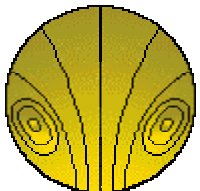


A HANDBOOK OF ELEMENTARY RHEOLOGY

Howard A. Barnes

Institute of Non-Newtonian Fluid Mechanics
University of Wales
2000



A HANDBOOK OF ELEMENTARY RHEOLOGY

Howard A. Barnes

Principal Scientist, and Science Area Leader
in Rheology and Fluid Mechanics
Unilever Research Port Sunlight
Wirral England

**University of Wales
Institute of Non-Newtonian
Fluid Mechanics, Aberystwyth, 2000**

Published by The University of Wales Institute of Non-Newtonian Fluid Mechanics, Department of Mathematics, University of Wales Aberystwyth, Penglais, Aberystwyth, Dyfed, Wales, SY23 3BZ.

First published 2000

© Howard A. Barnes, 2000

ISBN 0-9538032-0-1

Printed by Cambrian Printers, Llanbadarn Road, Aberystwyth SY23 3TN

FOREWORD

'One of the principal objects ... in any department of knowledge is to find the point of view from which the subject appears in its greatest simplicity', J. Willard Gibbs

In an earlier book—*An Introduction to Rheology*—we stated that rheology is a difficult subject. However, even though we then tried to make it as simple as possible, a number of people still told us that they found the book hard going. This present book is meant to satisfy this group. For this reason, the mathematical content has been kept to a minimum, and the text is as descriptive as possible: there are no integrals and only the occasional differentiation symbol, with all the equations in the simple algebraic form of $A = B$.

The book is suitable as a first introduction to the subject of Rheology for any student of science or engineering. However, having worked in industry for thirty years, I am also trying to meet the needs of my industrial colleagues who—often without any previous training in the subject of rheology—find themselves having to work on the formulation and processing of non-Newtonian liquids. The contents of this book are expansions of lectures that I have given to both these groups of people over the years, in introductory rheology courses run by rheometer companies, training organisations and universities around the world.

Before leaving this foreword I must mention two rheologists and two rheology books. Dr. George Scott Blair, the ‘grand old man’ of British Rheology, was the first author to produce a book called *Elementary Rheology* (Academic Press, London, 1969), written as he said, on Rheology, but ‘not intended for rheologists’! The present author worked in his laboratory for a few months during a summer vacation as an undergraduate in the early 1960’s. His parting words on that occasion were ‘I hope you catch the Rheology bug’. The bug was truly caught, and this book is intended to spread the infection even further!

Then, *An Introduction to Rheology* for me marks my gratitude to Prof. Ken Walters FRS, one of my co-authors of that book. He introduced me to the world of theoretical rheology as a postgraduate student at the University of Wales, Aberystwyth and thereby gave me of a wide appreciation of most aspects of rheology. Over 5000 copies of *An Introduction ...* have now been sold and this present book has been written, in effect, as an introduction to *An Introduction ...*.

This book is offered in the spirit of Skovoroda, the 18th century Ukrainian philosopher who said that *‘We must be grateful to God that He created the world in such a way that everything simple is true and everything complicated is untrue’*.

My special thanks go to members of the Institute of Non-Newtonian Fluid Mechanics for reading through the manuscript and making useful suggestions—*dioch yn fawr!*

Port Sunlight, January 2000

A BRIEF GUIDE TO THE HANDBOOK

The handbook begins with a short introduction (*chapter 1*) to the viscosity of everyday liquids, and shows the way in which rheology interacts with in-use situations which most of us come across in everyday life at home and work. Then a few chapters follow on the explanation of the different kinds deformation (*chapter 2*); the use of graphs in general (*chapter 3*), and rheology graphs in particular (*chapter 4*). A consideration of the simplest kind of liquid that we will meet comes next – the Newtonian liquid (*chapter 5*), and we then show how we can calculate its flow behaviour in lots of simple geometries (*chapter 6*).

Two chapters cover rheology measurement (*chapters 7 & 8*), thus equipping us for non-Newtonian behaviour in liquids. A discussion of such liquids—where the viscosity varies with shear rate (or shear stress)—then follows (*chapters 9 & 10*), with a special section devoted to very shear-thinning liquids that appear to have a yield stress (*chapter 11*). To complete this part, we discuss the flow, i.e. creep, of solids (*chapter 12*) under long-term stress.

Viscoelastic behaviour is then covered (*chapters 13 and 14*), first linear viscoelasticity with its manifestations in the time and frequency domain. Then non-linear displays of viscoelasticity are introduced, these effects being usually encountered in steady-state flow, where overt normal-force effects such as the Weissenberg rod climbing and the extrudate-swell phenomena are seen.

The origins of viscous and viscoelastic behaviour are then investigated for suspensions (*chapter 15*) and polymer systems (*chapter 16*), showing the important effects of colloidal interactions. Extensional (or stretching) flow results in a very different interaction between microstructural elements such as rods and coils and the surrounding stretching flow field, and this results in very divergent behaviour compared to shear flow (*chapter 17*).

Two applied areas are then covered, first the rôle of rheology in the surfactant systems (*chapter 18*) found in so many everyday products, and then we give a short overview of the rheology of food systems (*chapter 19*).

For those interested in buying journals or books on the subject of rheology, an extensive list is given (*chapter 20*). The last chapter (*chapter 21*) considers the growing importance of computing in rheology, where one can now predict the flow of viscoelastic liquids in complex geometries.

The book concludes with an Appendix which covers the area of on-line or process viscometry, which although not of great interest to all readers, is nevertheless very important to some.

Note:

Where possible useful Internet websites are referred to in the text, but readers are encouraged to explore such possibilities for themselves, starting at

<http://www.ncl.ac.uk/rheology/esr/> (lots of links!)
<http://www.ncl.ac.uk/rheology/bsr/noframes/index.html>
<http://www.rheology.org>
<http://www.engr.wisc.edu/centers/rrc/what.html>
<http://www.staff.ncl.ac.uk/chris.petrie/links.html>
<http://www.rheology.co.uk>

CONTENTS

FOREWORD AND GUIDE.....	iii
1. THE VISCOSITY OF LIQUIDS - SOME SIMPLE IDEAS	
1.1 Introduction	1
1.2 Rheology, packaging and product delivery	2
1.3 Where Rheology is important	2
2. WHAT IS FLOW AND DEFORMATION?	
2.1 Introduction	5
2.2 Shear rate and shear stress	6
2.3 The range of shear rates	6
2.4 Basic dimensions and units	7
2.5 Everyday Rheology units	9
3. HOW TO INTERPRETE GRAPHICAL DATA	
3.1 Introduction	11
3.2 Logarithmic plotting	11
3.3 Different ways of plotting the data	12
3.4 Plotting start-up	13
3.5 Long-distance running	14
3.6 Other running regimes	14
3.7 Summary	15
4. DRAWING RHEOLOGICAL GRAPHS	
4.1 Introduction	17
4.2 Figure legends	17
5. THE NEWTONIAN LIQUID	
5.1 Introduction	19
5.2 Viscosity	19
5.3 Viscosity of common Newtonian liquids	20
5.4 The variation of Newtonian viscosity with temperature	21
5.5 The effect of pressure on viscosity	22
5.6 The everyday perception of viscosity	23
5.7 The limit of Newtonian behaviour	23
References	24
6. SOME EQUATIONS FOR THE FLOW OF NEWTONIAN LIQUIDS	
6.1 Introduction	25
6.2 Flow in rotational viscometers	25
6.2.1 Narrow-gap concentric cylinder geometry	26
6.2.2 Small-angle cone-and-plate geometry	26
6.3 Flow in straight pipe circular pipes	27
6.3.1 Velocity profile and pressure drop in fully developed laminar flow in a tube	27
6.3.2 Flow from large reservoirs into small tubes	28
6.3.3 Filling a tube with constant suction	29
6.3.4 Tube emptying under a constant pressure	29
6.3.5 Flow through a packed bed of spheres in a tube	29
6.4 Spheres falling in Newtonian liquids	30
6.4.1 An isolated falling sphere	30
6.4.2 A falling/rising cloud of spheres	30
6.4.3 A sphere rolling down an inclined tube	31
6.5 Other important flows	31
6.5.1 Drainage down a wall	31
6.5.2 Flow along a slot	31
6.5.3 Flow through an annulus	32

6.5.4 A rod being pushed into a cup filled with liquid	32
6.5.5 Flow between squeezed circular plates	32
6.5.6 One tube moving inside another with the space between filled with liquid	33
6.5.7 An angled plate moving across a trapped liquid	33
6.5.8 A cylindrical indenter being pushed into a viscous liquid	34
6.5.9 A disc rotating in a sea of liquid	34
6.6 Interaction between viscosity and density in flows	34
6.6.1 Flow into the entrance of a tube	35
6.6.2 Turbulent flow in tubes	35
6.6.3 The size of the liquid jet coming out of a tube	36
6.6.4 Stokes flow with inertia	36
6.6.5 Taylor vortices in concentric-cylinder flow	36
6.7 Some flows where surface tension is important	38
6.7.1 Free coating	38
6.7.2 Levelling of surface undulations	39
6.7.3 Flow up a capillary tube	39
6.7.4 A large bubble moving in a tube	39
7. VISCOMETRY	
7.1 Introduction	41
7.2 Some important things to note about using viscometers	42
7.2.1 Calibration	42
7.2.2 Artefacts	42
7.2.3 Wall effects	42
7.2.4 Evaporation	43
7.2.5 Sedimentation/separation	44
7.2.6 Chemical damage	44
7.2.7 Mechanical damage	45
7.2.8 Sampling	45
7.2.9 High-speed testing	45
7.2.10 Suspended particles	46
7.3 Viscometer design	
7.3.1 General considerations	46
7.3.2 Commercial controlled-stress viscometers	47
7.3.3 Evolution of the specifications of controlled stress viscometers	48
7.4 Non-simple viscometer geometries	48
7.4.1 Wide-gap concentric cylinders	49
7.4.2 The rotating parallel-plate viscometer	50
7.3.6 Tube/pipe viscometer	50
8. YOUR RHEOLOGY LABORATORY	
8.1 What's in a good rheology laboratory?	51
8.2 Which problem?	51
8.3 Which rheometer?	52
8.3.1 Standard laboratory viscometers	52
8.3.2 Rheometers	52
8.3.3 Elongational viscometers	52
9. SHEAR-THINNING LIQUIDS	
9.1 Qualitative features of flow curves	55
9.2 Mathematical descriptions of flow curves	58
9.2.1 The Cross model	58
9.2.2 The Bingham equation	58
9.2.3 The power-law equation	59
9.2.4 The Sisko model	60
9.3 Fitting models to data	60
10. EQUATIONS FOR THE FLOW OF NON-NEWTONIAN LIQUIDS	
10.1 Introduction	63
10.2 Flow in a straight circular pipe	63
10.2.1 Power-law liquids	63
10.2.2 Sisko model	64

10.2.3 Casson model	64
10.2.4 Bingham fluid	64
10.3 Drainage down a wall	65
10.4 A sphere moving under gravity in a power-law liquid	65
10.5 Flow in a slit (a very wide slot)	66
10.6 Radial flow between parallel discs	66
10.7 Flow out of a tank through a long exit pipe	66
10.8 Flow of a power-law liquid between squeezing plates	67
10.9 Flow through a converging nozzle	67
10.10 Levelling of surface undulations under the action of surface tension	68
10.11 A disc rotating in a power-law liquid	68
10.12 More formulas for liquids with an apparent yield stress	69
10.12.1 Flow in a mixer	69
10.12.2 Wide-gap concentric cylinders	69
10.12.3 Capillary rise for a yield stress liquid	70
References	70
11. VERY SHEAR-THINNING OR ‘YIELD - STRESS’ FLUIDS	
11.1 Introduction	71
11.2 The history of the ‘yield stress’	72
11.3 Values of yield stress	73
11.4 The arrival of commercial controlled-stress rheometers	74
11.5 The vane geometry	74
11.6 Some flow equations with yield stresses	75
References	76
12. THE FLOW OF ‘SOLIDS’	
12.1 Introduction	77
12.2 Non-linear ‘viscosity’ of solids	78
12.3 Conclusion	79
References	79
13. LINEAR VISCOELASTICITY AND TIME EFFECTS	
13.1 Introduction	81
13.2 Mechanical analogues of viscoelastic behaviour	82
13.3 Measuring linear viscoelasticity	84
13.3.1 General	84
13.3.2 Creep tests	84
13.3.3 The behaviour of model materials in creep tests	86
13.3.4 Oscillatory tests – or mechanical vibrational spectroscopy	88
13.3.5 Oscillatory tests with a Maxwell model	89
13.3.6 Double or multiple Maxwell models in oscillation	90
13.3.7 Oscillation with a Voigt model	92
13.3.8 The oscillatory response of real systems	92
13.3.8.1 Viscous/terminal region – simple Maxwell behaviour	94
13.3.8.2 Polymer systems	95
13.3.8.3 Dispersions	96
13.4 What can we get from oscillatory data?	98
13.5 The relationship between oscillatory and steady-state viscoelastic parameters	100
13.5.1 General considerations	100
13.5.2 Creep versus oscillatory testing	100
13.5.3 A simple link between creep and oscillatory parameters	100
13.6 Non-linear response in oscillatory testing	101
13.7 Using oscillatory data to monitor curing, and rebuilding after shear	102
13.8 Stress-relaxation testing	103
13.9 Start-up experiments	104
References	105
14. NON-LINEAR VISCOELASTICITY	
14.1 Everyday elastic liquids	107
14.2 Some visible viscoelastic manifestations	108
14.3 The proper description of viscoelastic forces	110

14.4 The measurement of viscoelastic forces	111
14.5 Examples of first normal-stress differences	112
14.6 Some viscoelastic formulas	115
14.6.1 General	115
14.6.2 Extrudate flow	115
14.6.3 Flow in a slightly inclined trough	116
14.6.4 Pressure in holes and slits	116
14.6.5 Inertia in a cone-and-plate geometry	116
14.7 Postscript – flow of a viscoelastic liquid through a contraction	117
References	117
15. THE FLOW OF SUSPENSIONS	
15.1 Introduction	119
15.2 Viscosity of dispersions and emulsions	119
15.2.1 The continuous phase	119
15.2.2 The effect of very low concentration of suspended particles	120
15.2.2.1 The effect of the continuous phase	120
15.2.2.2 The effect of the disperse phase	122
15.2.2.3 The effect of medium-to-high concentrations of particles	122
15.3 Particle-size effects in concentrated dispersions	125
15.4 Particle-shape effects in concentrated dispersions	126
15.5 Particle deformability	126
15.6 Particle interactions – an overview	126
15.7 The viscosity of flocculated systems	129
15.8 Thixotropy	131
15.9 Shear thickening	133
15.10 Apparent wall slip	133
15.11 Very high concentration pastes	136
15.12 Colloidal control of suspension viscosity	137
15.13 The stability of suspensions	138
References	139
16. POLYMER RHEOLOGY	
16.1 Introduction	141
16.2 Some of the different kinds of polymer chains	141
16.2.1 Long rods	142
16.2.2 Coils/strings	142
16.3 Polymer solutions	144
16.4 Highly branched polymers	145
16.5 ‘Living polymers’ or rod- or worm-like micelles	146
16.6 Associative polymers	147
16.7 A polymer solution as a standard non-Newtonian liquid	148
References	149
17. EXTENSIONAL FLOW AND EXTENSIONAL VISCOSITY	
17.1 Introduction	151
17.2 Where do we find extensional flows?	152
17.3 What’s so special about extensional viscosities?	153
17.4 The Trouton ratio	155
17.5 Some examples of extensional viscosity curves	156
17.6 The effect of time or extension on extensional viscosity	158
17.7 Other kinds of extensional flows	159
17.8 Viscometers to measure extensional viscosity	160
17.9 Commercially available extensional viscometers	162
17.10 Some interesting applications	162
References	163
18. RHEOLOGY OF SURFACTANT SYSTEMS	
18.1 Introduction	165
18.2 Surfactant phases	165
18.3 Rheology of surfactant systems	167

18.4 Necessary rheological properties	168
19. RHEOLOGY OF FOOD PRODUCTS	
19.1 Introduction	171
19.2 Liquid-like food rheology	172
19.3 In-vivo flow fields	172
19.4 Rheology and food processing	172
20. YOUR RHEOLOGY LIBRARY	
20.1 Introduction	175
20.2 Rheology books in print	175
20.3 General Rheology	175
20.4 Theoretical Rheology	177
20.5 Polymeric systems	178
20.6 Blood	179
20.7 Food	179
20.8 Other specific systems	180
20.9 Drag reduction	180
20.10 Geological subjects	181
20.11 Proceedings of meetings (not mentioned elsewhere)	181
21. RHEOLOGY AND COMPUTING	
21.1 Introduction	183
21.2 A brief description of how CFD works	183
21.3 The rheological description of a non-Newtonian liquid and CFD codes	184
21.4 When should CFD be used?	184
21.5 Some typical results of CFD calculations	184
21.6 A word of caution	185
APPENDIX: ON-LINE (PROCESS) VISCOMETRY	
A.1 Introduction	187
A.2 Desirable features of a good on-line viscometer	187
A.3 Types of measurement made by current instruments	189
A.4 The effect of non-Newtonian viscosity	190
A.5 Hygiene and cleaning	191
A.6 General comments on actual representative instruments	191
A.7 Detailed description of a particular instrument	192
A.8 Conclusions	192
References	193
INDEX	195
ANSWERS TO SOME EXERCISES	200

CHAPTER 1: THE VISCOSITY OF LIQUIDS

- SOME SIMPLE EVERYDAY IDEAS

'Everything should be as simple as possible, but not simpler', Einstein

1.1 Introduction

No one is really an absolute beginner when it comes to rheology, because the flow properties of liquids play such an important part in our daily lives—either deliberately or accidentally. This importance ranges, for instance, from the viscosity of the blood flowing around our bodies, through the thickness of the liquids that we swallow, to the grade of the oil that we put into our car engines. As consumers we are not only told that products are '*new and improved*', but also that they are '*thick and creamy*', because such rheological properties are more pleasing to the eye, mouth and hand. Providing for our unmet needs as potential customers by adjusting the rheology of products is an important part of the product development activity.

We use many words with a rheological connotation, e.g. viscosity, consistency and texture, and they can have both positive and negative implications. Hence, while '*thick and creamy*' might impart a positive inference; *gluey, gelatinous, sticky, tacky, gooey, gummy, cohesive*, could well convey the opposite idea with regard to liquids being too thick.

Watery and *runny* might communicate the idea of dilution, since in a consumer's mind a liquid with a high viscosity usually conveys (or reinforces) the idea of concentration and 'strength', since a similar product with a lower viscosity will often pass on the idea of 'weakness'. On the other hand, many products, if perceived as *too* thick will, in the consumer's mind, be anticipated to have problems in 'dissolving', i.e. dispersing.

In the context of everyday products it is a simple and useful exercise to go around your house and garden and note the following examples of structured liquids with interesting rheologies:

- | | | |
|--------------------|---|---|
| • kitchen | - | laundry liquids, surface cleaning liquids |
| • bathroom cabinet | - | personal products |
| • garage | - | oils, greases |
| • pantry | - | sauces, salad dressings |
| • tool shed | - | paints, glues, mastics |

Exercise 1: List other liquids with interesting flow properties, and ask 'why have they been made like this'?

Exercise 2: Obtain samples of similar products with low and high viscosities respectively, and carry out a small consumer test to see if viscosity is connected with perceived 'strength' and concentration in the minds of average consumers.

1.2 Rheology, packaging and product delivery

Having considered the consistency of a product, we now need to think about its packaging and means of delivery. These probably range over the following sequence of packaging, consistency and delivery action:

Package	Consistency	Action	Example
pressure cans	thin and watery	Spray	paint, hair spray
bottles, cans	oily	Squirt	washing-up liquid, oil
tubes	pasty	Squeeze	toothpaste, tomato paste
tubs	soft-solid like	Scoop	face cream, Swarfega

Clearly anyone interested in these areas should be thinking very carefully about rheology.

1.3 Where rheology is important

As well as adjusting rheology to suit consumer tastes, it is sometimes necessary to control the rheology for specific technical reasons. Some examples that are easily appreciated are:

Slowing things down	- draining on vertical surfaces - suspending particles - thickened sauces	- paint, bleaches - paint, abrasive cleaners - mayonnaise.
----------------------------	---	--

We often need a high viscosity to resist flow at the low forces posed by gravity, but at the same time one needs a low viscosity for the same product under the high forces experienced in pouring, squirting or brushing. This is where the non-Newtonian—viscosity varying with applied force or flow rate—properties are very important. Some other examples where this is true are:

- **Hair shampoos** that need to be thick enough to pour onto the hands for transferring to the hair without flowing away through the fingers. The same is also true of skin creams and other personal products.
- **Toothpastes** that need to be viscous enough to sit on the brush without draining into the bristles, but at the same time are easily extruded from the tube. (However, some modern tooth-cleaning products are sold in bottles, and have a much lower viscosity.)
- **Thixotropic or 'solid' paints** that have very special properties built into them so that they appear to be solid after storing, but on brushing out or stirring, they thin down. They will then re-thicken on standing.
- **Printing inks** that need to spread easily when squeezed onto the type or transfer surface, but once deposited/printed onto a surface, in order to maintain a sharp edge, they must not spread by the action of surface tension or gravity.

- **Ink** in biros and roller-ball pens that must have a low viscosity as it is being dispensed through the high-shear-rate roller-ball mechanism. However, when the ink is sitting on the writing surface, its viscosity must be high to stop it spreading far.
- **Concentrated liquids** that often have suspended solid particles, either as crystals above their solubility limit, or that have been deliberately added such as abrasive particles: these have to be suspended for long periods of time. The product has also to be pourable.
- **Cement** pastes that have to be as concentrated as possible, but flowable—this can be achieved by vibrating.

Exercise 3: think of other areas where the property of high viscosity at low stress and low viscosity at high stress is important.

Epilogue:

Please note that the words ‘fluid’ and ‘liquid’ are often used interchangeably (as sometimes in this book). However, while the word ‘fluid’ covers both gases and liquids, gases are not liquids. So all liquids are fluids, but not all fluids are liquids—think about it! And while you’re thinking about it, don’t forget solids!



CHAPTER 2: WHAT IS FLOW AND DEFORMATION?

'Insufficient facts always invite danger, Captain', Mr Spock

2.1 Introduction

Rheology has been properly defined as the study of the flow and deformation of materials, with special emphasis being usually placed on the former. However, we might ask the simple question—‘what is flow?’. If we carry water carefully in a bucket, it is certainly moving, but it is not flowing, however if we pour out the water it *is* flowing. What is the difference? In flow, elements of the liquid are deforming, and adjacent points in the liquid are moving *relative* to one another.

There are two basic kinds of flow with relative movement of adjacent particles of liquid; they are called *shear* and *extensional* flows. In shear flows liquid elements flow *over* or *past* each other, while in extensional flow, adjacent elements flow *towards* or *away from* each other, see figure 1 for illustrations of shear and extensional deformation and flow respectively.

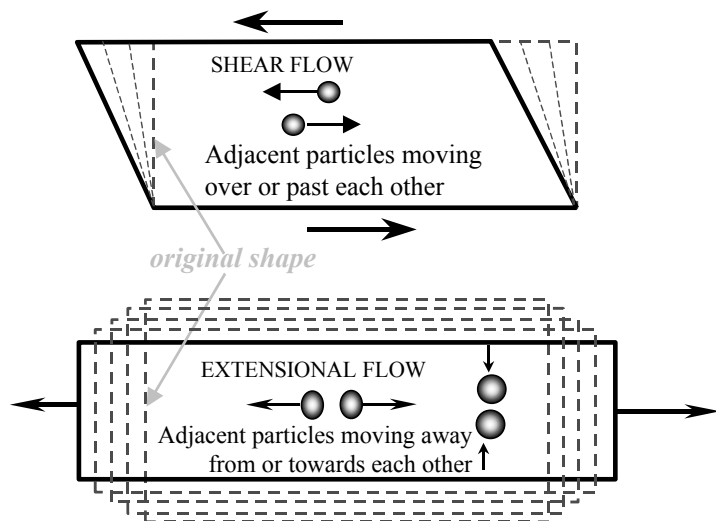


Figure 1: Particle motion in shear and extensional flows.

Exercise 1: When a liquid is being rubbed, poured or stirred, imagine that you are an element of the liquid and consider whether you are experiencing shear or extensional flow or both.

All flows are resisted by viscosity, so if we poured out a bucket of water, it would flow much quicker than if we had poured out a bucket of motor oil. Liquids are made to flow by imparting a velocity—as in stirring with a spoon—or else by applying a force, as with squeezing a bottle of sauce. For a given *velocity*, the

resulting force *increases* when the viscosity is increased, whereas for a given *force*, the velocity is *reduced* when the viscosity is increased.

Exercise 2: Try to think of a number of situations where flow is initiated by imparting a velocity or else by applying a force.

2.2 Shear rate and shear stress

As we have seen in figure 1, simple shear flow is the continual movement of particles of liquid *over* or *past* each other, while extensional (or *elongational*, or *stretching*) flows are where particles of liquid flow *towards* or *away from* each other (see below). In figure 2 we visualise shear flow alternatively as the movement of hypothetical *layers* sliding over each other. In the simplest case the velocity of each layer increases linearly with respect to its neighbour below, so that layers twice the distance from any stationary edge move at *double* the speed, etc. The *gradient* of the velocity in the direction at right angles to the flow is called the *shear rate* (*sometimes called the velocity gradient or strain rate*), and the force per unit area creating or produced by the flow is called the *shear stress*. In our simple example, the shear rate is V/h and is described by the symbol $\dot{\gamma}$ (pronounced ‘gamma dot’), while the shear stress is given by F/A and is given the symbol σ (sigma).

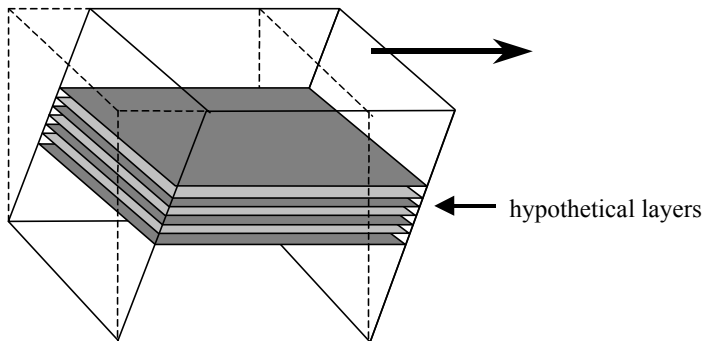


Figure 2: Hypothetical layers in shear flow.

The shear rate has the units of velocity divided by distance, i.e. metres per second / metres, leaving us with the units of reciprocal (i.e. one over) seconds, or s^{-1} . Shear stress—force per unit area—has the units of newtons per square metre, $N\ m^{-2}$, but in the SI system, stress, like pressure, it is given in units of pascals, Pa, in honour of the famous French scientist. For reference, standard atmospheric pressure, previously known to many as 14.7 pounds per square inch (psi), is 10^5 Pa.

2.3 The range of shear rates

The approximate value of the shear rate encountered in a wide variety of circumstances found in everyday life or in industrial situations is shown in table 1. Readers may relate these numbers to their own field of interest by simply dividing a typical velocity in any flow of interest by a typical dimension. An example of this is the average velocity of a liquid flowing in a pipe divided by the pipe radius, or the velocity of a moving sphere divided by its radius.

Situation	Shear Rate Range / s ⁻¹	Examples
Sedimentation of fine powders in liquids	$10^{-6} - 10^{-3}$	Medicines, paints, salad dressing
Levelling due to surface tension	$10^{-2} - 10^{-1}$	Paints, printing inks
Draining off surfaces under gravity	$10^{-1} - 10^1$	Toilet bleaches, paints, coatings
Extruders	$10^0 - 10^2$	Polymers, foods soft solids
Chewing and swallowing	$10^1 - 10^2$	Foods
Dip coating	$10^1 - 10^2$	Paints, confectionery
Mixing and stirring	$10^1 - 10^3$	Liquids manufacturing
Pipe flow	$10^0 - 10^3$	Pumping liquids, blood flow
Brushing	$10^3 - 10^4$	Painting
Rubbing	$10^4 - 10^5$	Skin creams, lotions
High-speed coating	$10^4 - 10^6$	Paper manufacture
Spraying	$10^5 - 10^6$	Atomisation, spray drying
Lubrication	$10^3 - 10^7$	Bearings, engines

Table 1: Typical shear rate ranges of various physical operations.

2.4 Basic dimensions and units

It is worth spending a little time on this subject, since it arises so often in Rheology and is an area in which it is very easy to become confused, so that many mistakes have been made by the unwary. We shall be following the SI (*Système International d'Unités*) convention, which, for our purposes is built around the five basic units of mass, length, time, temperature and amount of substance, as shown in table 2, from which all other units of rheological interest are derived. Table 3 gives a number of such units, which have special names, their symbols and their full equivalents.

The decade prefixes—as shown in table 4—should be used before units in order to bring them into the sensible range of 0.1 to 1000 as a numerical value used with any particular unit, e.g. 2 kN, but *not* 2000 N, and 10 Pa.s, but *not* 0.01 kPa.s. Note that all prefixes representing 10^6 or greater are capitalised (e.g. M for 10^6), but all below 10^6 are in lower case, e.g. m for 10^{-3} . There should be no space between the prefix and the unit, and combined prefixes should not be used, e.g. mmPa should be μ Pa. When units have to be written out in full, any prefix should also be written out in full, beginning with a lower-case letter, e.g. megahertz not Megahertz or Mhertz and millipascal seconds not mpascal seconds.

Quantity	Unit Name	Unit Symbol
Mass	kilogram	kg
Length	metre	m
Time	second	s
Temperature	kelvin	K
Amount of substance	mole	mol

Table 2: SI base units used in Rheology

Quantity	Special Name	Symbol	Equivalent
Frequency	hertz	Hz	s^{-1}
Force	newton	N	$kg\ m/s^2$
Pressure or stress	pascal	Pa	N/m^2
Work, energy, heat	joule	J	$N\ m, kg\ m^2\ s^{-2}$
Power	watt	W	J/s

Table 3: Some derived SI units with special names

Factor	Prefix	Symbol
10^6	mega	M
10^3	kilo	k
10^2	hecto	h
10^1	deka	da
10^{-1}	deci	d
10^{-2}	centi	c
10^{-3}	milli	m
10^{-6}	micro	μ

Table 4: Usual SI decade prefixes used in Rheology

The convention followed in this book is that all physical quantities are in *italic* type, while symbols for units are in normal type, so for instance we might say that ?the force F is 15 N; the viscosity η is 10 Pa.s and the shear rate $\dot{\gamma}$ is 0.1 s^{-1} . Symbols for unit names derived from proper names begin with a capital letter *but* the unit names themselves are not capitalised, *i.e.* N for newton, P for pascal and Hz for hertz. The unit name should not be followed by a full stop, and plurals of unit symbols should not be followed by an 's', e.g. 3 kg but *not* 3 kgs. If we are quoting temperature T in absolute units, *i.e.* kelvin, then no $^\circ$ symbol is needed, e.g. 200 K. However if you are quoting the temperature in Celsius or similar, you should put $^\circ$ C.

Chapter 2: What is flow and deformation?

Inserting a raised dot properly indicates multiplication of units, but a full stop (period, US)—as used here—is usually acceptable because some people only have access to a limited character set on their keyboards. However leaving a space between the units is also acceptable, so we can happily write either N.m, N.m or N m, but *not* Nm! Here we shall keep to the full-stop/period convention (as in Pa.s) which is well understood and easily typed, but when writing for particular companies or scientific journals, you should check their preferred house-style. Division is indicated by the use of a forward slash / or a negative exponent, but repeated use of a forward slash is not allowed, so for acceleration we write m/s² or m.s⁻² but *not* m/s/s.

The numerical value and the unit symbol should be separated by a space, even when used as an adjective in normal writing, e.g. 35 mm, not 35mm or even 35-mm. A zero should always be placed in front of the decimal point for numbers less than one, e.g. 0.3 J but not .3 J. The SI unit for volume, the litre, is best represented by L and not the lower case l which is easily confused with the numeral 1 in most character fonts.

Exercise 3: Check out <http://physics.nist.gov/Document/checklist.pdf> on the Internet for the US government's official view on the rules and style conventions for SI units. Standard rheological nomenclature, as approved by the (American) Society of Rheology may be found at www.umecheme.maine.edu.

2.5 Everyday Rheology units

Units that you will come across most frequently in Rheology are shown in table 5.

Quantity	Symbol	Units
Shear	γ (pronounced gamma)	-
Shear rate	$\dot{\gamma}$ (pronounced gamma dot)	s ⁻¹
Shear stress	σ (pronounced sigma)	Pa
Shear viscosity	η (pronounced eta, i.e. 'eater')	Pa.s

Table 5: Some commonly used rheological quantities and their units.
Note that the units of viscosity are Pa.s and *not* Pasecs!

Note that although it is good practice to write *shear* viscosity to distinguish it from *extensional* viscosity, it is usually referred to simply as viscosity.

The Greek symbol γ (gamma) represents deformation in simple shear, this is illustrated in figure 3, where shear stress σ (sigma) is also defined.

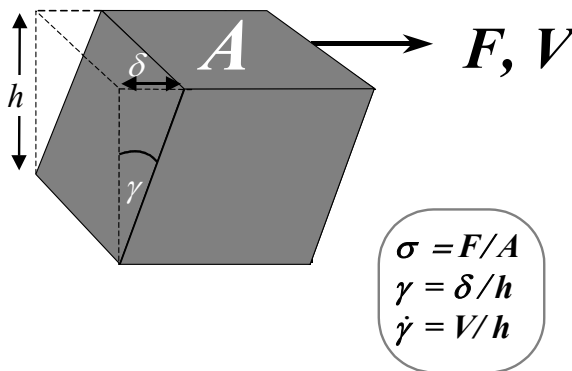


Figure 3: Definition diagram for shear flow.

Similarly, for uniaxial extension the proper measure of deformation is ε (epsilon) and stress (sometimes called *tension*) σ_e as shown in figure 4.

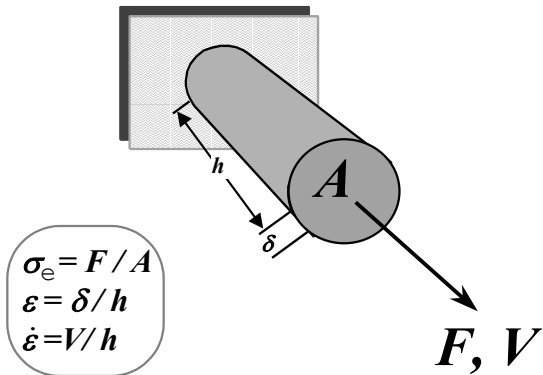


Figure 4: Definition diagram for uniaxial extensional flow.

Using the same diagrams we can also define deformation rate, where now the deformation δ (delta) is continuous and $V = d\gamma/dt$, and $\dot{\gamma} = dV/dh$, and is called the *shear rate*. The dot above the deformation symbols is used to signify differentiation with respect to time, and follows Newton's calculus convention ('Newton's dot'), so that γ is an *amount* of shear, and $\dot{\gamma}$ is the *rate* of shear, or shear rate $d\gamma/dt$ (usually referred to as 'd γ by dt'), which is sometimes called the *rate of strain or strain rate*.

For Newtonian liquids in simple shear flows we can write

$$\sigma = \eta \dot{\gamma}.$$

For uniaxial extensional or stretching flows, the equivalent symbols are σ_e and $\dot{\varepsilon}$ and η_e and then for Newtonian liquids,

$$\sigma_e = \eta_e \dot{\varepsilon}.$$

Exercise 4: Convert a flow rate of 100 US gallons per hour into SI units (assume 1 US gallon = $3.7854 \times 10^{-3} \text{ m}^3$).

CHAPTER 3: HOW TO INTERPRETE GRAPHICAL DATA

'Few things are harder to put up with than the annoyance of a good example', Mark Twain

3.1 Introduction

One of the most important considerations in rheology is making sense of data collected from viscometers or rheometers, especially when that data is to be plotted visually, as in a graph. (Here we will follow the modern practice—see the latest Oxford dictionaries—and take the word ‘data’ as singular, in the sense of a particular collection of numbers.) In order to master some of the principles involved in constructing, using and interpreting graphs, we will look at some interesting non-rheological data, viz. the world records for men and women’s running races (the data was collected from various Internet sites). We will use the world records ranging from the 50 m indoor event, through the various outdoor sprint distances, middle distances, the marathon, right through to *very* long distances.

3.2 Logarithmic Plotting

Once we have compiled the particular data-set of interest, the first thing we do is to plot the record times T as a function of race distance D , as shown in figure 1, but noting the first lesson that we must reduce all the data to *the same units*, in our case (mega-)metres and (mega-)seconds, and *not* a mixture of seconds, minutes and hours, etc.

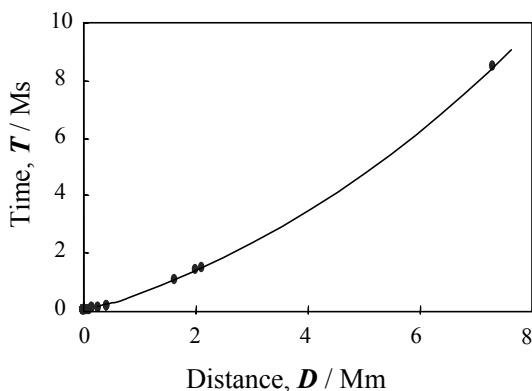


Figure 1: Men's world records, time versus distance.

Once we have produced this plot we immediately see a substantial problem: if we want to display *all* the data which covers a very wide range of distances—50 to over 7,000,000 m—on a simple *linear* plot, the points for distances less than 1,000,000 m are compressed into the corner of the graph, and we cannot even see them! One answer is to plot the results on a *logarithmic* basis, see figure 2, where we see that the spacing between 100 m, 1000 m and 10,000 m etc., is now the same on the distance axis. The facility of plotting logarithmic-based graphs is available on most modern graph-plotting software

packages, or they can even be generated manually on specially printed logarithmic graph paper.

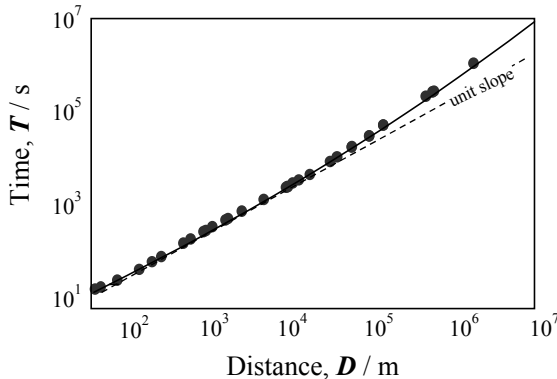


Figure 2: Men's world records, time versus distance, logarithmic plot.

3.3 Different ways of plotting the same data

Next we will show that the basic distance/time data can be manipulated and plotted in different ways. For instance if we now divide the distance by the time for each record, we get the average speed, V , in metres per second. For physiological reasons this is now plotted as a function of time—again on a logarithmic basis—to see how the body produces power (measured by velocity) as a function of time, see figure 3.

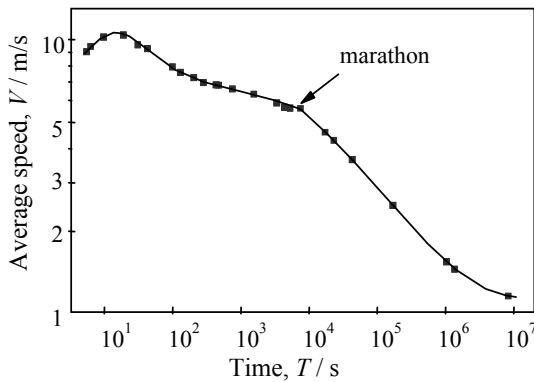


Figure 3: Men's world records, average speed versus time, logarithmic plot.

Notice that there is far more ‘structure’ in the speed/time graph than its innocuous time/distance equivalent and quite different regimes can now be identified. For instance, we notice that for short distances, the average speed seems to rise from the 50 m event to a maximum at around 150 m and then drop off. The reason for this is quite simple: because the runner starts from rest, he/she needs to accelerate up to maximum speed, then, after a certain time, he/she begins to tire and hence slows down, see figure 4.

How can this data be best represented and what further information can we extract from it? If we now plot the distance/time data over the range 50 to 400 m on a *linear* basis—as shown in figure 4—three things are obvious. First, the data we have plotted *appears* to extrapolate to a non-zero intercept on the time axis when the distance is zero. We can call this time the acceleration time, T_o , (the more mathematically

adventurous might like to work out what this means in terms of real features such as force being mass times acceleration and resistance being proportional to speed).

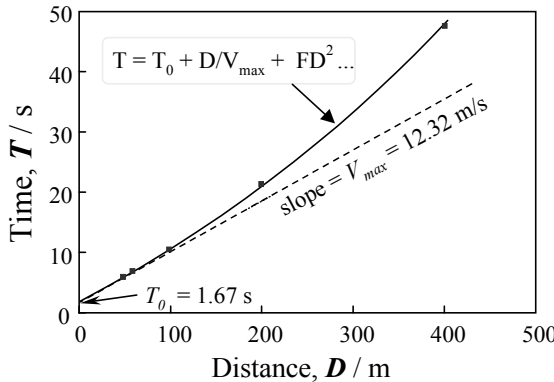


Figure 4: Men's world records, time versus distance, for short distances.

This acceleration time does contain a real time, that is the reaction time from the gun being fired to start the timing to the runner's legs receiving the nerve-impulse message to commence running, i.e. a fraction of a second.

3.4 Plotting start-up

The fastest speed shown on the graph is the initial slope at zero on the time axis, i.e. $\frac{dD}{dT}_{T \rightarrow 0}$, which we shall call V_{max} , and in this case it is nearly 14 m/s. Then the curve slopes upwards off the tangential line dictated by this maximum speed, indicating that running speeds are progressively reduced as fatigue sets in. We can now attempt to describe this curve in the simplest possible mathematical way. We will try the function $T = T_0 + D/V_{max} + FD^2$, where T_0 and V_{max} are, as described above, the acceleration time and maximum velocity, and F we shall call the 'fatigue factor', which arises from the run-down of energy and the build-up of lactic acid in the body. This equation can be fitted to the data using a regression package available on most spreadsheet applications, e.g. Microsoft Excel. From such a fit we find that V_{max} is 13.9 m/s and the acceleration phase T_0 is 1.8 s. We can subtract the acceleration phase and reconstruct the average speed data to illustrate the effect of the fatigue factor alone. This is shown in figure 5 where we have subtracted T_0 from all the time data.

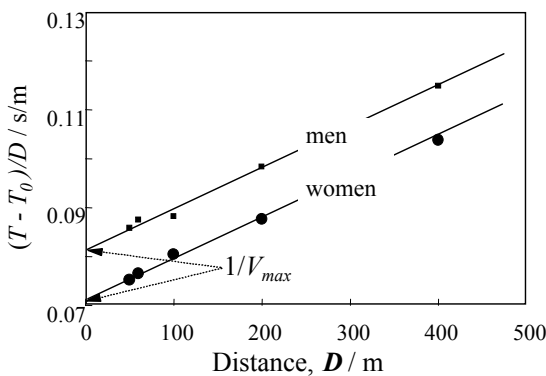


Figure 5: The inverse of the corrected speed for men's and women's world records for short distances, versus distance.

This would be the result if the runner could start the race at his maximum speed, or another way of combining these two numbers is to say that if the runner had started a distance $\approx V_{max} \cdot T_o$ (i.e. about 25 m) *before* the line, then he would have been up to maximum speed by the starting line (neglecting the very small amount of fatigue during that time).

3.5 Long distance running

If we now consider the longer-distance races, we see an important change in slope at around the marathon distance of approximately two hours, see figure 3. It so happens that the end of a marathon race occurs near a critical point in terms of the body's store of energy, because after about two hours the glycogen stored in the blood runs out and the body starts to burn fat. When this happens two things are important; first, when his supply of glycogen runs out, the runner 'hits the wall', and second the rate of conversion of fat to energy is thereafter slower, hence the greater slackening in speed as a function of time above two hours, shown as a distinct change in the slope of the curve shown in figure 3.

3.6 Other running regimes

Last we shall show how to plot data from parts of the original log graph that seemed to show different regimes. If we take the middle-distance data from 1000 to 10,000 m, we see that this shows a logarithmic straight-line relationship, see figure 6.

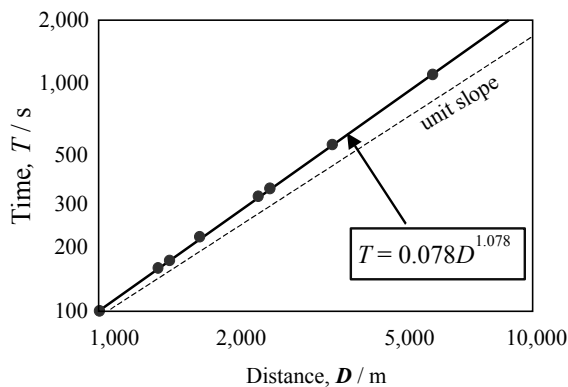


Figure 6: Men's world records, time versus distance for middle distance, logarithmic plot.

This implies a power-law relationship of the form $T = aD^n$, which in this particular case gives $T = 0.078D^{1.078}$. Again this kind of mathematical fit can be obtained from most spread-sheet software packages using regression analysis of the data, this one was obtained using Lotus *Freelance Graphics*. Remember that this relationship only works within the distance range we have chosen.

If we choose another range and combination of data, say average speed as a function of time for *very* long time events, we see another kind of logarithmic plot, see figure 7. This time we can describe the relationship between average speed and time by the expression $V = cT^m$, but now we note that m is negative because the speed is a *decreasing* function of time. The relationship is in fact given by $V = 61.36T^{-0.265}$. If we try to extrapolate this relationship *outside* its range, then large errors are introduced. For instance, if we attempt to use the relationship to predict the speed down at $T = 1$ s, the

result is very easy to calculate, because if $T = 1$, then 1 raised to any power is still 1, so then V is predicted to be 61.36 m/s. In fact V is no more than 14 m/s!

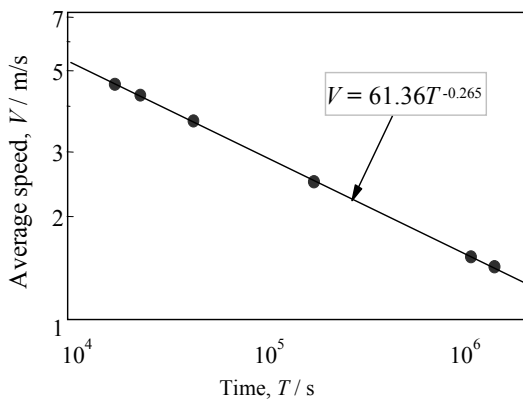


Figure 7: Men's world records, average speed versus time for long distances, logarithmic plot.

The equivalent data for women's running records tell the same story, but now we see that women are slower by about 13% ($\sim L$) over almost all distances/times, see figure 8 for some examples of this fact. In the plots of various ranges of distance and time, the power-law indices— m and n —describing men and women's performance are virtually identical.

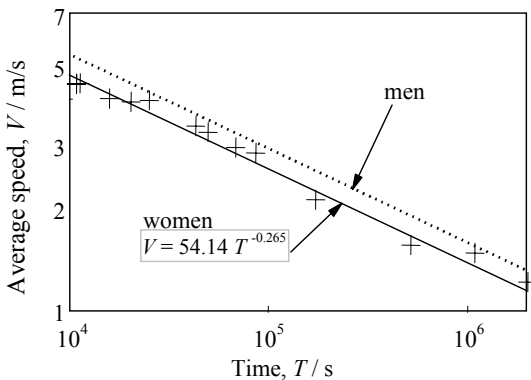


Figure 8: Women's world records, average speed versus time for long distances, logarithmic plot.

3.7 Summary

The lessons we have learned above—each of which has its own rheological counterpart—can be summarised as follows

- widely spread data is better plotted logarithmically,
- the same data set can be plotted in a number of ways, e.g. D vs. T ; T vs. D ; D/T vs. D ; D/T vs. T ,
- limited data can be extrapolated to zero distance to give an *apparent* intercept on the time axis,
- simple mathematical expressions can be fitted to the data, either linear, power law or more complicated, and
- mathematical fits must *not* be extrapolated outside the range of data collection.

These points will be constantly referred to in the following chapters where graphical representation of rheological behaviour is discussed at length.

Exercise: find some weight-lifting data on the Internet, and plot graphs of records as a function of weight, using the ideas given above.



CHAPTER 4: DRAWING RHEOLOGICAL GRAPHS

'First, get the facts, then you can distort them at your leisure', Mark Twain

4.1 Introduction

In the same way as we have described in Chapter 3 for data on running, graphs of rheological quantities are also best plotted on logarithmic axes so that the wide range of shear rates usually used and viscosities obtained are represented in the optimum manner. In this case the axis divisions are in decades, and the better way of representing these large numbers is to use decade exponents, i.e. 10^6 , (the normal decade number can be used if your plotting package only allows this form, but for very high viscosities, these can be quite long, e.g. 1,000,000) since other ways of representing this can be clumsy and confusing, e.g. E+6.

The axis labels can also be confusing and in order to overcome this the standard format should show (in the following order)

- the name of the quantity being plotted, e.g. Viscosity (note capitalisation),
- its symbol, e.g. η (remember, physical quantities are always in italics), and
- its units, e.g. Pa.s, *but shown as a division*, so that the quantities plotted on the graph are then pure numbers.

Thus, a complete axis label would look like

Viscosity, η / Pa.s Shear stress, σ / Pa.

If the units being plotted are large, then the unit size should be increased, so for instance, we might put

Tensile stress, σ_e / MPa,

then the numbers plotted are in megapascals, the original quantity having been divided by 10^6 . Sometimes graphs are plotted to show qualitative relationships only, and in that case the units should be omitted, hence

Viscosity, η , Time, t Strain, γ

4.2 Figure legends

In addition to labelling the axes carefully, equal care should be taken in composing the text for the figure legends. For instance, 'Figure 1' is not enough to identify a graph, with the details of what is being plotted being described only in the text. Figure legends should therefore be complete in themselves, so that a graph tell the whole story, without the reader needing to refer back and forth to the place in the

text where the graph is mentioned. Therefore, put into the legend (or perhaps within the graph itself), all the necessary information describing the variables and the system being represented.

Do not put too many curves on one graph, remember a graph is meant to enlighten and not to confuse! Use grids where necessary, but only where you want to draw attention to local particular values of points. Also, if your are plotting coloured graphs, beware of colours such as yellow are sometimes difficult to see, and do not copy well.

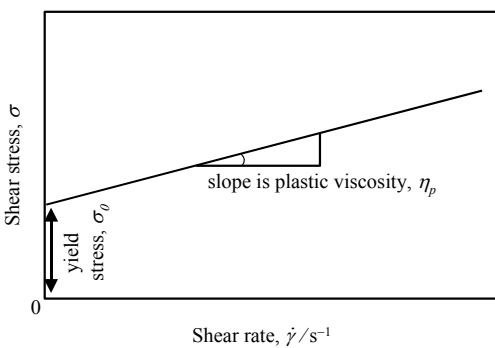


Figure 1: Hypothetical flow curve obeying the Bingham equation.

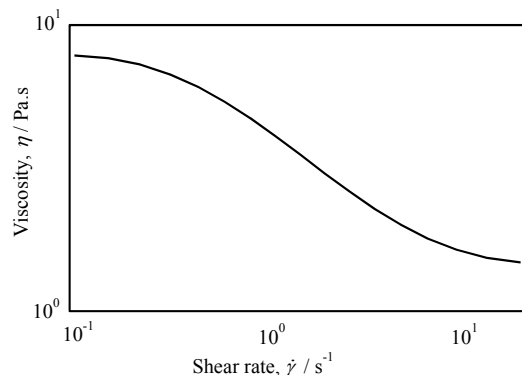


Figure 2: Viscosity versus shear rate for a dilute polymer solution, logarithmic scale.

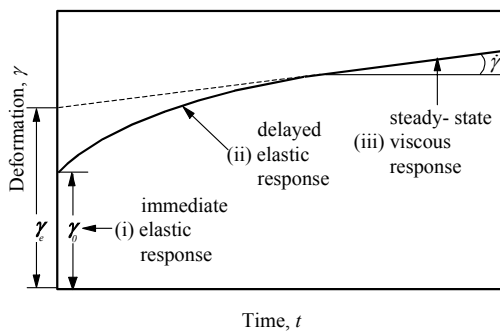


Figure 3: Hypothetical creep curve for a Burger model.

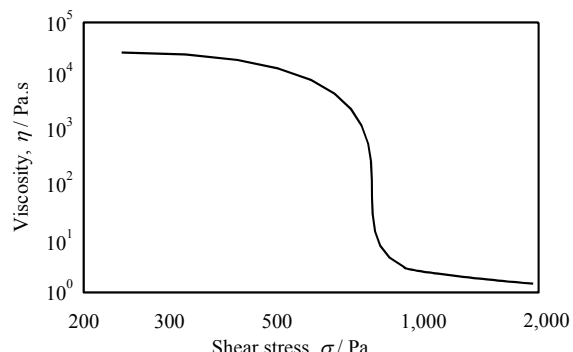


Figure 4: Viscosity versus shear stress for a very shear-thinning suspension; logarithmic plot.

Anticipating the contents of future chapters, figures 1 - 4 illustrate the points made here for some typical real and hypothetical rheological data.

Exercise 1: write down the graph axes for stress as a function of strain, and viscosity as a function of time.



CHAPTER 5: THE NEWTONIAN LIQUID

'The beginning of wisdom is to call things by their right names', A Chinese proverb

5.1 Introduction

A Newtonian liquid is one for which the viscosity—although varying with temperature and pressure—does not vary with deformation rate or time; nor does such a liquid display any elastic properties or extensional anomalies—these deviations will be explained later. A Newtonian liquid is of course an idealisation, but in many cases it is a very good representation of a large number of liquids under normal ‘everyday’ conditions, however see section 7 below. We shall now examine the ideas of viscosity in general and then the Newtonian liquid in particular.

5.2 Viscosity

Long before viscosity was recognised as a quantifiable material property of a liquid, there was obviously universal recognition that liquids could be viscous (from the Latin *viscum*, the mistletoe, which exudes a gelatinous juice when squeezed). Later, scientists knew qualitatively that viscosity was that property of a liquid which was a measure of its resistance to flow, so that high viscosity liquids flowed slowly and low viscosity liquids flowed quickly.

If we were able to explain to Isaac Newton (1642 - 1727) what we mean by viscosity, he would well understand, but he would call it '*defectus lubricitatis*—lack of lubricity', or the internal friction of a liquid. Neither would he recognise the idea of it having numbers with particular units associated with viscosity, because that came a lot later. In fact it was Wiedemann (1856) who proposed '*Zähigkeits-Koeffizient*', or 'coefficient of viscosity' as an absolute measure of the property. Then Hagenbach (1860) measured the value for water at 10 °C as 0.13351 in units of grams and square metres; this compares very well with the present internationally accepted value of 0.1307 in the same units. In 1890 Couette introduced the concentric-cylinder viscometer and found that the viscosity of water so measured agreed with Poiseuille’s value evaluated in tube flow. The first special unit for viscosity was the Poise, signified by P, in honour of Poiseuille (1797 - 1869), the French physician who had been interested in blood flow, and who, around 1840, had conducted extensive work on flow in tubes. The everyday unit from this system was the centipoise, being a hundredth of this value, i.e. the famous cP, with water being (very conveniently!) nearly 1 cP at room temperature.

Viscosity measurements began to be used by colloid chemists when Thomas Graham investigated the peptisation of silicic acid in the 1860’s. Soon, with the introduction of the Ostwald U-tube viscometer, viscometry became one of the most widely used methods of investigating colloidal solutions—and to a large extent it still is used for this purpose.

To be precise, we now say that shear viscosity is the ratio of shear stress to shear rate, i.e. $\sigma/\dot{\gamma}$ so the units of viscosity are pascals divided by reciprocal seconds,

giving us pascal seconds, or Pa.s. As this unit is only about 0.001 Pa.s for water at room temperature, the prefix m is necessary, hence 1 mPa.s. The pascal-second unit of viscosity is 10 times bigger than the older cgs equivalent, the Poise, but numerically, $1 \text{ mPa.s} \equiv 1 \text{ cP}$, which is precisely the viscosity of pure water at 20.2 °C.

Usually the limiting values of the viscosity of non-Newtonian liquids at very low and very high shear rate respectively (the so-called zero-shear and infinite-shear viscosities) are symbolised by η_0 and η_∞ . It is also worth noting that the following viscosity-related quantities are often quoted (with the appropriate symbols and units)

- the viscosity of the solvent or continuous phase, η_s , Pa.s;
- dimensionless relative viscosity, η_r , which is the ratio of the viscosity of a suspension to its continuous phase viscosity, η/η_s ;
- the dimensionless specific viscosity, η_{sp} , given by $\eta_r - 1$;
- the intrinsic viscosity, $[\eta]$ (with dimensions $\text{m}^3 \cdot \text{kg}^{-1}$) which is the specific viscosity divided by the concentration c of a dispersed phase, $(\eta_r - 1)/c$;
- the kinematic viscosity, $\nu = \eta/\rho$ which in pre-SI days had the dimensions of centi-Stokes, cS, for thin liquids, with water at 20 °C $\sim 1 \text{ cS}$.

Note: (i) in the engineering literature, the viscosity is often represented by the Greek letter mu, μ , and
(ii) the word '*non-Newtonian*' is often spelt incorrectly – the prefix has a lower case '*n*' and the word is hyphenated.

5.3 Viscosity of common Newtonian liquids

Many liquids display Newtonian behaviour under a wide range of shear rates, and many more show this behaviour within limited ranges. If we limit ourselves to 'everyday' shear rates, then the liquids in table 1 show Newtonian behaviour and encompass a large range of viscosities, best shown—like the race distances of chapter 3—on a logarithmic basis.

Liquid or gas	Approx. viscosity in Pa.s
Hydrogen	10^{-5}
Air	2×10^{-5}
Petrol	3×10^{-4}
Water	10^{-3}
Lubricating oil	10^{-1}
Glycerol	10^0 (i.e.1)
Corn syrup	10^3
Bitumen	10^9

Table 1: Approximate viscosities of some common Newtonian fluids.

Exercise: estimate the approximate viscosities of the following Newtonian liquids
- wine, baby oil, liquid honey.

It should be noted that even the international standard for the viscosity of water (1.002 at 20 °C) is only quoted to an accuracy of $\pm 0.25\%$. Commercially

available standard-viscosity liquids of the highest quality vary in the uncertainty to which they quote the viscosity: this ranges from (a very optimistic) 0.2% for 5 mPa.s, through 0.28% for 0.5 mPa.s to 1% for 500 Pa.s (ISO 9002). Cheaper variants will only quote viscosities to an accuracy of a few percent. Everyday measurements of viscosity cannot with much confidence be quoted as better than $\pm 5\%$.

5.4 The variation of Newtonian viscosity with temperature

The viscosity of all simple liquids decreases with increase in temperature because of the increasing Brownian motion of their constituent molecules, and generally the higher the viscosity, the greater is the rate of decrease. For instance, while the viscosity of water reduces by about 3% per degree Celsius at room temperature; motor oils decrease by about 5% per degree, while bitumens decrease by 15% or more per degree. Many attempts have been made to describe the viscosity/temperature dependence mathematically, so that by 1951 Partington had listed nearly 50 [1]. The most widely-used expression is that due to Andrade [2]

$$\log_{10} \eta = A + B/T$$

where T is the temperature in degrees absolute ($^{\circ}\text{C} + 273.15$), i.e. K. Note that this equation is also known by other names [3], for instance the Arrhenius law where B is replaced by E/R where E is an activation energy for viscous flow and R is the universal gas constant. The activation energy E is said to be a measure of the height of a potential energy barrier associated with the force needed to produce elemental quantum steps in the movement of molecules. In terms of what we said above—*that the viscosity decreases more with increase in temperature if the viscosity is higher (see [4] figure 2.1)*—we see that in the Andrade equation this implies that B increases with increase in A , and this is shown for instance in figure 1 for a collection of 132 single-phase, organic liquids [5].

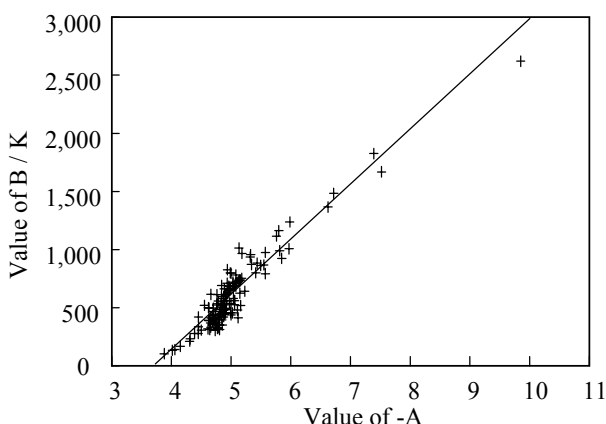


Figure 1: The values of A and B in the Andrade viscosity/temperature equation for a range of organic liquids.

As we see, a typical liquid has $A \sim -4.8$ and $B \sim 500$ K; this means a viscosity of around 0.8 mPa.s at room temperature (20°C) has a temperature variation of viscosity of -1.34% per degree Celsius. A liquid with a higher viscosity might have say $A = -10$ and $B = 3000$ K, which would give a room-temperature viscosity of around 1.7 Pa.s, and a viscosity-temperature sensitivity of $-7.84\%/\text{ }^{\circ}\text{C}$. On the other hand, a lower-viscosity liquid fitting this equation might have $A = -3.8$ and $B = 100$

K; this would give a viscosity of 0.35 mPa.s (similar to petroleum) and a temperature sensitivity of only around - 0.27% / °C. In a severe winter diesel oil is said to freeze, thus causing severe problems for transportation. In fact, all that happens is that the viscosity increases to levels where the pumps cannot operate, thus stopping the flow.

Water over the range 0 - 100 °C fits a slightly modified form of the Andrade law, viz. $\log_{10} \eta = A + B/(C - T)$, with $A = - 4.5318$, $B = - 220.57$ K and $C = 149.39$ K, and at room temperature water changes viscosity at a rate of - 2.54% per degree Celsius, [5]. This means that to perform reasonably reproducible experiments on water-based liquids, we should be careful to control the experiment to within ± 1 °C.

5.5 The effect of pressure on viscosity

The effect of pressure on viscosity is such that as the pressure goes up, the viscosity increases; however the amount is quite small for the situations normally encountered in everyday life. A useful rule-of-thumb is to remember that for most single-phase, organic liquids,

(a) on average the viscosity approximately *doubles* when the pressure is increased from atmospheric pressure to 100 MPa (1000 bar or atmospheres) and

(b) the increase is nearly linear with pressure up to that level [6], but the dependence is greater than linear above that level, so that at around 200 MPa the viscosity might increase tenfold, and at 400 MPa might be 100-fold etc., with the precise values depending on the particular liquid being considered.

One important exception to the insignificance of pressure on the viscosity of everyday materials is the very large increase in pressure and hence viscosity in the contacts between intermeshing gears in car engines, etc. The pressures in this situation are enormous during the very short times at the points of contact, and the viscosity of oil then becomes as high as that of bitumen at normal pressure. To be precise, at 10,000 bar, the viscosity of an oil could easily be 10^7 times greater than its original value! It should also be remembered that in injection moulding of plastics, the pressure can rise to 1000 bar. Then the viscosity of the melt can increase by a factor of 10 - 100 depending on the molecular weight of the polymer.

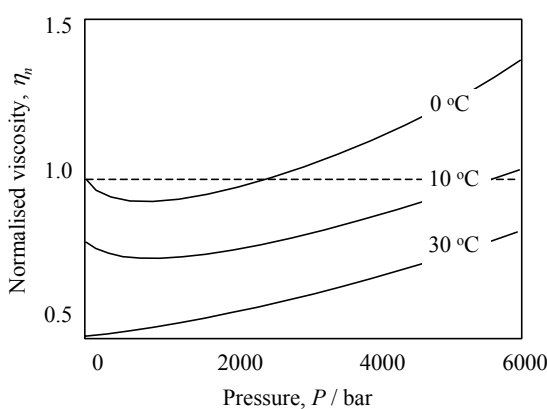


Figure 2: The viscosity of water normalised to the value at 0 °C and atmospheric pressure as a function of pressure.

Water is one major anomaly with respect to the normal viscosity/pressure rule, in that its viscosity—at least from 0 °C to around 30 °C—first *decreases* with increase in pressure, and only increases in viscosity at very high pressures, i.e. well above 100 MPa (1000 bar or atmospheres). Figure 2 shows these points graphically: this kind of dependence is also true for most water-based liquids.

5.6 The everyday perception of Newtonian viscosity

How does an average person judge viscosity without a viscometer? Although an expert can be trained to judge the viscosity of a Newtonian liquid quite accurately and thereafter give a reasonable estimate at its quantitative value, the same is not true for an untrained person. The normal perception of the level of viscosity of Newtonian liquids by such an untrained person is described by Stevens' general power-law of psycho-physical cognition [7], which for viscosity states that the estimates are approximately proportional to the *square root* of the real numerical value. Hence, if the viscosity of a 10 mPa.s Newtonian liquid was assigned unit value, the perceived viscosity of a 1000 mPa.s liquid when compared with the lower viscosity liquid would be seen as roughly 10 times higher, and similarly, a 10^6 Pa.s liquid would be estimated as about 100 times more viscous. This should always be borne in mind by those who are trying to produce a product with a particular viscosity. If the potential consumer of the liquid product cannot differentiate to a precise degree, then extensive efforts to adjust the viscosity to an exact value are wasted.

5.7 The limit of Newtonian behaviour

At a high-enough shear rate, all liquids become non-Newtonian, but the liquids we have been considering so far only do so at very high values of shear rate. For instance, the values of the critical shear rates for glycerol and mineral oils are above 10^5 s $^{-1}$. The viscosity of a set of typical silicone oils is shown as a function of shear rate in figure 3: these oils, which are often used as Newtonian standards, become non-Newtonian at lower and lower values of shear rate as their molecular weight—and hence general viscosity level—is increased.

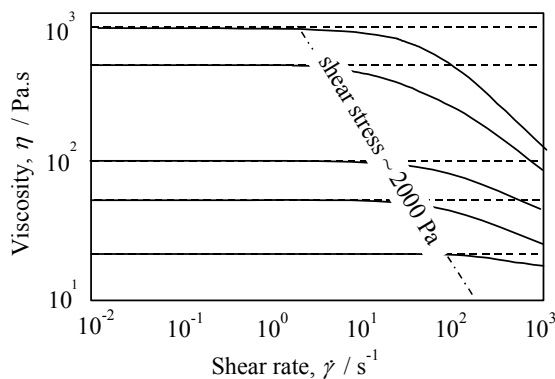


Figure 3: Flow curves for a series of silicone oils.
Note the onset of non-Newtonian behaviour
at a shear stress of around 2000 Pa.

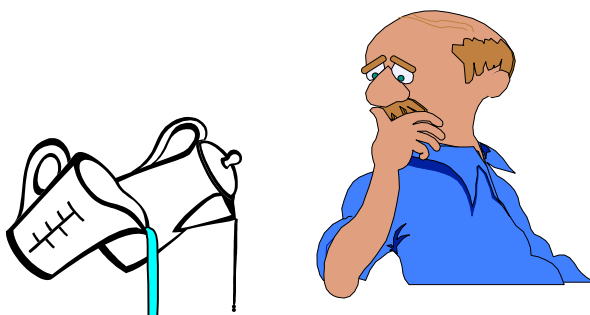
It has even been estimated that pentane becomes non-Newtonian above shear rates of 5×10^6 s $^{-1}$, while water would have to be sheared at an impossible 10^{12} s $^{-1}$ in order to see any non-Newtonian behaviour!

Exercise: Ask a number of untrained people to estimate how much thicker the following liquids are than water (the approximate value of the real difference is shown in brackets),

- a motor oil, SAE 10W (~ 100)
- washing-up liquid (~ 300)
- glycerol ($\sim 1,500$)
- liquid honey ($\sim 10,000$)

References

- [1] Partington, J.E., 'An Advanced Treatise on Physical Chemistry', Vol. 2: *The properties of liquids*', Longmans, Green & Co., London, 1951.
- [2] E.N. da C Andrade, Phil. Mag. 17, 497 & 698, 1934.
- [3] Scott Blair, G. W., 'A Survey of General and Applied Rheology', Pitman & Sons, London, 2nd edition, 1949, p. 33
- [4] Barnes, H A; Hutton, J F; Walters, K, 'An Introduction to Rheology', Elsevier, Amsterdam 1989.
- [5] D.S. Viswanath; Natarajan, G., "Data Book on the Viscosity of Liquids, Hemisphere, New York, 1989.
- [6] Hatschek, E., 'The Viscosity of Liquids', G. Bell and Sons, London, 1928, pp. 84 - 86.
- [7] Stevens, S.S; Guirao, M, Science, 144, 1157 - 8, 1964.



CHAPTER 6: SOME EQUATIONS FOR THE FLOW OF NEWTONIAN LIQUIDS

'Look at it this way Steve—every equation will halve your sales!', Stephen Hawking's publisher

6.1 Introduction

In this chapter we will look at a number of situations where, if we know the (Newtonian) viscosity of a liquid, we are able to predict something about its flow in certain simple geometries. First we will look at flows where the viscosity alone is important, and then we will see what happens when we have to take the liquid's density into account, so that secondary flows and eventually turbulence are seen in high-speed flows. Lastly, we will consider some flow situations where surface tension as well as viscosity is important. Learning to use these equations is a very useful precursor to looking at non-Newtonian equations. They can also be used to obtain an order of magnitude estimate of many complicated flow situations.

Important: One of the greatest difficulties for beginners is to realise that consistent units must be inserted into equations, and here we adhere to the SI system, see Chapter 2, where all parameters are reduced to a seconds, meters and kilograms basis.

6.2 Flow in rotational viscometers

The simplest possible flows are those where the shear rate is more or less the same everywhere in the flowing liquid. These flows are in fact the ideal geometries for viscometers for *non-Newtonian* liquids, where we want to measure the shear viscosity at a given shear rate or shear stress.

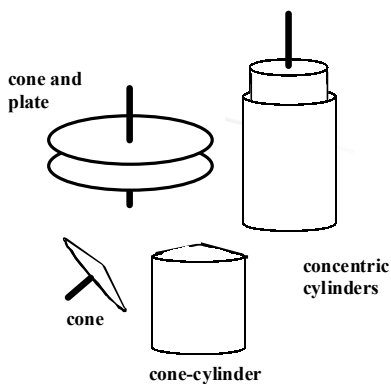


Figure 1: Viscometer geometries where the shear rate is approximately the same everywhere.

Two of this class of flows will now be considered. The first is circular flow between closely-fitting, narrow-gap concentric cylinders, and the second is circular flow in a small-angle, cone-and-plate geometry, see figure 1. Also shown is the cone-cylinder or Mooney geometry where the shear rates in the concentric-cylinder and the cone-and-plate parts of the geometry are arranged to be the same.

6.2.1 Narrow-gap concentric-cylinder geometry

If both cylinders have a large radius, and the gap between them is small, then the shear rate is the almost the same everywhere in the liquid-filled gap. If the inner cylinder radius is a_1 , and an outer cylinder radius is a_2 , then if the inner cylinder is stationary and the outer is rotated, the shear rate $\dot{\gamma}$ in the contained liquid is given by

$$\dot{\gamma} = \frac{a_2 \omega}{a_2 - a_1}$$

where ω is the rotation rate of the outer cylinder in radians per second, (ω is also equal to $2\pi f$, where f is the rotation rate in hertz, i.e. revolutions per second).

The shear stress σ is given by the force per unit area on the inner cylinder. If the torque on the inner cylinder is T (otherwise known as the couple or moment, with units of N.m), the turning force F on the inner cylinder is given by T/a_1 . Since the surface area over which the force F acts is $2\pi a_1 H$, where H is the cylinder height, the shear stress σ is given by

$$\sigma = \frac{T}{2\pi a_1^2 H}.$$

If we insert this geometry into a suitable instrument, we have a viscometer! We can then either apply a torque T to the inner cylinder and measure the rotation rate ω (the *controlled-stress mode*), or else apply a rotation rate ω to the outer cylinder and measure the resulting torque T on the inner cylinder (the *controlled-strain mode*). This geometry forms the basis of an important viscometer geometry, but the simple formula only works for *small* gaps, where a_1 is only a few per cent different from a_2 . A suitable formula for wider gaps will be considered later, because many liquids with large suspended particles cannot be placed in very small gaps.

6.2.2 Small-angle cone-and-plate geometry

The second simple geometry we will consider is flow in a rotating cone-and-plate (or cone-and-cone) geometry. The velocity at any point on the rotating surface (either the cone or the plate) is given by $r\omega$ where r is the distance from the centre of rotation and again ω is the rotation rate. If the cone angle is small (less than 4°), then the distance between the cone and plate at this point is given by $r\phi$, where ϕ is the angle between the cone and plate in radians (remember 2π radians = 360°). Thus the shear rate is now given by $r\omega/r\phi$ or simply ω/ϕ . Since this quantity is the same everywhere in the liquid, it follows that the shear rate is also the same everywhere. In the same way as described above, we can now write down the shear stress σ as $3T/2\pi a^3$, where a is the radius of the plate. Thus we have our second geometry to place into our suitable apparatus, and we can apply rotation and measure torque or

vice versa to either the cone or the plate. For practical reasons, the cone is usually placed on the top, since it is easier to load a liquid sample onto a flat plate.

To help locate the cone relative to the plate, and to reduce wear, the cone is usually truncated to remove the tip to the extent of a few tens of microns. This makes no practical difference to the results, but does allow the use of liquids with small suspended particles.

6.3 Flow in straight circular pipes

A pipe or a tube is a useful geometry for viscometers, but the study of flow in this geometry is also of great importance in many industrial applications. Below we will examine a number of important aspects of the subject.

6.3.1 Velocity profile and pressure drop in fully developed laminar flow through a tube

We will consider first the laminar flow of a Newtonian liquid in a straight circular pipe—radius a , length L —well away from its entrance and exit. The flow rate is Q and the pressure drop down the pipe is P . If we were able to visualise the velocity of the fluid, we would find that it has a parabolic profile, with a value at any radius $u(r)$ given by

$$u(r) = \frac{P}{4\eta L} (a^2 - r^2).$$

This implies that the shear rate—the velocity *gradient*—varies linearly in the tube from a maximum at the wall, $\dot{\gamma}_w$, to zero at the centre. This in turn shows that the shear stress in the liquid also varies linearly from a maximum at the wall σ_w ($= Pa/2L$) to zero in the middle of the tube, see figure 2.

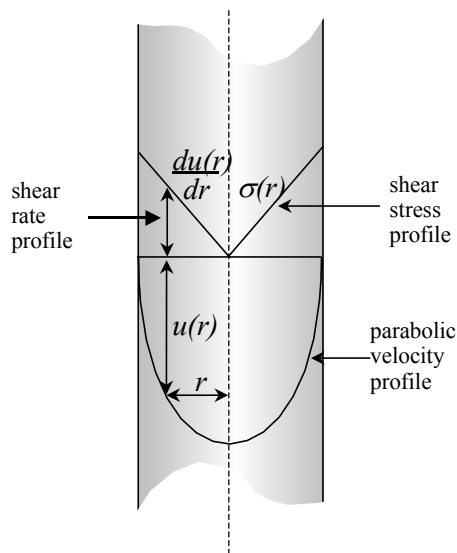


Figure 2: The physical parameters relating to flow in a tube: flow rate Q , pressure drop P along the pipe of length L and radius a .

This situation might seem paradoxical, in that the velocity is a *maximum* in the middle of the tube, but the shear rate is zero, whereas the velocity is zero at the wall and the shear rate is a *maximum* at the wall! If we follow a particle of liquid, then the time it takes to move through the tube is a minimum at the centre and if it is right at the wall, its velocity is zero, and theoretically it never gets through the tube!

These equations are based on the simple premise that there is no slip at the wall. This concept is very important, and is true for most of the liquids that we will consider here. However it is possible for very viscous materials such as polymer melts to lose adhesion and rip away from the wall when they flow very quickly, but this is the rare exception and certainly not the rule.

The overall equation governing laminar flow in a long pipe ($L/a > 100$) is

$$P = \frac{8Q\eta L}{\pi a^4}$$

where P is the pressure drop in pascals

Q is the flow-rate in cubic metres per second

L is the length of the pipe in metres

a is the radius of the pipe in metres

η is the viscosity of the liquid in pascal seconds.

Remember:

$$10^5 \text{ Pa} = 1 \text{ Bar} = 14.7 \text{ psi}$$

$$1 \text{ m}^3/\text{s} = 1000 \text{ L/s} = 15,852 \text{ US gal/min}$$

$$1 \text{ Pa.s} = 1000 \text{ cP.}$$

This equation works for flows with Reynolds number (the ratio of inertial force to viscous force), R_e – which is given by $2Q\rho/a\pi\eta$ – to around about 2300, and above this value the flow becomes turbulent, see below.

Another way of writing the equation for flow in a tube is given by:

$$\eta = \frac{\sigma_w}{\dot{\gamma}_w} = \frac{Pa/2L}{4Q/\pi a^3}$$

where we show the values of the wall shear stress $Pa/2L$ and the wall shear rate $4Q/\pi a^3$ being divided to give the viscosity. This equation forms the basis of using the tube as a viscometer. The wall shear stress is always given by $Pa/2L$, irrespective of the rheology of the liquid, but the value of the shear rate $4Q/\pi a^3$ does depend on the rheology, and has to be suitably modified for non-Newtonian liquids [1].

6.3.2 Flow from large reservoirs into small tubes

The entry pressure drop P_e generated when a Newtonian liquid flows very slowly (i.e. in ‘creeping flow’ where $R_e < 1$) from a large radius reservoir into a smaller tube is (approximately) given by

$$P_e = \frac{0.6Pa}{L}$$

where Pa/L is twice the wall shear stress σ_w produced by the flow well inside in the small tube. At the same time, the entry length L_e within the small tube needed to achieve a near steady-state velocity profile in creeping flow is given approximately by

$$\frac{L_e}{a} = 0.5 .$$

This means that under these circumstances, the velocity profile goes from an almost flat shape at the entrance to a fully developed parabolic profile within half a tube radius.

The volume of liquid V which flows out under its own weight in time t through a *vertical* tube of radius a from a wide reservoir is given by [2]

$$V = \frac{\pi a^4 t g \rho (h_1 - h_2)}{8 \eta L \ln\left(\frac{h_1}{h_2}\right)}$$

where h_1 and h_2 are any two heights in the wide reservoir. This may be rewritten as the efflux time T needed to drain a tank (but not the pipe below) as

$$T = \frac{8 \eta L R^2}{\rho g a^4} \ln\left[1 + \frac{H}{L}\right]$$

where H and L are now the height of the wide reservoir and the length of the pipe respectively, and R is the radius of the reservoir.

6.3.3 Filling a tube with constant suction

The distance l that is filled when a suction of P is applied for time t to a tube of radius a in contact with a liquid of viscosity η is given by [3]

$$l = \sqrt{\frac{P t a^2}{4 \eta}} .$$

6.3.4 Tube emptying under a constant pressure

The length of the liquid column l left when a liquid is blown from a tube of length L at constant pressure P is given by [3]

$$l = \sqrt{L^2 - \frac{P t a^2}{4 \eta}} .$$

6.3.5 Flow through a packed bed of spheres in a tube

The pressure drop P across a well-packed bed of small particles in a tube of diameter d , with a packing phase-volume $\varphi (= 1 - \varepsilon$, where ε is the porosity), a bed length L , for an average velocity v ($= 4Q/\pi d^2$) is given by the well-known Kozeny-Carman equation

$$P = \frac{180vL\eta}{d^2} \cdot \frac{(1 - \varepsilon)^2}{\varepsilon^3}.$$

For this equation to apply without taking the tube walls into account, the ratio of tube radius to that of the particle radius should be greater than 30. In some cases found in the flow of dispersions, it is easier for the liquid to flow through the particles than it is for the particles to flow with the liquid, and this equation then applies.

6.4 Spheres falling in Newtonian liquids

6.4.1 An isolated falling sphere

The movement of an isolated single solid sphere under the influence of gravity in a liquid is described by Stokes' law

$$V = \frac{2\Delta\rho g a^2}{9\eta}$$

where a is the radius of the sphere,

$\Delta\rho$ is the density difference between the spheres and the liquid,

η is the viscosity of the liquid, and

g is the acceleration due to gravity.

If the moving sphere is itself a liquid, immiscible with the liquid through which it is moving, then the velocity is given by the expression above multiplied by $\frac{3(\kappa + 1)}{(3\kappa + 1)}$

where κ is the viscosity ratio between the internal and external phases. Thus if the viscosity ratio is very large, we revert to Stokes law, but if it is very small, the velocity increases by 50%. For a gas bubble, the viscosity and density of the bubble may be taken as zero, so κ is zero, and the rise velocity is then given by $a^2g\rho/3\eta$ where ρ is the density of the liquid.

If the sphere is falling in a tube of radius R , it slows down relative to the Stokes velocity, and an approximate correction factor for the amount of retardation is given by $(1 - 2.1R/r [1 - (R/r)^2])$ for $R/r < 0.32$.

6.4.2 A falling/rising cloud of spheres

A cloud of solid spheres moving in a Newtonian liquid under the influence of gravity travels with a velocity of [4]

$$V = \frac{2\Delta\rho g a^2}{9\eta} (1 - \varphi)^{5 \pm 0.25}$$

where φ is the phase volume of the spheres.

The precise value of the exponent depends on the particle size, being about 4.75 for particles bigger than a micron, and about 5.25 for submicron particles, see later under §15.13.

6.4.3 A sphere rolling down an inclined tube

The viscosity η of a liquid can be calculated when a sphere of radius a rolls at a velocity V down a tube of radius R filled with viscous liquid from the expression

$$\eta = \frac{4a^2 \Delta \rho g \sin \theta}{15V} \left(\frac{R-a}{R} \right)^{5/2}$$

where θ is the angle the tube subtends to the horizontal and $\Delta\rho$ is the density difference between the sphere and the liquid.

When the sphere is small compared to the size of the tube, the formula simplifies to

$$\eta = \frac{\Delta \rho g a^2 \sin \theta}{V} .$$

These equations can be used for the rolling ball viscometer [2], see figure 3.

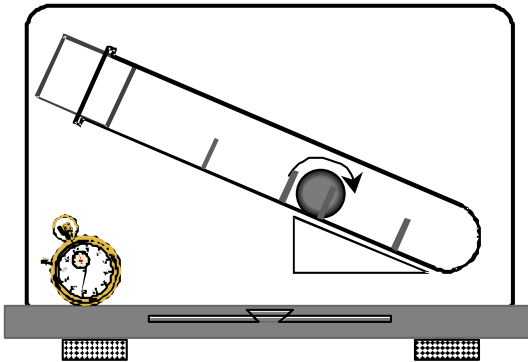


Figure 3: The rolling ball viscometer.

6.5 Other important flows

6.5.1 Drainage down a wall

A liquid that was originally a layer of constant thickness on a vertical wall eventually forms a parabolic wedge shape and the thickness h_x as a function of the distance x from top of the liquid sample is given by

$$h_x = \sqrt{\frac{x\eta}{gt\rho}} .$$

The maximum shear stress in this situation—whether for Newtonian or non-Newtonian liquids—is at the wall, and is given by $\sigma_w = \rho gh$ when the wall is vertical, and the expression is multiplied by $\cos\theta$ if the wall is at an angle θ with the vertical.

6.5.2 Flow along a slot

The pressure drop P for laminar flow along a long slot is given by

$$P = \frac{Q\eta Lr}{bh^3}$$

where b is the width and h the height. The value of r depends on the h/b ratio, so for $h/b = 1$ it is 28.6; for 2 it is 17.5, for 3 it is 15.3; for 4 it is 14.2; for 5 it is 13.7; for 10 it is 12.8 and for infinity it is 12.

6.5.3 Flow through an annulus

The volumetric flow rate Q for laminar flow through an annulus of length L with outer and inner diameters D and d is given by [2]

$$Q = \frac{\pi P}{8\eta L} \left[D^4 - d^4 - \frac{(D^2 - d^2)^2}{\ln \frac{D}{d}} \right].$$

It can be shown that for a very narrow annular gap $d \rightarrow D$ in the annulus this equation reduces to the wide-slot formula above.

6.5.4 A rod being pushed into a cup filled with liquid

The viscosity η of a very viscous liquid such as glucose syrup can be calculated from the force F needed to push a rod of radius a_1 centrally into a cup of radius a_2 at a velocity V as

$$\eta = \frac{F}{2\pi LV} \left[\frac{\beta^2 - 1}{\beta^2 + 1} \right] (\ln \beta - 1)$$

where L is the depth of the rod (well away from the bottom of the cup) and β is the ratio of cup inner to rod outer diameters. This equation applies to the piston viscometer used in on-line viscosity measurement. For a thin rod falling under its own weight in a large cup under its own weight, the expression simplifies to

$$\eta = \frac{\delta\rho g a_2^2}{2V} \left[1 + \ln \left(\frac{a_1}{a_2} \right) \right]$$

where $\delta\rho$ is the density difference between the rod and the liquid. The wall shear stress in that case is given by $\delta\rho g a_2^2/a_1$.

6.5.5 Flow between squeezed circular discs

The rate of change of the separation h with respect to time t is given by

$$\frac{dh}{dt} = \frac{2Fh^3}{3\pi\eta a^4}$$

where F is the force, a the disc radius and η the liquid viscosity, see figure 4. This can be integrated up from any position to another [2].

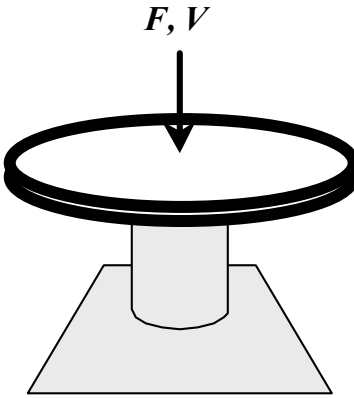


Figure 4 : The parallel-plate plastometer

Where a given volume of liquid is used, initial radius R_o , and height h_o , then if it keeps within the plates,

$$F = \frac{3\pi\eta VR_o^4 h_o^2}{h^5} .$$

6.5.6 One tube moving inside another with the space between filled with a liquid

The force F needed to push the inner tube length L through the outer cylinder with velocity V with a liquid viscosity η is given by

$$F = \frac{2\pi LV \eta}{\ln(\frac{a_2}{a_1})}$$

where L is the length of the liquid band and a_2 and a_1 are outer and inner the radii respectively. This is a simple viscometer for very viscous materials.

6.5.7 An angled plate moving across a trapped liquid

If a plate of length l and inlet and outlet heights defined by $h = h_o(1 + kx/l)$, then the upward lift force, F_l is [5]

$$F_l = \frac{6\eta VBl^2}{k^2 h_o^2} \left[\ln(1+k) - \frac{2k}{2+k} \right],$$

and the drag force, F_d is

$$F_d = \frac{\eta VBl^2}{kh_o} \left[4\ln(1+k) - \frac{6k}{2+k} \right]$$

where B is the breadth of the plate, see figure 5.

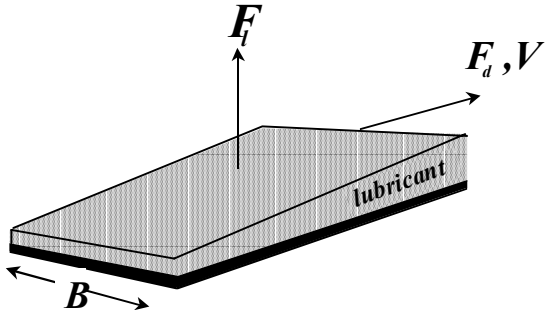


Figure 5: The angled-plate lubrication geometry.

It is easy to show that the thrust force maximises at around $k \sim 1.2$, and then

$$F_{\max} \approx \frac{\eta Vl^2 B}{6h_o^2} .$$

This simple equation gives us the basis of lubrication, where an angled surface is forced away from another with a viscous force generated inside the lubrication layer.

6.5.8 A cylindrical indenter being pressed into a very viscous liquid

The viscosity of a very viscous material such as asphalt may be conveniently measured using a small flat cylindrical indenter. If the radius is a , the velocity V and the force F in pascals, then the viscosity is simply given by

$$\eta = \frac{W}{8Va} .$$

6.5.9 A rotating disc in a sea of liquid

The couple C on a thin rotating disc of radius a immersed in a sea of liquid is given by

$$C = \frac{32}{3} a^3 \omega \eta$$

where ω is the rotation rate in rad/s, and η is the viscosity of the liquid. This forms the basis of the simple Brookfield viscometer often used to measure an equivalent Newtonian viscosity of non-Newtonian liquids.

6.6 Interaction between viscosity and density in flows

The energy needed to accelerate liquids in flow situations can have a marked effect. This energy compared with the energy needed to overcome viscous forces can be substantial, and the relative effects can be judged in different situations via an appropriate Reynolds' number, R_e , which is—as we have seen above—the ratio of inertial to viscous forces. In all such situations, the inertial force is proportional to the density of the liquid.

6.6.1 Flow at the entrance of tubes

The entry pressure drop P_e when a Newtonian liquid flows *quickly* from a large reservoir into the tube is given approximately by [6]

$$P_e = \frac{0.6Pa}{L} \left(1 + \frac{0.1167Q\rho}{a\pi\eta}\right).$$

The entry length L_e to achieve a near steady-state velocity profile in laminar flow where inertia is important is given approximately by

$$\frac{L_e}{a} = 0.5 + \frac{0.225Q\rho}{a\pi\eta}.$$

The velocity profile is dictated by a boundary layer that moves out from the wall as illustrated in figure 6. The form of the equation governing this velocity-profile development means that just below turbulent flow at a Reynolds number of say 2300, a length of 138 diameters is needed to achieve fully-developed flow. (However for turbulent flow—see next section—lengths are much shorter because the relationship is given by $L/d = 4.4 R_e^{0.167}$, so that just above the transition to turbulence, we only need 16 diameters to obtain fully developed flow [7].)

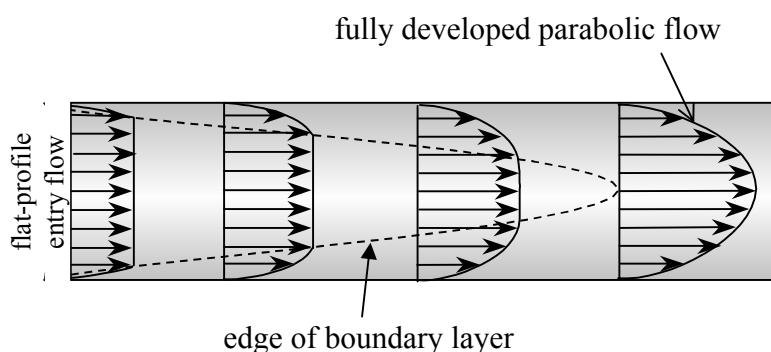


Figure 6: The developing velocity profile in laminar flow.

6.6.2 Turbulent flow in tubes

There is nothing ‘as unstable as water’, Gen. 49. 4, and as soon as we have any reasonable flow rate in a pipe for water-like liquids, the flow becomes turbulent and elements of fluid undergo local chaotic movement because inertial-driven instabilities can no longer be damped out by viscosity. In this situation the following equations are useful. For Reynolds numbers, R_e , from around 2300 up to 60,000, the pressure drop down the tube is given by [8]

$$P = \frac{0.008\rho L Q^2}{a^5} \cdot R_e^{-\frac{1}{4}},$$

which can be rewritten as

$$\sigma_w = 0.04\rho V^2 R_e^{-\frac{1}{4}}$$

where $\sigma_w = Pa/2L$, the wall shear stress, see above. The often-quoted friction factor ($f = 8\sigma_w/\rho V^2$) is

$$f = \frac{0.3164}{R_e^{\frac{1}{4}}}.$$

The ratio of the average to the maximum velocity in the flow is

$$\frac{V_{av}}{V_{max}} = \frac{1}{1 + 1.43\sqrt{f}},$$

thus the velocity profile becomes flatter at higher flow rate when f decreases, as [9]

$$V_x = V_{max} \left[1 - \frac{r}{a} \right]^{\frac{1}{4}}.$$

Even though the bulk of the flow is turbulent, there is laminar sublayer at the wall, the thickness of which is given by

$$\delta = \frac{5\sqrt{8}D}{Re\sqrt{f}}.$$

6.6.4 The size of the liquid jet coming out of a tube

If the Reynolds number $R_e (= 2aV_{av}\rho/\eta)$ is less than 16, the eventual diameter of Newtonian jet emerging from tubes swells slightly compared with the tube diameter; at $R_e = 16$ it is the same diameter as the tube and above 16 it contracts to below that value. At very slow flows the swelling amounts to around 12 %, and at very high flow rate the contraction is around 13%.

6.6.5 Stokes flow with inertia

If we used the Stokes equation to calculate the viscosity in a falling-ball viscometer when the Reynolds number is high, the viscosity appears to be too large, and we need to apply a correction to the formula. For small Reynolds numbers up to 2 this is accounted for by a factor of $1/(1 + R_e/16)$, where $R_e = 2\alpha\rho V/\eta$. Figure 7 shows the form of the inertia-driven secondary flows developing behind the sphere in this situation which account for the extra energy in the flow that could be misinterpreted as higher viscosity.

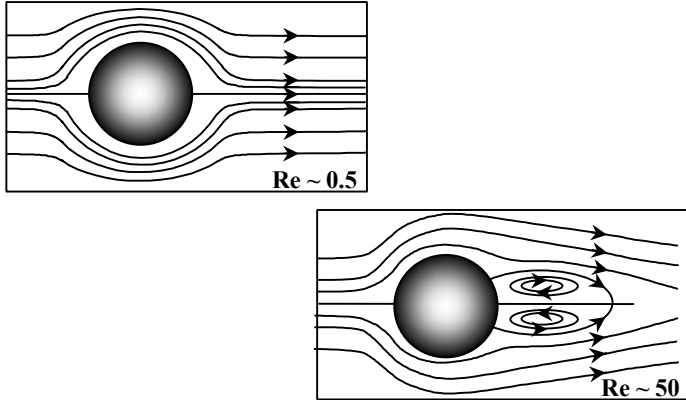


Figure 7: The streamlines around a sphere for very slow and moderate velocities.

6.6.6 Taylor vortices in concentric-cylinder flow

For low-viscosity liquids flowing in concentric cylinders, with the inner cylinder rotating at high velocities, we see the appearance of inertia-driven secondary flow cells called *Taylor vortices*, see figure 8. The onset of these vortices is controlled by the Taylor number which is given by

$$T = 2 \left(\frac{a_1}{a_2} \right)^2 \cdot \frac{\{a_2 - a_1\}^4}{\left\{ 1 - \left(\frac{a_1}{a_2} \right)^2 \right\}} \cdot \left(\frac{\rho\omega}{\eta} \right)^2$$

where a_1 is the inner radius

a_2 is the outer radius

ρ is the density of the liquid

ω is the rotational speed of the inner cylinder in rad/s

($= 2\pi f$ where f is in revs. per second) and

η is the fluid viscosity.

The onset of the vortices is governed by the critical Taylor number, T_c , which for small gaps ($a_1/a_2 > 0.95$) is about 1700, but for larger gaps is given by

$$T_c = 1700 \left(1 + \frac{a_2}{10a_1} \right) \text{ for } \frac{a_2}{a_1} < 1.25 .$$

The cell pattern becomes wavy for a Taylor number 50% greater than the onset value, T_c , and above that value soon becomes turbulent.

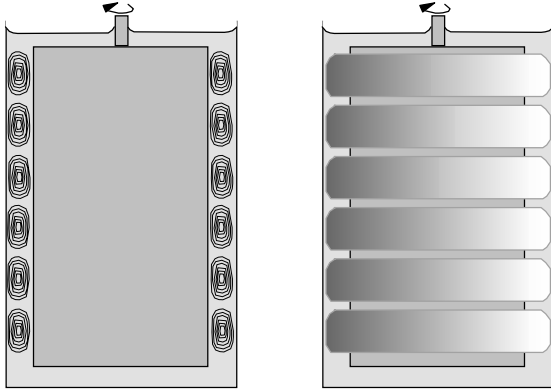


Figure 8: Taylor vortex secondary flow pattern between rotating concentric cylinders.

On the other hand, if in this flow geometry the outer cylinder is rotated and the inner is kept stationary, there is a sharp and catastrophic transition to turbulence (without any Taylor-like secondary flows) at a simple Reynolds number, R_e , of about 15,000, which is given by

$$R_e = \frac{(a_2 - a_1)a_2\omega\rho}{\eta}.$$

These two kinds of inertial-driven behaviour (secondary flow and turbulence) limit the range over which concentric-cylinder viscometers can be used for low-viscosity liquids.

6.7 Some flows where surface tension is important

The following are some examples of flows where there is an interaction between the viscosity and the surface tension ς of Newtonian liquids of viscosity η . In these situations, the relative effect of surface tension may be judged from the so-called Capillary number, $C_a = \eta V / \varsigma$ which is the ratio of viscous to surface tension forces.

6.7.1 Free coating

When pulling a thin sheet out of a Newtonian liquid at velocity V , a good approximation for the final thickness of the liquid coating formed on the sheet h_∞ is given by

$$h_\infty \approx 0.75 \left(\frac{\eta V}{\rho g} \right)^{1/2} \left(\frac{\eta V}{\varsigma} \right)^{0.132},$$

for values of the Capillary number up to 2, see figure 9.

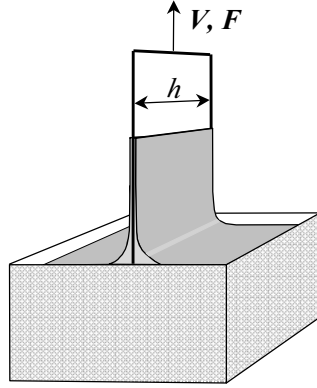


Figure 9: A sheet being pulled out of a liquid.

6.7.2 Levelling of surface undulations

The rate at which the amplitude α of a sinusoidal undulation on the surface of a liquid decreases with time as it is pulled out by surface tension forces is given by [10]

$$\frac{da}{dt} = -\frac{h^3 \sigma a}{3\eta} \cdot \left[\frac{2\pi}{\lambda} \right]^4 \quad (\text{or halflife } t_{1/2} = \eta \lambda^4 / \sigma h^3)$$

where λ is the wavelength of the sinusoidal undulation, see figure 10.

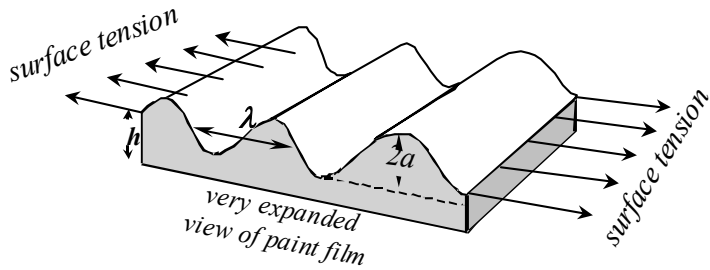


Figure 10: Definition diagram for the levelling of surface undulations on a liquid.

6.7.3 Flow up a capillary tube

The height H that a liquid rises in a capillary tube of radius a , in time t , (compared to the ultimate height H_o) is given by

$$\frac{H}{H_o} = 1 - e^{-\frac{t}{\tau}}$$

where τ is given by $\frac{8\eta H_o}{\rho g a^2}$ and H_o the equilibrium height is given by $\frac{2\zeta \cos \theta}{\rho g a}$, where

θ is the contact angle (this means that the height will decrease for mercury, since $\theta = 140^\circ$).

6.7.4 A large flattened bubble moving up a tube

The approximate thickness of a Newtonian liquid layer trapped at the tube wall by a large flattened bubble moving at a velocity U up/along a tube of radius a is given by

$$\delta = 0.643a\left(\frac{3\eta U}{\zeta}\right)^{\frac{2}{3}}.$$

Exercise: Calculate the rate of seepage of water through a crack 10 micron by 2 mm which is at the bottom of the wall of a dam 2 m thick. The water is 10 m deep, and remember that the pressure at a depth h is $P = \rho gh$, where ρ is the density of water and g the acceleration due to gravity (9.8 m.s^{-2}). Give the answer in litres per day.

References

- [1] Barnes, H A; Hutton, J F; Walters, K, '*An Introduction to Rheology*', Elsevier, Amsterdam 1989.
- [2] Bird R.B; Armstrong R. C; Hassager O, *Dynamics of Polymeric Liquids*, , Volume 1, Fluid Mechanics, 2nd ed., Wiley, 1987
- [3] Scott Blair, G.W, '*A Survey of General and Applied Rheology*', 2nd Edition, Pitman & Sons, London, 1949.
- [4] Barnes, H A, '*Recent advances in rheology and processing of colloidal systems*' Keynote Address in 'The 1992 IChemE Research Event', pp. 24-29, IChemE, Rugby, 1992, ISBN 0 85295 290 2.
- [5] Tanner R.I, '*Engineering Rheology*', Clarendon Press, Oxford, 1985.
- [6] Mujumdar A.S; Mashelkar, R.A, '*Advances in Transport Processes*', Wiley Eastern Ltd., New Delhi, 1982.
- [7] Gupta V; Gupta S.K, '*Fluid Mechanics and its Applications*', Wiley Eastern Ltd., New Delhi, 1984.
- [8] Pao R.H.F, '*Fluid Mechanics*', Charles E. Merrill Books, Columbus, 1967.
- [9] Darby R, '*Chemical Engineering Fluid Mechanics*', Marcel Dekker, New York, 1996.
- [10] Barnes, H A, '*Dispersion Rheology 1980, a survey of industrial problems and academic progress*', 190 pages, Royal Soc. Chem., Industrial Div., London, 1981.

CHAPTER 7: VISCOMETRY

'It is a capital mistake to theorise before one has data', Arthur Conan Doyle

7.1 Introduction

Viscometry is the science of the measurement of viscosity*. Such viscometric measurements generally have to do with applying either a force F or a velocity V at a surface in contact with a contained test liquid. The response of this liquid to either the velocity or the force is measured at that surface or at some other nearby surface which is also in contact with the liquid. Examples of the geometries used for this purpose include tubes, parallel plates, cone-and-plate arrangements, and concentric cylinders. Sometimes artefacts arise whereby the presence of these surfaces interferes with the local liquid microstructure, giving apparent slip effects—these will be discussed in detail later.

The aim of such viscometry is then

- (a) to convert the applied force F to a shear stress σ , and
- (b) to convert the velocity V to a shear rate $\dot{\gamma}$.

This is done using geometric constants, and is evaluated at a standard reference point such as the immediate vicinity of the tube wall or the inner cylinder or the outer edge of the cone and plate, etc. Then, for instance, the calculated shear stress σ and shear rate $\dot{\gamma}$ can be plotted as a function of one another, or else the shear stress can be divided by the shear rate to give the viscosity η .

In simple geometries the shear rate—and hence the shear stress—are the same everywhere in the liquid, and cone-and-plate and narrow-gap concentric-cylinder geometries are examples of this situation used in viscometers, see chapter 6. In some other situations, either the shear rate or the shear stress varies in a known manner independently of the rheology of the test liquid, and this information can be used to reduce the measured data to viscosity/shear-rate or viscosity/shear-stress, however we must make some assumption about the form of the viscosity/shear-rate curve, for example that it approximately obeys a power-law relationship. Examples of this known relationship are found in

- (a) flow in a straight tube, where (see chapter 6) the *shear stress* varies *linearly* from zero at the centre to $Pa/2L$ at the wall,
- (b) flow in the parallel-plate viscometer, where the *shear rate* varies *linearly* from zero at the centre to $a\omega/h$ at the edge of the plates, and
- (c) flow in a wide-gap concentric-cylinder, where the *shear stress* falls off as the *inverse square* of the distance r from the centre of rotation as $T/2H\pi r^2$.

* See APPENDIX for a discussion of on-line (process) viscometry.

Appropriate formulas to deal with these situations will be given at the end of this chapter.

If the measured viscosity η is constant with respect to shear rate, then the liquid is said to be *Newtonian* as described above. However, as is usually the case for structured liquids such as polymer solutions and suspensions, the viscosity *decreases* with increasing shear rate: such liquids are described as *shear thinning*. Occasionally, situations arise where the opposite is true, and the viscosity *increases* with increasing shear rate: these are called shear-thickening liquids, see chapter 15.

7.. Some important things to note about using viscometers

7.2.1 Calibration

While it is possible to calibrate a viscometer from first principles by using weights and pulleys etc., it is more usual to use previously-calibrated standard liquids (mostly oils). These may be purchased from viscometer suppliers, or ordered from laboratory-suppliers' catalogues. They provide calibrated fluids starting (for instance) from 0.29 mPa.s at 25 EC, then in 18 steps that double the viscosity, arriving eventually at 80 Pa.s; a typical cost would be around £66 per pint ($\sim \$US100$ for 0.5 kg). The fluids are NIST-traceable and ISO 9002 registered. The viscosity ranges covered by these standardised liquids should match the ranges of viscosities that are being routinely measured. In most cases, you will find that the calibration is quite near that given by the viscometer manufacturer, and gross differences means that you have a major mechanical or electrical problem.

7.2.2 Artefacts

Small zero errors and zero drift on the meters or on the electrical output of viscometers due to mechanical and electronic changes are found more frequently than actual calibration errors, and zero settings should be checked regularly (at least once a month) by extrapolating low-speed data for standardised liquids.

7.2.3 Wall effects

Difficulties arises in smooth-walled viscometers because placing a structured liquid next to the wall changes the local microstructure [1]. For a simple suspension of smooth spherical particles, the spatial concentration of particles deep in the bulk of the sample, well away from the wall, is random. However, right at the wall, the particle concentration is zero. How do these two points join? The answer is that the concentration rises rapidly as one moves away from the wall; shows a decaying oscillatory behaviour, then it smoothes to the bulk concentration, see figure 1. This whole process from zero to average concentration takes about five particles diameters. The result is that the material near the wall is essentially different from the bulk, however worse than this is the effective lubricating layer near the wall where the particle concentration is first zero, and is small even up to half a particle diameter. The phenomenon of lower concentration next to the wall is called wall depletion, but is popularly known as slip, see chapter 15 section 10 for more details.

The effect is very particle-size dependent, and here particle size for flocculated suspensions means floc size, which is shear-rate dependent. Hence, flocs are biggest at low shear rate, and therefore for flocculated systems where this problem is mostly seen, wall slip is a low shear rate phenomena. There are various

tell-tale features that enable us to see even from superficial results if this effect is present. These are shown in figure 2, where the measured flow curve for a flocculated system is compared with the expected flow curve without slip.

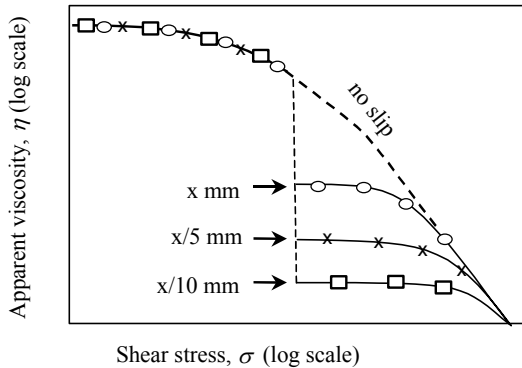


Figure 1: Viscosity versus stress plot for a flocculated suspension showing slip effects, as a function of (hypothetical) concentric-cylinder gap.

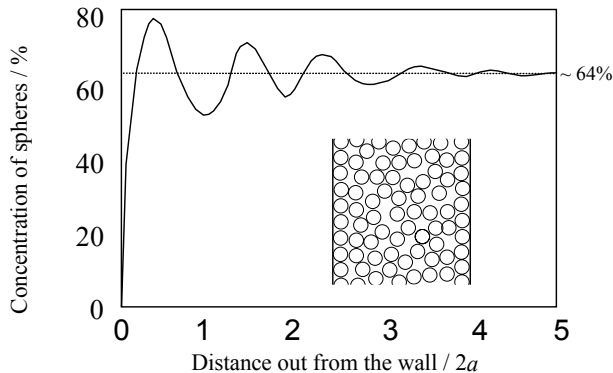


Figure 2 : The local concentration of spheres as a function of distance from the wall, measured in sphere diameters.

How do we eliminate these wall-depletion/slip effects? The answer is to take the viscometer wall motion into the bulk of the liquid, which is done most easily by either roughening or profiling the wall. Sandblasting with a coarse grit should be enough, since this results in approximate 10 - 20 micron surface variations. However, most rheometry manufacturers supply grooved geometries.

There is one wall effect seldom referred to, that is where the sample is fibrous. In this case as well as upsetting the local concentration, a smooth wall upsets the random orientation of the fibres. This too gives a lowering of the local viscosity, since any alignment along the direction of flow makes flow easier. To avoid problems with fibrous suspensions, a vane geometry might be needed. The vane is the ultimate in a profiled wall, and should be supplemented by some roughening of the outer container, or else sliding in a gauze sleeve, see figure 3 and chapter 11.

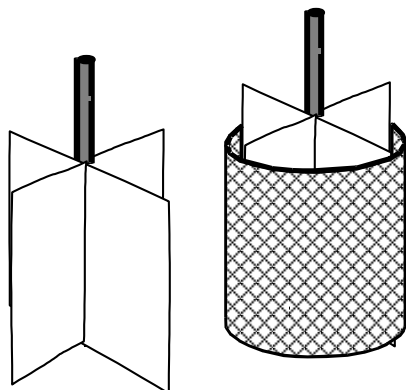


Figure 3 : The vane and the vane-and-basket geometries

7.2.4 Evaporation

Evaporation is often critical in cone-and-plate and parallel-plate geometries, where drying at the edge of the samples leads to large errors in the measured torque, given that the effect is at the greatest distance from the centre. The way around these problems is two-fold: you either create a saturated atmosphere in the air next to the sample, or else you can flood the same area with solvent, see figure 4.

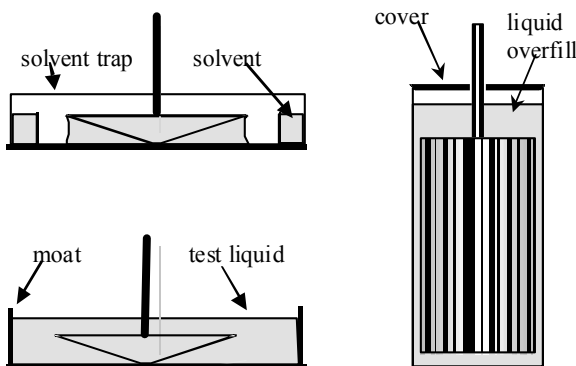


Figure 4 Various ways of overcoming evaporation in viscometers.

7.2.5 Sedimentation/separation

Another problem that can arise with long-term shearing is enhanced sedimentation. Even if the suspension continuous phase has been thickened to slow down sedimentation at rest (as for instance in storage), when the sample is sheared, the continuous phase viscosity is greatly reduced and its ability to keep particles in suspension can be severely impaired. The only answer to this problem is to slowly circulate the suspension, pumping it out of the bottom of the viscometer and returning it to the top. The flow rate should be adjusted so that the average velocity of the liquid down the viscometer gap is small compared with the velocity of the wall, say 5%. This pumping/recirculating arrangement is suitable for naturally unstable suspensions such as coal and mineral slurries in water.

7.2.6 Chemical attack

In some older instruments, chrome-plated brass geometries can be attacked by a number of everyday liquids. Steel and plastic geometries (or even titanium in certain circumstances) are usually recommended, but note the difference between stainless and mild steels, since the latter can produce ions in solution which might alter the viscosity of some aqueous liquids.

7.2.7 Mechanical damage

Accidental bending of spindles can lead to eccentric motion. Although this might still give the correct answer for Newtonian liquids, the high/low shear rate oscillatory flow then encountered in the gap, will give the wrong answer for *non-Newtonian* liquids. Always have a few spare sets of geometries around – dropping a cone or cylinder can ruin a tight measurement schedule!

7.2.8 Sampling

Viscometers usually contain small samples, and these must be representative of large batches of material, so care should be taken in obtaining samples.

7.2.9 High-speed testing

High-speed testing of low-viscosity liquids can lead to secondary flows, as shown for cone-and-plate and concentric-cylinder geometries in figure 5.

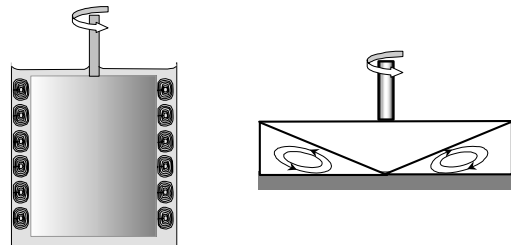


Figure 5: Inertial secondary flow patterns in concentric-cylinder and cone-and-plate geometries.

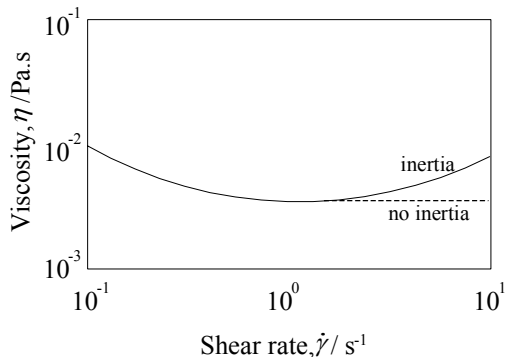


Figure 6: Typical effect of inertia in a concentric-cylinder and cone-and-plate geometry.

Little can be done about this phenomenon, but choosing a different geometry might be helpful. Figure 6 shows the typical effect of high-speed testing using a low-viscosity liquid in a concentric-cylinder geometry, where the extra dissipation that could be mistaken for an increase in viscosity is really due to Taylor vortices.

The resulting increased couple in the inertial case T_i , for a cone-and-plate instrument, compared with that for no inertia T , is given for Newtonian liquids by

$$\frac{T_i}{T} \approx 1 + \frac{6}{10^4} \left(\frac{\rho \omega \theta^2 a^2}{\eta} \right)^2$$

where ρ is the density of the liquid of viscosity η , and a is the cone radius whose angle in radians is θ . From this equation it is easy to see that the correction becomes important when $\frac{\rho\omega\theta^2 a^2}{\eta}$, which is a form of Reynolds number, exceeds 10. This gives a useful guide to the highest shear rates available for testing liquids.

7.2.10 Suspended particles

Suspended particles can lead to two kinds of problem. First, large solid particles can become jammed in narrow parts of certain geometries, such as the cone and plate. However, the cone truncation often used to prevent wear of the tip, often helps. Second, if the viscometer gap is not around five to ten times larger than the largest particles, then the correct viscosity of the material is not being measured, since the particle spatial distribution is being altered by the wall.

7.3 Viscometer design

7.3.1 General considerations

As we have seen, viscometers are instruments that can either apply a force and measure a speed, or apply a speed and measure a force, to or from a simple geometry. This might be as simple as a U-tube viscometer that measures the time taken for a gravity-driven flow to move from one vertical position to another, or a similar situation for flow from the hole at the bottom of a carefully manufactured cup called a flow-cup, see figure 7.

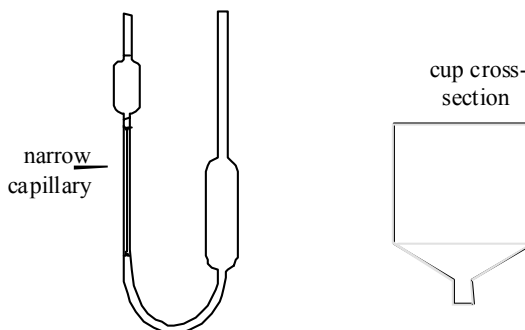


Figure 7 : A schematic diagram of a simple U-tube viscometer and a flow-cup.

In both these situations, the shear stress experienced by the liquid being tested varies

- *in time* as the vertical driving-force reduces;
- *in space* because the flow is quite different at different places, and
- *in kind* because the flow-cup is not a simple shear flow with the liquid being 'squeezed' into the hole as an extensional flow.

These cups are perfectly adequate for Newtonian liquids, once a correction has been made for the effect of fluid density, but because of the variations mentioned, the measurement of viscosity for non-Newtonian liquids becomes impossible. However, if we want to apply a more well-defined situation, such as a fixed shear stress or shear rate everywhere in the liquid, we need more control.

Originally, such controlled viscometers were based on an applied shear stress which was generated by a weights-and-pulleys arrangement, as shown for instance in figure 8.

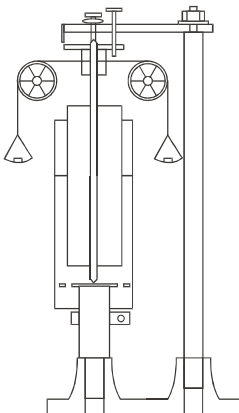


Figure 8: Schematic diagram of the 1912 Searle controlled-stress, concentric-cylinder viscometer (D. Hopkins).

Limitations were soon found with this type of instrument in terms of attaining *low* shear rates—due to bearing friction—as also were the limitations of prolonged shearing at *high* shear rates—the finite length of the string! These methods were then superseded by electrically driven motors and the (what we now call) controlled-strain instruments had arrived, largely replacing the controlled-stress variants. These became more and more sophisticated, and eventually with logarithmic mechanical gear boxes were able to span a shear-rate range typically from $\sim 10^{-4} \text{ s}^{-1}$ to $\sim 10^4 \text{ s}^{-1}$ (e.g. the Weissenberg Rheogoniometer).

7.3.2 Commercial controlled-stress viscometers

In the mid-1970s, a new generation of *controlled-stress* rheometers began to appear, as opposed to the controlled-strain type of viscometer commonly used in laboratories [2]. The first had been developed by Jack Deer and colleagues at the London School of Pharmacy, who used air bearings and an air-driven turbine to provide the torque. It was claimed that ‘with such an instrument the application of a known and controlled stress provides the rheologist with vital information of this critical region in the form of a “CREEP” curve’. These claims could be made because they had introduced a ‘specially designed air bearing ... and an air turbine drive system for the application of torsional stress that is independent of rotational speed ... throughout the operational range’. (Air bearings and air turbines had been and still are used for dentists’ drills, but of course at much higher speeds, hence the whine!) Using a pre-commercial version of the air-turbine rheometer in the creep mode, it was found that the ‘creep’ (i.e. zero shear) viscosity of wool fat BP at 25 °C over a shear rate range of $1.76 - 6.14 \times 10^{-6} \text{ s}^{-1}$ was constant (to within a small experimental error) at $\sim 2 \times 10^6 \text{ Pa.s}$.

Then around 1980, commercial versions of the new generation of electrically driven controlled-stress rheometers began to appear, still based on air bearings that greatly reduced friction, but now using so-called drag-cup electrical motors that allowed controlled stresses to be more easily applied, but still independent of rotational speed. Along with these features came new ways of measuring smaller and smaller rotation and rotation rates. The use of the latest optical-disc technology

now means that rotation rates as low as 10^{-8} rad/s (~ 1 revolution in 20 years!) can be measured. Access to these ultra-low shear-rate regions is now called creep testing, by analogy to the testing of solids under similar low-deformation-rate, long-time conditions; albeit solids creep testing is usually performed in extension rather than in shear.

7.3.3 Evolution of the specifications of controlled-stress viscometers.

Table 1 compares the specifications of some typical controlled-stress viscometers as they have evolved over the last thirty years or so. It is clear that an amazing increase in sensitivity and range has been brought about, especially in the lower-and-lower minimum torques (and thus stresses) and rotation rates (and thus shear rates) achievable.

Date	~ 1970	~ 1978	~ early 1980s	~ late 1980s	~ 1999
Typical instrument	Air Turbine rheometer	Deer Rheometer	Carrimed Mk1	Carrimed CSL 100	TA Inst. AR 1000
Torque (N.m)					
min.	10^{-4}	10^{-5}	10^{-6}	10^{-6}	10^{-7}
max.	10^{-2}	10^{-2}	10^{-2}	10^{-2}	0.1
resolution	10^{-4}	10^{-5}	10^{-7}	10^{-7}	10^{-9}
Ang. veloc. (rad/s)					
min. (creep)	-	-	-	-	10^{-8}
max.	50	50	50	50	100
resolution	-	-	10^{-2}	10^{-4}	-
Creep (strain)					
resolution	2×10^{-2}	2.5×10^{-3}	2.5×10^{-4}	10^{-5}	6.2×10^{-7}
max.	-	-	-	-	1300

Table 1: Some typical commercial controlled-stress rheometer specifications.

7.4 Non-simple viscometer geometries

There are a number of popular viscometer geometries where the shear rate is not the same everywhere. In order to convert the basic experimental data into unambiguous viscosity/shear-rate data, an intermediate calculation step is needed. This uses an assumption about the liquid, usually that at any particular value of shear rate, the *local* viscosity/shear-rate data can be described by a power-law-type behaviour, where the slope of the log/log curve is given by n' . (For true power-law liquids, this is the same as n , the power-law index.) The following are the necessary equations for wide-gap concentric cylinders; the parallel-plate geometry and tubes used as viscometers. In each case the viscosity data is related to a certain shear rate calculated at some fixed point in the geometry, and n' is related to the basic measured parameters.

7.4.1 Wide-gap concentric cylinders

The software provided by some viscometer manufacturers for calculating viscosities in concentric-cylinder geometries only makes use of the narrow-gap approximation (you should check this in your manual). However, this only applies to gaps of at most a few percent of the outer-cylinder radius, and assumes that the shear rate and shear stress are approximately constant throughout the gap. This is not the case in many practical cases, and if for instance the inner cylinder is being rotated, the value of the shear stress decreases as the inverse square of distance from the centre of rotation as one moves away from the inner cylinder.

If non-Newtonian liquids are being measured and the narrow-gap approximation is used, the data from different-sized gaps does not coincide. However, the data can be corrected by the use of a number of lengthy analytical methods. However, a simple correction of the data can be made as follows, using an empirical correction factor worked out by the author, for the viscosity at the inner-cylinder, uncorrected shear rate:

$$\eta = \eta_{ng} [b + n'(1 - b)]$$

where η is the correct viscosity at the inner-cylinder shear rate, η_{ng} is the *calculated* viscosity based on the narrow-gap approximation, n' is the local power-law index at that shear rate at which the viscosity is being evaluated, calculated as $d\log T/d\log \omega$ where T and ω are the torque and rotational speed respectively, and, b is the gap ratio (inner-cylinder radius divided by the outer-cylinder radius). When this formula is used, data for different gap ratios, b , which would have originally appeared as a set of different curves if calculated using the narrow-gap approximation now lie on a single curve. Table 2 shows the viscosity correction factors predicted by our simple equation for a range of possible values of b and n .

Values of b	$n' = 0.8$	$n' = 0.7$	$n' = 0.5$
0.9	0.98	0.97	0.95
0.7	0.94	0.91	0.85
0.5	0.90	0.85	0.75

Table 2: Viscosity correction factors for non-Newtonian liquids measured in wide-gap concentric cylinder viscometers.

Complete equations for the evaluation of the viscosity in the wide-gap situation should be used for *very* shear-thinning liquids (say $n' < 0.3$), i.e.

$$\dot{\gamma} = \frac{2\omega}{n(1 - b^{\frac{2}{n'}})},$$

and

$$\eta = \frac{Cn(1 - b^{\frac{2}{n'}})}{4\pi r_i^2 L \omega}$$

where ω is the rotation rate of the inner cylinder,
 C is the couple on the inner cylinder, and
 r_i is the radius of the inner cylinder of length L .

7.4.2 The rotating parallel-plate viscometer

In a parallel-plate geometry, the upper plate is usually rotated and the couple C is like-wise measured on the upper plate. The shear rate varies from zero at the centre to $a\omega/h$ at the edge of the plates, where a is the plate radius, h the gap and ω the rotation rate in rad/s. The shear rate at the edge is given by

$$\dot{\gamma}_a = \frac{a\omega}{h},$$

and the viscosity (evaluated at the edge shear rate $\dot{\gamma}_a$) is given by

$$\eta = \frac{3Ch}{2\pi a^4 \omega \left(1 + \frac{1}{3} \frac{d \log C}{d \log \omega} \right)}.$$

For a power-law liquid $d \log C / d \log \omega$ is simply n .

7.4.3 Pipe/tube viscometer

Tube or pipe viscometers take many forms, but they should all be able to give the pressure-drop P as a function of flow rate Q for situations where the tube is long enough to be able to neglect entrance and end effects, say $L/a > 50$. In this case we can calculate the viscosity as a function of the wall shear rate, $\dot{\gamma}_w$, which is given by

$$\dot{\gamma}_w = \frac{4Q}{\pi a^3} \left(\frac{3}{4} + \frac{1}{4} \frac{d \log Q}{d \log P} \right).$$

The viscosity η is then given by

$$\eta = \frac{\pi a^4 P}{2QL \left(3 + \frac{d \log Q}{d \log P} \right)}$$

where for power-law liquids, $d \log Q / d \log P$ is simply $1/n$.

References

- [1] Barnes, H A, JNNFM, 56, 221 - 251 (1995).
- [2] Barnes, H A, JNNFM, 81(1&2), 133 - 178 (1999).

CHAPTER 8: YOUR RHEOLOGY LABORATORY

'The ultimate object is to measure something which we have already seen ... to obtain a numerical estimate of some magnitude', James Clark Maxwell

8.1 What's in a good rheology laboratory?

What do you expect to find in a good rheology laboratory? The answer depends very much on the particular field of interest. Here we shall discuss what we would anticipate for a number of industrial situations, but the same would be true for academic studies in the same general area:

<i>Areas of interest</i>	<i>Types of liquid</i>
Personal products and cosmetics	creams, lotions, pastes
Paints, coatings and inks	suspensions
Polymers	solutions, melts
Lubricants	oils, greases
Detergents	suspensions, pastes
Pharmaceuticals	dispersions, lotions, creams
Food and biotechnology	dispersions, emulsions, pastes
Minerals	slurries, suspensions

This is not an exhaustive list (for which see Whorlow's book [1]), but liquids found in any other areas fall somewhere within those examples found in this list.

8.2 Which problem?

Obviously in each area, certain specific items of test equipment will be used, such as small extruders, paint rigs, Stevens texture testers and penetrometers, etc. However, here we are interested in those pieces of *rheological* equipment that we should also find. The following important features are generally measured in rheological studies for typical liquids listed above, with some specific examples:

Product Property	Examples
general 'thickness'	- consumer-perceived flow properties
suspendability	- long-term physical stability
technical attributes	- slow draining
microstructural characteristic	- state of flocculation
Processing	Examples
machineability	- 'fly' or misting in ink or coatings machines
process engineering	- heat transfer, pump specification, mixing efficiency

8.3 Which rheometer?

The following are some general classes of rheometer:

8.3.1 Standard laboratory viscometers,

Standard laboratory viscometers have a shear rate range $\sim 0.1 - 1000 \text{ s}^{-1}$. At the moment these include the

Brookfield DV3
Haake VT7, VT500/550, RV1
Bohlin Visco 88
Rheometrics RM 180, 265
Reologica ViscoCheck
Physica MC1

Typical output: viscosity/shear-rate as a function of time of shearing for the shear rate specified, so that the general flow curve and thixotropy can be studied for a range of temperatures, usually in the range -10 to 100 EC.

8.3.2 Rheometers,

Rheometers available today, and the typical viscoelastic parameter(s) they can measure are shown in table 1.

8.3.3 Elongational viscometers

Rheometric Scientific RME (for polymer melts only)

Typical output: Extensional stress as a function of extensional strain rate/time.

Exercise: Find the Internet websites of the most prominent viscometer and rheometer manufacturers, viz. Brookfield Engineering, Haake, Bohlin, TA Instruments, Reologica Instruments AB, Rheometric Scientific and Physica, start at <http://www.staff.ncl.ac.uk/chris.petrie/links.html>

Exercise: Imagine you are working in the following areas, and discuss the kinds of rheometers you would like to use in setting up a laboratory to study asphalt, blood flow, cosmetics, chocolate.

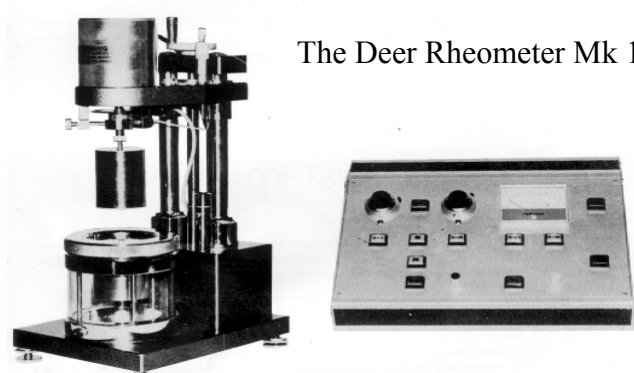
Normal Force (to give N_1)*	Oscillation (to give G' , G'')	Controlled Stress (to give $J(t)$)
Bohlin - CVO 50/120	Bohlin - CS, CVO 50/120, DSR CSR	Bohlin - CS, CVO 50/120, DSR CSR, CVR
-	-	Brookfield - RSCPS
Haake - RT20, RS75/150	Haake - RheoWave 1, RS 75/150	Haake - RS1, RS 75/150
Physica - UDS 200	Physica - DSR 4000 UDS 200	Physica - DSR 4000 UDS 200
Reologica - STRESSTECH/HR	Reologica - STRESSTECH/HR	Reologica - STRESSTECH/HR VISCOTECH
Rheometrics - ARES SR 2000/5000	Rheometrics - SR5/2000/5000 ARES	Rheometrics - SR5/ 2000/5000 ARES (controlled-rate instrument using feed back)
TA(Carri-med) - AR1000N	TA(Carri-med) - AR 1000 CSL ² 500	TA(Carri-med) - AR 1000 CSL ² 500

* some instruments only give a *qualitative* value of normal force - check with manufacturer.

Table 1: Commercial rheometers available today and their available functions.

References

- [1] Whorlow, R.W., 'Rheological Techniques', Second Edition, Ellis Horwood, New York, 1992



The Deer Rheometer Mk 1

CHAPTER 9: SHEAR-THINNING LIQUIDS

'[The viscosity] varies with the speed of shearing', Schwedoff (1890)

9.1 Qualitative features of flow curves

Employing the well-defined viscometers we discussed earlier, *viz.* the small-gap, concentric-cylinder or the cone-and-plate type, we are able to measure directly the viscosity of structured liquids such as polymer solutions, emulsions, dispersions, etc., as a function of either the applied stress or the applied shear rate. When we do this over a wide-enough range of either shear rate or shear stress, we generally see the kind of behaviour shown in figures 1 - 8, when, as described in chapter 4, we plot the results on logarithmic axes.

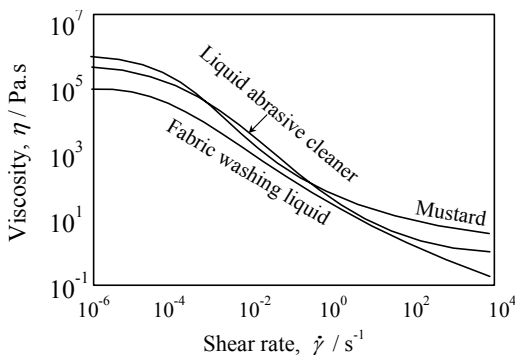


Figure 1: Viscosity/shear-rate curves for various products.

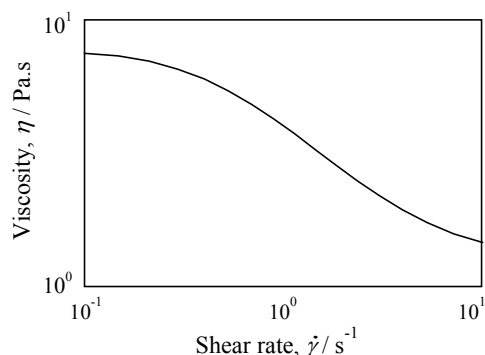


Figure 2: Viscosity/shear-rate curve for a dilute solution of polyacrylamide in glucose syrup.

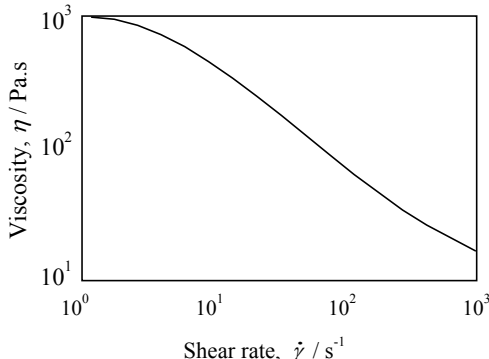


Figure 3: Viscosity/shear-rate curves for a typical printing ink.

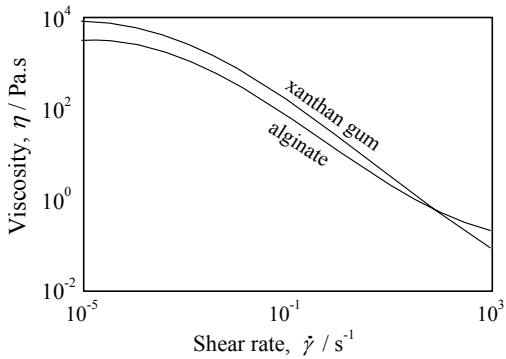


Figure 4: Viscosity/shear-rate curves for 1% aqueous solutions of two natural polymeric thickeners.

At low-enough shear rates or shear stresses, the viscosity is constant (with a value η_0), but at some point it begins to decrease, and usually enters a straight-line region on a logarithmic plot, which indicates power-law behaviour, see figure 9.

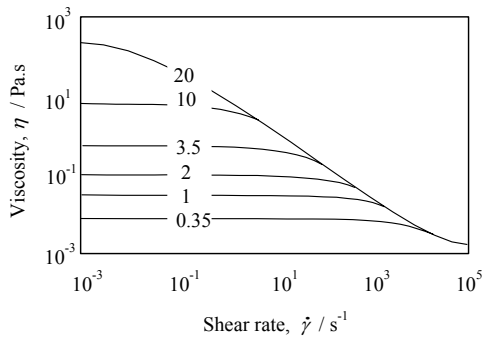


Figure 5: Viscosity/shear-rate curves for 3% by weight polystyrene in toluene: parameter - various molecular weights in millions.

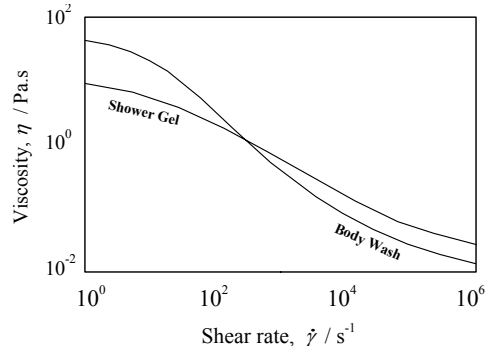


Figure 6: Viscosity/shear-rate curves for two personal products.

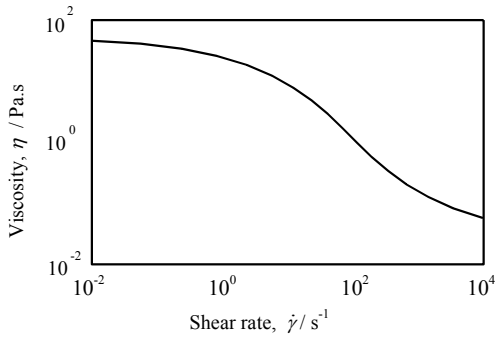


Figure 7: Viscosity/shear-rate curves for 2% by weight, polyisobutylene in decalin.

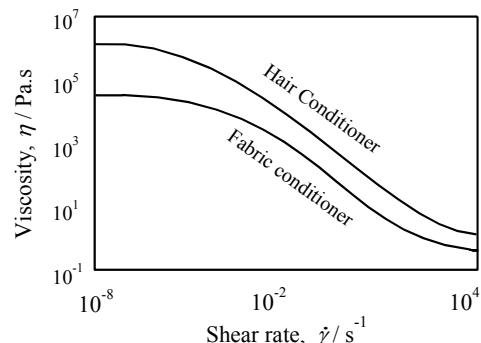


Figure 8: Viscosity/shear-rate curves for two conditioners.

This decrease of viscosity with shear rate is called *shear thinning* and must be distinguished from a decrease of viscosity with *time of shearing* which is called *thixotropy*, see later. At some point well down the viscosity curve, we see the beginnings of a flattening out, and if data at a high-enough shear rate or shear stress is available, then a second constant viscosity region, (with value η_∞), is usually seen. Thus we have the two limiting Newtonian viscosities, η_0 and η_∞ separated by a power-law region.

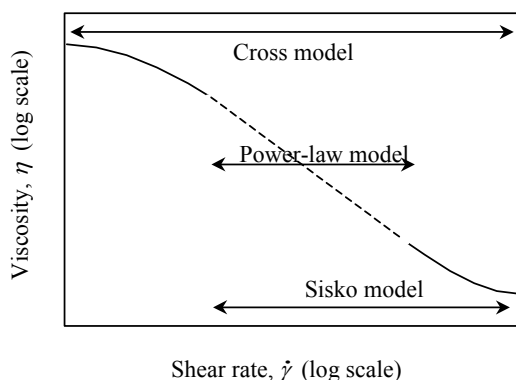


Figure 9: Definition diagram of the various models and the ranges that they cover.

Sometimes the position of the typical behaviour along the shear-rate axis is such that the particular measurement range used is too low to pick up the higher-shear-rate part of the curve, see for instance figures 10 - 13 (note that the typical shear-rate range of most laboratory viscometers is ~ 0.1 to 10^3 s $^{-1}$). This is particularly true for polymer melts and shampoos. On the other hand, if the shear-rate range is too *high*, then the

lower shear-rate behaviour is not seen, then the kind of behaviour shown in figures 14 and 15 is observed.

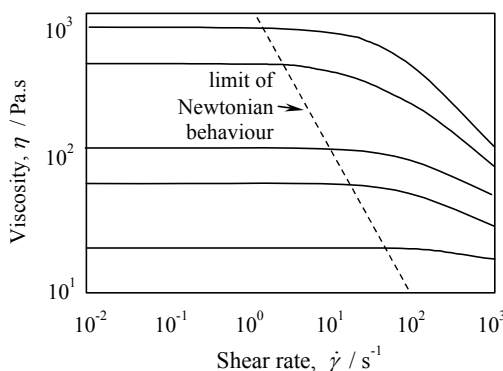


Figure 10: Viscosity/shear-rate curves for a range of silicone oils sold as viscosity standards.

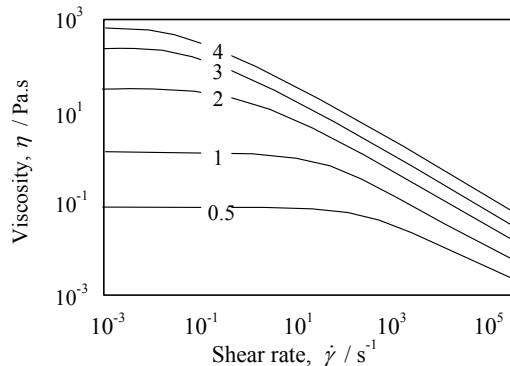


Figure 12: Viscosity/shear-rate curves for polystyrene ($M_w = 20M$) in toluene: parameter - weight %.

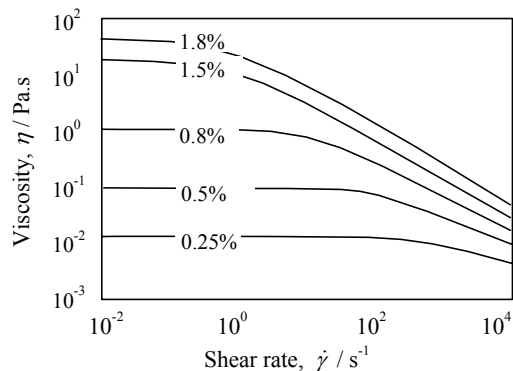


Figure 11: Viscosity/shear-rate curves for aqueous solutions of locust bean gum.

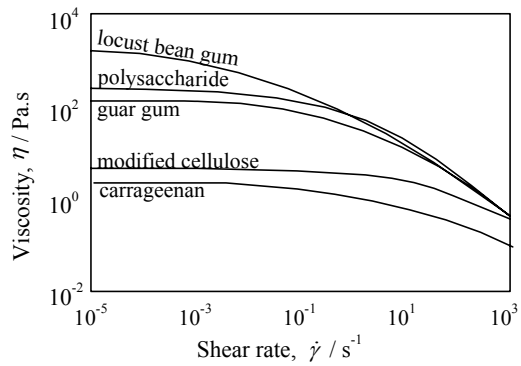


Figure 13: Viscosity/shear-rate curves for 1% by wt. various natural polymeric thickeners in water.

This is often seen for dispersions and emulsions measured in typical laboratory viscometers. Lastly, the situation sometimes arises where both the lower and higher shear rate behaviour is difficult to see, and then only the power-law region is seen. This is shown to be the approximate behaviour seen in figure 16. This is fairly typical of most situations where the power-law is forced to fit the data, when careful scrutiny – try looking along the curve from the side – will show that there is always some curvature.

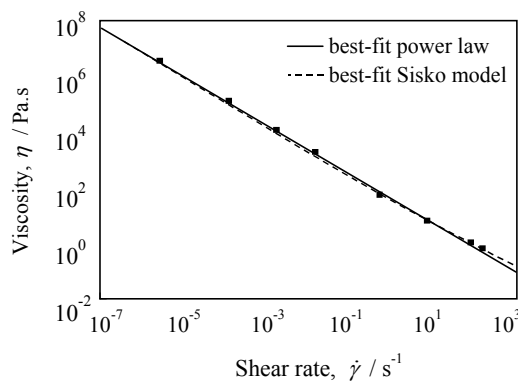


Figure 14: Viscosity/shear-rate curves for 0.35% aqueous Carbopol solution.

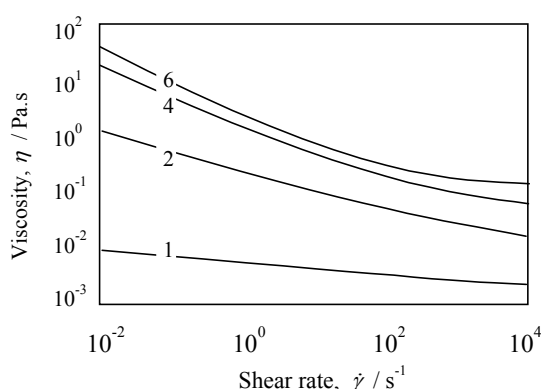


Figure 15: Viscosity/shear-rate curves for aqueous starch dispersions: ordinate weight %.

9.2 Mathematical descriptions of flow curves

All the features described above can be captured using simple equations relating viscosity and shear rate via a minimum number of parameters. The following are some examples of just some of the simpler forms of equations which fit different parts of the flow curve, see figure 17 for an overall picture.

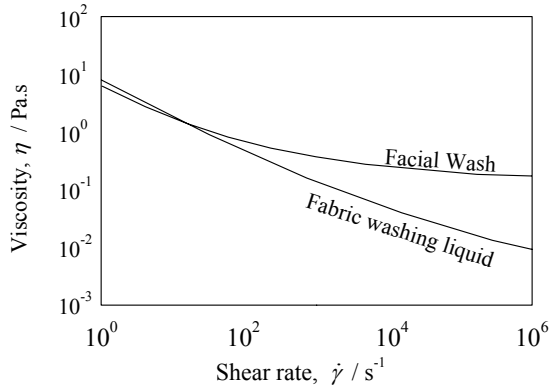


Figure 16: Viscosity/shear-rate curves for two personal products.

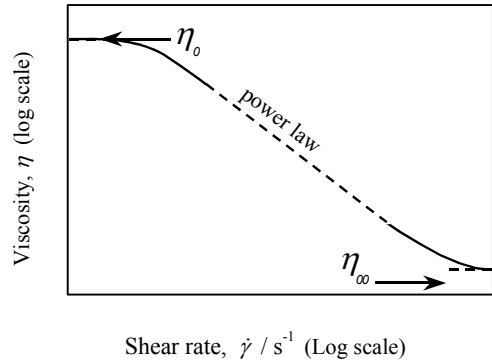


Figure 17: Definition diagram of parts of the flow curve.

9.2.1 The Cross model

First, we will consider one equation that describes the whole curve: this is called the Cross model, named after Malcolm Cross, an ICI rheologist who worked on dye-stuff and pigment dispersions. He found that the viscosity of many suspensions could be described by the equation of the form

$$\frac{\eta - \eta_\infty}{\eta_0 - \eta_\infty} = \frac{1}{1 + (K\dot{\gamma})^m}$$

where, written in this particular way, K has the dimensions of time, and m is dimensionless. When this model is used to describe non-Newtonian liquids, the degree of shear thinning is dictated by the value of m , with m tending to zero describes more Newtonian liquids, while the most shear-thinning liquids have a value of m tending to unity.

If we make various simplifying assumptions, it is not difficult to show that the Cross equation can be reduced to Sisko, power-law and Newtonian behaviour, see below. There is another Cross-like model which uses the stress rather than the shear rate as the independent variable, it has been called the Ellis or sometimes the Meter model, and for some specific values of the exponent, it has been given other names: for an exponent of unity it has been called the Williamson or Dougherty and Krieger model, while for an exponent of two it has been called the Philippoff model, etc.

The Carreau model is very similar to the Cross model, but with the whole of the bottom line within brackets, i.e. $(1 + (K\dot{\gamma})^2)^{m/2}$: the two are the same at very low and very high shear rates, and only differ slightly at $K\dot{\gamma} \sim 1$.

9.2.2 The Bingham equation

For most structured liquids at high shear rates, $\eta_0 \gg \eta_\infty$ and $K\dot{\gamma} \gg 1$, and then it is easy to show that the Cross model simplifies to the Sisko equation

$$\eta = \eta_\infty + \frac{\eta_0}{(K\dot{\gamma})^m} .$$

For the most shear-thinning liquids, m is unity, and the equation above can easily be recast as the **Bingham** equation by multiplying throughout by shear rate, so

$$\sigma = \frac{\eta_0}{K} + \eta_\infty \dot{\gamma} \quad \text{or} \quad \sigma = \sigma_o + \eta_p \dot{\gamma}$$

where the Bingham parameters are the yield stress σ_o , which is now given by η_0/K , and the plastic viscosity η_p which is now given by η_∞ .

Figure 18 shows the typical form of the results that would normally have been measured and plotted graphically over the last 50 years. Over a reasonable range of shear rates, the shear stress seemed to be a linear function of shear rate, but now displaced upwards by a constant value, which is called the yield stress. This was found by extrapolation to where the shear rate was zero. This seemed to show that there would be no flow at all unless the stress was higher than this critical value. Bingham investigated systems like this, and this simple straight-line-with-intercept-type behaviour bears his name, and such liquids are called *Bingham plastics*, and as we have said above, the intercept is called the *Bingham yield stress* σ_o and the slope of the straight line is called the *plastic viscosity*, η_p .

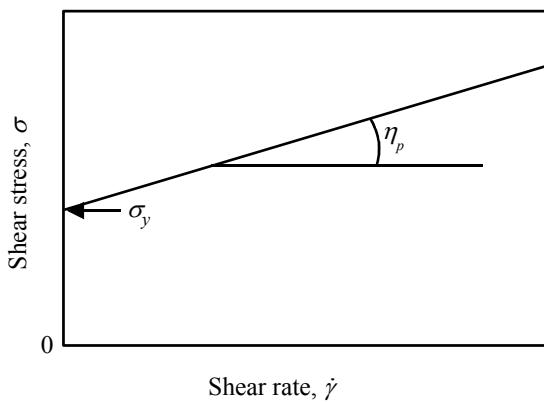


Figure 18: Definition diagram of the Bingham model.

9.2.3 The Power-law liquid

In many situations, $\eta_0 \gg \eta_\infty$, $K\dot{\gamma} \gg 1$, and η_∞ is small. Then the Cross equation (with a simple change of the variables K and m) reduces to the well-known *power-law* (or Ostwald-de Waele) model, which is given by

$$\sigma = k\dot{\gamma}^n \quad \text{or} \quad \eta = k\dot{\gamma}^{n-1}$$

where k is called the consistency and n the power-law index.

While Bingham linear plots are still favoured by many physical chemists, most engineers were happy to utilise the next most obvious two-parameter model, the power-law equation. In the power-law model, the consistency k has the strange units of Pa.sⁿ and the power-law index is dimensionless and usually ranges from 1 for Newtonian liquids towards 0 for very non-Newtonian liquids. This law alone is sufficient to describe many non-Newtonian flows, and the use of it is described in chapter 10 with many examples, which are analogous the Newtonian examples shown above. The power-law description does well for most structured liquids from shear rates around 1 to 10³ s⁻¹ or so, but at about 10³ s⁻¹, there is usually some flattening. However, for engineering calculations, power-law predictions are quite reasonable if limited to the medium range.

9.2.4 The Sisko model

Many real flows take place for structured liquids at shear rates where the viscosity is just coming out of the power-law region of the flow curve and flattening off towards η_∞ . This situation is easily dealt with by simply adding a Newtonian contribution to the power-law description of the viscosity, giving

$$\eta = k\dot{\gamma}^{n-1} + \eta_\infty, \text{ where } K^n = k,$$

or in terms of shear stress

$$\sigma = k\dot{\gamma}^n + \eta_\infty\dot{\gamma}.$$

This is called the Sisko equation, and it is very good at describing the flow behaviour of most emulsions and suspensions in the practical everyday shear rate range of 0.1 to 1000 s⁻¹.

Exercise: In figure 19, which models would you attempt to fit to each the flow curves shown?

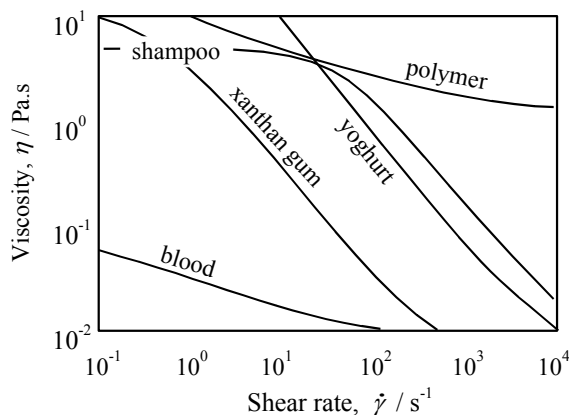


Figure 19: Viscosity/shear-rate curves for blood, liquid crystalline polymer, shampoo, yoghurt and an aqueous xanthan gum solution.

9.3 Fitting data to equations

Let us suppose we have a set of shear-stress/shear-rate data $(\sigma, \dot{\gamma})$ which we want to fit to an appropriate equation. First we plot the data on a linear basis to see if it fits the Bingham equation. If it does, then all we need to do is to perform a linear regression on the data, using a simple spread-sheet software package, or the software usually provided nowadays with the viscometer/rheometer we have used. Then the values of σ_0 and η_p can be used to predict flows of the liquid in other geometries, see chapter 10.

If the linear plot shows curvature, the data should be plotted on a logarithmic basis. From this plot we can see if we have a reasonable straight line, or a straight-line and some curvature. If a fair straight line is seen, then the data can be submitted for power-law regression and the k and n extracted and used for prediction. Last, if there is considerable curvature, then the Sisko model, or if necessary the complete Cross equation is indicated. However, here we have a problem, because the equation is non-linear and simple regression analysis is inadequate. However, most modern viscometers have suitable software for this purpose, otherwise other specialised commercial mathematical software.

Chapter 10 will show how these simple non-Newtonian equations – Bingham, power-law and Sisko – can be used to describe the flow of liquids in various geometries. However a note of warning must be sounded – the equations should only be used to predict behaviour within the range of the measurements taken to produce the various fitting parameters. In simple terms this is done by finding a representative shear rate, which is a typical size dimension and a typical velocity, so for a pipe we use the radius a and the average velocity V derived from the volumetric flow rate Q , so $V = Q/\pi a^2$. Then our representative shear rate would be given by V/a or $Q/\pi a^3$. Then the range of shear rates in both situations – the viscometer and the pipe – should be approximately in the same range of decades, say 10 - 100 s⁻¹.

A Handbook of Elementary Rheology

CHAPTER 10. EQUATIONS FOR THE FLOW OF NON- NEWTONIAN LIQUIDS

'An equation is for eternity', Einstein

10.1 Introduction

Just as we have collected a series of simple mathematical solutions for flows involving Newtonian liquids (Chapter 6), here we do the same for non-Newtonian liquids. These are generally power-law equations, but some other flow laws are also included. For most engineering applications the power law description is adequate if the parameters for the flow law relate either to the local point where the calculation is being made, or generally over the range being considered, see chapter 8, see also [1 – 3].

10.2 Steady-state flow in a straight circular pipe

10.2.1 Power-law liquids

If the liquid obeys a power-law flow law over the range of interest, then

$$P = \frac{2kL}{R} \left[Q \cdot \frac{\frac{3}{n} + \frac{1}{n}}{\pi R^3} \right]^n$$

where k is the consistency and n the power law index; Q is the flow rate through the pipe of radius a , with a pressure drop of P over a length L .

The radial velocity profile $u(r)$ across the tube is given by

$$u(r) = \left(\frac{n}{n+1} \right) \left(\frac{P}{2Lk} \right)^{1/n} a^{n+1/n} \left\{ 1 - \left(\frac{r}{a} \right)^{n+1/n} \right\}$$

where r is the distance out from the centreline towards the pipe wall. The wall shear rate is given by

$$\dot{\gamma}_w = \frac{Q}{\pi a^3} \left[3 + \frac{1}{n} \right].$$

We can use the tube as a viscometer, and plot of the wall shear stress σ_w as a function of $\dot{\gamma}_w$. If the value of n only changes slowly over a range of flow rates, then this approach can be used to deal piecewise with the whole flow-curve, even though it does not strictly follow power-law behaviour over a wide range of shear rates.

The entry pressure needed for a power-law liquid to get into a pipe from a large reservoir for slow (creeping) flow, see chapter 6, is less than that for Newtonian liquids ($\Delta P = \frac{0.6Pa}{L}$) by the factor

$$\frac{3(3n + 1)^2}{2(2n + 1)(5n + 3)}.$$

10.2.2 Sisko model

If the liquid flowing in a pipe/tube can be described by the Sisko model ($\eta = k\dot{\gamma}^{n-1} + \eta_\infty$), then the pressure drop is given (to a very good approximation) by

$$P = 2 \frac{L}{R} [k \left[\frac{V}{R} \cdot \frac{3n+4s+I}{n+s} \right]^n + \eta_\infty \frac{V}{R} \cdot \frac{3n+4s+I}{n+S}]$$

$$\text{where } S = \frac{\eta_\infty}{k \left[4 \frac{V}{R} \right]^{n-1}}.$$

Where V is the average velocity in the pipe ($= Q/\pi a^2$) of radius a and length L . This equation reduces to the power-law version (see relevant equation above) when η_∞ is zero. It is very good for describing the flow of most emulsions and dispersions through pipes.

10.2.3 Casson fluid

The Casson fluid is essentially the same as its Bingham cousin, but with all the components raised to the half power, so

$$\sigma^{1/2} = \sigma_0^{1/2} + (k\dot{\gamma})^{1/2}.$$

Then the flow rate in a pipe is given by

$$Q = \frac{\pi a^4 P}{8\eta_p L} \left[1 - \frac{16}{7} \sqrt{\frac{\sigma_0}{\sigma_w}} + \frac{4\sigma_0}{3\sigma_w} - \frac{\sigma_0^4}{21\sigma_w^4} \right].$$

Notice that this equation reduces to the Newtonian version at very high wall shear stresses, when the wall shear stress σ_w is much greater than the yield stress σ_o .

Workers who handle molten chocolate favour the Casson model; blood is also believed to conform to this model.

10.2.4 Bingham fluid

The Bingham model applied to pipe flow is one of the oldest mathematical flow solutions, and it is called the Buckingham-Reiner equation:

$$Q = \frac{\pi Pa^4}{8\eta_p L} \left[1 - \frac{4\sigma_o}{3\sigma_w} + \frac{1}{3} \left(\frac{\sigma_o}{\sigma_w} \right)^4 \right].$$

If the ratio of stresses σ_o/σ_w is small (as when the yield stress is small anyway or the flow stress is quite high), we can ignore the third term in brackets. The formula is then simpler, and can be re-arranged to give P as a function of Q , hence

$$P = \frac{8\eta_p L Q}{\pi a^4} + \frac{8L\sigma_o}{3a}.$$

In order to accommodate a Bingham fluid flowing down a pipe with a Newtonian slip layer (usually made up of the continuous phase), we need to add the term $\frac{\pi \delta a^3 P}{2 L \eta_s}$ to the full equation for flow rate, where δ is the thickness of the Newtonian slip layer whose viscosity is η_s . In most practical cases where slip layers are observed, they are usually less than one micron in thickness, but because the viscosity is so low, they can still dominate the flow.

10.3 Drainage down a wall under the action of gravity

The surface velocity V of a power-law liquid draining down a vertical surface is given by

$$V = \left[\frac{\rho g}{k} \right]^{\frac{1}{n}} \cdot \frac{n}{1+n} \cdot h^{\frac{1+n}{n}}$$

where ρ is the liquid density, g the acceleration due to gravity, k the consistency, n the power-law index, and h is the liquid-film thickness.

10.4 A sphere moving in a non-Newtonian liquid

The various expressions found in the literature for the Stokes flow of a sphere of radius a under the force of gravity in a power-law liquid have been simplified by the present author to give the average shear rate and shear stress as

$$\dot{\gamma}_{av} = \frac{V}{2a} [9 - 7n],$$

and

$$\sigma_{av} = \frac{ga\Delta\rho}{9} [1 + n].$$

The viscosity is then given by:

$$\eta = \frac{2ga^2\Delta\rho}{9V} \left[\frac{1+n}{9-7n} \right].$$

These expressions simplify to the correct Newtonian values when n is set to 1. We can invert these expressions so that given a known shear stress and a measured viscosity at that stress, the velocity can be calculated.

10.5 Flow in a slit (a very wide slot)

The wall shear rate $\dot{\gamma}_w$ and wall shear stress σ_w for the flow of a power-law liquid in a slot (see above, with $b \gg h$) are given by

$$\dot{\gamma}_w = \frac{2Q}{bh^2} \left[2 + \frac{1}{n} \right],$$

and

$$\sigma_w = \frac{hP}{2L}.$$

The viscosity corresponding to these values of shear rate and shear stress is then given by

$$\eta = \frac{Ph^3b}{4QL \left(2 + \frac{1}{n} \right)}.$$

This reduces to the expression for a very wide slot, see above.

10.6 Radial flow between parallel discs

If two circular discs are separated by a distance $2h$, with a pressure-drop P for radial flow between any two radii a_1 and a_2 , the flow rate is given by

$$Q = \frac{4\pi h^2}{2 + \frac{1}{n}} \left[\frac{Ph(1 - n)}{k(a_2^{1-n} - a_1^{1-n})} \right]^{\frac{1}{n}}.$$

10.7 Flow out of a tank through a long exit pipe

The efflux time T of a liquid flowing from a tank through a long exit tube is given by

$$T = \left[3 + \frac{1}{n} \right] \left[\frac{2kL}{\rho ga} \right]^{\frac{1}{n}} \frac{R^2}{a^3} \left(\frac{(H + L)^{1 - \frac{1}{n}} - L^{1 - \frac{1}{n}}}{1 - \frac{1}{n}} \right).$$

The height and radius of the tank are H and R and those of the outlet pipe L and a . This approach assumes that the emptying is slow enough to leave no material on the walls of the vessel.

10.8 Flow of a power-law liquid between squeezing plates

The power-law solution for squeezing flow between plates of radius a for a power-law liquid of original thickness h_0 and current thickness h at time t is given by

$$\left[\frac{h_0}{h} \right]^{\frac{n+1}{n}} = I + \left[I + \frac{1}{n} \right] \left[\frac{h_0}{2} \right]^{\frac{n+1}{n}} Kt$$

where K is given by

$$K^n = \frac{(n+3)F}{\pi k a^{n+3}} \left[\frac{2n}{2n+1} \right]^n,$$

see figure 1.

F, V

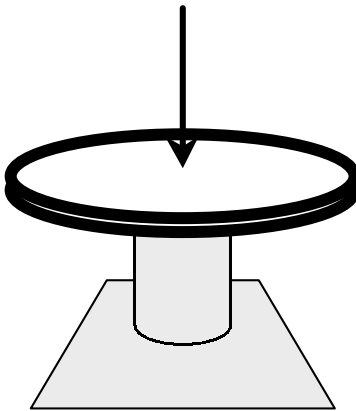


Figure 1 : The parallel-plate plastometer.

The expression for calculating the apparent yield stress in a parallel-plate plastometer is

$$\sigma_o = \frac{W h_e^{\frac{5}{2}} \pi^{\frac{1}{2}}}{2V^{\frac{3}{2}}}$$

where W is the applied weight, V the volume of the sample, and h_e the equilibrium distance between the plates. The plastic viscosity, η_p , can also be calculated, using the speed of approach of the plates, see §10.8 above.

10.9. Flow through a converging nozzle

The pressure drop P along a tube of length L that reduces in radius from a_1 to a_2 for a power-law liquid at a flow-rate Q is given by

$$P = \frac{2kL}{3n} \left[\frac{Q}{\pi} \left(\frac{1}{n} + 3 \right)^n \right] \left[\frac{a_1^{-3n} - a_2^{-3n}}{a_1 - a_2} \right].$$

10.10 Levelling of surface undulations under the action of surface tension

If the surface undulations are assumed to maintain a sinusoidal cross-section, we can say that

$$a^{\frac{n-1}{n}} = a_0^{\frac{n-1}{n}} - \left[\frac{(n-1)}{(2n-1)} \left(\frac{\sigma}{k} \right)^{\frac{1}{n}} \left[\frac{2\pi}{\lambda} \right]^{\frac{3+n}{n}} h^{\frac{2n+1}{n}} \right] t$$

where a is the amplitude of the undulation, a_0 is the initial amplitude of the undulation, λ is the wavelength, h is the mean film thickness, σ is the surface tension, k and n are the power-law constants and t is time. The maximum stress σ_m in that situation is given by $8\pi^3 \cdot \sigma a h / \lambda^3$.

10.11 A disc rotating in a power-law liquid

One of the simplest and cheapest viscometers on the market today is the Brookfield viscometer based on a thin disc rotating in large volume of liquid. While the viscosity is normally quoted as the equivalent Newtonian viscosity as a function of rotation speed in rpm for a given spindle, it is possible to evaluate the power-law parameters k and n for suitable liquids using the following equations [4]

$$n = \frac{d \log C}{d \log \omega},$$

and

$$k = \frac{3C}{4\pi \left(\frac{8}{\pi n} \right)^n R^3 \omega^n}$$

where C is the torque on the rotating disc,
 ω is the disc rotation rate in rad/s, and
 R is the radius of the disc.

It is also possible to define an average shear stress and shear rate for this situation as

$$\dot{\gamma}_{av} = \frac{8\omega}{\pi n} \quad \text{and}$$

$$\sigma_{av} = k \left(\frac{8\omega}{\pi n} \right)^n.$$

While these equations properly relate to true power-law liquids only, it is possible to obtain a reasonable estimate of the true flow curve by correcting the data collected at each point using the *local* value of $d\log C/d\log \omega$ for n .

10.12 More formulas for liquids with an apparent yield stress [5]

10.12.1 Flow in a mixer

When very non-Newtonian liquids are mixed in a vessel, a ‘cavern’ of visibly moving liquid is seen around the impeller, while liquid outside the cavern appears to be motionless, see figure 2.

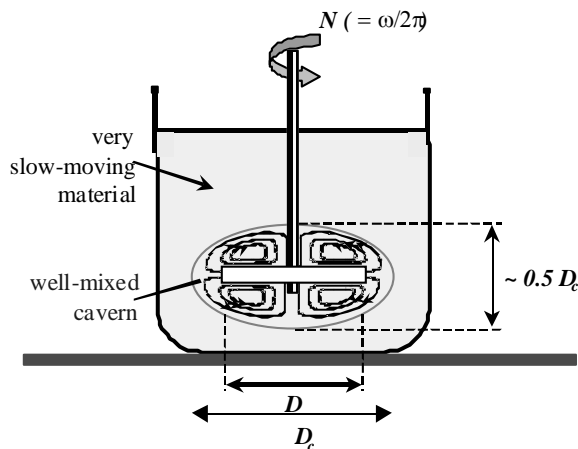


Figure 2 : Cavern flow in a simple mixer.

The size of this mixing cavern is given by

$$\left[\frac{D_c}{D} \right]^3 = \frac{1.36 P_o}{\pi^2} \left[\frac{\rho N^2 D^2}{\sigma_0} \right]$$

where D_c is the diameter of the cavern, D is the diameter of the impeller, N is the impeller speed in revolutions per second (rps) and P_o , the impeller power number is given by $P_o = \frac{2\pi C}{\rho N^2 D^5}$, where C is the couple on the impeller.

10.12.2 Wide-gap concentric cylinders

For a Bingham plastic between widely spaced concentric cylinders, at large stresses (i.e. where $C > 2\pi\sigma_o r_2^2$), the rotation rate ω (in rps) is given by

$$\omega = \frac{C}{4\pi\eta_p} \left(\frac{1}{a_1^2} - \frac{1}{a_2^2} \right) - \frac{\sigma_o}{\eta_p} \ln \frac{a_2}{a_1}$$

where C is now the couple *per unit height* of the cylinder; a_2 and a_1 are the outer and inner radii of the cylinders respectively. By plotting C against ω , the values of σ_o and η_p could be found.

10.12.3 Capillary rise of a yield-stress liquid

Recently, Kotomin [S. Kotomin, Moscow, personal communication, Sept. 1998] has suggested a simple means of measuring yield stress using two open-topped capillaries immersed in a yield-stress liquid. The value of yield stress σ_o is given by the simple equation

$$\sigma_o = \frac{\rho g (r_2 h_2 - r_1 h_1)}{h_1 - h_2}$$

where h_1 and h_2 are the equilibrium heights of the liquid of density ρ in the capillaries with radii a_1 and a_2 , respectively.

References

- [1] Bird, R.B., Armstrong, R.C.; Hassager, O, 'Dynamics of Polymeric Liquids' Volume 1, John Wiley, New York, 1977.
- [2] Macosko, C.W., 'Rheology Principles, Measurements and Applications', Wiley-VCH, New York, 1994.
- [3] Tanner, R.I, 'Engineering Rheology', Clarendon Press, Oxford, 1985.
- [4] Wein, O.J, JNNFM 1, 357 (1976).
- [5] Barnes, H A, JNNFM, 81(1&2), 133 - 178 (1999).



CHAPTER 11: VERY SHEAR-THINNING OR ‘YIELD-STRESS’ FLUIDS

‘Difference of opinion leads to enquiry, and enquiry to truth’ Thomas Jefferson

11.1 Introduction

Special attention has been paid over the years to very shear-thinning liquids that *appear* to have a yield stress [1]. It was usually thought that at stresses below the yield stress no flow takes place, and only elastic behaviour is seen. This is in fact only half the story, since indeed although there are such materials which *appear* to show this kind of behaviour, in reality there is as much happening in terms of flow below as above the ‘yield stress’. Figures 1 – 10 (see [1] for details) show a number of examples of such liquids, where the viscosity falls many orders of magnitude over a narrow range of shear stress, and indeed when approaching this critical stress region from regions of high stress it appears that the viscosity goes to infinity at a certain minimum stress. However, careful and patient measurement *below* this stress shows that the viscosity is still finite, and eventually levels off to a constant, but very high value at low stress.

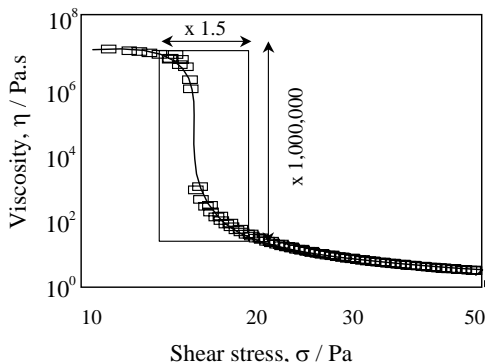


Figure 1: Flow curve of molten chocolate measured in a vane geometry to eliminate slip.

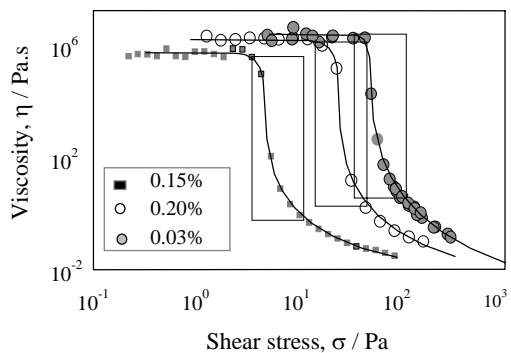


Figure 2: Flow curves for various concentrations of Carbopol 980 in water, each box showing a million-fold drop in viscosity for a three-fold increase in shear stress.

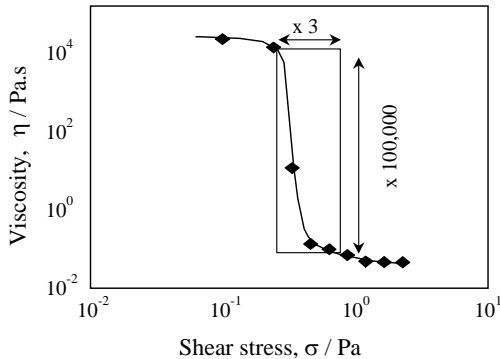


Figure 3: Flow curve of penicillin broth.

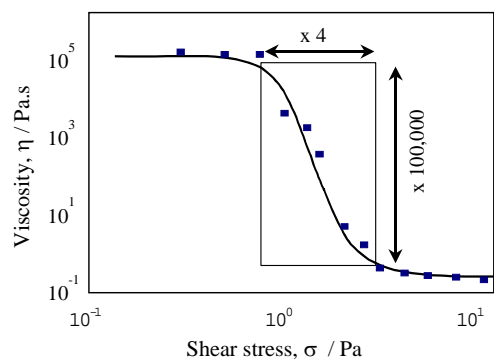


Figure 4: Flow curve of 6% iron oxide in mineral oil.

Here we take a little time to explain how the situation came about whereby yield stresses were supposed, and how we explain it these days. We finally comment on how to make proper use of the mathematical constant that is often called the ‘yield stress’, but which has no physical reality, see Barnes [1] for fuller details.

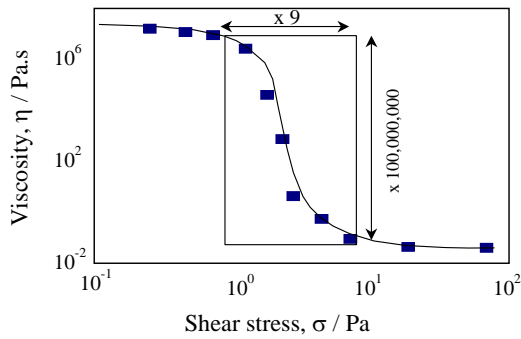


Figure 5: Flow curve of 10% suspension of Bentonite.

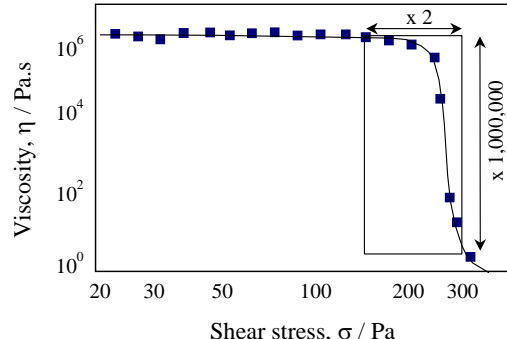


Figure 6: Flow curve of a mayonnaise.

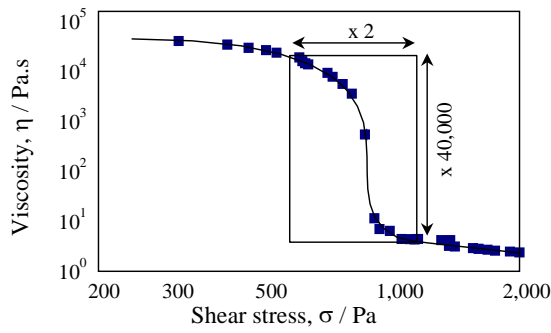


Figure 7: Flow curve of a flocculated ink.

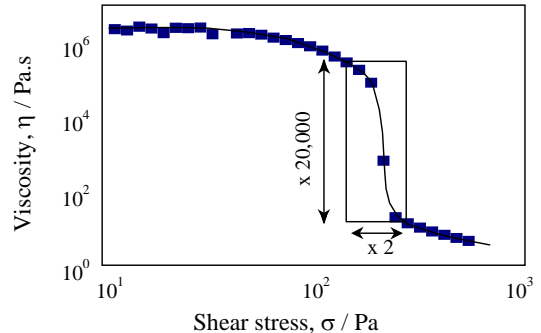


Figure 8: Flow curve of a toothpaste.

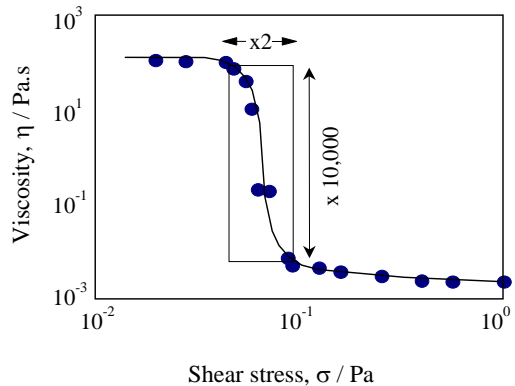


Figure 9: Flow curve of saliva at room temperature.

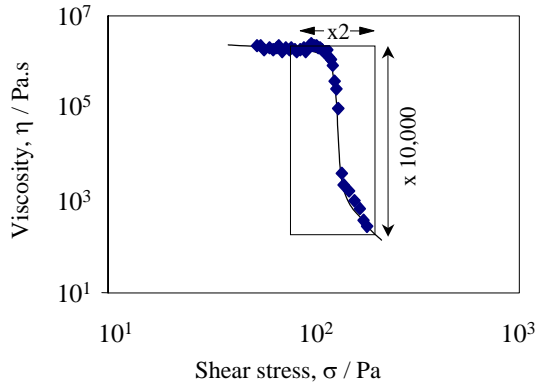


Figure 10: Flow curve of tomato paste at room temperature.

11.2 The history of the ‘yield stress’

A typical dictionary definition of the verb ‘*to yield*’ would be ‘*to give way under the action of force*’ and this implies an abrupt and extreme change in behaviour to a less resistant state. The yield stress of a solid material, say a metal like copper, is the point at which, when the applied stress is *increased*, it first shows liquid-like behaviour in that it continues to deform for no further increase in stress. Similarly,

for a liquid, one way of describing its yield stress is the point at which, when decreasing the applied stress; it first appears to show solid-like behaviour, in that it does *not* continue to deform.

Anyone testing a very shear-thinning liquid (e.g. toothpaste, Carbopol, tomato puree, etc.) in a viscometer with a limited range of shear rates—say the typical ~ 1 to 1000 s^{-1} of a laboratory viscometer—and plotting the results *linearly*, is almost *bound* to come to the conclusion that the liquid has a yield stress. However, measurement of the complete flow curve—using the appropriate equipment—shows that no real yield stress exists. When plotted as, say, the *logarithm* of viscosity against the *logarithm* of applied stress, the phenomenon is much better illustrated. Within the limited range of measurable shear rates, it *looked as though* the viscosity of such a 'yield-stress' liquid was increasing asymptotically as the applied shear stress was decreased. Indeed, for all *practical* purposes it looked as though there was a definite stress where the viscosity did become infinite. These materials can easily show a million-fold drop in viscosity over a very small region of increasing shear stress, often around or even less than a decade, see again figures 1 – 10 [1].

The liquids that appear to have a yield stress are legion. Among them are many original examples noted early in the century such as

clay, oil paint, toothpaste, drilling mud, molten chocolate, etc., then later, materials as diverse as creams of all sorts, ketchups and other culinary sauces, molten filled rubbers and printing inks, etc.,

were found to show similar behaviour. Nowadays such disparate systems as

ceramic pastes, electro-viscous fluids, thixotropic paints, heavy-duty washing liquids, surface-scouring liquids, mayonnaise, yoghurts, purees, liquid pesticides, bio-mass broths, blood, water-coal mixtures, molten liquid-crystalline polymers, plastic explosives, foams, battery and rocket propellant pastes, etc.,

may be added to the extensive list.

11.3 Values of yield stresses

The values of apparent yield stresses measured for different sorts of liquid-like foods range over the following values,

ketchup and drilling muds	$\sim 15\text{ Pa}$
spaghetti sauce	$\sim 25\text{ Pa}$
mustard, and apple sauce	$\sim 60\text{ Pa}$
mayonnaise	$\sim 90\text{ Pa}$
tomato paste	$\sim 125\text{ Pa}$

Within the limited time-scale of eating a meal, it is obvious what the concept of a yield stress means to the non-expert, in terms of, for instance, the confined spreading out of a liquid-like food when poured out, which seems to come to a constant thickness, e.g. thick sauces and ketchup.

In food processing, given the limited time-scales of many processing operations, the thickness of layers of liquid-like foodstuffs left on vertical walls after drainage has taken place can be calculated from the yield stress σ_o , for $\sigma_o = \rho gh$, where ρ is the fluid density, g is the acceleration due to gravity, and h is the layer

thickness. Having, for instance, emptied a vat of such a liquid product, we could then calculate, at least in the short-to-medium term when the liquid does not *appear* to flow, the thickness of the layer left on the wall of the vessel, which has to be removed in any ensuing cleaning operations.

Sherman [2] listed the following values of yield stress (in pascals) and their every-day significance for soft-solid, food-like, spreadable materials (such as margarine and butter) -

5,000	-	10,000	<i>means</i>	very soft, not pourable
10,000	-	20,000		soft, but already spreadable
20,000	-	80,000		plastic, and spreadable
80,000	-	100,000		hard, but satisfactory <i>[sic]</i> spreadable
100,000	-	150,000		too hard, limits of spreadability

The yield stress of such materials can be easily calculated as $\sigma_0 = W/\pi a^2$ for a right-angled cone of radius a at the plane of penetration, where W is the loading of the cone in newtons.

11.4 The arrival of commercial controlled-stress rheometers

As we have seen in chapter 7, the new generation of commercial electrically driven, controlled-stress rheometers with the latest optical-disc technology now means that rotation rates as low as 10^{-8} rad/s (~ 1 revolution in 20 years) can be measured! This has opened up a new range of previously unobtainable flow behaviour for structured liquids that *seemed* to have a yield stress. Measurement in these ultra-low shear-rate regions is now called creep testing, by analogy with the testing of solids under similar low-deformation-rate, long-time conditions; albeit solids creep testing is usually performed in extension rather than in shear.

The reason why these types of rheometers lend themselves to measurement of the whole curve is as follows: the complete range of shear rates needed to encompass the whole range of flow can be very large, say 10^{10} decades. However, the concurrent range of shear stress for the same conditions can be as low as 10^3 . The ability to apply this range of stress in a controlled fashion via the couple T applied to a typical geometry is relatively easy compared to generating the equivalent range of shear rates that would need to be applied. *Measuring* a wide range of shear rates is much easier than *generating* them and this measurement is done very accurately these days using optical discs.

11.5 The vane geometry

Last of all in our consideration of appropriate equipment to measure materials that appear to have a yield stress, we must consider the steps necessary to avoid wall-depletion or slip artefacts that very often arise in low shear rate measurement of the kind of highly structured liquids that appear to have yield stresses, see figure 11. Apart from roughening the walls of existing geometry members, the most widely used geometry suitable for this purpose of eliminating wall effects is the vane geometry (where the vane is used instead of an inner cylinder of a viscometer / rheometer), with its diversity as to vane number and aspect ratio.

It offers the possibility of inserting the thin vanes into an existing rested or stored sample with the minimum of disturbance.

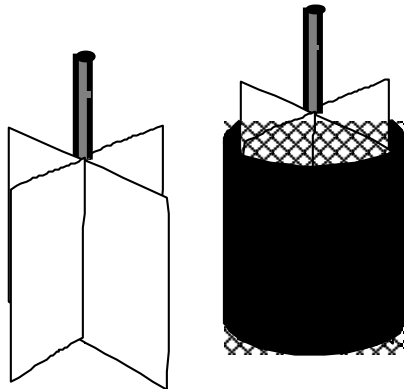


Figure 11: The vane and the vane-and-basket geometries

Barnes [1] went further than simply using a vane when he introduced a close-fitting wire-mesh cylinder inside the outer containing cylinder to prevent slip there also, which can often occur, but is usually ignored, see figure 11. Of course, use of a vane geometry at very high rotation rates is precluded due to secondary flow developing behind the vanes.

Theoretical analyses of this geometry has been carried out by several workers who all essentially concluded that for yield-stress/very-shear-thinning liquids, the vane geometry acted as a circumscribing cylinder defined by the tips of the vane blades, with the material inside the virtual cylinder essentially acting as a solid body, and the material outside being sheared in the normal way [1]. This ensures that slip is completely overcome at the rotating member.

11.6 Some flow equations with yield stresses

Many of the liquids whose flow curves we have just examined will obviously appear to have a yield stress if scrutinised only over the shear-rate/shear-stress region just above the large increase in viscosity. Much useful progress has been made for these kinds of liquids by using simple, yield-stress-containing equations that fit steady-state, shear-stress/shear-rate data quite well over a *limited* range of shear rates. Then, if these equations are used to predict flow in any other situation, where *the same general range of shear rates applies*, this is completely acceptable and uncontroversial, and can indeed be very effective.

The most popular equations that have been used to describe liquids with yield stresses are the Bingham, Casson and Herschel-Bulkley (sometimes called the generalised Bingham) models, i.e.

$$\sigma = \sigma_o + \eta_p \dot{\gamma} \quad \text{Bingham},$$

$$\sqrt{\sigma} = \sqrt{\sigma_o} + \sqrt{\eta_p} \dot{\gamma} \quad \text{Casson},$$

and $\sigma = \sigma_o + k \dot{\gamma}^n$ Herschel - Bulkley.

The Bingham model is the most non-Newtonian example of the Sisko model, which is itself a simplification of the Cross (or Carreau model) under the appropriate conditions [3].

A simple but versatile model that can cope with a yield stress, yet retain the proper extreme of a finite zero and infinite shear-rate viscosity is the Cross model with the exponent set to unity, so

$$\frac{\eta - \eta_\infty}{\eta_0 - \eta_\infty} = \frac{1}{1 + k\dot{\gamma}},$$

the behaviour of which is shown in figures 12 and 13, plotted either linearly as stress against shear rate or logarithmically in terms of stress versus shear rate or viscosity versus stress.

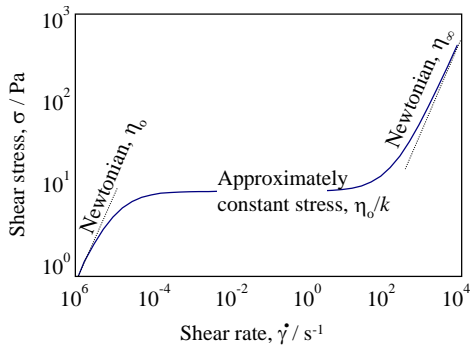


Figure 12: The Cross model with $m = 1$ and typical values of the parameters, showing the apparent yield stress region and upper and lower Newtonian regions.

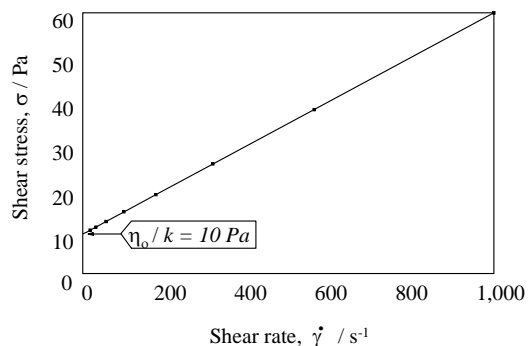


Figure 13: The Cross model with $m = 1$, plotted linearly to show Bingham-type behaviour.

This behaviour is then very similar to figures 1 to 10, where we note the large drop in viscosity for only a moderate increase in stress for all the results shown. Above the ‘yield stress’ where $\eta \ll \eta_0$, and $k\dot{\gamma} \gg 1$ and it is easy to show that the equation simplifies to

$$\sigma = \frac{\eta_0}{k} + \eta_\infty \dot{\gamma},$$

which is the same as the Bingham equation, but with $\sigma_0 = \frac{\eta_0}{k}$ and $\eta_p = \eta_0$.

References

- [1] Barnes, H. A, JNNFM, **81**(1&2), 133 - 178 (1999).
- [2] Sherman, P, ‘Industrial Rheology’, Academic Press, London, 1970.
- [3] Barnes, H. A; Hutton, J F; Walters, K, ‘An Introduction to Rheology’, Elsevier, Amsterdam 1989.

CHAPTER 12: THE FLOW OF SOLIDS

'There are solids in rheology, even if they ... creep', Markus Reiner

12.1 Introduction

There is a widespread but mistaken belief that solids do not flow, but only show elastic behaviour. However, *all* solids when stressed, while certainly deforming elastically on a time-scale of less than a second, consequently creep (i.e. continue to deform very slowly) over a very long time scale of days, months and even years. If we replace the word 'creep' with 'flow', we have moved smoothly from material science into rheology, and we can happily talk about the viscosity of solids, because, as we have seen so far, viscosity determines flow-rate.

Arnstein and Reiner [1] showed that 'solidified' cements have viscosities of 10^{16} - 10^{17} Pa.s., while Sherman [2] later showed that ice-cream viscosities at low stresses were in the order of 10^8 Pa.s. He quoted earlier measurements of the viscosities of various English cheeses in the range 10^{10} - 10^{11} Pa.s, and for concentrated oil-in-water emulsions with 65 % w/w disperse phase; the creep range had viscosities of over 10^6 Pa.s. He even measured Madeira cake and came out with viscosities of around 10^9 Pa.s! These kinds of numbers can be compared with the more recent work of Harnett et al on the creep of butter [3], who found values of the steady-state creep viscosity at 10 °C to be in the range 2.4 — 11.0×10^{11} Pa.s. Similar creep measurements were made on various kinds of solid soap by Pacor et al, who found values of creep viscosity—depending on formulation and moisture content—in the range 5 - 160×10^{11} Pa.s [4].

The approximate values of steady-state 'creep' (zero-shear) viscosity η_0 for a range of 'solid' materials (mostly at room temperature) are shown in table 1, showing typical examples for each viscosity decade from 10^{21} down to 10^6 Pa.s, arranged in \log_{10} decrements.

21 - the Earth's mantle	17 - marble	13 - ice	9 - bitumen
20 - glass	16 - cement	12 - solid soap	8 - ice cream
19 - steel	15 - polyethylene	11 - asphaltic concrete	7 - resins
18 - mortar	14 - tin	10 - cheddar cheese	6 - gelatine gel

Table 1: Some steady-state creep viscosities of solid-like materials.

In these systems, we either have materials in a super-cooled, glassy state, and hence their flow is the same as that of other liquids but is very slow, or else 'solid' polycrystalline materials where flow is usually via the integrated effect of atomic 'jumping' movements along grain boundaries.

12.2 Non-linear ‘viscosity’ of solids

If solid materials are heated to temperatures of about half their melting point (in degrees kelvin, K), they are still ‘solid’, but the long-term creep rates are then considerably higher and usually within the measurable range, i.e. $> 10^{-9} \text{ s}^{-1}$. When results from this type of experiment are collated, a simple picture emerges, so that

- after a long-enough time, a steady creep rate is achieved; then
- this creep rate, at low-enough applied stress, usually becomes directly proportional to the applied stress—in the language of the rheologist, this proportionality signifies *Newtonian* behaviour—and is governed by atomic diffusion, while,
- at higher stresses, the creep rate increases faster than the stress, and usually shows a power-law-like behaviour.

Above the power-law region, other phenomena lead to different kinds of creep behaviour, but among them is a situation where the creep rate (often quite large by now) tends again towards a linear function of applied stress—the so-called drag-controlled plasticity—i.e. in rheological parlance an upper Newtonian behaviour. If we express this response as would normally be done for a structured liquid, the identical behaviour would be as shown in figures 1 - 9 of chapter 11.

The creep results of most solid materials, in the customarily observed linear followed by power-law regions, can be fairly well described by the empirical Ellis equation (omitting the usual high-shear-stress asymptotic viscosity), viz.

$$\frac{\eta}{\eta_0} = \frac{1}{1 + \left[\frac{\sigma}{\sigma_c} \right]^m}$$

where η is the steady-state creep viscosity measured at a stress of σ ; η_0 is the zero-shear-rate viscosity; σ_c is the critical stress which determines the *region* of shear stress where the material shows significant departure from linearity, and m is another material parameter—this time dimensionless—which determines the *rate* of departure from linearity. (The results can be expressed equally well using the Cross model, which is essentially the same as the Ellis model, but where the stress is replaced by the shear rate).

Some further examples of this kind of behaviour are shown in figures 1 and 2.

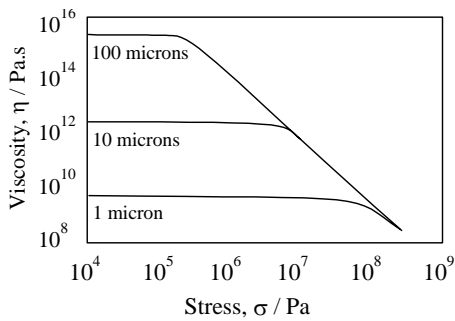


Figure 1: Creep viscosity versus shear stress for magnesium oxide at 1000 °C, for various values of grain size.

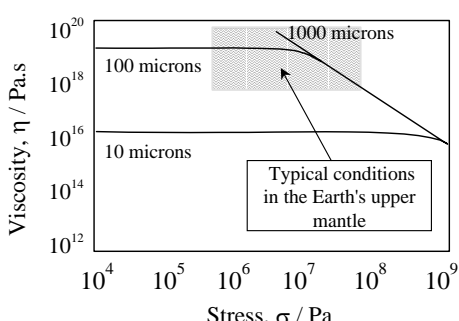


Figure 2: Creep viscosity versus shear stress for olivine (a rock) at 1000 °C, for various values of grain size.

The approximate parameters for other solid materials are collected together in table 2. The data has been read off graphs in Frost and Ashby's book [5] and has been fitted to the Ellis model.

Material	Temp. °C	η_0 Pa.s	σ_0 Pa	m
Spinel, a mineral	1000	4.64×10^{16}	7.4×10^7	1.2
α-Alumina	1200	1.25×10^{16}	4.8×10^7	1.1
Zinc carbide	1600	2.00×10^{16}	1.5×10^6	2.9
Lithium fluoride	500	2.45×10^{14}	2.7×10^6	4.6
Sodium chloride	400	3.02×10^{14}	1.7×10^6	4.3
304 Stainless steel	600	6.20×10^{15}	2.5×10^7	3.6
Titanium	900	1.00×10^{15}	1.0×10^6	2.9
Ice	-8	1.02×10^{13}	3.2×10^5	2.1

Table 2: Approximate values of the Ellis model parameters that describe the creep of some 'solid' materials.

Plasticine, which is considered to be a typical soft solid, also shows characteristic non-Newtonian, steady-state liquid behaviour as seen in figure 3, where the results of a creep test are compared to those obtained at the higher deformation rates experienced in extrusion through a short orifice.

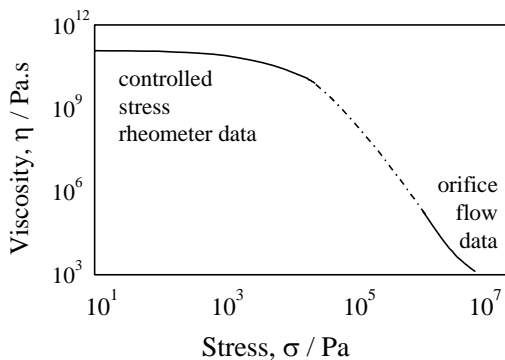


Figure 3: Flow curve as viscosity versus shear stress for Plasticine at room temperature.

12.3 Conclusion

The conclusion of this chapter is that everything flows, and 'solids' flow very slowly [6]. Nevertheless their overall flow behaviour is essentially the same as that of structured liquids. One thing worth noting about the degree of 'shear-thinning' seen for solids is that if we compare the steepness of the shear-thinning regions of the very shear-thinning (yield-stress) liquids shown in chapter 11, they are much 'steeper' than for the solids shown here. This is because their viscosity often arises from structures that are not space-filling (as for solids), but are composed of tenuous arrangements such as chains and flocs that collapse above a critical shear stress to a low viscosity, while solids are always space filling.

References

- [1] Arnstein, A; Reiner, M, Civ. Engng., Sept 1945, p3.
- [2] Sherman, P, '*Industrial Rheology*', Academic Press, London, 1970.
- [3] Harnett, M; Lambert, R.K; Lelievre, J; Macgibbon, A.K.H; Taylor, M.W; in

A Handbook of Elementary Rheology

- [4] Pacor, P; Lander, L.H; Papenhuijzen, J.M.P; *Rheol. Acta*, 9(3), 455, 1970
- [5] Frost, H.J; Ashby, M.F, '*Deformation-Mechanism Maps*', Pergamon Press, Oxford, 1982.
- [6] Barnes, H A, 'Yield stress - a review, or παντα ρει - everything flows?' *JNNFM*, 81(1&2), 133 - 178 (1999).



'The mountains flow before the Lord'

CHAPTER 13: LINEAR VISCOELASTICITY AND TIME EFFECTS

'Time is nature's way of keeping everything from happening all at once', anon.

13.1 Introduction

In all structured liquids there is a natural rest condition of the microstructure that represents a minimum-energy state. When these liquids are deformed, thermodynamic forces immediately begin to operate to restore this rest state, just like a stretched spring will always seek to return to its unextended length. Also like a spring, movement from the rest state represents a storage of energy, which manifests itself as an elastic force trying to reproduce the static *status quo*. This kind of energy is the origin of elasticity in structured liquids. Some examples of rest states are

- unextended, isolated polymer coils with a random, undeformed configuration,
- unstretched inter-entanglement polymer chains,
- spatially random distribution of particles in a suspension at rest, or
- undeformed particles in an unsheared emulsion.

Initially, the restoring force increases linearly with the distance that any deformation takes the material away from its rest state, but eventually non-linearities will be encountered. The rate of increase of force with deformation then diminishes, until at very large deformations a steady-state situation arises and the elastic force becomes constant. By the time that these large elastic forces are evident, the microstructure has changed radically, and has become anisotropic. The elastic force manifests itself at *small* deformations as various elastic moduli, such as the *storage modulus*, and at steady state (i.e. very large deformations) by a *normal-stress difference* (see chapter 14). Alongside these elastic forces are the ever-present viscous forces due to the dissipation, and proportion to the *rate* not extent of deformation, so that together these produce *viscoelastic* (i.e. viscous plus elastic) effects.

Most concentrated structured liquids show strong viscoelastic effects at *small* deformations, and their measurement is very useful as a physical probe of the microstructure. However at large deformations such as steady-state flow, the manifestation of viscoelastic effects—even from those systems that show a large *linear* effects—can be quite different. Polymer melts show strong non-linear viscoelastic effects (see chap. 14), as do concentrated polymer solutions of linear coils, but other liquids ranging from a highly branched polymer such as Carbopol, through to flocculated suspensions, show no overt elastic effects such as normal forces, extrudate swell or an increase in extensional viscosity with extension rate [1].

If the stresses and strains in deformations are relatively large, then many time effects are *thixotropic* in nature. The difference between the two situations – viscoelastic and thixotropic—is that in the linear viscoelastic region the microstructure responds over a certain time scale *without changing*, while in thixotropy the microstructure does change—by breaking down or building up—and

such changes take time. In this chapter we shall deal only with linear viscoelasticity, and the resulting viscoelastic responses shown in various test situations.

Before embarking on an investigation of liquids that show obvious elastic effects such as recoil and normal force, it is well to remember that *all* liquids show elastic effects at a short-enough time or a high-enough frequency. Put in terms of a Maxwell relaxation time (see next section), even what we would think of as simple Newtonian liquids have elastic properties (see [2]). Table 1 shows a number of such liquids compared to others that we would normally think of as elastic, giving the modulus that would describe their behaviour at times less than their relaxation time, which is also given. This is the converse of what we found in chapter 12, where we saw that all solids flow, since here we are saying that all liquids show solid-like properties under appropriate, if extreme, conditions.

Liquid	Viscosity $\eta / \text{Pa.s}$	Relaxation time τ / s	Modulus G / Pa
Water	10^{-3}	10^{-12}	10^9
An oil	0.1	10^{-9}	10^8
A polymer solution	1	0.1	10
A polymer melt	10^5	10	10^4
A glass	$>10^{15}$	10^5	$>10^{10}$

Table 1: Values of approximate Maxwell parameters for a very wide range of liquids (following Tanner [2]).

13.2 Mechanical analogues of viscoelastic liquids

For those not familiar with viscoelasticity, one of the simplest ways of understanding the subject is to make use of simple mechanical models. These consist of combinations of linear elastic and viscous elements, i.e. springs and dashpots, see figure 1, that visualise the concepts that we discussed above.

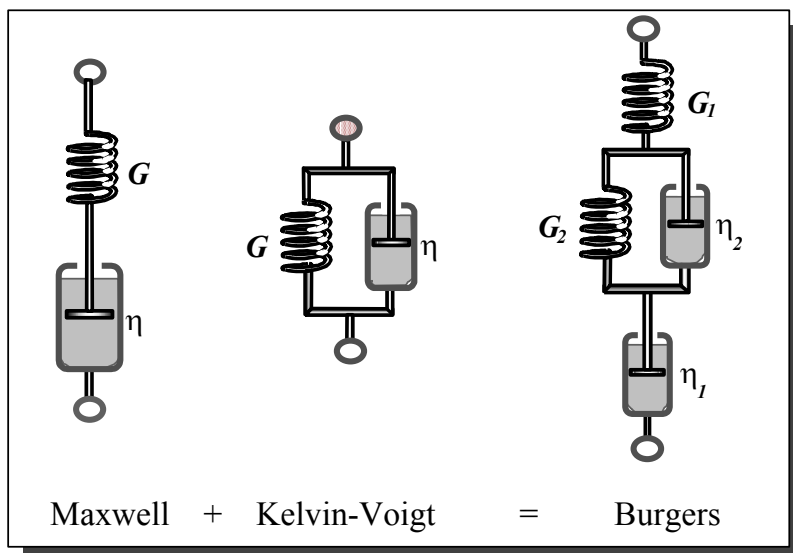


Figure 1: The Maxwell, Kelvin-Voigt and Burgers models.

A spring is a representation of a linear elastic element that obeys Hooke's law—i.e. the strain is proportional to the applied stress. In a simple shear deformation the constant of proportionality is the elastic modulus, G , so that

$$\sigma = G\gamma.$$

Notice that time does not come into this behaviour, so that if we apply a strain γ to the unstrained model, the resultant stress σ suddenly appears, and then, if we remove the strain, the stress σ falls immediately to zero (and vice versa when a stress is applied).

Similarly, linear viscous response can be modelled using a dashpot. A plunger moving through a very viscous Newtonian liquid physically represents this. The response of this element is described mathematically by the equation

$$\sigma = \eta\dot{\gamma}.$$

Note that now only the *rate* of deformation matters, and if we switch on a stress σ , the dashpot immediately starts to deform and goes on deforming at a constant deformation rate $\dot{\gamma}$ without any change with time until the stress is removed, and then the deformation stops immediately (again vice versa if a shear rate is applied). Note that again there are no time effects.

If we connect a spring and a dashpot in *series* we have the simplest representation of a viscoelastic *liquid*, and such a combination is called a Maxwell model, in honour of the famous Scottish physicist of the last century (1831 - 1879), who introduced it in the 1870's.

If we connect the single elastic and viscous elements in *parallel*, we end up with the simplest representation of a viscoelastic *solid*, and this has been named after Voigt, the German physicist (1850 - 1919), while some workers call it the Kelvin or the Kelvin-Voigt model, linking it with Lord Kelvin (1824 - 1907), another Scottish physicist: to please as many as possible, we shall call it the Kelvin-Voigt model.

The Maxwell and Kelvin-Voigt models may be expanded to give either multiple Maxwell models, which are usually combined in parallel, or else multiple Kelvin-Voigt models, which are usually combined in series. However, if we combine a Maxwell model and a Kelvin-Voigt model in series, we obtain a Burgers model, named in honour of the Dutch physicist (1895 - 1981) of that name. This model is the most complicated that we need to consider, since it describes all the basic features of interest to us. Below we will see how all these various combinations of springs and dashpots begin to describe real viscoelastic materials.

Of course, looking down a microscope, we would never see real springs and dashpots, so what are the real physical entities being modelled by them? First, as we saw above, elastic elements represent any physical system in the microstructure that can store energy. This might be potential energy or entropic energy, so a bond or a polymer segment being stretched would be an example of the former, while an isolated polymer random coil being deformed from its spherical rest state being but one example of the latter. A spring can also represent many other energy-storing mechanisms. In each case, the movement of any entity through a liquid continuous phase will dissipate energy and this can be modelled by a dashpot. Even in a polymer melt where there is no liquid around the chains, there is friction as the chains slide over one another.

To use these mechanical models we need to establish for any particular liquid the number and configuration of springs and dashpots.

13.3 Measuring linear viscoelasticity

13.3.1 General

There are a number of ways of measuring linear viscoelastic response. One of the simplest is the sudden application of a constant stress to the liquid being tested, and the monitoring of the resulting strain thereafter – this is called *creep testing*. Another frequently used method is *oscillatory testing*, i.e. applying an oscillating stress or strain as an *input* to the liquid and monitoring the resulting oscillatory strain or stress *output*. The same repetitive sinusoidal straining motion recurs over and over again, with each cycle taking a certain time, and having a frequency that is inversely proportional to that time.

One other method used occasionally is the sudden application of a constant strain, and the monitoring of the consequent stress, which then decays away with time – this is called a *stress relaxation* test. The only other test we need to mention here is the application of a steady shear rate, as in the start-up of a simple viscometer – so not surprisingly this is called a *start-up* test. All these tests are shown in figure 2. The first two tests mentioned – creep and oscillatory – will now be dealt with at some length, since they are the most frequently used tests, while the other two – stress relaxation and start-up – will only be mentioned briefly.

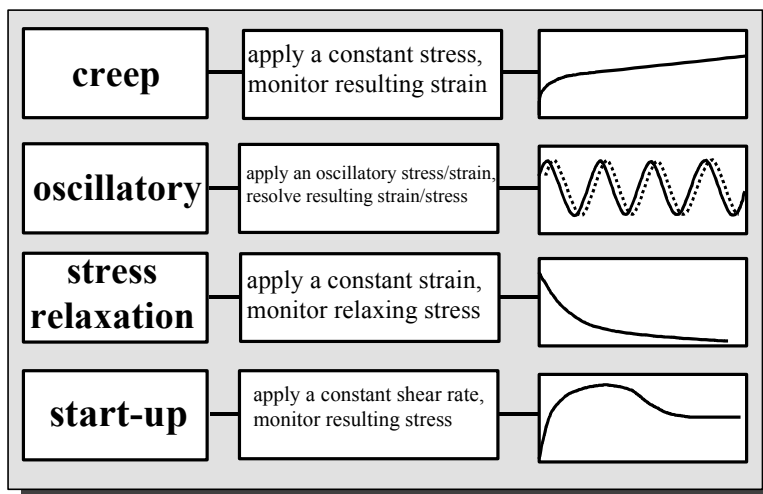


Figure 2: Various tests that measure the time response of a liquid.

13.3.2 Creep tests

For many years, metallurgists performed tests in which they stressed long, thin samples of metal, and measured the (usually small) resultant deformation as a function of time. In some cases the testing time was very long (months or even years!), and they then found that the samples were still deforming long after the initial elastic response; however the deformation they measured was so slow that the phenomenon was called *creep*. Creep properties are very important in studying certain practical situations where high stresses and long times (and sometimes high temperatures) are involved, such as suspension bridges or pressurised nuclear-reactor vessels. This kind of stress-controlled test was later used for softer materials such as ice cream, butter and soap, and the name *creep stuck*, so that when the new

generation of controlled-stress instruments for structured liquids came along, they had testing regimes called *creep analysis*.

The behaviour normally seen for typical *viscoelastic* liquids – represented for convenience and simplicity by a Burgers model – in a creep test is shown in figure 3.

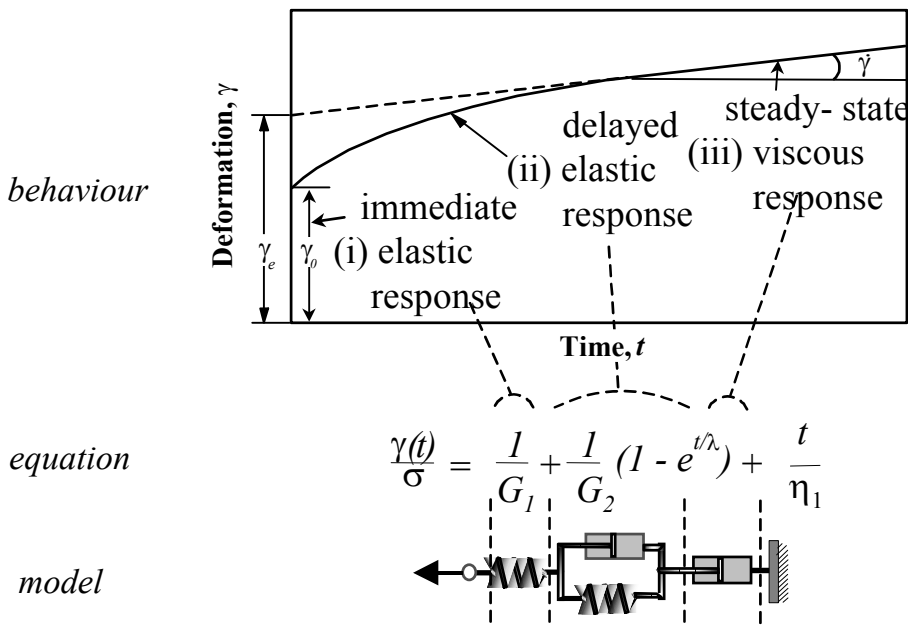


Figure 3: The Burgers model in detail.

There is an initial elastic response, which for gel-like liquids can produce an unwanted instrument artefact called ‘ringing’ that arises from the large inertia of the moving member of the rheometer. Thereafter there is a so-called *delayed elastic response* where the deformation rate becomes slower and slower, ending up as a very slow but steady-state deformation at the longest times, i.e. the material is in steady flow. Sometimes it is difficult to be sure when this steady state has been reached. If the controlled-stress instrument used does find it difficult to detect the steady-state slope for structured liquids, it often measures a slope that is too steep, and the typical result of this common artefact is seen in figure 4, where the long-time, steady-state viscosity *appears* to decrease with decreasing shear stress.

The answer to this problem is to tighten the level of scrutiny with which the instrument decides if steady state is achieved, and then the normal viscosity plateau is seen.

The ‘universal’ curve that describes the creep response of most structured liquids and gels is shown in figure 5, with some examples shown in figure 6. The behaviour is depicted over a very long time period, which, as ever, is best shown on a logarithmic scale. The response for most materials measured under normal conditions is such that we first see the immediate elastic response (the horizontal dotted line), then we see the delayed elastic response, and eventually the viscous flow predominates, and the slope approaches unity at very long times (see the second dotted line).

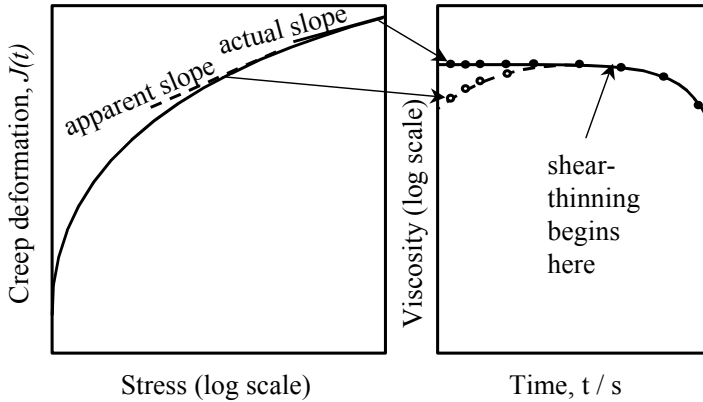


Figure 4: The artefact found in creep testing where the rheometer reads the creep slope too early.

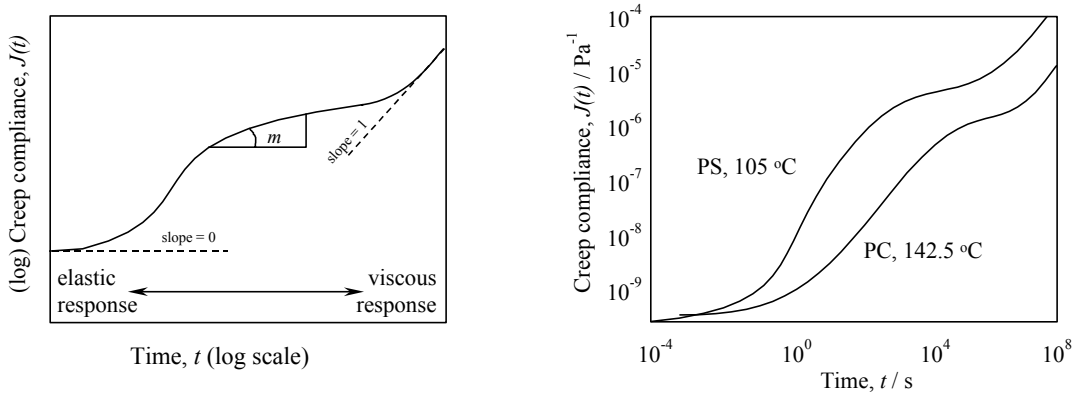


Figure 5: A typical creep curve plotted on a logarithmic basis. **Figure 6:** Creep curves for polystyrene and polycarbonate melts [3].

13.3.3 The behaviour of model materials in creep tests

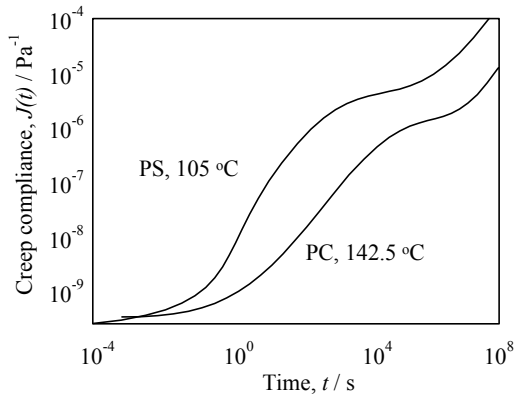
In a creep test, a simple elastic solid—a spring—shows an immediate response to give a constant deformation (i.e. strain). On the other hand, a simple Newtonian liquid—a dashpot—would show an ever-increasing strain, which displayed on a graph of strain against time would be a straight line starting at the origin, with the slope giving the shear rate, $\dot{\gamma}$.

If we now perform a creep test on a Maxwell model, the behaviour can be described by the simple equation

$$\dot{\gamma} = \sigma \left(\frac{1}{G} + \frac{t}{\eta} \right),$$

which, at very short times, is characterised by an immediate elastic response, $\dot{\gamma} = \sigma/G$, and at very long times, when $t \gg \eta/G$, by simple viscous behaviour, $\dot{\gamma} = \sigma t/\eta$. Here η/G is called the relaxation time τ .

If a creep test is performed on a Kelvin-Voigt model, the strain gradually builds up to a constant value as described by



$$\gamma = \frac{\sigma}{G} \left[1 - e^{-t/\tau} \right].$$

Here τ is called the *retardation time*, since it characterises the retarded response of the model, and its value is again given by η/G . At *very short times*, the response is viscous, and $\gamma \sim t\sigma/\eta$. At $t = \tau$, the strain has risen to $\sim 63\%$ of its final, asymptotic value of σ/G .

If we now stress the Burgers model in a creep test, it is easy to see what will happen, see figure 3: first, the unrestrained spring G_1 will instantaneously deform to its expected extent, while the isolated dashpot will start to deform at its expected rate. However, the spring in the Kelvin-Voigt element cannot immediately respond, being hindered (i.e. retarded) by its dashpot. Nevertheless, it does begin to deform, and eventually comes to its expected steady-state deformation. It is possible to show that the overall deformation can be written down as:

$$\gamma = \sigma \left(\frac{1}{G_1} + \frac{1}{G_2} \left(1 - e^{-t/\tau} \right) + \frac{t}{\eta} \right)$$

where τ is the retardation time, now given by η_2/G_2 .

Some examples of real materials whose creep deformation at low stresses are described quite well by the Burgers model are

- concentrated corn starch dispersions, see Liao et al. [4]
- titanium dioxide dispersions, see Zupancic [5]
- liquid crystals, see Shi et al [6]

Any number of extra Kelvin-Voigt elements can be added in series within the Burgers model, and each will add one extra term to the creep equation, so that most practical creep curves can be reasonably described, with the behaviour at the very shortest times captured by G_1 and at the longest times in steady flow by η , so

$$\frac{\gamma(t)}{\sigma} = J(t) = \frac{1}{G_1} + \frac{1}{G_2} \left(1 - e^{-t/\tau_2} \right) + \frac{1}{G_3} \left(1 - e^{-t/\tau_3} \right) + (\dots) \dots + \frac{t}{\eta} .$$

If the long-time behaviour predicted by this model is extrapolated back to zero time, the intercept is γ_o . If this is divided by the applies stress, we get the so-called equilibrium compliance, J_e , which can be related to the elastic elements we used by

$$J_e = \frac{\gamma_o}{\sigma} = \frac{1}{G_1} + \frac{1}{G_2} + \frac{1}{G_3} + \dots .$$

In fact this extrapolated line is exactly the behaviour of a single Maxwell model, where we have only a spring and a dashpot in series, with the spring elasticity G given by

$$\frac{1}{G} = \frac{1}{G_1} + \frac{1}{G_2} + \frac{1}{G_3} \dots,$$

and a viscous element still given by η . The deformation is then given by

$$J_e = \frac{1}{G} + \frac{t}{\eta}.$$

For many applications, J_e and η are the most useful data to collect, the former being a measure of elasticity at short times and the latter a measure of steady-state deformation at long times. Both eventually become non-linear at large stresses, figure 7 shows a typical example.

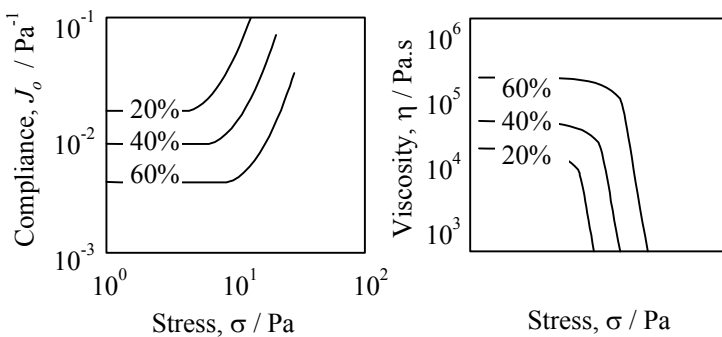


Figure 7: Non-linear creep properties of oil-in-water emulsions with various amounts of oil [7].

13.3.4 Oscillatory tests, or mechanical vibrational spectroscopy

As well as doing creep tests over a range of *time*, we can equally perform oscillatory tests over a range of *frequency*. Then short times correspond to high frequencies, and long times relate to low frequencies. We shall find that for real materials, just as the behaviour at short time is dominated by an elastic response, so too is the behaviour at *high frequency*, and likewise the viscous response that dominates at long times in creep, now shows up as being most import at *low frequencies*.

If we perform an oscillatory test by applying a sine-wave-shaped input of either stress or strain, we can then, using suitable electronic methods, easily resolve (i.e. separate) the resulting sinusoidal strain or stress output into a certain amount of *solid-like* response, which is *in phase* with the input, and a corresponding amount of *liquid-like* response which is $\pi/2$ (i.e. 90°) *out of phase* with the input, see figure 8.

The solid-like component at any particular frequency is characterised by the *storage modulus*, G' , and the liquid-like response is described by the complementary *loss modulus*, G'' . The units of both these moduli are pascals. The values of both these parameters vary with applied frequency, ω , which is given by $2\pi f$, where f is the frequency in hertz (Hz). As all modern rheometers are well able to handle the complicated mathematical calculations necessary for determining these moduli, we do not need to consider the calculation procedure here.

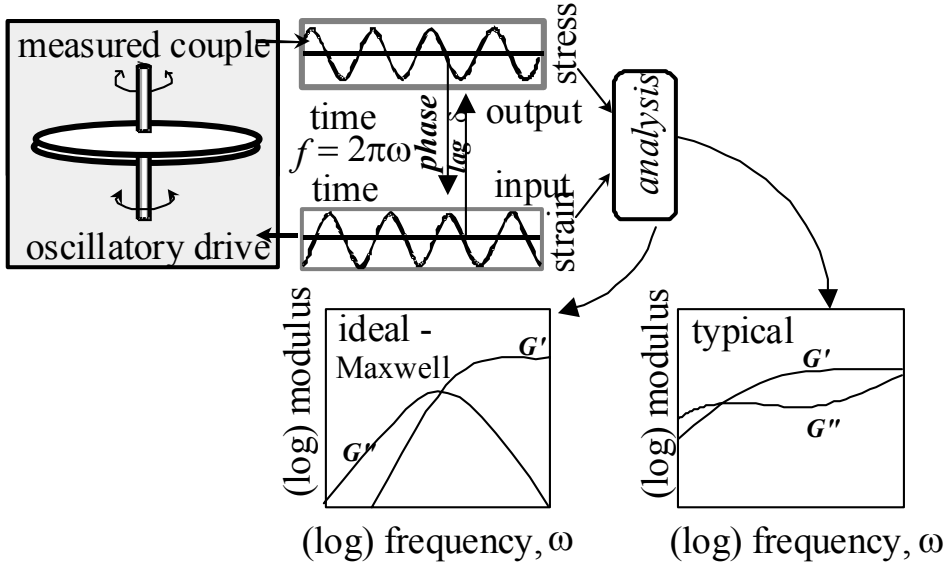


Figure 8: A schematic representation of oscillatory testing.

Note that the G' and G'' data produced by rheometers is sometimes reported in different ways, as for instance

- the dynamic viscosity - $\eta' = G''/\omega$,
- the loss tangent - $\tan \delta = G''/G'$,
- the complex modulus - $G^* = \sqrt{G'^2 + G''^2}$,
- the complex viscosity - $|\eta^*| = \left[(\eta') + \left(\frac{G'}{\omega^2} \right)^{\frac{1}{2}} \right]$.

Note: It is important to realise that there is *no extra information* in any of these other derived parameters compared with that which is contained in the basic G' and G'' information. Hence, we shall only be using these basic G' and G'' parameters.

In the same way that instrument mechanical inertia can cause problems at *short times* in creep tests, so too can it cause difficulties at *high frequencies* in oscillatory tests, especially with respect to the G' data. Even fluid inertia can become important at the latest highest frequencies of around 100 hertz. Fortunately, in good rheometers, these effects are dealt with in the software and the displayed results have had the inertial components eliminated, see figure 9 for a typical example of viscoelastic results corrected for inertia.

13.3.5 Oscillatory tests with a Maxwell model

If we oscillate an ideal spring, at all frequencies $G' = G$ the spring modulus, and G'' is zero. If, on the other hand, we oscillate a perfect dashpot, the loss modulus is given by $G'' = \eta\omega$, and the storage modulus G' is always zero. However, the response of the simplest combination of these two elements in series –

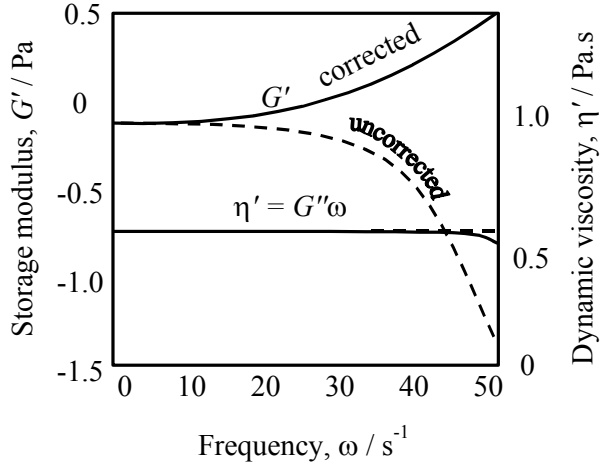


Figure 9: Inertial effects in oscillatory flow illustrated for a silicone fluid [8].

the Maxwell model – gives a far more complex and interesting behaviour over a range of test frequencies, as shown in figure 10, which is given mathematically by

$$G'' = \frac{\eta\omega}{1+(\omega\tau)^2} \quad \text{and} \quad G' = \frac{G(\omega\tau)^2}{1+(\omega\tau)^2}$$

where the relaxation time $\tau = \eta/G$.

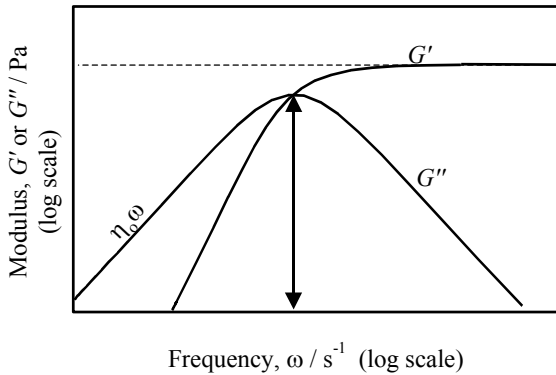


Figure 10: Typical Maxwellian behaviour in oscillatory testing, with the crossover point indicated.

At very low frequencies, G'' is much larger than G' , and hence liquid-like behaviour predominates. However as the testing frequency is increased, G' takes over and solid-like behaviour prevails. The determinant of which kind of behaviour is most significant is the value of the test frequency ω relative to the relaxation time τ . This is a simple way to define a Deborah number, D_e – the ratio of the relaxation time to the test time – and a measure of D_e in this case is $\omega\tau$. Hence, low Deborah numbers always indicate *liquid-like* behaviour, whereas high Deborah numbers means *solid-like* response. At the midpoint, where G'' goes through a maximum; $G' = G''$, and this takes place at a critical crossover frequency of $\omega = 1/\tau$.

As shown above, we can define the dynamic viscosity $\eta' = G''/\omega$, and then for the Maxwell model we see that

$$\frac{\eta'}{\eta} + \frac{G'}{G} = 1 \quad \text{or put another way} \quad \eta' = \eta - \tau G'.$$

This shows a linear relationship between η' and G' over a range of frequencies, which is a quick way to check if data really corresponds to the Maxwell model!

13.3.6 Double or multiple Maxwell models in oscillation

If we combine *two* Maxwell models in parallel, we begin to see features that will later become quite familiar as we examine practical examples of oscillatory curves. The overall behaviour is seen in figure 11, and is the simple sum of the two Maxwell units, so

$$G'' = \frac{\eta_1 \omega}{1 + (\omega \tau_1)^2} + \frac{\eta_2 \omega}{1 + (\omega \tau_2)^2} \quad \text{and} \quad G' = \frac{G_1(\omega \tau_1)^2}{1 + (\omega \tau_1)^2} + \frac{G_2(\omega \tau_2)^2}{1 + (\omega \tau_2)^2}.$$

If the two relaxation times are different by more than a decade, then at very low frequencies η_1 dominates, and at very high frequencies, the elastic response is governed by $G_1 + G_2$.

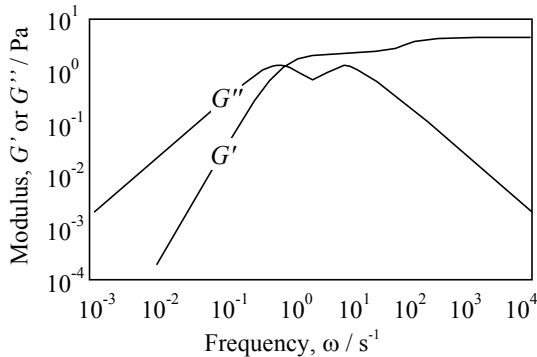


Figure 11: Typical oscillatory response of a double Maxwell model, with both spring moduli set at unity and the time constants set at 1 and 0.1 seconds respectively.

The last in our series of models is the multiple Maxwell model obtained by putting any number of Maxwell elements in *parallel*. The multiple Maxwell model is to oscillatory flow what the multiple Burgers model is to creep testing, in that it begins to represent real systems in a sensible way. The values of the overall storage and loss moduli, G' and G'' , at any frequency ω , are then given by the sum of i contributions from i Maxwell elements

$$G'(\omega) = \sum_i G_i \frac{\omega^2 \tau_i^2}{1 + \omega^2 \tau_i^2} \quad \text{and} \quad G''(\omega) = \sum_i G_i \frac{\omega \tau_i}{1 + \omega^2 \tau_i^2}.$$

Here the dynamic response of a viscoelastic liquid over a range of frequencies can be modelled by choosing a range of Maxwell elements with appropriate values of G and τ chosen to cover the range used in the experiment for which G' and G'' values are available, as say $\tau = 10^{-3}$ s, 10^{-2} s, ... 10^3 s for a frequency range of 10^3 down to 10^{-3} rad/s, together with the appropriate values of G_i . It is obvious that at very high

frequencies the overall storage modulus G' will be given by $G_1 + G_2 + G_3 \dots$, while at the very lowest frequencies, the overall dynamic viscosity η' is given by $\eta_1 + \eta_2 + \eta_3 \dots$, though η_1 will usually dominate.

13.3.7 Oscillation with a Kelvin-Voigt model

The behaviour of a Kelvin-Voigt model is quite simple, since $G' = G$ and $G'' = \eta\omega$, or $\eta' = \eta$. We will not discuss the combination of Kelvin-Voigt models in oscillatory flow, since this is rarely considered. However, as we shall see later, Kelvin-Voigt-type behaviour is seen in at least one part of the viscoelastic spectrum of real materials.

13.3.8 The oscillatory response of real systems

The most general overall G' , G'' response of real examples of structured liquids is shown in figure 12. The exact values of the moduli and their position in the frequency domain will of course vary, but the indicated overall qualitative behaviour is usually seen if data is available over a wide-enough frequency range. A number of specific regions can often be differentiated, namely

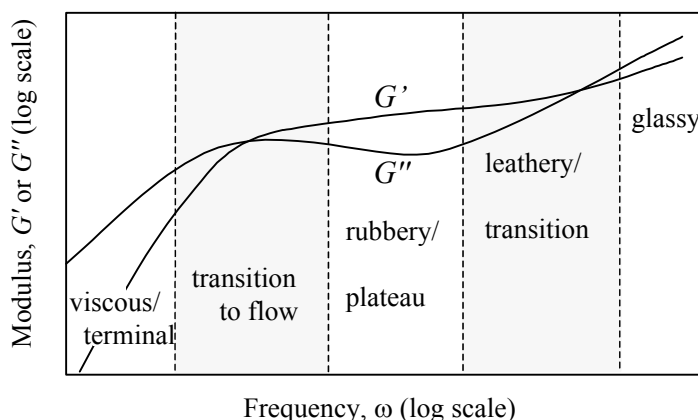


Figure 12: The various regions in the viscoelastic spectrum of non-Newtonian liquids.

(a) the *viscous* or *terminal* region, where G' predominates and viscous (flow) behaviour prevails. All materials have such a region, even solids (because they creep at long times), but the frequency where this is seen is often so low that most oscillatory instruments cannot detect this part of the curve. At low-enough frequencies, G'' is linear with increasing frequency and G' is quadratic, and the longest relaxation time, τ_{max} is given by $G'/(G''\omega)$.

(b) the *transition-to-flow* region is so called because, when viewed from higher frequencies (where elastic behaviour dominates and $G' > G''$), the loss modulus G'' , describing viscous or flow behaviour, becomes significant. The point where the two moduli cross over is sometimes noted, and for a Maxwell model, this crossover frequency is given by the inverse of the relaxation time τ .

(c) the *rubbery* or *plateau* region is where elastic behaviour dominates. While in many cases we see what *appears* to be a flat plateau, there is always a slight increase of G' with frequency, but it can be as small as a few percent increase in modulus per decade increase in frequency. The value of G'' is of course always lower than that of G' , but sometimes it can be considerably so. When the slope of the

storage modulus versus frequency curve (G', ω) is small, the value of G'' decreases with increase in frequency, towards a minimum before rising again. The lower the slope of the (G', ω) curve, the deeper is the G'' 'valley', so that sometimes at the minimum point, G/G'' is greater than 15. This fact is a good example of a very useful approximation in linear viscoelasticity, that is, at any particular frequency

$$G'' \approx \frac{\pi G'}{2} \frac{d \ln G'}{d \ln \omega}$$

where the second term is the local slope of the logarithmic plot of G' versus ω at that frequency. If we express this slope as m , then we can also write

$$\tan \delta \approx \frac{\pi m}{2}.$$

(d) a *leathery* or higher *transition* crossover region is also seen, where, due to high-frequency relaxation and dissipation mechanisms, the value of G'' again rises, this time faster than G' . Once more at $G' = G''$, a crossover frequency can be defined, from which another characteristic time can be obtained.

(e) at the highest frequencies usually encountered in this form of testing, a *glassy* region is seen, where G'' again predominates and continues to rise faster than G' .

When the typical range of frequencies available on most rheometers is used, say 10^{-2} to 10^2 rad/s, it is quite usual to see only two of the regions described above. The particular ones seen depend largely on the longest relaxation time, τ_{max} , of the material being tested, so that if $\omega\tau_{max} \sim 1$, then the *viscous* and *transition-to-flow* regions are seen. If $\omega\tau_{max} > 1$, then often only the plateau region is seen, perhaps with the higher transition point before the *glassy* region. On the other hand, for many dilute polymer solutions, $\omega\tau_{max} < 1$, and G'' always predominates.

If the range of testing is artificially extended by using different temperatures (the so-called time/temperature superposition principle), then for many materials, it is often possible to see all the regions described by superimposing the data using suitable shift factors, see Ferry [9].

The behaviour of a real system, especially a gel or very high molecular weight polymer melt, can be simplistically modelled by dividing it into Maxwell behaviour at low frequencies giving way to Kelvin-Voigt behaviour at high frequencies, see figure 13. In both cases we have crossover frequencies where the critical time is given by $\tau = \eta/G$ from the Maxwell or Kelvin-Voigt models respectively. In the intermediate region, obviously elastic behaviour dominates, and we have the plateau region seen for so many structured liquids, melts and gels.

We will now show various practical examples of viscoelastic behaviour in oscillatory flow.

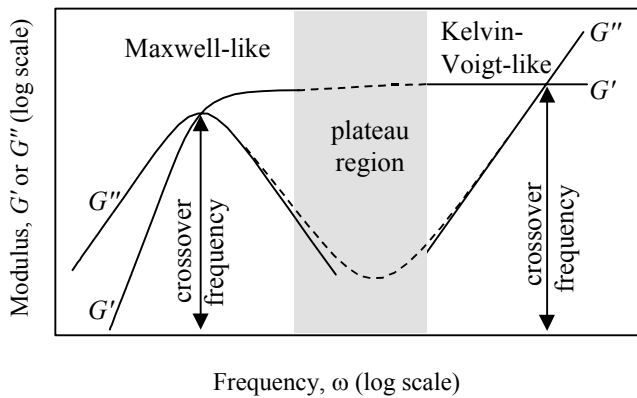


Figure 13: Low and high frequency oscillatory behaviour shown as Maxwellian and Voigt-like behaviour.

13.3.8.1 Viscous/terminal region - simple Maxwell behaviour

There are two specific examples of liquids that often show simple Maxwell-like behaviour within the normal measuring range (10^{-2} - 10^2 Hz), with the expected shapes of the G' and G'' curves and a single relaxation time, *viz.* associative-thickener-type polymers (see chapter 16 for details) and worm-like surfactant micellar systems, otherwise known as threadlike or rod-like micelles (linear or branched). (The latter are also called ‘living polymers’ because if they break under large stresses, they can reform under conditions of rest or low stress (see chapter 18).) The typical response of such a system is shown in figure 14, where a representative relaxation time would be around 1 s, see [10].

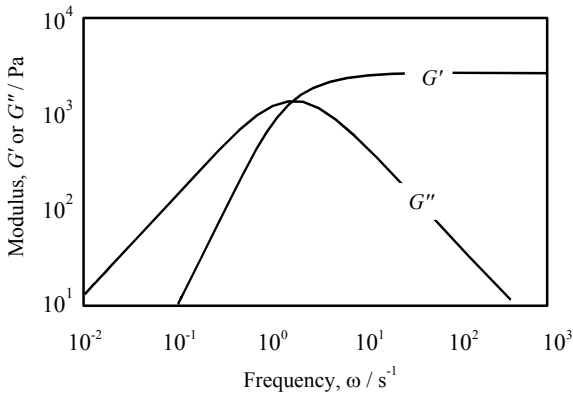


Figure 14: Oscillatory behaviour of an associative thickener.

Some particular examples of these two kinds of systems are:

- associative polymers such as hydrophobic ethoxylated urethane (HEUR), see Annable et al [11].
- aqueous surfactant solutions containing thread-like micelles, see [12-16].

Occasionally other systems have also been reported as showing simple Maxwell behaviour, such as

- an water-in-oil emulsion, see Pons [17]
- the child’s toy Bouncing Putty™, see Benbow et al [18] with, $\eta \sim 10^5$ Pa s, $G = 2.5 \times 10^5$ Pa.

- some organic glasses, Benbow [19].

There are also some systems that show *near*-Maxwell behaviour, and an example is given in figure 15, where in this case a surfactant phase responds with a major relaxation time of around 10 s which is responsible for the prominent maximum in G'' , see [20]. However the contributions from some other faster relaxation mechanisms give a slower-than-expected fall-off of G'' with increase in frequency.

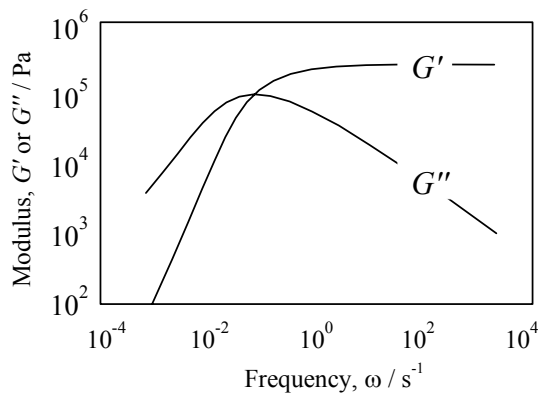


Figure 15: Oscillatory behaviour of the cubic phase of a branched nonionic detergent.

13.3.8.2 Polymer systems

The particular oscillatory regions seen for polymer systems depend on their concentration and molecular weight, as well as the range of frequencies used. The behaviour of concentrated low-molecular-weight systems is shown in figures 16 and 17, where at low frequencies we see the characteristic viscous/terminal regions which correspond more or less to Maxwell-type behaviour, with G'' dominating and at the lowest frequencies being proportional to frequency, but eventually curving over. This feature of the behaviour moves to lower and lower frequencies as the concentration is increased, so that more and more plateau-like behaviour takes over within the experimental 'window' (10^{-2} - 10^2 Hz).

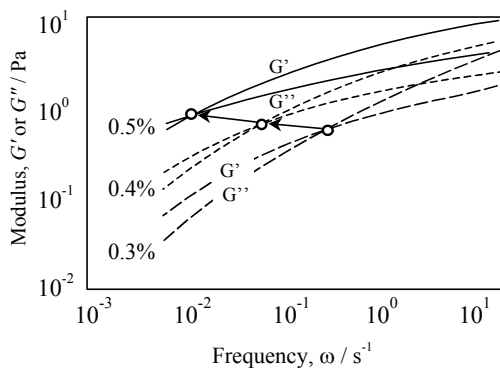


Figure 16: Oscillatory behaviour of aqueous xanthan gum solutions, at various weight percentages, [21].

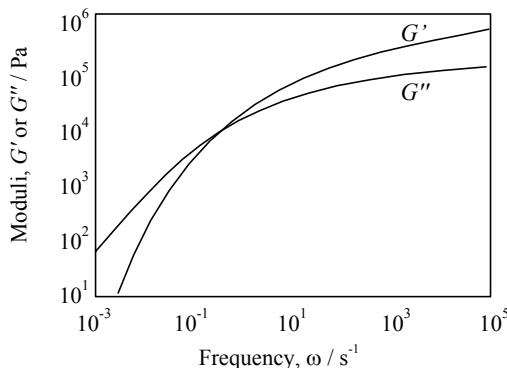


Figure 17: Oscillatory behaviour of low molecular weight polyethylene melt at 150 °C.

For higher molecular weight polymers, whether melts or more concentrated solutions, a pronounced plateau region is seen. Examples of increasing molecular weight and resulting deepening of the G'' valley and the introduction of other

associated features is shown in figures 18 - 21. Figures 18 - 20 are redrawn from Haake Instruments promotional literature, and figure 21 arises from reference [22].

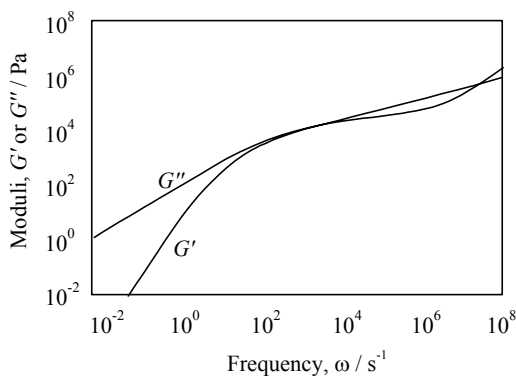


Figure 18: Oscillatory behaviour of polydimethylsiloxane of molecular weight 133,000 at 20 °C.

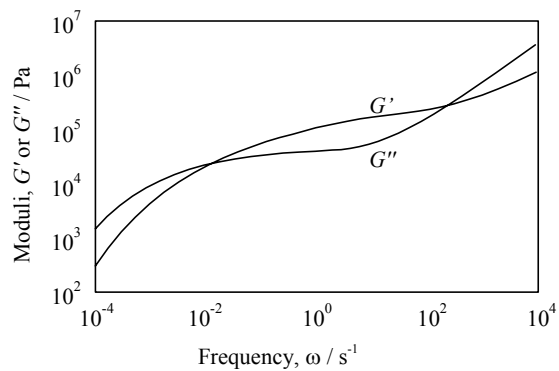


Figure 19: Oscillatory behaviour of 0.4 M broad molecular weight polystyrene at 150 °C.

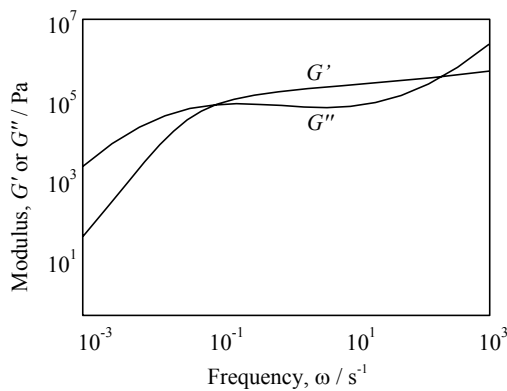


Figure 20: Oscillatory behaviour of PMMA, Mw = 0.12M, polydispersity 1.08, at 185 °C.

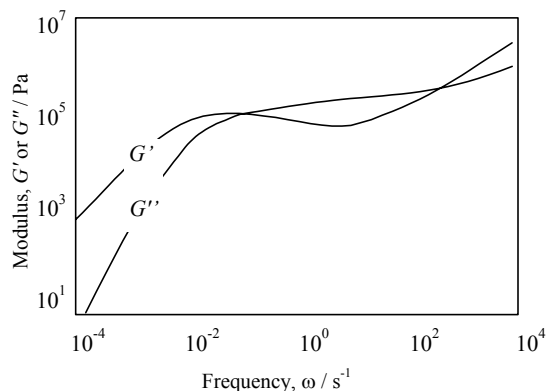


Figure 21: Oscillatory behaviour of narrow molecular weight polystyrene, mol. weight 0.39 M, at 160 °C.

This deepening of the G'' valley with increase in molecular weight is particularly well illustrated in figure 22.

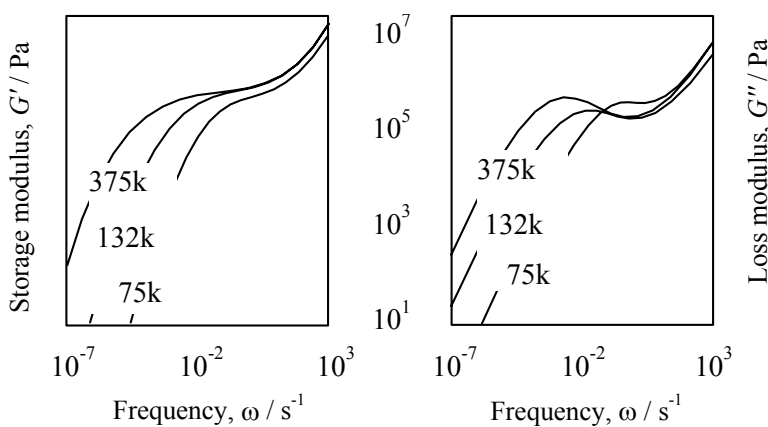


Figure 22: Oscillatory behaviour of a polypropylene melts of various molecular weights.

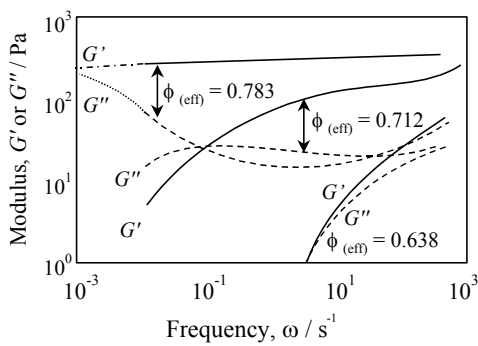


Figure 23: Oscillatory behaviour of 84 nm PMMA particles in decalin, at various effective phase volumes, [23]

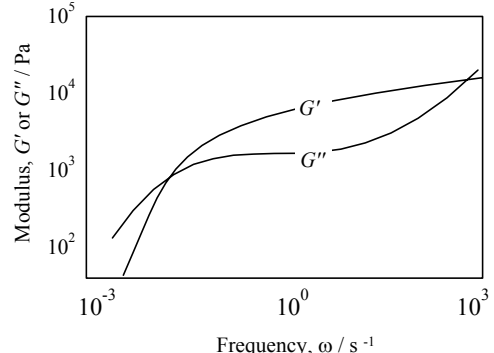


Figure 24: Oscillatory behaviour of a nonionic hexagonal liquid crystalline phase, [24].

13.3.8.3 Dispersions

All dispersions show some viscoelastic behaviour, and hence a measurable value of G' in the *viscous* region; figure 23 shows such a situation where G' and G'' begin to rise as expected at low frequencies, with G'' proportional to ω and G' proportional to ω^2 , but as the concentration rises one moves to a plateau situation, see also figures 24 - 26, where the situation is very analogous to concentrated polymer solutions. Similarly, the possibility of a minimum in G'' and an apparent plateau in G' in a *plateau* or *rubbery* region is often seen, as in figures 27 - 32 showing the response of a range of concentrated dispersions and gels.

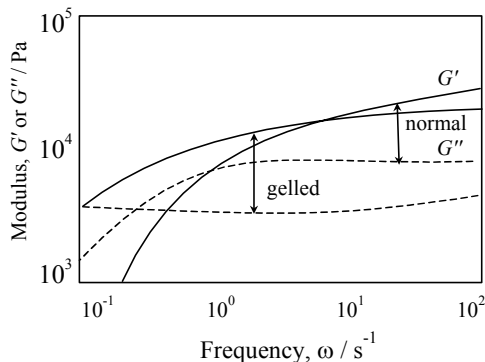


Figure 25: Oscillatory behaviour of two toothpastes, [25].

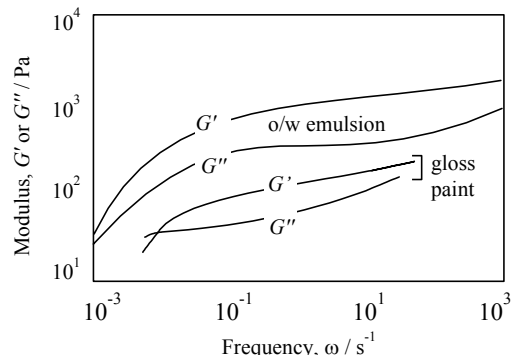


Figure 26: Oscillatory behaviour of a typical oil-in-water emulsion and a gloss paint [26].

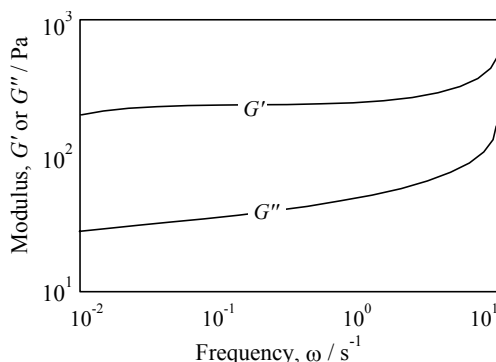


Figure 27: Oscillatory behaviour of a 3% by weight Laponite dispersion in demineralised water.

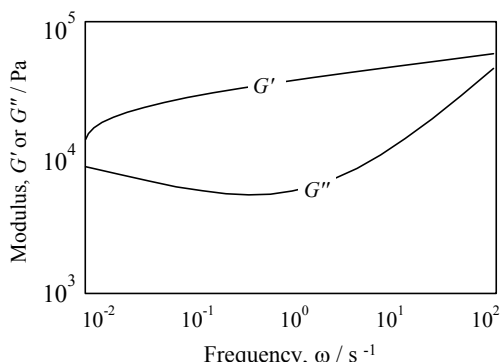


Figure 28: Oscillatory behaviour of a lubricating grease at room temperature, [27].

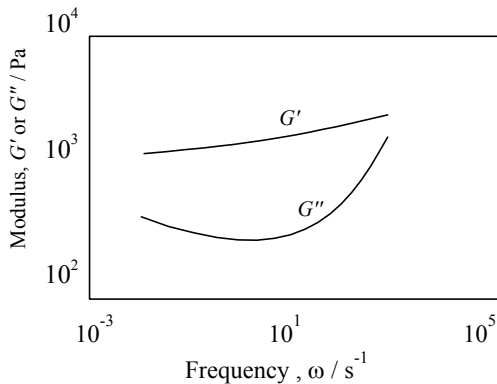


Figure 29: Oscillatory behaviour of a Bentonite, polymer and aqueous electrolyte solution, [28].

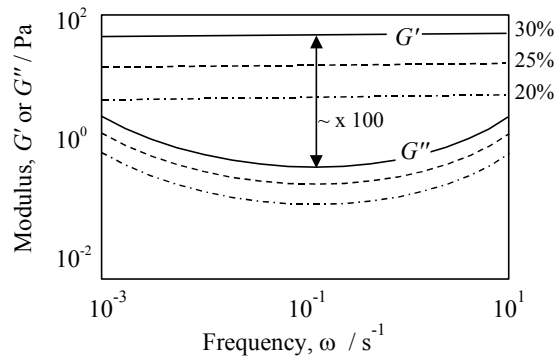


Figure 30: Oscillatory behaviour of a highly charged latex suspension, at three volume fractions, [29].

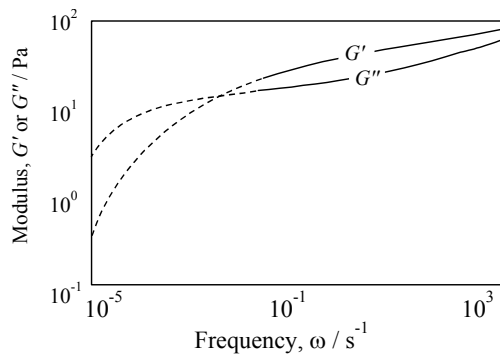


Figure 31: Oscillatory behaviour of a polymer latex suspension; particle size 0.4 microns and phase volume 60%, [30].

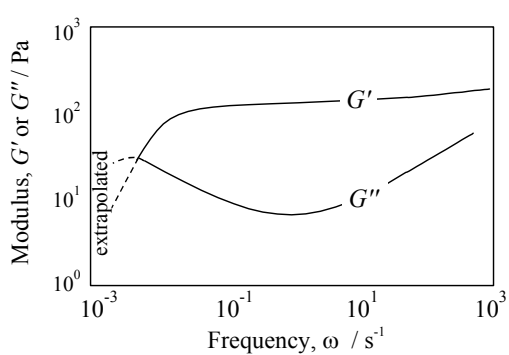


Figure 32: Oscillatory behaviour of a 5% crosslinked starch gel, [31].

13.4 What can you get from oscillatory data?

In qualitative terms the oscillatory curves give a fingerprint of the state of the microstructure in the same way as does an NMR or an infrared spectrum. Just as various mechanisms can be identified and quantified by the position on the frequency axis and the height of the signal so too can oscillatory curves. A number of examples are follow:

(a) At low-enough frequencies, it is possible to obtain η_0 , the zero-shear-rate viscosity, since in that region, $G' = \eta_0\omega$, see figure 33. This can be used in a number of microstructural calculations, as well as for stability predictions. Also, the point where G' departs from being a linear function of frequency is a measure of the departure of the steady-state (σ, γ) curve from linearity, at a shear rate given by the same numerical value of the frequency in radians per second.

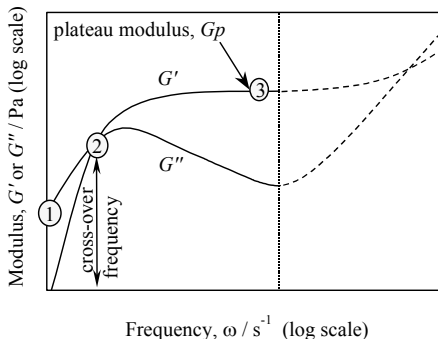


Figure 33: Important features of low-frequency oscillatory data.

(b) The crossover frequency at which $G' = G''$ is a measure of the longest relaxation time, and is given by the inverse of the numerical value in radians per second. This can easily be shown as the case when the Maxwell model is used, where the crossover coincides with the maximum value of G'' and at a frequency such that $\omega\tau = 1$. This has been used as a measure of molecular weight.

(c) If the viscous-to-rubbery region does not overlap the transition-to-glassy region, then a plateau modulus G_p can often be identified where the modulus G' is *nearly* constant. This too can be seen from the use of a single or a multiple Maxwell model, where the modulus is dictated by purely elastic elements. In the ideal case the loss modulus is then much smaller than the storage modulus by over an order of magnitude. This is not always the case, and the plateau modulus is often defined as the value of G' when G'' is a minimum. In fact, the flatter the plateau in G' , the deeper will be the valley in G'' curve beneath it. If G'' does not have a deep minimum, then sometimes one should look for a minimum in G''/G' ($= \tan \delta$) instead, to define the frequency necessary to evaluate G_p .

Once a plateau modulus G_p has been evaluated, it can be used for a number of purposes, see figure 33. First, for polymeric systems, the value of the molecular weight of the chain segments between temporary entanglements, M_e , can be evaluated, since $M_e = \rho RT/G_p$, where R is the universal gas constant ($8.314 \text{ J mol}^{-1} \text{ K}^{-1}$), ρ is the polymer density and T is the absolute temperature, see figure 34.

In disperse systems, the inter-particle force may be evaluated from the value of G_p , since the plateau modulus is given by a mathematical function that contains the radial distribution function and the force that particles exert on one another as a function of their separation, see [32]. If one makes various approximations to the radial distribution function such as a delta function or a cubic lattice, then the force between the particles can be calculated. An example of the use of the plateau modulus for emulsions is given by Sanchez et al [33].

At frequencies above the plateau modulus and loss modulus minimum, other more complicated mechanisms begin to dictate the values of the moduli as both moduli increase again. These are beyond the scope of this book, but anyone interested should read Ferry's excellent book [35].

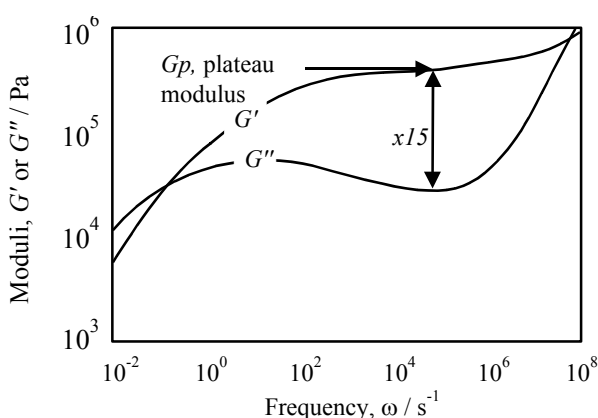


Figure 34: Oscillatory behaviour of atactic polypropylene at 463 °C, [34].

(d) In some cases it is difficult to measure the steady-state viscosity and normal forces for very elastic liquids, since they often flow out of the measuring geometry or else fracture. In this case it is possible to use oscillatory data to reconstruct the steady-state data, at least for polymeric systems, see [1] and [36].

However, this is not possible (and often not necessary) for disperse systems such as suspensions or emulsions, where the elastic forces in steady state are much smaller than the equivalent values in oscillatory flow. In some cases such as a flocculated suspension, the very elastic structure at low stresses gives way to a low viscosity, inelastic liquid at high stresses.

13.5 The relationship between oscillatory and steady-state viscoelastic parameters

13.5.1 General considerations

The following identities are always true for viscoelastic liquids

$$\eta'(\omega)_{\omega \rightarrow 0} = \eta(\dot{\gamma})_{\dot{\gamma} \rightarrow 0} \quad \text{and} \quad \frac{G'(\omega)}{\omega^2}_{\omega \rightarrow 0} = \frac{N_1(\dot{\gamma})}{2\dot{\gamma}^2}_{\dot{\gamma} \rightarrow 0}.$$

These relationships mean that we can extend any oscillatory plot if steady-state data such as zero-shear-rate viscosity from a creep experiment is available (or vice versa). This then dictates the G'' curve, at least to the shear rate where the viscosity departs from η_0 , which in turn prescribes the frequency at which G'' departs from $\eta_0\omega$.

There are various other formulas of this form that can be used for suitable systems over a wider range of shear rates/frequencies, see [37] for details. By and large they fit polymeric liquids, but often fail when used with colloidal systems.

13.5.2 Creep versus oscillatory testing

Which experiments are best, creep or oscillatory? This question is often asked, and the answer is – it depends! First, what do we need the answers for? If we need to look at the long-term behaviour, creep is usually the best kind of test, since the equivalent very low frequencies are difficult to generate. If on the other hand we want to assess quantitatively how ‘wobbly’ a material looks in a bottle, oscillatory testing is ideal. Another important point is that the amplitude of oscillatory testing can be limited, and the test will not exceed the critical amplitude where non-linearities set in, and the material is broken down. This can take some time to recover due to thixotropy. Hence slowly increasing the amplitude of testing and carefully monitoring the output will define the linear region. In creep testing, the amplitude increases relentlessly, and could easily take the material into the non-linear region, see below.

13.5.3 A simple link between creep and oscillatory parameters

Is there any relationship between results from creep and oscillatory experiments? In other areas of science, similar tests can be carried out that utilise either time or frequency as parameters, e.g. NMR and various other spectroscopic techniques, which are analogous to this form of *mechanical* spectroscopy. As in all these areas, the relationship between data in the frequency and time domains is complicated, see such books as [38]. However, in simple terms, we can write down a relationship as follows according to a very approximate formulation worked out by the author, see table 2.

Range of m	G' at $\omega = 1/t$	G'' at $\omega = 1/t$
$m \propto 0.35$ (solid like)	$1/J(t)$	$\approx \frac{1.85m}{J(t)}$
$m \chi 0.35$ (liquid like)	$\frac{\pi}{2} \cdot \frac{(1-m)}{J(t)}$	$1/J(t)$

Table 2: Approximate relationship between creep and oscillatory parameters, where m is the local log/log slope of the creep curve.

These approximate relationships give us a way of comparing and even predicting results between the one test and the another, at least to the extent of being able to check if the results are in reasonable agreement. The correspondence between the inverse of the creep curve and oscillatory behaviour becomes obvious by comparing figures 5 and 6 with figure 12.

13.6 Non-linear response in oscillatory testing

In oscillatory testing, great care has to be taken to ensure that the experiment takes place in the linear region where G' and G'' are independent of the maximum amplitude or stress of the oscillation. A number of examples of non-linear testing are shown in figures 35 - 40 where we see that the most sensitive parameter to breakdown is usually G' , since it eventually falls faster, whereas when G'' does change it can increase before decreasing.

The extent of the linear region can vary from a fraction of one per cent strain up to a strain of unity for certain rubbery systems. In most cases the strain at which non-linearities first become apparent are nearly independent of frequency. This means that for controlled-stress experiments, results can be difficult to compare with corresponding controlled-strain results unless both sets of results are reduced to the same basis.

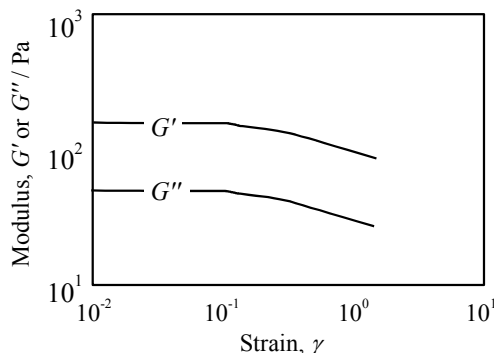


Figure 35: Non-linear oscillatory behaviour of a hair gel at 3 Hz, [39]

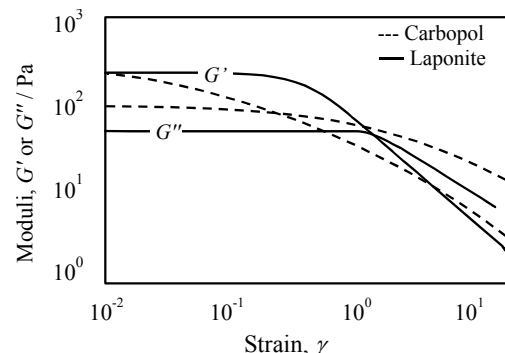


Figure 36: Non-linear oscillatory behaviour of a Laponite suspension at 1Hz compared with a similar dispersion of Carbopol.

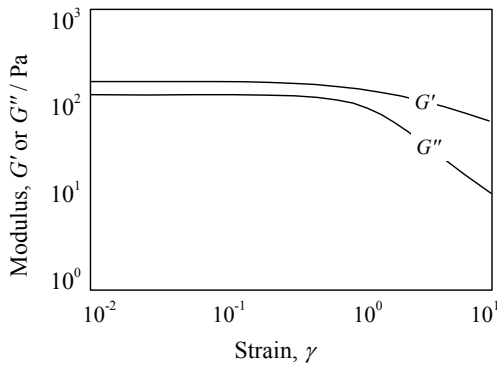


Figure 37: Non-linear oscillatory behaviour of Bonjela, a commercial oral preparation, at 1 Hz.

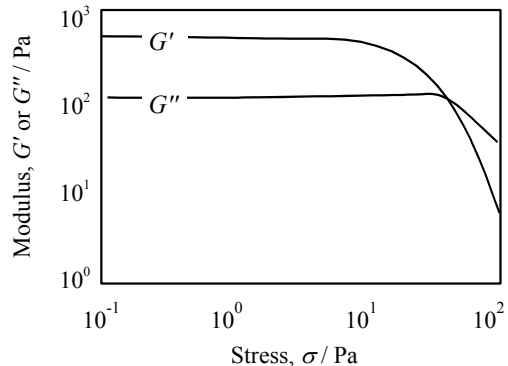


Figure 38: Non-linear oscillatory behaviour of a commercial sample of ketchup, see [40].

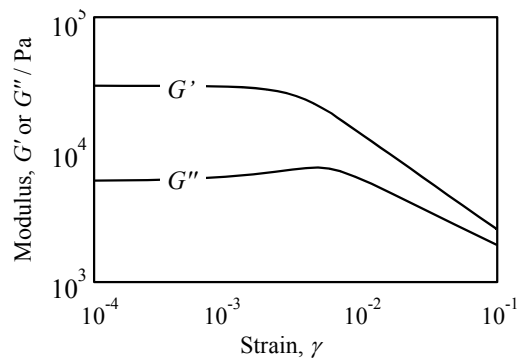


Figure 39: Non-linear oscillatory behaviour of a strong flour dough at 10 Hz.

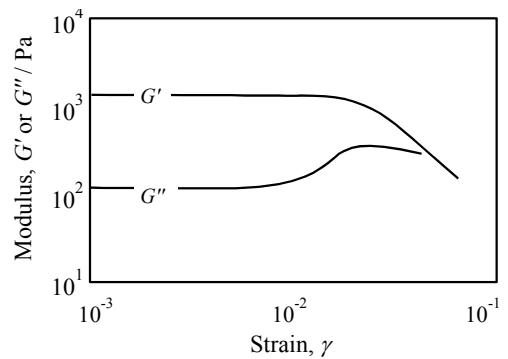


Figure 40: Non-linear oscillatory behaviour of a Bentonite suspension.

13.7 Using oscillatory data to monitor curing, and rebuilding after shear

Oscillatory testing is ideal for following the rebuilding of the microstructure of sheared systems, or for tracking the setting or curing of gelling systems. This is because when we operate in the linear G' and G'' regions, the amplitude is small enough so as not to interfere with the microstructure or the curing/setting mechanism. An example is shown in figure 41, where the response changes from a loss-modulus-dominated (G'') viscous situation at short times, to a storage-modulus-dominated (G') elastic situation at long times.

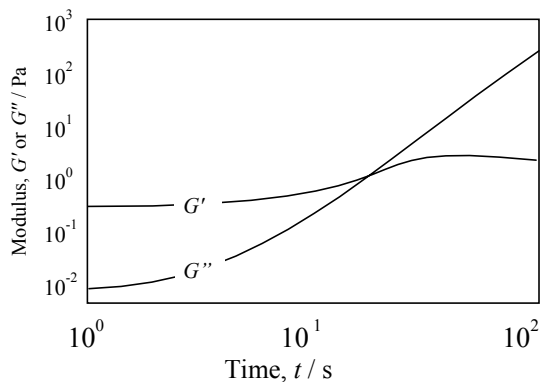


Figure 41: Oscillatory parameters during the gelation of a guar-gum/borate dispersion.

Obviously the gelling times are crucial in, for instance, dental applications, where patients will not tolerate very long curing times for moulding materials in

their mouths. Besides, simple dental economics would dictate a reasonable time which is long enough to manipulate the setting material around the teeth, but is not too long for eventual curing, see figure 42 for an example of a good and bad material. Epoxy resins can be allowed to set over longer times if the strengths produced are better with slower setting, see figure 43, or again, time might be at a premium.

An example of rebuilding after shear is given by the silica gel in polydimethyl siloxane sample shown in figure 44, here the complete G' and G'' curves are given, but again it is obvious that the G' build-up is most significant—as the case of curing and setting—showing once again the sensitivity of this parameter to microstructure. The development of the plateau region is clearly seen as an evidence of the formation of a network. Another example, but for a single frequency (~ 1 hertz) is shown in figure 45.

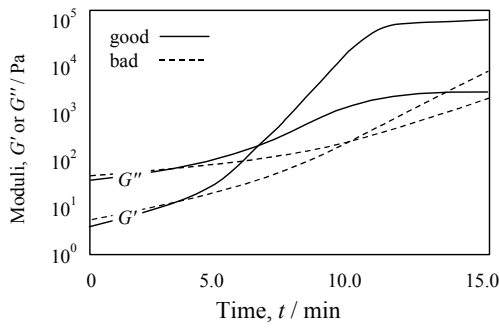


Figure 42: Oscillatory parameters during the curing of two orthodontic silicone gels at 2 Hz, see [39].

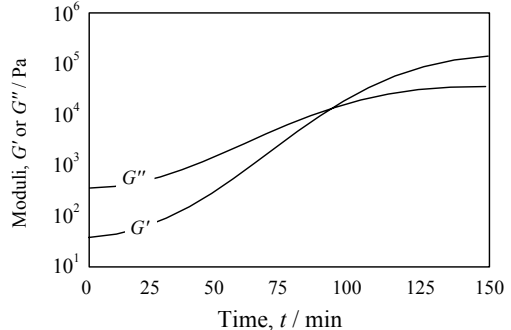


Figure 43: Oscillatory parameters during the curing of an epoxy resin, measured at 0.5 Hz, see [39].

At very short times, we have simple elastic behaviour, and $\sigma = G\gamma$, but then the stress begins to fall, first of all it does so linearly (expanding the exponential to the first term gives $\sigma/\gamma = G(1 - t/\tau \dots)$). The stress then continues to die away, so that when $t = \tau$, the stress has dropped to $1/e$ ($\sim 37\%$); for $t = 2\tau$, to $1/e^2$ ($\sim 13.6\%$), etc., and on a semi-logarithmic scale displays a straight line, see figure 46. Thus at the shortest times the Maxwell model does not know it has liquid-like properties, and at the longest times it has forgotten that it has solid-like properties!

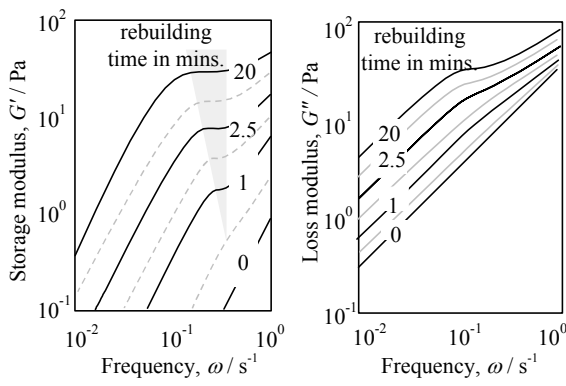


Figure 44: Oscillatory parameters during the rebuilding of a silica gel in polydimethyl siloxane after shearing.

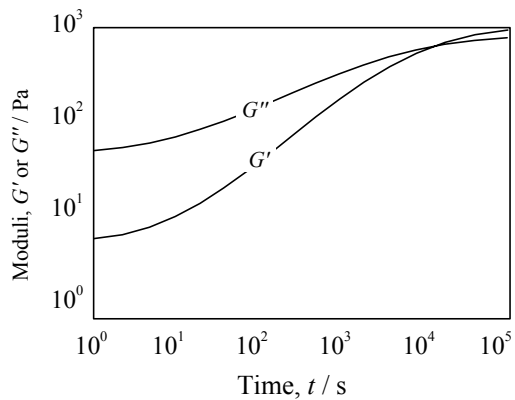


Figure 45: Oscillatory parameters during the rebuilding of a flocculated sepiolite suspension after shearing at 30 s, see [42].

13.8 Stress relaxation testing

Suddenly deforming a viscoelastic liquid to a predetermined strain results in a stress that, once attained, begins to fall off rapidly with time. This decrease eventually slows down, and sometimes appears to approach a steady-state value at long times.

If the liquid under test corresponded to a Maxwell model, the behaviour is given by

$$\frac{\sigma(t)}{\gamma} = Ge^{\frac{-t}{\tau}}$$

where again $\tau = \eta/G$, see figure 46.

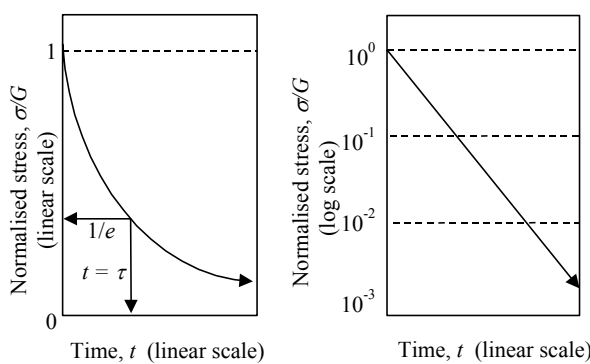


Figure 46: Stress relaxation of a Maxwellian liquid plotted as either a linear or a logarithmic function of the normalised stress.

For real viscoelastic liquids, the stress relaxation curve is usually described by a series of Maxwell models in parallel, so

$$\frac{\sigma(t)}{\gamma} = G_1 e^{\frac{-t}{\tau_1}} + G_2 e^{\frac{-t}{\tau_2}} + G_3 e^{\frac{-t}{\tau_3}} \dots$$

where the various parameters are usually obtained by non-linear curve fitting programmes.

13.9 Start-up experiments

Normal viscometer-type operation consists of applying a constant shear rate to a sample and monitoring the ensuing stress. If the liquid being tested is viscoelastic, the stress can take a finite time to come to its equilibrium value. If the shear rate is low and the steady-state viscosity is constant as a function of stress, then the stress builds up slowly. If however the shear rate is high, the stress can overshoot, going through a maximum before reaching a lower steady-state value, because the response has moved into the non-linear region.

If we suddenly start deforming the simple Maxwell model at a shear rate of $\dot{\gamma}$, the stress slowly builds up as

$$\sigma = \eta \dot{\gamma} (1 - e^{-t/\tau}).$$

At very short times this simplifies to $\sigma = G \dot{\gamma} t$, or $\sigma = G\gamma$ which is simple elastic behaviour. Then at $t = \tau$, the stress is $1/e$ of its value at steady state, where it is $\sigma = \eta \dot{\gamma}$, i.e. purely steady-state viscous behaviour. The start-up of real viscoelastic liquids may need to be modelled using a number of Maxwell elements. However, for most realistic experiments using this kind of test, the response quickly enters the non-linear region since the strain is continually increasing.

Last of all, for a Kelvin-Voigt model, if we apply a constant strain rate, $\dot{\gamma}$, then simply $\sigma = \dot{\gamma} [Gt + \eta]$, so that at zero time, $\sigma = \eta \dot{\gamma}$, i.e. viscous behaviour, and at *very* long times, $\sigma \sim G \dot{\gamma} t$, which is complete elastic behaviour. However, this kind of behaviour is rarely, if ever, seen in practice.

References

- [1] Al-Hadithi, T. S. R; Barnes, H. A; Walters, K., Colloid and Polym. Sci., 270(1), 40-46 (1992).
- [2] Tanner, R.I, 'Engineering Rheology', Clarendon Press, Oxford, 1985.
- [3] Kaschta, J; Schwarzl, F.R., in 'Theoretical and Applied Rheology', Proc. XIth Int. Congr. on Rheol., ed. P. Moldenaars; Keunings, R., Elsevier Science, Amsterdam, 1992.
- [4] Liao, H.J; Okechukwu, P.E; Damodaran, S; Rao, M.A., J. Texture Studies, 27(4), 403 - 418 (1996).
- [5] Zupancic, A., Applied Rheology, 7(5), 219 - 226 (1997).
- [6] Shi, H.Q; Chen, S.H; deRosa, M.E; Bunning T.J; Adams, W.W., Liquid Crystals 20(3), 277 - 282 (1996).
- [7] Gladwell, N; Rahalkar, R.R; Richmond, P., Rheol. Acta, 25, 55 - 61 (1986).
- [8] Jones, T.E.R; Davies, J.M; Barnes, H.A, in 'Advances in Rheology', Proc. IXth Int. Congr. on Rheology, Ed. B Mena et al, Universidad Nacional Autonoma de Mexico, Vol. 4, pp. 45-52, 1984.
- [9] Ferry, J.D., 'Viscoelastic Properties of Polymers', 2nd Edition, John Wiley, New York, 1970.
- [10] Fannum, G; Bakke, J; Hansen, F.K., Coll. & Polym. Sci., 271(4), 380 - 389 (1993).
- [11] Annable, T; Buscall, R; Ettelaie, R; Shepherd, P; Whittlestone, D., Langmuir, 10(4), 1060 - 1070 (1994), and Annable, T; Buscall, R; Ettelaie, R; Whittlestone, D., Langmuir, 37(4), 695 - 726 (1993).
- [12] Shikata, T; Hihon Reoroji Gakkaishi, 25(5), 255 - 265 (1997).
- [13] Fischer, P; Rehage, H., Langmuir, 13(26), 7012 - 7020 (1997),
- [14] Ali, A.A; Makhloifi, R., Physical Review, 56(4), 4474 - 4478 (1997),
- [15] M.E. Cates, J. Phys.-Condensed Matter, 8(47), 9167 - 9176 (1996), and Structure and Flow in Surfactant Solutions, 578, 32 - 50 (1994).
- [16] Hoffmann, H., Structure and Flow in Surfactant Solutions, 578, 2 - 31 (1994),
- [17] Pons, R; Erra, P; Solans, C; Ravey, J.C; Stebe, M.J., J. Phys. Chem., 97(47), 12320 - 12324 (1993)
- [18] Benbow, J.J; Cogswell, F.N; Cross, M.M., Rheol. Acta, 15, 231 - 237 (1976)
- [19] Benbow, J.J., Lab. Practice, 12, 6 (1973).
- [20] Richtering, W; Linemann, R; Langer, J., 'Progress and Trends in Rheology', 4th European Rheology Conference, Ed. Gallegos, C., Steinkopff, Darmstadt, 1994, pp. 597 - 599.
- [21] Carnali, J., J. Appl. Polym. Sci., 43, 929 - 941 (1991).

- [22] Cassagnau, P; Montfort, J.P; Marin, G; Monge, P., *Rheol. Acta*, 32(2), 156 – 161 (1993).
- [23] Mewis, J., unpublished IFPRI report.
- [24] Cordobes, F; Gallegos, C., Proc. 5th European Rheology Conference, Stein-Koppf, Darmstadt, 1998, pp. 519 & 520.
- [25] Bohlin Instruments promotional literature.
- [26] Gallegos, C., Proc. XIIth Congr. on Rheology, ed. Ait-Kadi et al, Canadian Rheology Group, Laval University, 1996, pp. 785 & 786.
- [27] Haake promotional literature.
- [28] Marchal, P; Moan, M; Choplin, L., 'Progress and Trends in Rheology', 4th European Rheology Conference, ed. Gallegos, C., Steinkopff, Darmstadt, pp. 669 – 671.
- [29] van der Vorst, B; Toose, M; van der Ende, D; Mellema, J., 'Progress and Trends in Rheology', 4th European Rheology Conference, Ed. Gallegos, C., Steinkopff, Darmstadt, 1994, pp. 699 – 701.
- [30] Mewis, J., unpublished IFPRI report.
- [31] Gluck-Hirsh, J.B; Kokini, J.L., *J. Rheol.*, 41(1), 129 – 139 (1997).
- [32] Zwanzig, R; Mountain, R.D., *J. Chem. Phys.*, 43, 4464 (1965).
- [33] Sanchez M. C; Berjano, M; Guerrero, A; Brito, E; Gallegos, C., *Can. J. Chem. Eng.*, 76(3), 479-485 (1998).
- [34] Echstein, A; Sulm, J; Friendrich, C; Maier, R. -D; Sassmannhausen, R; Bochmann, M; Mulhaupt, R., *Macromolecules*, 31(4), 1335 – 1340 (1998).
- [35] Ferry, J.D., 'Viscoelastic Properties of Polymers', 2nd Edition, John Wiley, New York, 1970.
- [36] Cox, W.P; Merz, E.H., *J. Polym. Sci.*, 28, 619 (1958).
- [37] Barnes, H. A; Hutton, J. F; Walters, K., 'An Introduction to Rheology', Elsevier, Amsterdam 1989.
- [38] Tschoegl, N.W., 'The Phenomenological Theory of Linear Viscoelastic Behaviour', Springer-Verlag, Berlin, 1989.
- [39] Haake Instruments promotional literature.
- [40] Lapasin, R; Martorana, A; Grassi, M; Pricl, S., Proc. 5th European Rheology Conference, ed. Emri, I, Steinkopff, 1998, pp. 579 & 580.
- [41] Phan-Thien, N; Safari-Ardi, M., *JNNFM*, 74(1-3), 137-150 (1998).
- [42] Mewis, J., unpublished IFPRI report.

CHAPTER 14: NON-LINEAR VISCOELASTICITY

'In any real material ... rearrangements necessarily require a finite time ... [therefore] all real materials are viscoelastic', Nicholas W. Tschoegl.

14.1 Everyday elastic liquids

There are many situations encountered in everyday life around the home where elastic (or to be more precise, *viscoelastic*) liquids are encountered, and their *viscoelasticity* is very evident. They are either stringy when poured or wobbly when shaken or swirled. Various other overt elastic properties are sometimes seen, such as *die swell* as very viscoelastic liquids expand when squeezed out of tubes.

Among everyday liquids that show some of these effects are

- egg-white
- toothpaste
- shower gels
- half-set jelly
- thickened bleaches
- hair shampoos
- oven cleaners (very caustic!)
- low-calorie vinegraites
- thixotropic paints
- flour doughs

There are also more viscous gelled materials that show strong elastic properties, such as Swarfega™, Jungle Gel™ or similar hand-washing products, as well as some kinds of greases, where the product is so elastic that it resonates or 'rings' in its plastic container when the container is struck.

In most of these cases the elastic behaviour arises from high-molecular-weight polymers dissolved in the continuous phase, or else from the presence of rodlike-micellar ('living' polymers) structured surfactant phases.

Although all these examples also manifest large elastic effects in linear measurements as described in chapter 13, the same is not always true for non-linear measurements. There are many 'colloidal' systems that show large values of storage modulus in small-amplitude testing that do not show any visible large-amplitude elastic effects such as die swell or other similar phenomena (hence large G'), see [1]. Examples of such systems include flocculated dispersions and emulsions, where the linear viscoelasticity arises from the formation of chains of particles, which easily break on shearing at large strains and in steady-state flows.

Exercise: collect some elastic liquids from your home, and rank them in terms of their viscoelasticity, using whatever criteria seem appropriate.

14.2 Some visible viscoelastic manifestations

There are many situations where, if viscoelastic forces manifest themselves on a grand scale, large changes can occur in flow and force patterns. Figures 1 to 7 show some striking examples of these effects.

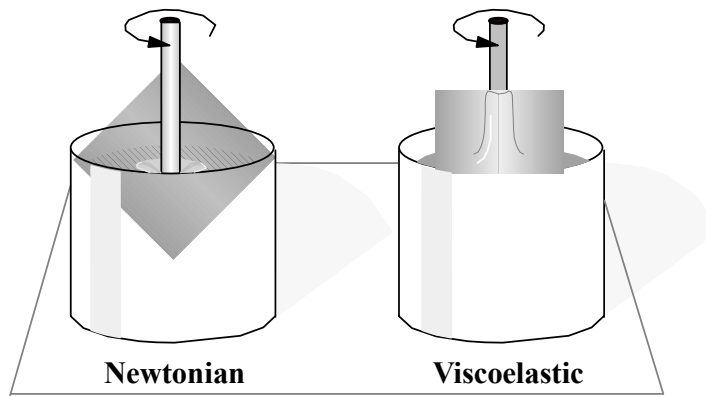


Figure 1: The Weissenberg effect, seen as the rod-climbing in an elastic liquid, as opposed to the inertial dipping in a Newtonian liquid.

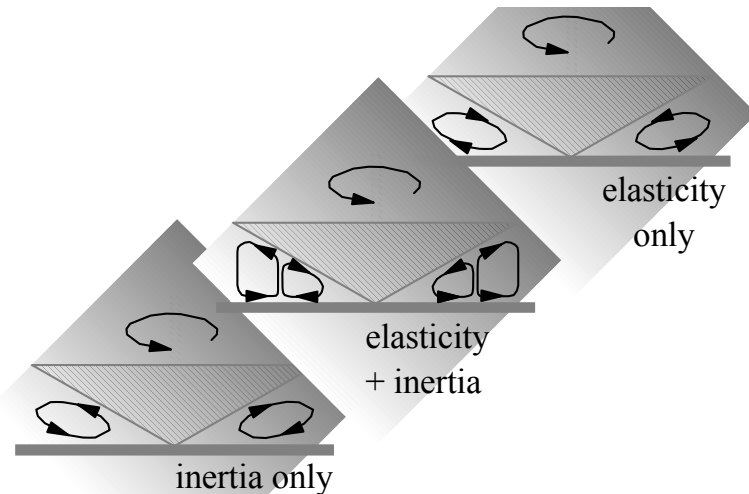


Figure 2: The effect of viscoelasticity in a cone-and-plate configuration, in conjunction with the competing inertial force.

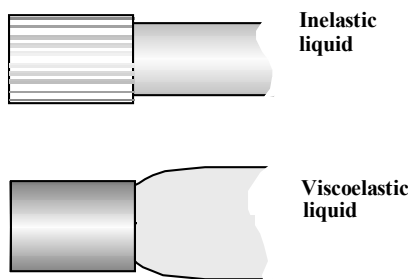


Figure 3: The flow of a Newtonian and a viscoelastic liquid out of a tube, showing viscoelastic 'extrudate swell'.

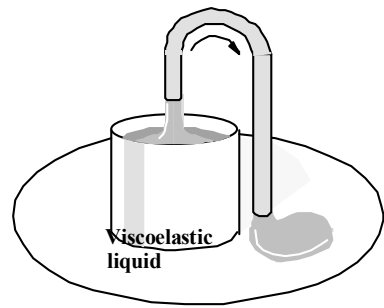


Figure 4: The tubeless siphon: look, no tube!

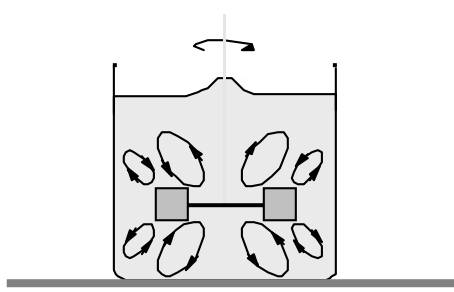


Figure 5: The effect of viscoelasticity in a simple turbine mixer configuration, with the effect of the competing inertial force.

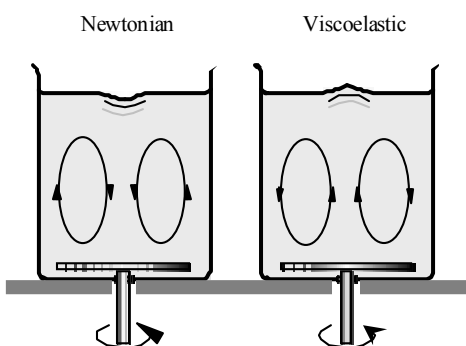


Figure 6: The Weissenberg effect, as seen within an elastic liquid, compared with the inertial effect in a Newtonian liquid.

Clearly they are important in many practical and industrial applications. All these effects arise essentially because of tension along the streamlines generated in the flow of these viscoelastic liquids which are not present in Newtonian liquids, and this tension is associated with the so-called *first normal-stress difference*.

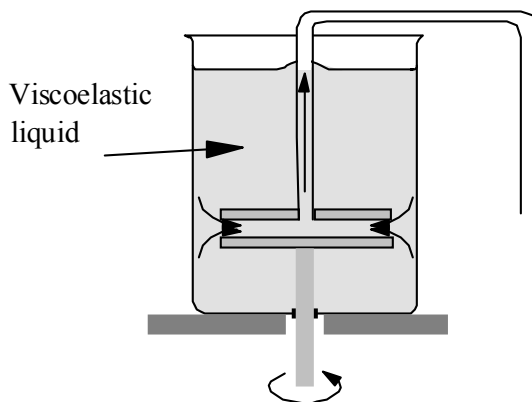


Figure 7: The 'normal force' pump.

Figure 8 shows a simple but useful analogy to this situation. It compares a squeezed solid rubber cylinder and a sheared viscoelastic liquid cylinder, where in both cases a force emerges at right angles—or normal—to the squeezing direction: hence we talk about a *normal force*.

In the case of a viscoelastic liquid the squeezing action arises from the tension along the circular streamlines which result in an inward ‘strangulation’ force, otherwise called a *hoop stress* [2].

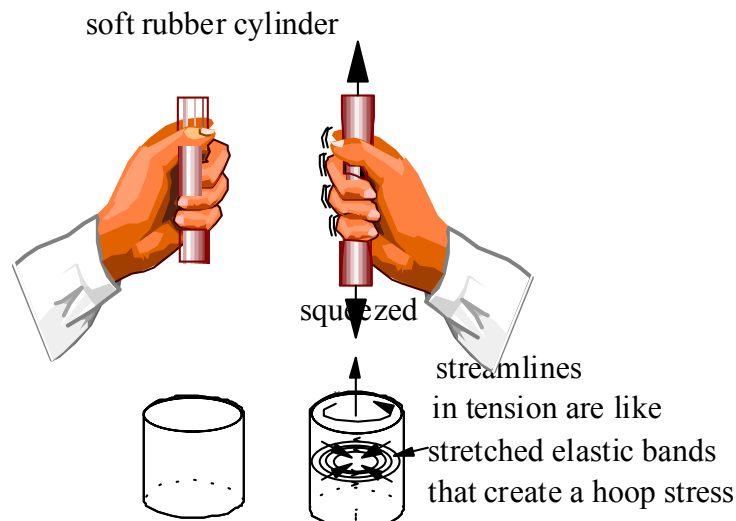


Figure 8: An analogy to the normal force created in a sheared cylinder of elastic liquid.

Another (but smaller) non-linear viscoelastic force called the *second normal-stress difference* (see later for an explanation of this term) has a special rôle to play in a number of other situations such as

- shear fracture in rotational instruments such as cone and plate
- Taylor instabilities
- die swell
- flow in non-circular pipes

14.3 The proper description of viscoelastic forces

The viscoelastic forces that produce the remarkable manifestations illustrated above are properly characterised in shear flow by the so-called first and second normal-stress differences, N_1 and N_2 , which occur in addition to the shear stress σ (with which we are already familiar) –note that occasionally N_1 and N_2 are called the primary and secondary normal stress differences. The complete stress distribution in a flowing viscoelastic liquid may be written down formally as follows,

$$\sigma = \eta \dot{\gamma},$$

$$\sigma_{xx} - \sigma_{yy} = N_1, \text{ and}$$

$$\sigma_{yy} - \sigma_{zz} = N_2$$

where η , N_1 and N_2 are called *viscometric functions*. At this stage we do not need to be too concerned about understanding the origins and mathematics of these forces,

but we do need to appreciate the general form of the curves shown later in this chapter just as we have examined non-Newtonian viscosity.

The viscoelastic equivalents to viscosity—the stress divided by the shear rate—are the so-called first and second normal-stress *coefficients*, Ψ_1 and Ψ_2 . These are given by the first and second normal-stress differences divided by the shear rate *squared*, so

$$\Psi_1 = \frac{N_1}{\dot{\gamma}^2},$$

and

$$\Psi_2 = \frac{N_2}{\dot{\gamma}^2}.$$

The typical form of these coefficients is not unlike that of the non-Newtonian viscosity, with a high plateau at low shear rate, giving way to a decreasing power-law form above a critical shear rate, and at high-enough shear rates it begins to flatten out again. This means that at low-enough shear rates, both N_1 and N_2 increase quadratically with shear rate. Then in the shear-thinning region, the coefficients always drop off faster than the complementary viscosity. At higher shear rates, the rise is not so steep, and is often nearly linear. At the highest shear rates, the dependence increases again towards a quadratic dependence on shear rate. All these features are shown in figures 9 and 10.

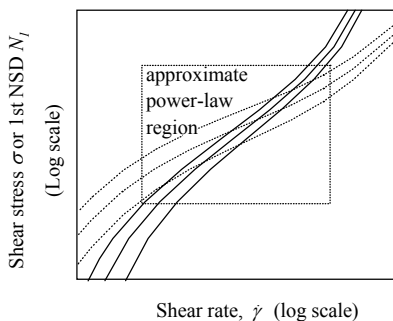


Figure 9: An idealised plot of the shear stress (dotted line) and first normal-stress difference (1st NSD, solid line) as a function of shear rate for a wide range of shear rate and concentration or molecular weight.

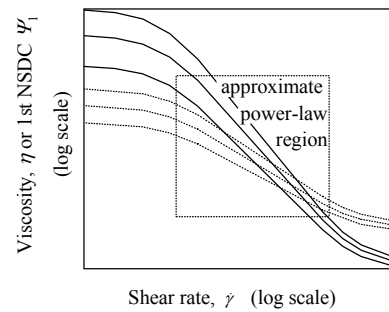


Figure 10: An idealised plot of viscosity (dotted lines) and first normal-stress difference coefficient (1st NSDC, solid lines) as a function of shear rate for a wide range of shear rate and various concentrations or molecular weights.

Generally speaking, the second normal-stress difference is a fraction of the first—usually less than a quarter—and of the opposite sign.

14.4 The measurement of viscoelastic forces

There are a number of ways in which N_1 and N_2 can be measured as a function of shear rate. The easiest and most convenient measurements can be made using a combination of rotating cone-and-plate and parallel-plate tests. When a viscoelastic liquid is sheared in these geometries, not only is the customary drag force experienced, but a force now arises that tends to push the plates apart. This force, F , when measured, can be used to evaluate the respective normal-stress differences. The following formulas apply to the cone-and-plate, parallel-plate and

re-entrant cone-and-plate geometries respectively, see figure 11, (in all cases the radius of the plates is a),

$$N_1 = \frac{2F}{\pi a^2},$$

$$N_1 - N_2 = \frac{2F}{\pi a^2} \left(1 + \frac{1}{2} \frac{d \log F}{d \log \dot{\gamma}} \right),$$

$$N_2 = \frac{h + a \tan \beta}{h} \left[N_1 - \frac{F}{\pi a^2} \left(2 - \frac{\partial F}{\partial h} \right) \right]_{\omega}$$

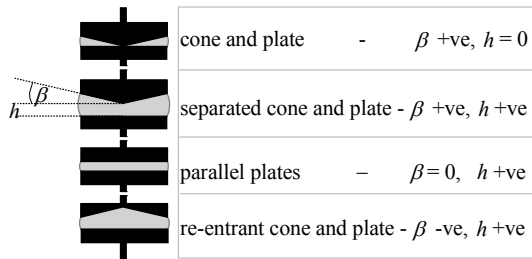


Figure 11: Various cone-and-plate and parallel-plate configurations used to measure normal force, showing the values of the gap and cone angle.

where F is, as stated above, the total normal force or thrust on the configurations, h is the edge gap between the plates, and β is the cone angle (which is either positive or negative). In all the experiments, h is a variable. In the last formula, all the evaluations are made at the same rotation speed ω , see [3].

The normal-force differences are evaluated in every case at the edge shear rate, which is given by $\dot{\gamma}_a = a\omega/h$. From a combination of two or more of these measurements, N_1 and N_2 can be separately determined.

14.5 Examples of first normal-stress differences

Particular examples of the first normal-stress difference N_1 or its coefficient Ψ_1 are shown in figures 12 - 29, where a comprehensive collection of examples is given for polymer solutions and melts, as well as an emulsion. These are compared with either the equivalent shear stress or the viscosity. All the different possible combinations of shear and normal-stress difference, and viscosity and normal-stress coefficient are displayed to show the way that results are presented in the rheological literature. The figures are set out to illustrate overall behaviour, with especial emphasis on low shear-rate and mid-range (i.e. power-law) behaviour.

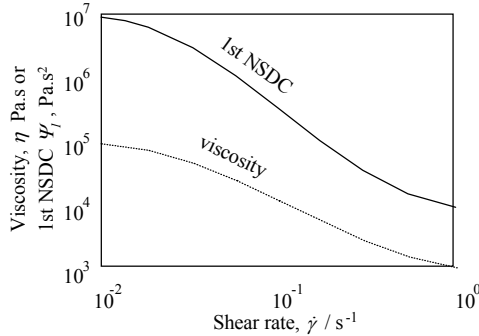


Figure 12: The viscosity and first normal-stress difference coefficient (1st NSDC) as a function of shear rate at room temperature for 20 wt. % polystyrene (Mw ~ 2 M) in tricresyl phosphate, [4].

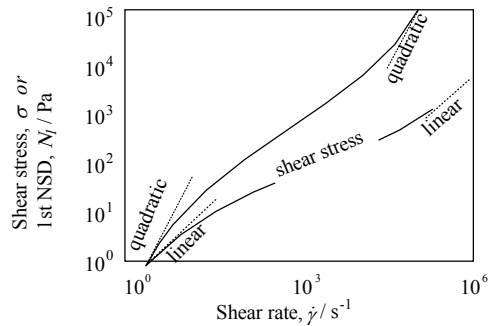


Figure 14: The shear stress and first normal-stress difference (1st NSD) as a function of shear rate at room temperature for a 0.5% hydroxyethyl cellulose solution, [6].

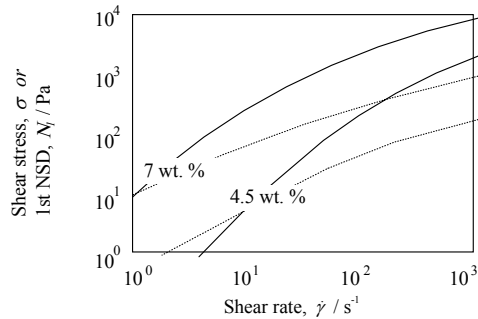


Figure 16: The shear stress (dotted lines) and first normal-stress difference (1st NSD, solid lines) as a function of shear rate at room temperature for solutions of polyacrylate in dipropylene glycol methyl ether, [8].

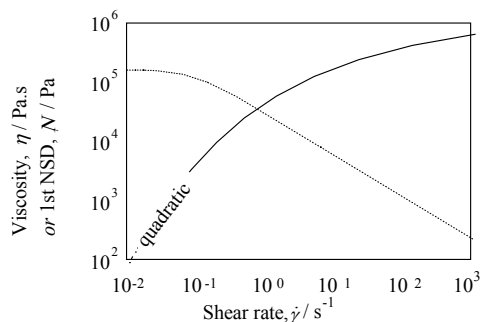


Figure 18: The viscosity (dotted line) and first normal-stress difference (1st NSD, solid line) as a function of shear rate for a HDPE melt at 200°C, [10].

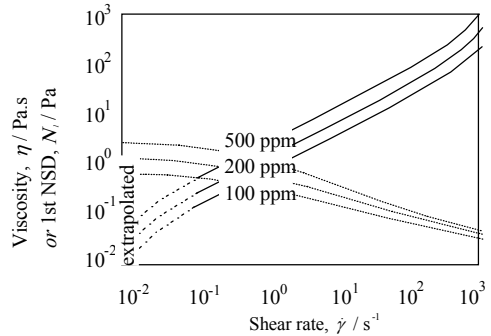


Figure 13: The viscosity (dotted lines) and first normal-stress difference (1st NSD, solid lines) as a function of shear rate at room temperature, for 100, 200 & 500 ppm polyacrylamide (AP-30) solutions respectively, [5].

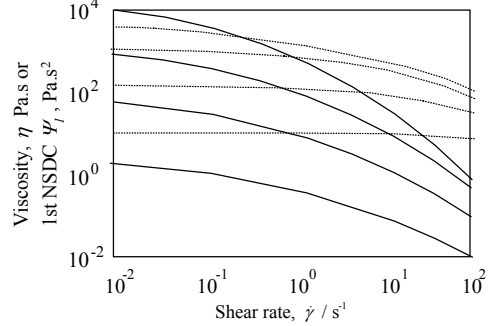


Figure 15: The viscosity (dotted lines) and first normal-stress difference coefficient (1st NSDC, solid lines) as a function of shear rate for solutions of polyvinyl acetate in benzyl alcohol, [7].

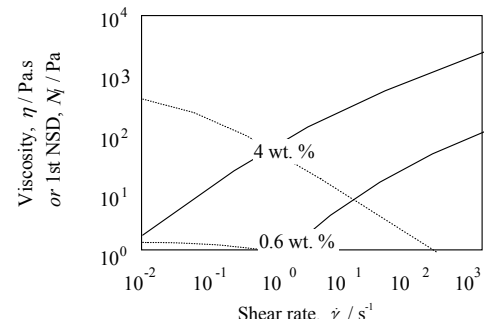


Figure 17: The viscosity (dotted lines) and first normal-stress difference (1st NSD, solid lines) as a function of shear rate at room temperature, for 0.6 wt. % and 4 wt.% aqueous polyacrylamide solutions, [9].

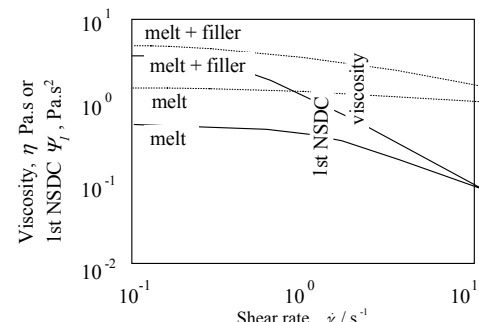


Figure 19: The viscosity and first normal-stress difference coefficient (1st NSDC) as a function of shear rate for polystyrene melt at 232°C, with and without rubber filler particles, [11].

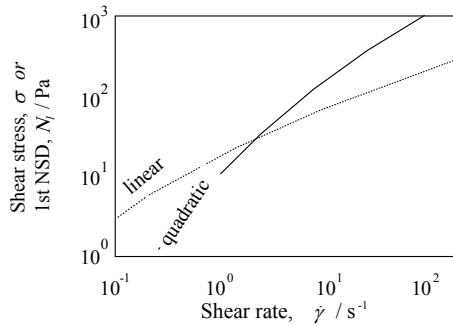


Figure 20: The shear stress (dotted line) and first normal-stress difference (1st NSD, solid line) as a function of shear rate at room temperature for a solution of polystyrene in toluene.

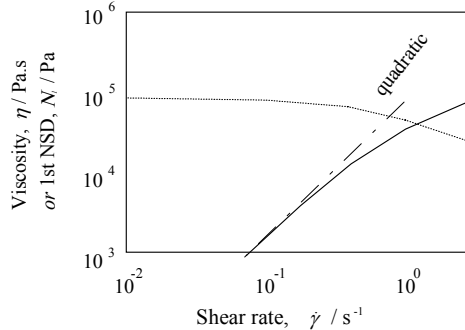


Figure 22: The viscosity (dotted line) and first normal-stress difference (1st NSD, solid line) as a function of shear rate at room temperature for a polystyrene melt, [13].

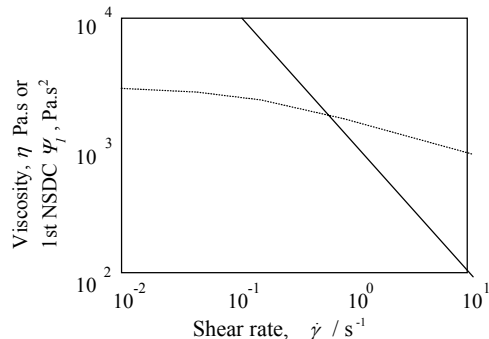


Figure 24: The viscosity (dotted line) and first normal-stress difference coefficient (1st NSDC, solid line) as a function of shear rate for a polypropylene melt at 240°C, [15].

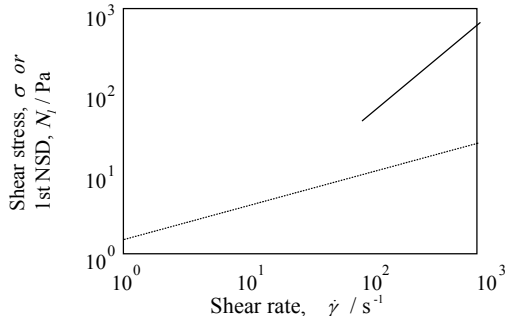


Figure 26: The shear stress (dotted line) and first normal-stress difference (1st NSD, solid line) as a function of shear rate at room temperature for a 1% aqueous solution of polyacrylamide.

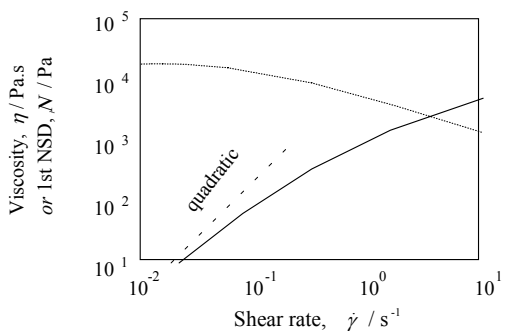


Figure 21: The viscosity and first normal-stress difference coefficient (1st NSD) as a function of shear rate at room temperature for a solution of polyisobutylene in cetane, [12].

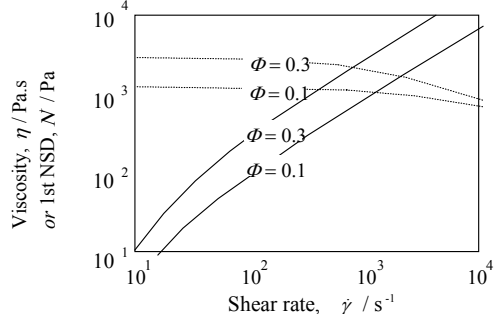


Figure 23: The viscosity (dotted line) and first normal-stress difference coefficient (1st NSD, solid line) as a function of shear rate at room temperature for an emulsion of low-molecular weight polybutene in glycerol, at two levels of phase volume, [14].

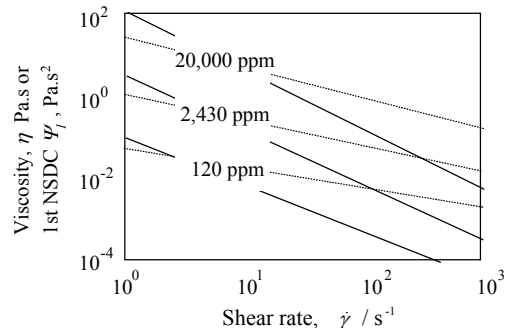


Figure 25: The viscosity (dotted lines) and first normal-stress difference coefficient (1st NSDC, solid lines) as a function of shear rate at room temperature for three aqueous polyacrylamide solutions, [16].

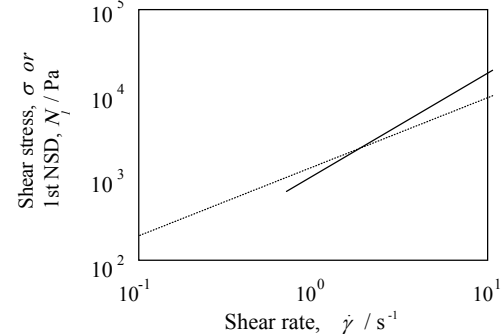


Figure 27: The shear stress (dotted line) and first normal-stress difference coefficient (1st NSD, solid line) as a function of shear rate at room temperature for a polypropylene copolymer at 230°C.

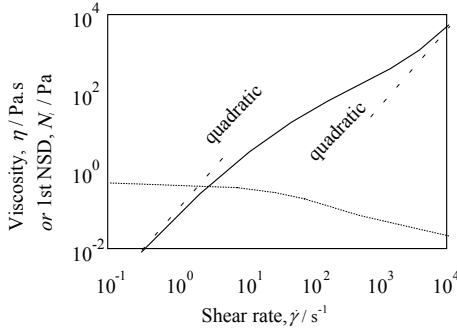


Figure 28: The viscosity (dotted lines) first normal-stress difference (solid lines) as a function of shear rate for a 2.5% solution of polyisobutylene ($M_w = 6.106$) in tetradecane at 25°C , [17].

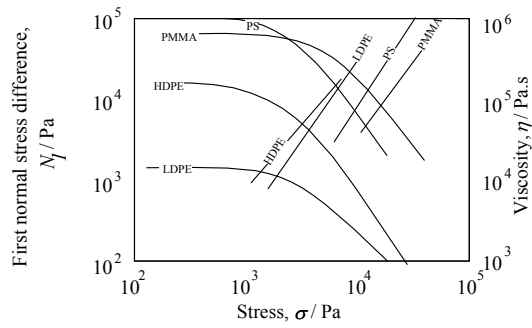


Figure 29: The viscosity (dotted lines) first normal-stress difference (solid lines) as a function of shear stress for a number of polymer melts at 160°C , [18].

When a filler is added to an elastic liquid, the viscosity always *increases*. However, the opposite is true when it comes to the normal stress situation, where the level of elasticity always *decreases*. One of the most obvious consequences of this effect is that extrudate swell *decreases* as the filler loading is increased. The only exception to this is for long, thin fibres, where an increase is seen, see [19] chapter 7 for a full discussion of this unexpected result.

14.6 Some viscoelastic formulas

14.6.1 General

Just as we wrote down some formulas that predicted the effect of Newtonian and non-Newtonian viscosity in flow, see chapters 6 and 10, so now can we quote some for the effect of N_1 and N_2 . (Conversely, these situations may also be used to evaluate the values of N_1 and N_2 .)

14.6.2 Extrudate swell

The extent of extrudate or *die swell* of a viscoelastic liquid emerging from a long tube, see figure 3, is given by the empirical Tanner equation [20]

$$\frac{D_e}{D} = \left[1 + \frac{1}{2} \left(\frac{N_1}{2\sigma} \right)_w^2 \right]^{\frac{1}{6}}$$

where D is the diameter of the tube, and D_e is the eventual diameter of the extrudate. The shear stress and the normal-stress difference values are evaluated at the wall of the tube.

Sometimes a numerical addition of 0.1 is added to the right-hand side of this equation to bring it into better alignment with experimental findings. Die swell of up to a few hundred percent have been observed for very elastic liquids.

As mentioned above, the addition of fillers (apart from long, thin fibres) decreases the N_1 level, and thus decreases the die swell. At levels of filler of about 40%, a typical polymer melt, which would swell by up to 40% when unfilled, will show no swell at all [19].

14.6.3 Flow in a slightly inclined trough

If b is the bulge on the surface of an elastic liquid flowing down a channel inclined at an angle β to the horizontal, then

$$N_2 = \rho g b \cos \beta.$$

This method can be used as a simple means of measuring N_2 .

14.6.3 Pressure in holes and slots

If P_H is the extra pressure generated at the bottom of a hole set into a wall when an elastic liquid flows past it, then its value for various geometrical configurations is given by the following formulas:

a circular hole

$$P_H = \frac{1}{3} \left(\frac{N_1}{n_1} - \frac{N_2}{n_2} \right)_w,$$

a transverse slot

$$P_H = \frac{1}{2n_1} (N_1),$$

an axial slot

$$P_H = -\frac{N_2}{n_2},$$

with all values of normal-stress difference evaluated at conditions relevant to the wall of the tube.

14.6.4 Inertia in a cone-and-plate geometry

When a low-viscosity viscoelastic liquid is tested at high rotational speed in a cone-and-plate geometry, there is an inertial force acting outwards that tends to pull the plates together, thus counteracting the normal-force effects which tend to push the plates apart. When this effect is just measurable, the overall force is then given by

$$F = \frac{\pi a^2}{2} \left[N_1 - \frac{\rho(a\omega)^2}{6} \right].$$

This can be used to correct the normal-force results. However, when the correction becomes large, secondary flows are present in the cone-and-plate gap, and this means that the results are then unreliable.

14.7 Postscript - flow of a viscoelastic liquid into a contraction.

One last item worth mentioning before we move on is the effect of viscoelasticity on flow into a contraction. This has been a ‘set piece’ for many years for rheologists interested in viscoelasticity, and the possibility of calculating its effect using formal mathematical methods or computer simulation. No one can attend a large rheological conference these days without hearing someone talking on the subject! It is often encountered in extrusion processes in the plastics industry, where viscoelastic polymer melts are pumped into and out of short dies.

All else being equal, an increase in flow-rate for an elastic liquid, or an increase in the level of elasticity (measured as, say, the first normal-stress difference) produces the effect on the flow pattern in a contraction shown in figure 30. The complex flow pattern shown on the right of the figure is very susceptible to flow instabilities. The onset of these instabilities dictates the maximum flow-rate possible for an extrudate emerging from the end of the die having a smooth, acceptable surface. (See chapter 17 for a discussion of the role of extensional viscosity in this kind of flow.)

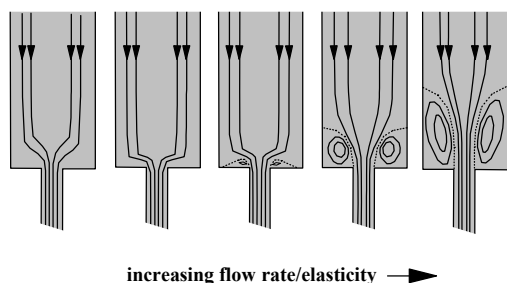


Figure 30: The flow of a viscoelastic liquid into a contraction; note that Newtonian liquids do not have recirculating vortices at high flow rates.

References

- [1] Al-Hadithi, T. S. R; Barnes, H. A; Walters, K., *Colloid and Polym. Sci.*, 270(1), 40-46 (1992).
- [2] Reiner, M., *'Deformation, Strain and Flow'*, 3rd edition, H.K. Lewis, London, 1969.
- [3] Barnes, H.A; Eastwood, A.R; Yates, B., *Rheol. Acta*, 14, 61-70 (1975).
- [4] Mhetar, V.R; Archer, L.A., *J. Rheol.*, 40, 549 – 571 (1996).
- [5] Han, C.D; Yoo, H.J., *J. Rheol.*, 24, 55 – 79 (1980).
- [6] Walters, K., *'Rheometry'*, Chapman and Hall, London, 1975.
- [7] Agarwal, S.H; Porter, R.S., *J. Rheol.*, 25, 171 – 191 (1981).
- [8] Joseph, D.D; Beavers, G.S; Cers, A; Dewald, C; Hoger, A; Than, P.T., *J. Rheol.*, 28, 325 – 345 (1984).
- [9] Chang, D.H; Yoo, H.Y., *J. Rheol.*, 24, 55 – 79 (1980).
- [10] Macosko, C.W., *'Rheology Principles, Measurements and Applications'*, Wiley-VCH, New York, 1994.
- [11] Kruse, R.L; Southern, J.H., *J. Rheol.*, 24, 755 – 763 (1980).
- [12] Zapas, L.J; Phillips, J.C., *J. Rheol.*, 25, 405 – 420 (1981).
- [13] Sugeng, F; Phan-Thien, N; Tanner, R.I., *J. Rheol.*, 32, 215 – 233 (1988).
- [14] Han, C.D; King, R.G., *J. Rheol.*, 24, 213 – 237 (1980).
- [15] Schmidt, L.R., *J. Rheol.*, 22, 571 – 588 (1978).
- [16] Argumedo, A; Tung, T.T; Chang, K.I., *J. Rheol.*, 22, 449 – 470 (1978).

A Handbook of Elementary Rheology

- [17] Schoonen, J.F.M; Swartjes, F.H.M; Peters, G.W.M; Baaijens, F.P.T; Meijer, H.E.H., *J. Non-Newton. Fluid. Mech.*, 79 (2-3), 529 - 561 (1998).
- [18] Feguson, J; Kemblowski, Z., '*Applied Fluid Rheology*', Elsevier Applied Science, London, 1991.
- [19] Shenoy, A; '*Rheology of Filled Polymer Systems*', Kluwer Academic Publishers, Dordrecht, 1999.
- [20] Tanner, R.I, '*Engineering Rheology*', Clarendon Press, Oxford, 1985.

CHAPTER 15: THE FLOW OF SUSPENSIONS

'The whole of science is nothing more than a refinement of everyday thinking', Einstein

15.1 Introduction

Many of the structured liquids that we come across in everyday life are suspensions/dispersions of particles in a liquid, with examples ranging from mud to blood, and custard to mustard. Other examples of the kind of suspensions we are dealing with here, and the places you might find them are

- under the sink - liquid abrasive cleaners, fabric washing liquids,
- pantry or cupboard - sauces, meat-pastes, custard, mustard, mayonnaise,
- garage or store-room - paints, greases, mastics, fillers, glues, cements,
- bathroom cabinet - medicines, ointments, creams, lotions, and toothpastes.

Everyday experience tells us that if we increase the concentration of the dispersed particles, the viscosity of a mixture increases, going from a free-flowing liquid through to a paste, and eventually to a soft solid, as more and more particles are added. A familiar example of this is when we add cement or flour to water. What we need to know is, what influences the increase in viscosity in terms of the character of the liquid phase and the added particles? For instance, what is the effect of the shape of the particles; their size distribution; the interaction between them, and their deformability, etc.? All these factors will be considered below.

N.B. We do not differentiate here between the words *suspension* and *dispersion*, but some people speak about the latter as made up of small particles, where small might mean sub-micron-sized so that colloidal factors are very significant.

Emulsions are dispersions of deformable liquid drops in a liquid continuous phase. However, if they are composed of very small drops, they are very much like a small-particle-sized dispersion since the drops are hardly deformable. As a result they follow essentially the same kind of rules given below for solid dispersions.

15.2 Viscosity of dispersions and emulsions

15.2.1 The continuous phase

The viscosity of dispersions is first of all controlled by the continuous phase liquid which might itself be Newtonian or non-Newtonian, and then the added dispersed phase where the size, shape, amount and deformability of the particles of dispersed material can vary considerably, as can the interaction between the individual dispersed particles.

For many liquids the continuous phase is Newtonian, and might be water, as found in most household or personal care products, modern paints, etc. On the

other hand, it might be a Newtonian oil, as in such oil-based products as in lubricants, greases, or even Plasticine™ the well-known modelling clay. Some paints and coatings are based on a Newtonian resin continuous phase.

15.2.2 The effect of very low concentration of suspended particles

Although much empirical progress had been made in the study of dispersions, the first important theoretical work was done by Albert Einstein at the beginning of this century, when he calculated that the viscosity of a dispersion with a very small amount of material, ϕ , in the form of solid spherical dispersed particles, is given by

$$\eta = \eta_0(1 + [\eta]\Phi)$$

where η is the measured viscosity and η_0 is the Newtonian continuous phase viscosity: $[\eta]$ is called the intrinsic viscosity, which for spheres Einstein calculated to be $\frac{5}{2}$. In the equation, ϕ is properly called the *phase volume*, because it represents that volume of the dispersion occupied by the dispersed phase; it does *not* mean weight fraction, because at this stage the particles are considered weightless.

15.2.2.1 The effect of the continuous phase

In all the suspension equations considered here, the viscosity is predicted to be *directly proportional* to the viscosity of the continuous phase. This is an important point to remember, because if we change the continuous-phase viscosity in any way, then, all else being equal, the overall suspension viscosity changes proportionally by the same amount. Thus, if the viscosity of the continuous phase is doubled, then so too is that of the dispersion. This proportionality is important when we think about the effect of temperature, concentration of soluble additives, etc.

The following concentrations of, for instance, sodium salts (% by weight) approximately double the viscosity of water at 20 °C: hydroxide (10.5), carbonate (11.5), acetate (15), phosphate (21), sulphate (18), tartrate (19), chloride (25), thiocyanate (35), and nitrate (37). The effect is obviously complicated, being a function not only of molecular weight, but also the shape of the dissolved molecules and the way in which they interact with the structure of water. Molecular weight alone will eventually give a large effect, as for instance with dextran ($M_w = 72,000$ daltons), which only needs to be added at a level of 2.75 wt. % to double the viscosity of water, whereas simple organic molecules like glucose, maltose and sucrose have to be added at concentrations around 22 % to produce the same effect.

In this context it is worth remembering that sometimes chemical additives can *decrease* the viscosity of water. Before the beginning of this century, Wagner [1] discovered that some salts of potassium, rubidium, caesium, and ammonium produce such a reduction at lower concentrations, before at higher concentrations increasing the viscosity as normal. These are the so-called 'structure-breakers', which interfere with the local intermolecular hydrogen bonding of water molecules. One of the biggest decreases is produced by the addition of 36% by weight of ammonium iodide to water at room temperature, when the viscosity decreases by around 13.5%. The complete curves for ammonium chloride, bromide and iodide are sketched out in figure 1 where the reduction is shown as a function of mol/L, which can be converted into weight percent by noting that the molecular weights are

55.5, 98 and 145 respectively. This kind of reduction has also been seen when potassium iodide was added to glycerol, with a 20 % by weight solution giving a viscosity reduction of 20 %.

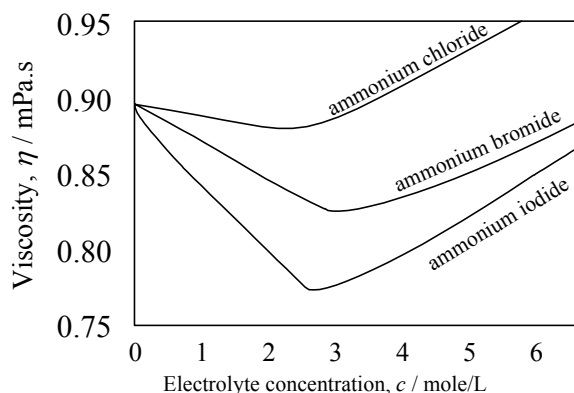


Figure 1: Viscosity versus concentration for some aqueous ammonium salt solutions at 25 °C, [2].

Last of all with respect to the viscosity of the continuous phase, we might consider the addition of other miscible liquids to water, where the mixture properties are complex, even though the mixture of the same liquid to an organic liquid will give simple mixing. A good example of complex mixing is seen in the addition of ethyl alcohol to water, when both have almost the same viscosity but their mixture viscosities are very different, see figure 2. This will have an obvious effect on the viscosity of dispersions of particles in such mixtures, and is an interesting way of thickening a suspension!

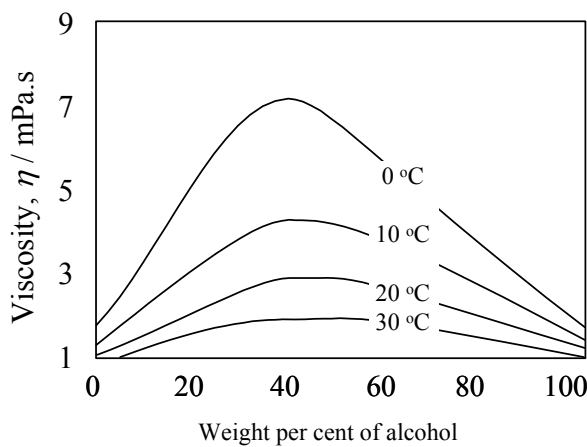


Figure 2: Viscosity of water/ethyl-alcohol mixtures as a function of temperature, [3].

The effect of temperature on the overall viscosity is—all else being equal—controlled by the viscosity/temperature variation of the continuous phase. This has already been discussed in §5.4. This means for instance that the variation of viscosity with temperature for water-based suspensions is around 3 % per degree, but it can be much higher for some oil-based systems.

15.2.2.2 The effect of the dispersed phase

When we say that the Einstein equation accounts for dispersions with ‘a very small amount’ of suspended particles, we mean that the particles are so widely spaced that they are completely unaware of each other’s existence. In reality this means a concentration of no more than a few percent phase volume. This formula was experimentally verified by Bancelin in 1911 [2] using particles of size 0.3, 1, 2 and 4 μm , and no effect of the size of the particle was found.

On the other hand, shape does matter, since the increase in viscosity comes from the diversion of streamlines in the flow as they are redirected around particles, thus leading to an increase in the viscous energy dissipation, i.e. viscosity. When the particles are non-spherical, this extra dissipation increases, and the incremental amount of viscosity also increases. The measure of the increase is the intrinsic viscosity $[\eta]$ and this increases when a sphere is pulled out towards a rod, or squashed down towards a disc, with the former giving the greater increase in viscosity. A typical example of a rodlike particle system is paper-fibre suspension, while red blood cells are approximately disc-shaped. Simple formulas for both kinds of particles have been derived by the present author [3] as

$$[\eta] = \frac{7}{100} p^{\frac{5}{3}}$$

for rodlike (prolate) particles and

$$[\eta] = \frac{3}{10} p$$

for disc-like (oblate) particles, and in both cases the axial ratio p is defined in such a way that it is greater than unity.

The presence of electrical charges on the surface of particles leads to extra energy dissipation due to flow distorting of the surrounding charge cloud. Von Smouluchowski accounted for the effect mathematically as

$$\eta = \eta_0 (1 + 2.5\phi \left\{ 1 + \left(\frac{\varepsilon\zeta}{2\pi} \right)^2 \left\{ \frac{1}{2\sigma\eta_0 a^2} \right\} \right\})$$

where ε is the relative permittivity of the continuous phase, ζ is the electrokinetic potential, σ is the specific conductivity of the continuous phase, and a is the radius of the spherical particles. This effect can easily double the effective phase volume [4].

For the first time, we have introduced a size effect, since the smaller the particle, the larger is the effect of the fixed-thickness electrostatic layer relative to the particle size, and hence the greater the effective phase volume, giving the inverse dependence on a^2 shown in the equation.

15.2.2.3 The effect of medium-to-high concentrations of particles

Although the Einstein equation is an important starting point, it gives little help for real situations, since individual particles are not aware of one another’s existence. Many empirical equations followed Einstein’s exact mathematical effort,

each of which sought to increase the concentration range into a more practical region. One of the more useful is known as the *Kreiger-Dougherty* (K-D) equation [5], which is given by

$$\eta = \eta_0 \left(1 - \frac{\Phi}{\Phi_m}\right)^{-[\eta]\Phi_m}$$

where Φ_m is called the *maximum packing fraction*, which is that concentration where just enough particles have been added for the viscosity to become infinite. For instance, at rest this is often near the random close-packing limit of approximately 64 %. However, as we shall see, the value of Φ_m varies according to the prevailing circumstances.

The K-D equation reduces to the Einstein equation in the limit of very small phase volume. (The basic form $\eta = \eta_0(1 + a\Phi)^n$ goes back to Baker [6], but has been given many names since.) Further examination of the K-D equation in the light of practical experience shows that the product of $[\eta]\Phi_m$ is often around 2 for a variety of situations. In the light of this fact we can simplify the equation to

$$\eta = \eta_0 \left(1 - \frac{\Phi}{\Phi_m}\right)^{-2}.$$

Now, surprisingly, the *only* real variable is Φ_m ! This variable is a function of particle size distribution (p.s.d.) and particle deformability, as well as the flow conditions. In terms of the former, the wider the particle-size distribution, the higher is Φ_m . Figure 3 gives an example of data due to Wakeman [7] for the packing of dry powders that illustrates this point.

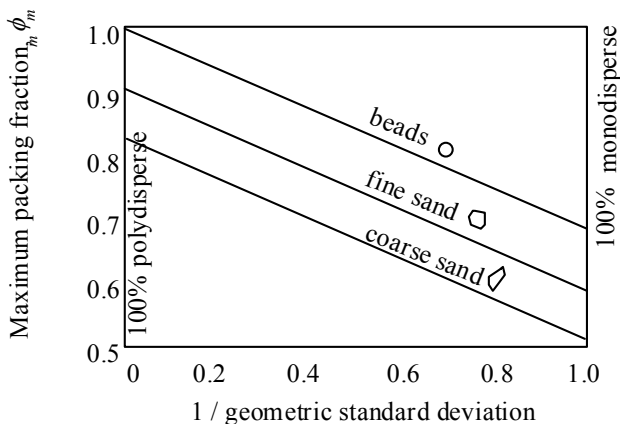


Figure 3: The maximum packing fraction of a powder as a function of its polydispersity (shown here as the inverse of geometric standard deviation) for a log-normal distribution.

In the same figure we also see that the effect is mirrored for slightly non-spherical particles such as sand grains. The particular kind of size distribution used in the powder illustration—log normal—is the usual consequence of many size-reduction operations such as the grinding up of solid particles or the break-up of liquid droplets in liquid-mixing operations.

If we want to control or understand the viscosity of concentrated dispersions, Φ_m is an important variable to manipulate. For instance, either a widening or

narrowing of the p.s.d. can be attempted, or else the deliberate mixture of particle sizes have a large effect on Φ_m . If the particles are monodispersed, then mixtures of particle sizes can reduce the viscosity if the size ratio is around 4:1, since the small particles can fit into the holes left when the large ones touch. This size-mixing manoeuvre is very effective for higher concentration suspensions, as shown in figure 4. If three sizes are mixed, under the same restriction of size ratio, the effect is equally as good, see figure 5, [8]. After three sizes of particles, the restriction on size becomes impractical. This exercise is used in the manufacture of concrete, when as aggregate material as possible needs to be added while keeping the concrete quite flowable.

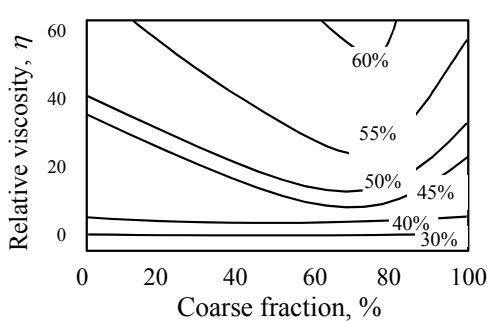


Figure 4: Relative viscosity of a binary mixture of particles, with size ratio $> 4:1$, for various total phase volumes.

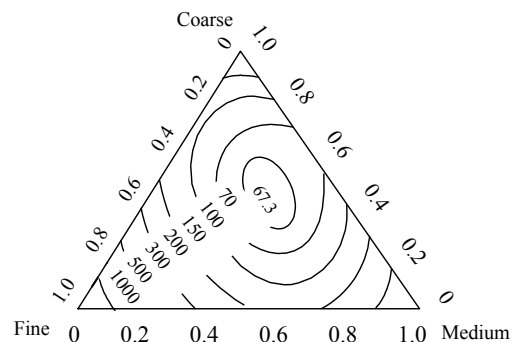


Figure 5: Relative viscosity of a ternary mixture of particles in suspension, where the total phase volume is 66%.

The consequences of concentration, Φ , are scaled by Φ_m , and they become very critical as Φ approaches Φ_m . This is easily understood by considering the situation when powders are dispersed in a liquid in such kitchen operations as making custard, where adding the critical final amount of water or milk transforms a stiff paste into a flowing liquid. In simple dispersions this becomes true for phase volumes above 50 %.

It is easy to show that the viscosity-concentration profile approaches a situation where the viscosity would double or halve if the phase volume increased or decreased by 1 %. There are a number of ways this can happen by the particles swelling or shrinking by that amount. This would mean that the particle size would change by around $\pm 1\%$. Since this very small change could not be measured on any commercial particle sizer, it leaves us with the interesting possibility that the viscosity of a product could change considerably for no obvious reason!

An interesting practical example of this was seen by the author when visiting a manufacturer of polymer lattices [3]. The lattices were manufactured in one solvent, then dried off and afterwards re-dispersed in a different solvent. Unfortunately, some of the second solvent absorbed to a small extent into the polymer particles, but only very slowly. Hence the viscosity increased continuously over the next few days due to the swelling, but for no reason obvious to the manufacturer, since the small increase in size of the latex particles was immeasurable.

15.3 Particle-size effects in concentrated dispersions

The effect of particle size of dispersions enters through a very important mechanism which relates to the spatial arrangement of the particles. When a dispersion is at rest, the particles are randomly dispersed throughout the continuous phase due to the perpetual action of Brownian motion. If the dispersion is sheared at very low shear rates, then there has to be a great deal of co-operative movement to allow these particles to move in the flow direction while maintaining the overall random distribution, and thus the viscosity is high. However, when the dispersion is sheared at a higher shear rate, the particles can be moved from the overall random arrangement towards a situation where they begin to form into strings and layers, see figure 6.

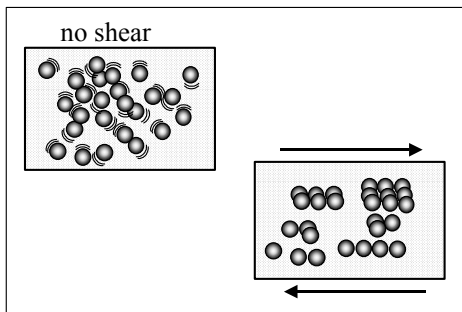


Figure 6: The formation of strings and layers in a suspension of non-interacting 'Brownian' spheres under the action of shear flow.

Then the *average* distance between the particles increases in a direction at *right angles* to the flow direction, and it decreases *along* the flow direction. This change of spatial arrangement makes their movement past each other much easier, thus lowering the viscosity. This manifests itself in the K-D equation by a small but significant *increase* in the value of Φ_m as the shear rate increases. Typical values of Φ_m are about 0.63 for a dispersion of monodisperse, spherical particles at very low shear rates and about 0.71 at very high shear rates. This seemingly small change produces large effects at high concentrations resulting in a large amount of shear thinning in concentrated suspensions.

As the backwards driving force towards randomness is Brownian, hence of thermal origin, we can see that shear thinning is easier for large particles where Brownian motion is less effective and the shear forces are correspondingly more important. When a small-particle-sized dispersion is sheared, the effect of Brownian motion is longer lasting along the shear rate axis, and higher values of shear rate are needed to produce the same amount of shear thinning, see figure 7.

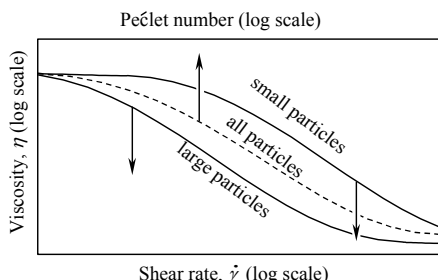


Figure 7: A schematic diagram of the viscosity as a function of shear rate or Peclet number for large and small particle size suspensions.

These effects can be properly scaled by plotting the so-called Péclet number instead of the shear rate, which then collapses the data onto a single curve. The Péclet number is described as the ratio of the hydrodynamic to the thermal force, so $P_e = a^3 \eta \dot{\gamma} / kT$. This curve can usually be described by the Cross-type equation, see chapter 9, with the shear rate term replaced by the Péclet number, see figure 7.

15.4 Particle-shape effects in concentrated dispersions

The thickening effect of particles with respect to their shape follows the descending order of rods > plates > cubes/grains > spheres, when the same phase volume of particles is added to a liquid. This is illustrated in figure 8, where we see the approximate order of thickening power of each shape, with rods/fibres being the most efficient for any given phase volume. The aspect ratio of fibres is a controlling factor in determining the precise effect, see figure 9. With regard to the viscosity parameters we have considered, i.e., $[\eta]$ increases for non-spherical particles as we have seen above for dilute suspensions, but ϕ_m decreases. However, the product of these two terms still does not differ greatly from 2, see [8].

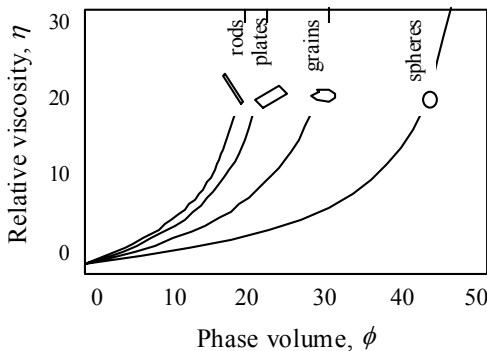


Figure 8: Viscosity as a function of phase volume for various particle shapes.

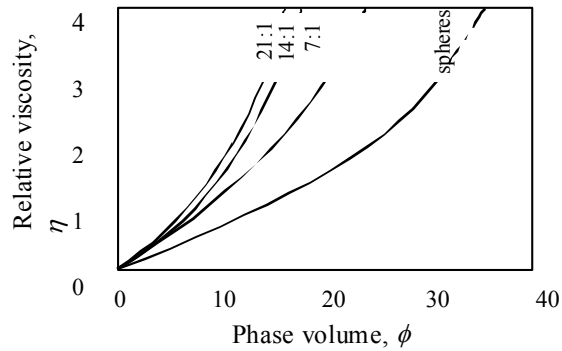


Figure 9: Viscosity as a function of phase volume for various aspect ratio of fibres.

15.5 Particle deformability

Particle deformability means that for the same amount of dispersed material, the viscosity at high concentrations is lower than the equivalent dispersion of solid particles, since the droplets are deformable and can thus accommodate each other at rest and squeeze past each other during flow, so that first the maximum packing fraction ϕ_m is higher and the intrinsic viscosity $[\eta]$ is lower [9].

15.6 Particle interactions - an overview

The simplest picture we can form of any dispersion of submicron particles, is of the particles being free to approach and depart from each other under the action of the ever-present Brownian motion, with no more resistance than that presented by the movement through the intervening viscous liquid. However for such small particles, significant interparticle forces can change this picture. For instance the ubiquitous van-der-Waals attraction force between particles, if not counteracted, will cause the particles to stick together on touching. This attractive force arises from correlated atomic motions in neighbouring particles and is always present in all particle-particle interactions. For particle separations in the nanometre range, the

van-der-Waals interaction potential present between two equal spheres can be described simply by

$$\Phi_{vdW} = \frac{-Aa}{12(r-a)}$$

where A is the relevant Hamaker constant for the particular situation, a is the radius and r is the centre-to-centre separation of the particles.

This force is usually significant in the range 1-10 nanometre for colloid-sized particles ($\sim 1 \mu\text{m}$). It does not increase indefinitely at very small distances—as indicated by the simple equation above—but approaches a minimum. If the particles are completely unprotected, the force minimum at these very small distances (the so-called *primary minimum*) can be large enough to give more-or-less permanent particle contact—this is called coagulation. In most situations, however, we are usually interested in the shallower *secondary minimum* caused by the combined effects of the van-der-Waals attraction and some repulsive force arising from the presence of a protecting moiety at the particle surface or an electrostatic repulsion between neighbouring particles carrying the same sign charge.

A strong repulsive force between particles arises from the repulsion between like charges on the surfaces of adjacent particles. The approximate operating distance of the electrostatic force resulting from charges adsorbed on particles in an aqueous environment is $1/\kappa$ where κ is known as the *double-layer thickness*. The thickness of this layer is strongly dependent on the electrolyte concentration and is given approximately (in nanometre units) by

$$1/\kappa = 0.3 c^{-1/2} [z]^{-1}$$

where c is the electrolyte concentration in mol/L, and $[z]$ is the valency of the electrolyte. This means that (assuming $[z] = 1$) the following is true for aqueous liquids

electrolyte concentration, $c = 10^{-5}$, then double layer thickness $1/\kappa \sim 100 \text{ nm}$

$c = 10^{-3}, \quad 1/\kappa \sim 10 \text{ nm}$
--

$c = 10^{-1}, \quad 1/\kappa \sim 1 \text{ nm}$

<p>If the repulsive forces are larger and longer-range, then they are able to counteract the van-der-Waals attractive forces; thus giving a (colloidally) stable dispersion. Polymers are available—called <i>block copolymers</i>—which have one end soluble in the continuous phase, and the other end insoluble and able to absorb onto the particle surface. These can protect particles that would otherwise flocculate—the protruding polymer loops and strands overlap to hold the particles far enough apart so that they are not strongly attracted—this is called <i>steric repulsion</i>. The system can then be regarded as non-interacting, but for very small particles, the effective phase volume must be increased to account for any polymer layer.</p>

<p>As well as producing repulsion by introducing a polymer onto the surface of the particles, one can combine both effects using absorbed polyelectrolytes, i.e. polymers with charge distributed along the chains. The particular nature of the forces arising is different in each case but the overall effect is always the same—they produce a repulsive force. We need say no more about normal polymers at this stage with respect to the details of these force, but it is useful to note that the</p>

approximate distance of action of a polymer adsorbed at random points along its backbone (a homopolymer) is approximately—when expressed in nanometres—one tenth of the square root of its molecular weight. If however the polymer is attached at one end only, the distance is about twice that value, thus for instance, for a terminally anchored polymer of molecular weight 10,000, then thickness of the layer would be around 20 nanometres, while the randomly attached equivalent would have a thickness of about 10 nanometres.

Another attractive force between particles has very surprising origins. If high molecular weight polymers are present in the continuous phase of a suspension, then the only effect we normally expect is that due to increasing the continuous-phase viscosity. However, another effect can also occur under certain circumstances. This arises because when particles come close to one another, and the gap between them is quite small, any large polymer molecules (or surfactant micelles) in the vicinity are excluded from the small space. The result is a depleted region with respect to polymer concentration and this leads to a local difference in osmotic pressure. The overall effect is that the two adjacent particles producing the small gap are pulled together. This pull can be so strong that it exceeds any repulsive forces, and with the addition of the van-der-Waals force, it can produce flocculation of the particles. The effect is called *depletion flocculation*, and it can also be caused by very small particles or detergent micelles present in the dispersion.

In summary we can say that the overall effect of the attractive van-der-Waals and depletion forces with the various repulsive forces shown in figure 10, where two extremes are shown—very large attractions due to van-der-Waal plus depletion forces, and the large repulsion present if we have very large surface charge and low electrolyte in aqueous systems.

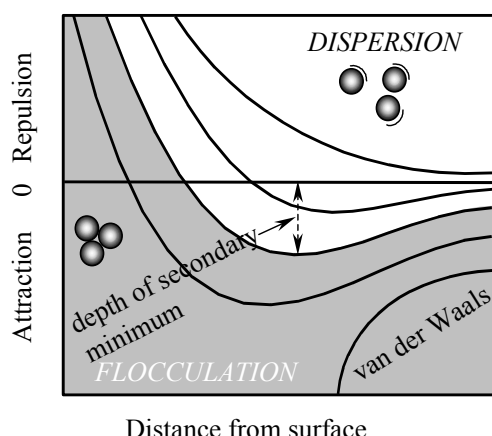


Figure 10: Force-distance curves for colloidal forces: van der Waals attraction forces balanced against increasing steric or electrostatic repulsion forces.

However, most systems have a mixture of both effects, so that we have the appearance of a *secondary minimum*. If this secondary minimum is shallow (only a few kT s), then the particles remain dispersed, but if it is much larger than that, then the particles stick together, that is they flocculate.

All these kinds of interactions lead to an increased viscosity. However, although these colloidal forces dictate the form of the dispersion at low shear rate, when the shear rate is greater than some critical value, the viscosity begins to decrease. Eventually, the viscosities approach similar values at high shear rates,

largely dictated by the hydrodynamic effects that we have previously seen, see figure 11.

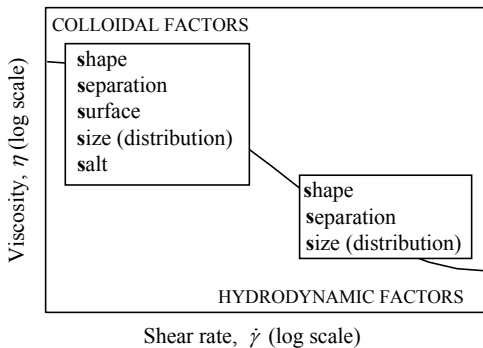


Figure 11: Flow curve of a suspension of colloidal particles.

In the figure we see that colloidal effects dictate the viscosity at low shear rates, and then the five S's are important ,

- shape of the particles and their
- size distribution, plus the
- separation of particles (i.e. concentration), their
- surface properties and the possible presence of
- salt in the continuous aqueous phase.

However, at very high shear rates, hydrodynamic effects largely control the situation, and only the first three factors are important, with some effect due to the presence of surface charge in the increase of the effective phase volume, but the effect is smaller than at low shear rates.

15.7 The viscosity of flocculated systems

While particles with a large overall repulsion are very interesting from a scientific point of view, giving us the crystal-type effect that can have very beautiful optical effects, they are rarely important in real products, since these systems cannot tolerate the presence of salts and surfactants in solution. However, a far more widespread situation is where flocculation is present, at least to some extent, resulting from an overall attraction between the particles. The individual flocs making up such dispersions can be easily broken down by shear, as for instance during vigorous shaking. This situation will now be described in some detail, especially its rheological consequences.

The depth of the secondary minimum formed due to the addition of the repulsive and attractive forces will vary from a few kT units—which means no flocculation because Brownian motion will keep the particles apart—to $\sim 10 - 20 kT$. Forces in this latter range mean that typical flows can break-up any flocs present, although they will reform under more quiescent conditions. The size and architecture of the flocs formed play a major rôle in determining the rheology and physical stability of the suspension.

Shearing hard enough will result in the flocs being reduced to the primary particles, but shearing at a low shear rate results in the partial breakdown or reformation of flocs. The form of the floc depends on the interaction force and to some extent on the flow history attending the floc formation. Depending on its

form, strength and duration, any flow will progressively break down these flocs: thereafter, further rest reforms them under the action of Brownian motion. (This process accounts for *thixotropy* as well as shear thinning in flocculated suspensions and it is completely reversible.)

We will spend a little time considering the nature of flocs. A floc is a collection of particles where the spatial arrangement often follows some simple law. It might be that the average particle concentration is the same throughout the floc, but usually the concentration decreases from the centre towards the outside. This is due to the way that the flocs are formed.

The simplest way of describing such a floc is to use fractals. In our case this simply means that the concentration falls off according to a power law with distance from the floc's centre. Then we can write down the following,

$$p \approx \left(\frac{R_0}{a} \right)^D$$

where p is the number of particles in a floc, a is the radius of the particles, R_0 is the radius of the smallest enclosing sphere for the floc, and D is called the *fractal dimension*, see figure 12.

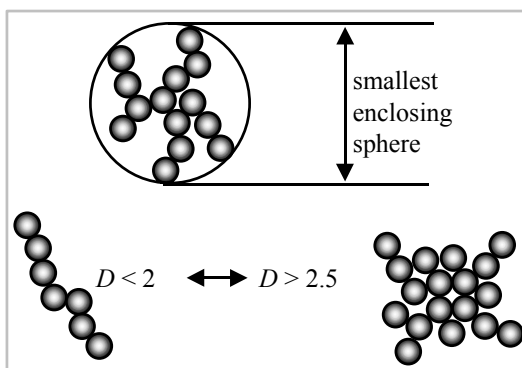


Figure 12: Fractal flocs: the dimensions and extremes of fractal flocs (shown in 2D).

D can vary from almost 3 for the densest floc down towards 1 for a very open 'linear' floc with a few radiating arms. The value of D depends on the particle interaction forces. If a suspension is sheared to completely deflocculate the particles, and then the flocs are allowed to reform under quiescent conditions, the architecture will depend on the forces in such a way that if the attractive forces are large, say around 10 kT, with D often less than 2. Here the particles '*hit and stick*', giving a very open structure. However if the attractive force is small, say a few kTs, the particles '*hit and roll*', forming a denser floc, with D greater than 2.5. Obviously small changes in D will give large changes in floc structure.

From the mathematical relationship above we can redefine the phase volume as the *effective* phase volume, assuming for the sake of simplicity that the phase volume is now that defined by the enclosing spheres of the flocs of radius R_0 . Then it is easy to show that

$$\phi_{\text{eff}} = \phi p^{\frac{3}{D}-1}$$

where ϕ is the total (real) phase volume of the particles, and ϕ_{eff} is the effective phase volume of the flocs. It is obvious now that the effective phase volume of the flocculated suspension is much higher than the real phase volume of the particles, and hence the viscosity of the suspension is much higher.

From this equation we also see the sensitivity of viscosity to interparticle force, for the exponent $3/D - 1$ will vary from 0 when D is 3 (for a small attractive force), to 0.5 for a D of 2 (for a large force). This would mean that for $p = 100$, the effective phase volume would vary by a factor of 10 for D going from 3 to 2. However we also see another important fact from this equation—the effective phase volume of the suspension now depends on the *size* of the flocs, via the value of p , the number of particles per floc. For example if $D = 2$ (for most real flocculated suspensions D usually varies in the range 2 ± 0.25), the effective phase volume decreases by a factor of 10 when the number of particles in a large floc is reduced from 10,000 to 100 under the action of shearing.

The most obvious way of reducing the number of particles in a floc is to subject the floc to shear. If such a shear field is applied to a flocculated suspension, then the floc size is approximately [10]

$$R_s = \frac{R_0}{1 + (b\dot{\gamma})^c}$$

where R_s is the radius of the sheared floc; b is a constant with the dimensions of time, and c is a dimensionless constant, and $\dot{\gamma}$ is the applied shear rate. From this relationship we can rewrite the effective phase volume, insert it into the K-D equation and arrive at a simple expression for the viscosity of a flocculated suspension as

$$\eta = \eta_0 \left(1 - \left[\frac{R_0}{a} (1 + (b\dot{\gamma})^c)^{3-D} \cdot \frac{\phi}{\phi_m} \right]^{-2} \right).$$

The effect of shear rate on viscosity in this equation is very strong, and demonstrates the typical situation with flocculated systems where severe shear thickening is seen, giving what looks like a yield stress.

15.8 Thixotropy

Thixotropy is the change of viscosity with *time* of shearing rather than *rate* of shearing, and is generally viewed as a troublesome property that one could well do without. All the advantages previously claimed for thixotropy are in fact better seen as the result of a high degree of shear thinning [11].

Thixotropy comes about first because of the finite time taken for any shear-induced change in microstructure to take place. Microstructure is brought to a new equilibrium by competition between, on the one hand the processes of tearing apart by stress during shearing, and on the other hand build-up due to flow- and Brownian-motion-induced collision, over a time that can be *minutes*. Then, when the flow ceases, the Brownian motion (the only force left) is able to slowly move the elements of the microstructure around to more favourable positions and thus rebuild the structure: this can take many *hours* to complete. The whole process is completely reversible.

If we refer back to the viscosity of flocculated suspensions, we had assumed there that if we started to shear the suspension at a particular shear rate, then we assumed that the floc radius immediately adjusted itself to that value appropriate to the shear rate. This of course is not the case, and a finite time is required for such changes to take place. During this time, if the shear rate has been changed from a lower to a higher shear rate, then initially the viscosity is that which is pertinent to the floc radius of the lower shear rate, then slowly the average radius of the flocs—and consequently the viscosity—decreases. On the other hand, if the shear rate is decreased, the average floc size gradually increases, and the viscosity subsequently increases also, see figure 13.

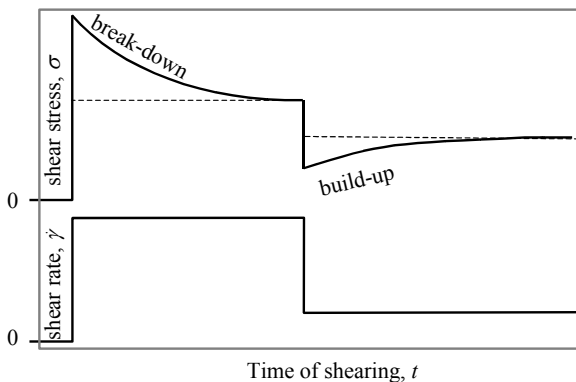


Figure 13: The behaviour of a thixotropic liquid, initially at rest, and then subjected to a high shear rate followed by a lower shear rate.

In fact, *any* shear-induced change in the microstructure of a suspension takes time to occur. This is true for the simplest changes such as the transition from the random-at-rest situation for simple suspensions to the breakdown of flocs to primary particles when flocculated suspensions are sheared hard. The former change is often over before the relatively slow mechanics of most viscometers could detect it, but the latter kind of change can take hours or even days to complete!

Thixotropy is a function of time and shear rate, and therefore cannot be properly accounted for in experiments where both these variables are changed simultaneously. This is true in *loop tests* where either shear rate or shear stress is varied in a triangular fashion with time, increasing linearly from zero to a maximum and back again. The measured results for the up- and down-curves are quite different for the first few loops, and the area between these curves is sometimes used as a measure of thixotropy, but these produce numbers that are impossible to relate to quantitative description of the phenomenon. For this reason, loop tests are *not* recommended for the serious study of thixotropy.

The best experiments to properly measure thixotropy are those where the sample to be tested is sheared at a given shear rate until equilibrium is obtained, then as quickly as possible the shear rate is changed to another value. The typical response to such a step-wise change from one steady-state condition to another is, in terms of the viscosity, often characterised by the so-called *stretched exponential model*:

$$\eta = \eta_{e,\infty} + (\eta_{e,\infty} - \eta_{e,0})(1 - e^{-\frac{t}{\lambda}})$$

where $\eta_{e,0}$ is the viscosity at the commencement of shearing; $\eta_{e,\infty}$ the viscosity after shearing for an infinite time and λ is a time constant. Note that this formula accounts for the fact that the eventual viscosity will be higher than the original value when we move

from a higher to a lower shear rate, and the viscosity recovers. The value of λ is a function of both the original and the final shear rate.

Further details on the subject of thixotropy may be found in a review published by the author [11].

15.9 Shear thickening

In very specific circumstances, the viscosity of a suspension can *increase* with increasing shear rate as well as decrease. After the flow field has organised the particles into strings and layers, there can come a time when, if the shear-rate/shear-stress is high enough, the particle ordering will break down and clumps of particles are formed. The form of these shear-induced clumps may be temporary strings aligned across the flow, or permanent or transient random groupings or strings of particles. The result of this disruption is an *increase* in viscosity. The form of this increase is shown in figure 14.

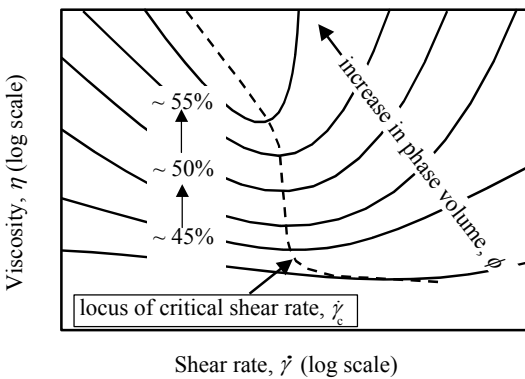


Figure 14: Schematic representation of the flow curve of a typical shear-thickening suspension, for various phase volumes.

The increase in viscosity follows on from the normal *decrease* of viscosity with increasing shear rate seen with all suspensions. The increase then seen becomes more and more abrupt as the concentration is increased. Since the viscosity is double-valued with respect to shear stress, strange things can happen when stress-controlled rheometers are used to measure this phenomena. For instance, if a stress-sweep programme is used, the shear rate will increase, but eventually decrease.

The overall situation with respect to the effect of particle size is shown in figure 15, where particle sizes from very small to quite large are responsible for the onset of shear thickening moving from very high to very low shear rates. In fact, the critical shear rate is approximately proportional to the inverse of the particle size *squared*. More details on this interesting but troublesome phenomenon may be found in a review written by the author [12].

15.10 Apparent wall slip

An apparent slip or lubrication occurs at the wall in the flow of any multi-phase systems if the disperse phase moves away from smooth walls. This arises from steric, hydrodynamic, viscoelastic and chemical forces present in suspensions flowing near smooth walls and constraints acting on the disperse phase particles immediately adjacent to the walls, see [13].

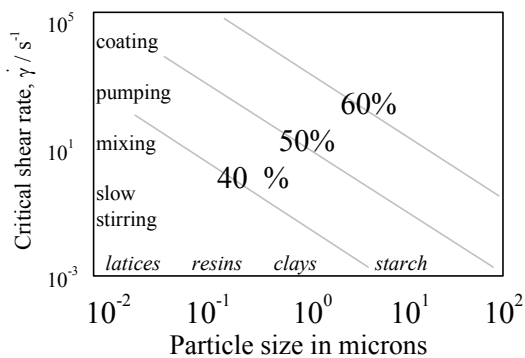


Figure 15: Critical shear rate 'map' for the onset of shear thickening as a function of particle size and phase volume, for various operations and materials.

The enrichment of the boundary near the wall with the continuous (and usually low-viscosity) phase means that any flow of the suspension near such a boundary is easier because of the lubrication effect. Because this effect is usually confined to a very narrow layer—with typical thickness of $0.1\text{-}10 \mu\text{m}$ —it so resembles the slip of solids over surfaces that it has historically been described by the same terminology. The restoring effect for all the forces that cause an increase in concentration as particles move away from walls is usually osmotic, and this will always limit the movement of particles away from the walls, thus also limiting the effective slip.

How do these effects occur? When any suspension of particles is placed next to a smooth wall, the original microstructure is locally disturbed. For a simple suspension at rest where the particles are randomly dispersed in space, the concentration of particles undergoes a damped oscillatory variation as one moves away from the wall, see figure 16, where the concentration is at the maximum packing fraction, so that the effect is enhanced. The new distribution has two effects, first that the variation in concentration does not die out until about five particle radii away from the wall, and secondly that the average particle concentration is zero at the wall and less than average for a small distance away from the wall.

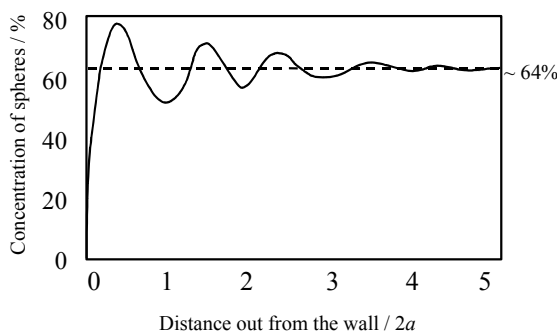


Figure 16 : The local concentration of spheres as a function of distance from the wall, measured in sphere diameters.

As well as these static—essentially geometric—effects that produce depletion at the wall, there are also dynamic effects which enhance the phenomenon. The existence of a shear rate and/or a shear rate gradient in the fluid next to the wall (as in a pipe) results in a further movement of particles away from the wall, towards areas of lower shear rates such as the centre of pipes. Solid particles, emulsion droplets and polymer molecules all show this tendency.

The result of these combined static and dynamic depletion effects is an effective lubricating layer at the wall. This can be modelled simply as a particle-free layer of about half a particle-radius wide. Hence the lubricating effect is larger for larger particles, and in this context large particles include flocs, so that at low shear rates, slip effects are stronger than at higher shear rates for flocculated suspensions.

Slip manifests itself in such a way that viscosity measured in different-sized viscometer geometries gives different answers if calculated the normal way - in particular the apparent viscosity *decreases* with decrease in geometry size (e.g. tube radius). Also, in single flow curves, unexpected lower Newtonian plateaus are sometimes seen, with an apparent yield stress at even lower stresses. Sudden breaks in the flow curve can also be seen. The typical effect of slip on flow curves measured in viscometers/rheometers is shown in figure 17. The effect is obviously very gap-size dependent, since the slip layer becomes more and more important as the gap size decreases.

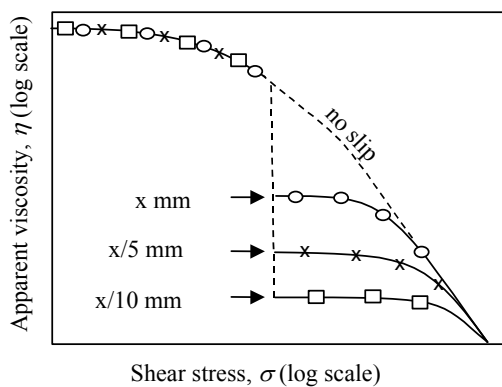


Figure 17: Viscosity versus stress plot for a flocculated suspension showing slip effects, as a function of concentric-cylinder gap.

What do we need to do about slip? First we might want to properly describe the slip in viscometers because it might also be happening in the situation we are dealing with, such as flow down smooth-walled process pipework. In this case we can for instance write down the following equation for flow in a pipe with a very thin Newtonian slip layer in a pipe of radius a ,

$$\frac{4Q}{\pi a^3} = \dot{\gamma}_w + \frac{4V_s}{a}$$

where Q is the overall flow rate and V_s is the velocity at the edge of the slip layer. The effect of this is shown in figure 18, where we see the possibility of extrapolating the apparent wall shear rate ($4Q/\pi a^3$) in pipes of different diameter but at the same values of wall shear stress σ_w (= $Pa/2L$), in order to extract the no-slip shear-stress/shear-rate data as well as obtaining the slip-velocity/shear-stress function from the slope of the curves. This type of graph is called a Mooney plot, and enables us to extract both the wall shear rate, $\dot{\gamma}_w$, and slip velocity, V_s , as a function of wall shear stress from simple plots of Q/a^3 vs. $1/a$ for fixed values of σ_w in different pipes.

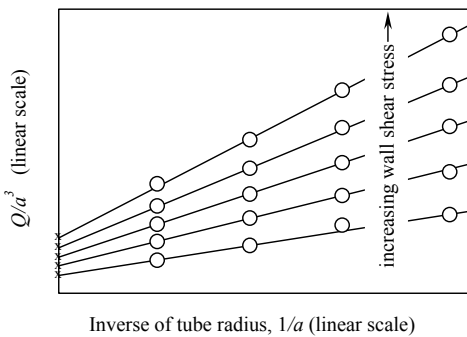


Figure 18: The apparent wall shear rate as a function of inverse diameter for various wall shear stresses.

Rather than *characterising* slip, we might want to *eliminate* it. This can often be done by sandblasting or otherwise roughening or profiling (with ribs etc.) the surfaces where the test liquid comes in contact with the viscometer. In fact, any regular surface undulations of the order of $10 \mu\text{m}$ should eliminate slip effects in most cases. See chapter 7 for a further discussion of the elimination of slip, especially by the use of the vane and basket geometry.

In summary we can say that slip becomes more and more important as

- concentration is increased, with greater difference between the slip layer and the plug viscosities,
- particle size is increased (flocs included),
- viscometer gap size (or tube radius) is decreased and
- (usually) shear rate is decreased, see figure 17.

15.11 Very high concentration pastes

In many situations, the concentration of a suspension is so high that the flow properties in *shear* are dominated by the shearing thin slip layer and an almost unsheared solid plug, while for any *extensional flow* that the paste encounters (such as flow into an orifice or the entrance of a tube) still demands the deformation of the whole paste. In these situations the flow of a typical paste into and along a tube, such as are found in ceramic and battery pastes etc., can be characterised by the formula

$$P = 2(\sigma_o + \alpha_1 V^m) \ln \left[\frac{D_0}{D} \right] + 4(\tau_o + \beta_1 V^n) L / D$$

where the first term describes the entry flow *into* the tube (dominated by extensional flow), and contains the yield stress of the *bulk* material, σ_o , see [14]. The second term describes the slip flow *along* the tube, and is characterised by a possible (but not always necessary) slip yield stress, τ_o , with a power-law index in each case, given by m and n respectively. In the simplest case, m and n are unity, and the slip yield stress, τ_o , is zero.

Cone penetrometry of paste-like materials can be used to measure the apparent extensional yield stress using the equation

$$\sigma_o = \frac{F}{\pi L^2 \tan^2 \theta}$$

where F is the applied force, θ is the half angle of the cone, and L is the penetration depth.

15.12 Colloidal control of suspension viscosity

Some very significant changes can be brought about by the alteration of colloidal conditions, since the overall force between particles can be made more attractive or repulsive in nature. We will now consider a few examples of such manipulation.

First, we see the effect of the addition of electrolyte to a suspension of highly-charged spheres. Particle surface charge results in a large repulsion between adjacent particles, causing them to form into a pseudo-crystalline state with particles sitting on regular lattice positions (but vibrating due to the incessant Brownian motion). In this state, it is difficult for particles to pass over each other in shear flow, jumping from one lattice position to the next, hence out of one potential well into another. The result of this is a high viscosity, see figure 19. If electrolyte (i.e. salt) is now added to the aqueous phase, the charges on the particle are shielded, and the interparticle repulsion is reduced and the viscosity—at least at low shear rates—drops significantly. There might also be an accompanying small drop in viscosity at high shear rate, see §15.2.2 above.

If enough salt is added, the particles are eventually neutral with respect to one another, and just bounce off each other if they collide. The viscosity is then at a minimum. If even more salt is added, the electrostatic repulsion is swamped, the van-der-Waals attractive force dominates, and the particles flocculate. The viscosity then increases again, as in figure 19.

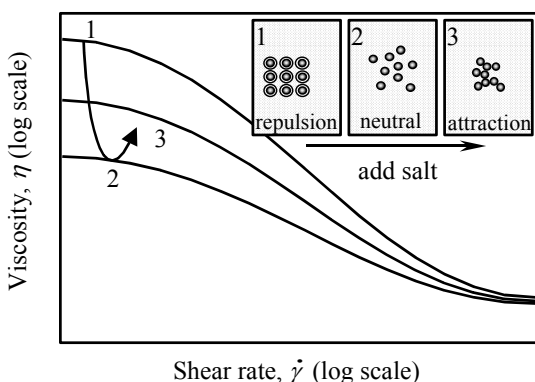


Figure 19 : Flow curves resulting from the addition of electrolyte (salt) to the aqueous phase of a suspension of charged particles.

Our second example is the change of surface forces brought about by change in solution pH. The hydroxyl groups on many mineral particles—chalk, titanium dioxide, quartz, etc.—become charged (in terms of degree and sign) according to the solution pH. Thus at very low pH we might have a large positive charge on the particle surfaces, while at very high pH the situation might completely reverse to a large negative charge. Between these values the charge can pass through zero—at the so-called *isoelectric point* (some examples of the isoelectric point in terms of pH

are, titanium dioxide ~ 8 , alumina ~ 10 , calcium carbonate ~ 12). The effect on the viscosity is shown in figure 20. At the isoelectric point the system flocculates and becomes very shear thinning.

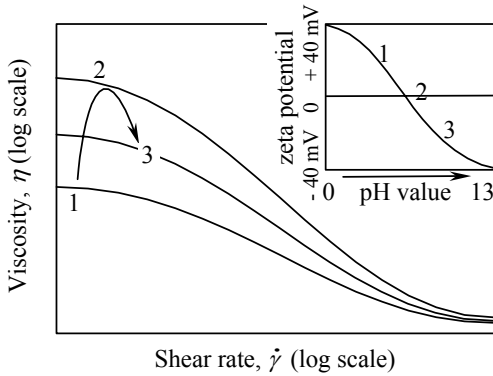


Figure 20: Flow curves resulting from changing the surface charge (via solution pH) on the suspended particles of a concentrated suspension.

Last, we will consider the effect of adding surface-active material or very high molecular weight polymers that absorb at one end or at intervals onto the suspended particle surface (block co-polymers). If we begin with a flocculated – and hence high viscosity – suspension, and add sufficient of this kind of material, then after vigorous stirring the viscosity drops significantly as the particle surface gets covered. The electrostatic or the steric repulsion (or both) causes the state of flocculation to reduce or disappear with its accompanying reduction in viscosity.

One other interesting effect is found with either shearing emulsions or grinding particles in a mill. If a certain amount of surface active material or polymers are adsorbed to reduce the viscosity, then when the particle size is reduced, the surface area increases greatly (as $1/a^2$), and hence the *surface coverage* (concentration per unit area) decreases, and hence the interparticle repulsion decreases. This can, under the appropriate conditions, lead to flocculation, and hence an increase in viscosity. Consequently, processing operations which involve size changes can greatly affect viscosity.

In summary, we note the following colloidal factors at our disposal that we could use to change the viscosity of a given suspension -

- continuous-phase electrolyte concentration
- change of surface charge by changing pH
- surface coverage of particles by surface active agents
- adsorption of block copolymers
- changing total surface area by size reduction

15.13 The stability of suspensions

The equation that we gave in §6.4.2 for the velocity of a cloud of spheres moving in a liquid under the influence of gravity, is sometimes applicable to the stability of non-flocculated suspensions or emulsions, viz.

$$V = \frac{2\Delta\rho g a^2}{9\eta} (1 - \varphi)^{5 \pm 0.25}$$

where

- $\Delta\rho$ is the density difference between the suspended and the continuous phases,
- a is the average particle radius,
- g is the acceleration due to gravity (9.8 m/s^2),
- ϕ is the phase volume of the suspended phase, and
- η is the continuous phase viscosity.

If either the continuous phase is Newtonian, or else has a low-shear rate Newtonian plateau controlling the velocity, then the equation can be used. If the particle size a is less than a micron, then the final exponent in the equation is ~ 5.2 , while for particles greater than a micron, it is lowered to ~ 4.8 . Figure 21 shows the effect graphically, and illustrates that for a phase volume ϕ of 50%, the sedimentation ($\Delta\rho > 0$) or creaming ($\Delta\rho < 0$) velocity reduces to around 0.05 or 0.025 times the velocity of a large or small isolated sphere respectively.

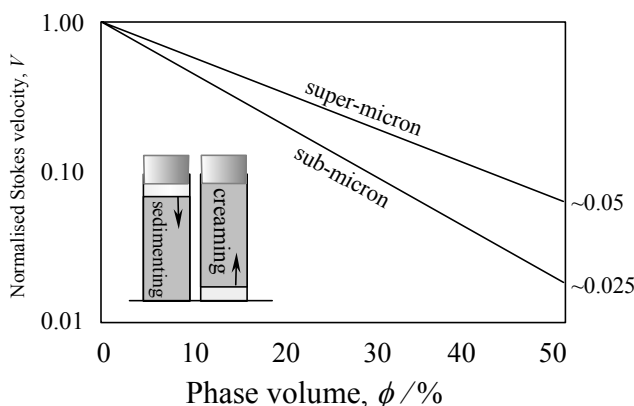


Figure 21: Normalised Stokes velocity as a function of phase volume for super- and sub-micron particles respectively.

Here the overall velocity V is the same as that of the interface between the concentrating suspension and the clear liquid left behind.

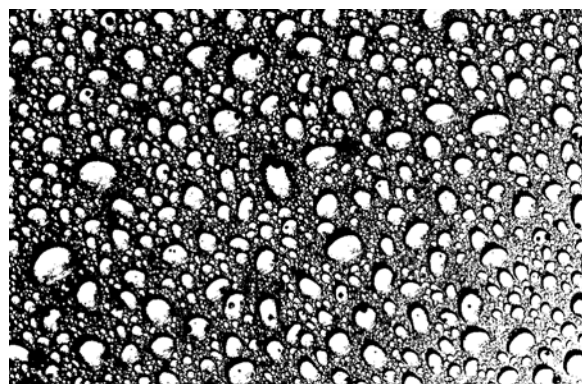
Exercise: consider what happens if salts are added to water to above their solubility limit, bearing in mind the effect of crystal shape.

References

- [1] Wagner, J., *Zeit. Physik. Chem.*, 5, 31 (1891).
- [2] Bancelin, M., *Comp. Rend.*, 152, 1382 (1911).
- [3] Barnes, H A, 'Dispersion Rheology 1980, a survey of industrial problems and academic progress', Royal Soc. Chem., Industrial Div., London, 1981.
- [4] Garcia-Salinas, M. J; de las Nieves, F.J., *Progr. Coll. Poly. Sci.*, 110, 134 – 138 (1998).
- [5] Krieger, I.M; Dougherty, T.J., *Trans. Soc. Rheol.*, 3, 137 – 152 (1959).
- [6] F. Baker, *Trans. Chem. Soc.*, 103, 1655 (1913).
- [7] Wakeman, R., *Powder. Tech.*, 11, 297 – 299 (1975).
- [8] Barnes, H.A; Hutton, J.F; Walters, K, 'An Introduction to Rheology', Elsevier, Amsterdam 1989.

A Handbook of Elementary Rheology

- [9] Barnes, H.A, Colloids and Surfaces A: Physicochemical and Engineering Aspects, 91, 89-95 (1994).
- [10] Barnes, H.A, '*Recent advances in rheology and processing of colloidal systems'* Keynote Address in 'The 1992 IChemE Research Event', pp. 24-29, IChemE, Rugby, 1992, ISBN 0 85295 290 2.
- [11] Barnes, H.A, JNNFM, 70(1/2), 1 - 33 (1997).
- [12] Barnes, H.A, J. Rheol., 33(2), 329-366 (1989).
- [13] Barnes, H.A, , JNNFM, 56, 221 - 251 (1995).
- [14] Benbow, J; Bridgwater, J, '*Paste Flow and Extrusion*', Clarendon Press, Oxford, 1993.



CHAPTER 16: POLYMER RHEOLOGY

'One cannot help but be in awe ... contemplating ... the marvellous structure of reality',
Einstein

16.1 Introduction

The flow of polymer systems, whether solutions or melts, has fascinated rheologists for many years. Since these systems often display very viscoelastic properties, they have attracted more-than-expected attention from a wide range of workers. We find polymer solutions in many every-day situations, especially among the macromolecular (i.e. polymeric) solutions found in the human body such as mucus, saliva, blood proteins, joint lubricating fluids, etc. In terms of natural products, various gums and resins have proved very useful in many practical situations. Then man-made polymers represent a huge industry, whose products pervade every part of our lives, ranging from consumer-product packaging through to the innumerable plastic articles of every-day life.

Sources of well-known polymeric material vary considerably, for instance

- | | |
|--------------------|--|
| • trees and plants | - gum-arabic, cellulose |
| • seeds | - Guar gum, locust bean gum |
| • seaweed | - carageenan, alginates, agar |
| • fruit | - pectins |
| • grains | - starches |
| • microbial | - xanthan gum |
| • animal | - gelatin, keratin and |
| • petroleum | - acrylic acid, polyacrylamide, and many plastics. |

The special properties of polymers arise because although macromolecules are long and intertwined, they are nevertheless small enough to be subject to Brownian motion that tends to randomise their configuration, giving linear chains that 'ball-up' to an approximate spherical shape. The ever-present Brownian randomising is in competition with flow effects that seek to straighten isolated polymer chains and 'comb-out' entangled chains. All these effects combine to give long-range interactions that persist to high shear rates. Also, when linear polymers are stretched, their unique configuration allows for the transition to highly aligned strings in the stretch direction. This gives a very high resistance to stretching manifested in a large extensional viscosity, see later.

16.2 Some of the different kinds of polymer chains

In order of complexity of their configuration, the general forms of macromolecules described in the following paragraphs are often encountered.

16.2.1 Long rods

Some polymers are naturally rod-like, for instance xanthan gum ($Mw \sim 2 \times 10^6$, with a typical length up to 1 micron and an aspect ratio, L/d , of ~ 600), while others can become rod-like. An example of the latter is a polyelectrolyte in a very low electrolyte solution, where the electrostatic charges along the polymer chains repel each other and force the convoluted chain to become straight. For rod-like polymers with an aspect ratio of up to around 200, the relative increase in viscosity compared with the solvent ($\eta_{sp} = (\eta - \eta_s)/\eta_s$) is given by the approximate relationship [1]

$$\eta_s \approx 2.5 + \frac{1}{10} \left[\frac{L}{d} \right]^{5/3}$$

when the shear rate is low and the rods are randomised by Brownian motion. However, when they become aligned along or across the flow at high shear rates, the specific viscosity in both cases drops to approximately 2.5, thus becoming independent of aspect ratio L/d . This is an obvious source of shear thinning, but also shows that the viscosity difference between low and high shear rate increases with aspect ratio. (Of course the Brownian motion is always trying to randomise the rods, and the result is an accompanying elastic restoring force.)

The *extensional* viscosity (see chapter 17 for details) of semi-dilute suspensions of long rod- or fibre-like entities (xanthan gum being a good example) is given by [2]

$$\eta_e = 3\eta_s \left[1 + \frac{4\phi \left(\frac{L}{d} \right)^2}{9 \ln \left(\frac{6}{\phi} \right)} \right].$$

This shows that the aspect ratio plays a dominant part in determining the extensional viscosity.

16.2.2 Coils/Strings

These types of polymers can either be linear or branched, but because they are usually made up of segments that are freely jointed, they can take up many transient configurations under the action of Brownian motion. At a low-enough concentration, when linear coils are isolated and non-interacting, they take up an approximate spherical shape, the size of which is dictated by thermodynamics, see figure 1. When they are sheared, these spheres become ellipses which are (slightly) aligned to the flow. At the highest shear rates, the coils can be unwound into strings completely aligned with the flow.

At high concentrations, the chains are completely intertwined and entangled (see figure 2), and being under the incessant action of Brownian motion, they move around like 'snakes in a snake pit', continuously sliding over each other, forming and disengaging from individual entanglements as they move. Polymer melts are of course made up of these chains alone, while concentrated solutions have solvent between the chains which strongly influences the overall rheology.

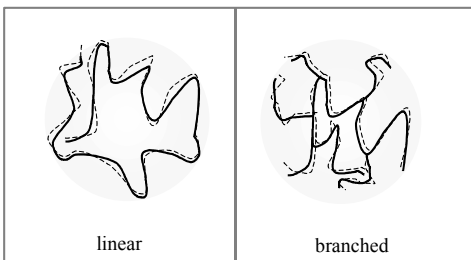


Figure 1: Isolated polymer coils subject to Brownian motion: note the space-filling efficiency of a small amount of material, with solvent immobilised within the coils.

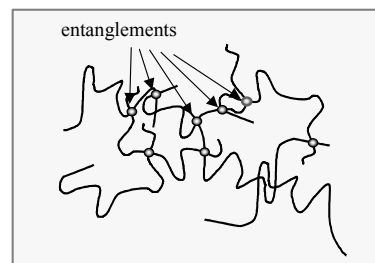


Figure 2: Concentrated coils overlapping, and highly entangled. Note that entanglements are continually forming, disappearing and reforming, but at any one instant there is a transient network.

Melts and concentrated solutions are elastic because tension in the chains between entanglements persists while the entangled chains slide over each other. The transient networks present in such situations are elastic on a short time-scale, but as the stretched chains slide over each other and loose entanglements, they relax and show normal viscous behaviour.

The controlling factors for polymer rheology include concentration, molecular weight distribution, and degree of branching, as well as temperature and pressure. Of course there is also the obvious difference between a melt and a solution, with concentration playing no part in melt rheology (except for additives to the melt such as plasticisers). Below a critical molecular weight, Mw_c , the viscosity of a molten polymer is almost directly proportional to the weight average molecular weight, Mw_{av} . However above this value of molecular weight, Mw , the proportionality dramatically increases to a power-law relationship of around 3.4 [3], so

$$\eta_0 = K[Mw_{av}]^{3.4}.$$

The critical molecular weight is the point at which entanglements become important, and below that value the chains may be considered as non-penetrating spheres. This critical molecular weight depends on the chain configuration, but apart from some important exceptions, it is of the order of tens of thousands. Obviously entanglements make flow more difficult, hence the higher dependence on molecular weight. However, at very high shear rates, the entanglements disappear as the flow ‘combs’ them out; the dependence on molecular weight disappears, and the viscosity is only dependent on concentration, see figure 3.

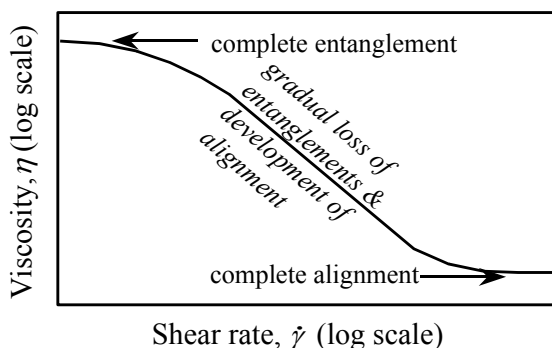


Figure 3: The flow curve for a polymer solution showing the two extremes of complete entanglement and complete alignment.

All the individual curves for a series of molecular weights, temperatures and shear rates can often be incorporated into a single master curve by plotting the non-dimensional quantity $\frac{\eta}{\eta_0}$ against $\frac{\eta_0 \dot{\gamma} Mw^\alpha}{\rho T}$, where α is a constant near unity, ρ is the polymer density at T , the temperature in degrees Kelvin.

All else being equal, broadening the molecular-weight distribution generally results in a polymer melt becoming non-Newtonian at lower values of shear rate, so by the time we come to those shear rates relevant to extruding etc., the polymer is easier to handle with a lower viscosity.

A small degree of branching of the polymer chains generally decreases the viscosity of a melt with the same average molecular weight since the branched chain is more compact. However, if the branching is extensive, for a reasonably high molecular weight ($\sim 10^6$) the viscosity at low shear rates may be much higher, given the difficulties for these complicated interpenetrating structures to move. Imagine the structure as a collection of stars, i.e.*. Nevertheless, in almost all cases branching results in a lower viscosity at high shear rates.

16.3 Polymer solutions

The viscosity of polymer solutions, as well as depending on shear rate and temperature (and in some extreme cases pressure), also depends on the molecular weight distribution and the concentration, see figures 4 and 5.

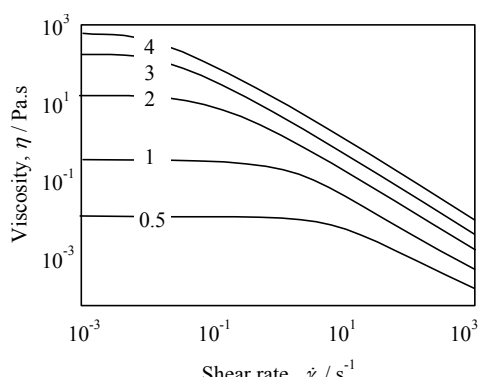


Figure 4: The flow curve for polystyrene in toluene, $Mw = 20M$, for different concentrations of polymer (shown as wt.%)

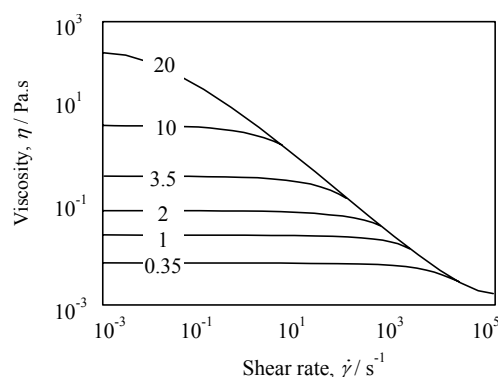
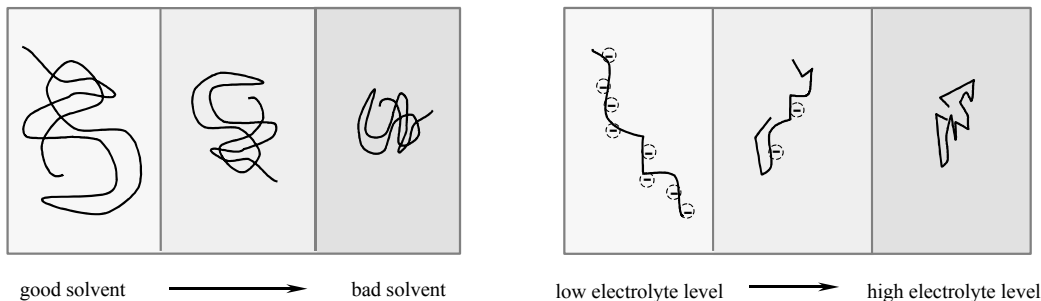


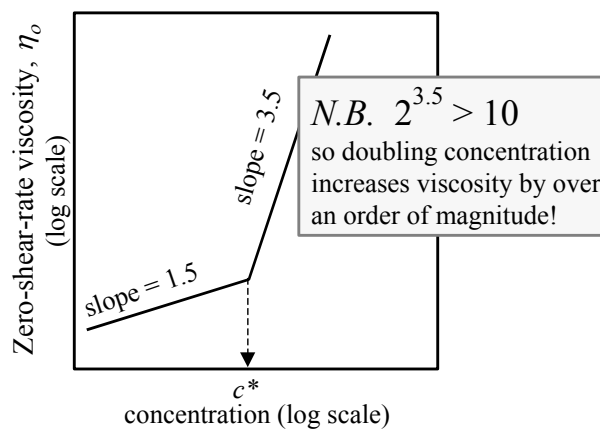
Figure 5: The flow curve for 3% w/w polystyrene in toluene, for different molecular weights (shown in millions).

The solvent properties are also important since the quality of the solvent can vary for organic liquids from 'good' to 'bad', and have the effect shown in figure 6, with the effect on the viscosity being then obvious.

In aqueous systems, some polymers have charges distributed along the chains. In that case, the amount of electrolyte (salt) in the aqueous solvent will affect the overall shape of the chain, see figure 7. In the absence of electrolyte, the charges are unshielded and repel one another. This results in the chain being stretched out. However, when electrolyte is present, the charges are shielded and their effect is suppressed, resulting in the chain tending to shrink towards its natural random configuration. This change from a rod to a sphere obviously causes the viscosity to decrease.

**Figure 6:** The effect of solvent quality on polymer coil dimensions.**Figure 7:** The effect of electrolyte on the coil dimensions of a polyelectrolyte.

As in polymer melts, there is a point at which entanglements take place in polymer solutions. However, in the solution case it is controlled by concentration as well as molecular weight. Figure 8 shows the dependence, which changes from a low to a high dependence, being governed by the critical concentration c^* .

**Figure 8:** The zero-shear-rate viscosity of a polymer solution versus polymer concentration, showing the critical overlap concentration c^* .

The intrinsic viscosity of many polymer solutions is given by the so-called Mark-Houwink equation [3]

$$[\eta] = KM^\alpha$$

where M is the molecular weight and K and α are constants for particular kinds of polymers, for instance α varies from 0.5 for a random coil to 2 for a rigid rod.

16.4 Highly branched polymers

When highly branched chains are sheared, they too unwind, but they cannot form very long strings because of the branching. For this reason they do not give 'stringy' liquids, see chapter 17. This is important for thickening consumer products, and for this reason the highly-branched Carbopol polymers are highly prized for thickening without causing stringiness. Highly cross-linked polymers like these are called *micro-gels* for obvious reasons. At quite low concentrations—often less than 1% by weight—these microgel particles form a space filling network, which give a

high viscosity, but at the same time is extremely shear thinning, giving the appearance of a high apparent yield stress, see chapter 15.

16.5 'Living polymers' or rod- or worm-like micelles

If the right molecular proportions and electrolyte concentrations are chosen, mixtures of many surfactant molecules form themselves into rods or worm-like threads, which are sometimes called '*living polymers*', see chapter 18. Figure 9 shows a schematic representation of these micelles.

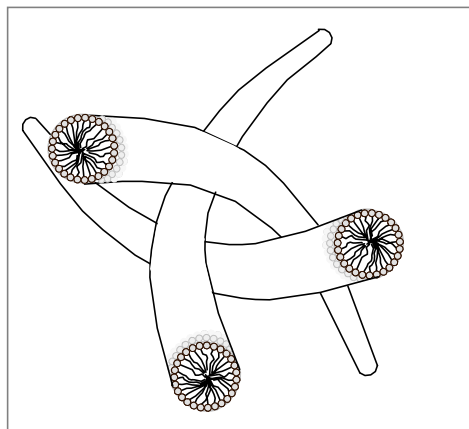


Figure 9: A schematic diagram of worm-like micelles.

At concentrations of a few weight percent, these rods/worms behave in exactly same way as the equivalent macromolecules, and entangle with each other to form transient networks. The end result is strong viscoelastic behaviour. This is often seen in transparent hair shampoos, shower gels, thickened bleaches, etc. The rods so formed give the best possible thickening for a given amount of surfactant. In their efforts to use this efficient thickening, some manufacturers overdo the viscoelastic effect and produce liquids that are very stringy and verge on being unpleasant to use.

'Living polymers' have one extra property that the normal polymer system lack, and hence their name, as we now show. If either polymer chains or surfactant worm-like micelles are subjected to a high extensional force, they can be snapped in half. While polymer fragments always remain thereafter at this lower (halved) molecular weight, the broken surfactant micelles can reform under more quiescent conditions, since they are thermodynamic objects held together by reversible bonds. If elastic liquids are needed to withstand continual damage, and yet survive, then these micellar systems are much more mechanically robust—a good example of this is in turbulent drag reduction. For this reason they have been suggested for drag-reducing fluids in central-heating systems. On the other hand, they are more prone to chemical breakdown if electrolytes or metal ions enter the system.

Like all fibrous microstructures, the viscosity is high when the system is randomly dispersed in space and highly entangled, but once the flow has aligned the microstructures, the viscosity is quite low. This change from very high to very low viscosity takes place over a narrow range of stress, see figure 10. This is the situation for shampoos and shower gels.

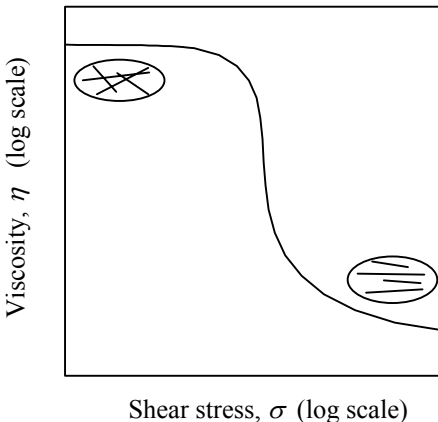


Figure 10: The form of the flow curve for worm-like micelles, e.g. shampoos.

16.6 Associative polymers

These are an interesting class of polymers which have hydrophobic (water-hating) pendant (side) and/or terminal groups on their hydrophilic (water-loving) chains, making them similar in some respects to surfactant molecules. These end/side-groups naturally clump together, either with similar groups nearby on the same chain, or else with similar groups on adjacent chains, the latter interaction producing a loose network. Each group only spends a given amount of time in such an association before Brownian motion dislodges it, but sometime later the same randomising force brings the end-group into another association. Thus if we take a snapshot at any time, there is a gel-like network (showing viscoelastic properties), but over time, there is flow (see [4]). The molecular weight of each polymer chain can be quite low (10^4 - 10^5 daltons), but the overall effect is to produce a high viscosity. The kind of network formed is visualised in figure 11.

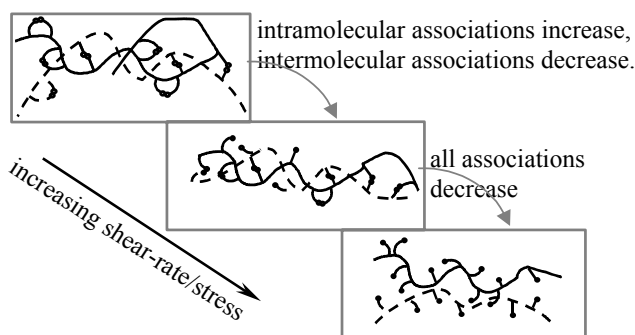


Figure 11: The interactions between the hydrophobic endgroups in associative polymers, [5].

It is also possible for shearing to produce new junctions between polymer chains at the expense of those between end-groups along particular chains, and hence the viscosity can *increase* after the low-shear-rate Newtonian plateau by up to 100%. However, the normal effect of shearing soon takes over afterwards when associations are lost due to large stresses and then the viscosity decreases as usual, see figure 12: this effect has also been seen in extensional flow [6]. These kind of

thickeners are often used in water-based coatings, drilling fluids, liquid laundry additives and personal-care products.

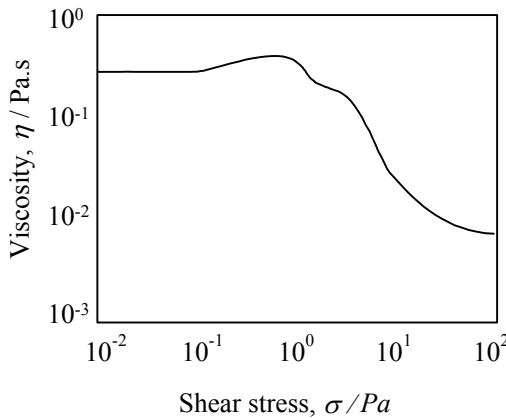


Figure 12: The typical form of the flow curve for an associative polymer solution, [5].

Obviously, the sites where the hydrophobic ends can interact can be blocked by ordinary surfactant molecules and the viscosity decreases, or interestingly, the associations can be strengthened by the addition of electrolyte. Thus the usefulness of associative polymers is very formulation dependent.

16.7 A polymer solution as a standard non-Newtonian liquid

It is worth giving especial consideration to a particular polymer solution which has been extensively researched around the world and has now become a commercially-available, non-Newtonian standard liquid. It is a 2% w/v solution of poly(isobutylene) (molecular weight $4.3 \cdot 10^6$ daltons) in a mixture of *cis*- and *trans*-decalin. It is marketed by the Pure and Applied Chemistry department, University of Strathclyde, Scotland, as Standard Fluid SUA1.

Data is provided on the complete rheological characterisation, relative to steady-state shear stress and first and second normal stress differences as a function of shear rate, as well as the complementary oscillatory data, see figures 13 and 14. The measured extensional properties are also available, see figure 15 [7].

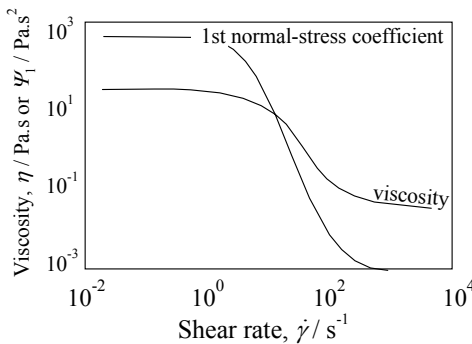


Figure 13: The viscosity and first normal-stress coefficient as a function of shear rate for the SUA1 standard polymer solution.

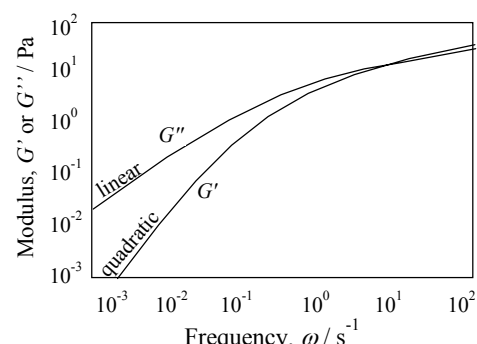


Figure 14: The linear viscoelastic parameters G' and G'' as a function of frequency for the SUA1 standard polymer solution.

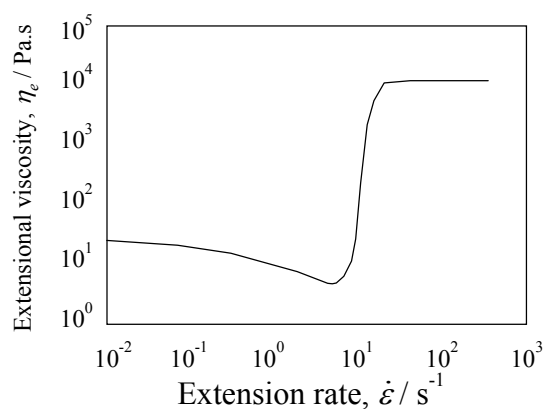


Figure 15 : The extensional viscosity as a function of extension rate for the SUA1 standard polymer solution.

References

- [1] Scheraga, H.A., J. Chem. Phys., 23, 1526 (1955).
- [2] Acrivos, A; Shaqfeh, E.S.G., Phys. Fluids, 31(7), 1841 – 1844 (1988).
- [3] Ferry, J.D., ‘Viscoelastic Properties of Polymers’, 2nd Edition, John Wiley, New York, 1970.
- [4] Annable, T; Buscall, R; Ettelaie, R; Whittlestone, D., J. Rheol., 37(4), 695-726 (1993).
- [5] English, R.J; Gulati, H.S; Jenkins, R.D; Khan, S.A., J. Rheol., 41(2), 427 - 444 (1997).
- [6] Kennedy, J.C; Meadows, J; Williams, P.A., J. Chem. Soc. Faraday Trans., 91(5), 911 – 916 (1995).
- [7] Hudson, N.E; Jones, T.E.R., JNNFM, 46, 69 – 88 (1993).



CHAPTER 17: EXTENSIONAL FLOW AND VISCOSITY

*'There was things which he stretched, but mainly he told the truth', Mark Twain
in 'The Adventures of Huckleberry Finn'*

17.1 Introduction

Although most viscometric and rheological studies are carried out in simple shear flows such as rotational viscometers, *real* flows experienced by *real* liquids are very often *extensional* (stretching or elongational) in nature, and for some liquids there can be a very large difference between their shear and extensional viscosities.

To recap, in extensional flow the elements of a fluid are stretched out or squeezed down rather than sheared. A good example of this is found in the flow in and out of a short tube, see figure 1, which is the kind of flow experienced when liquids such as ketchup, washing-up liquid and skin lotion are squeezed from plastic bottles, or when toothpastes, meatpastes and processed cheese are squeezed from tubes.

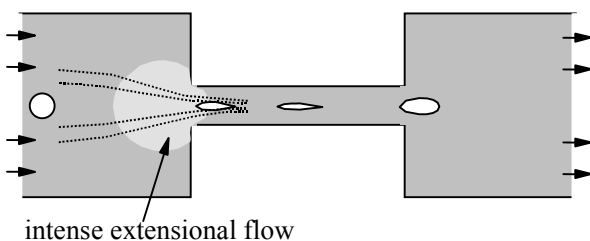


Figure 1: The deformation of a droplet from a larger to a smaller diameter tube, where the entrance region is dominated by extensional flow.

The history of a typical element of fluid in such a flow is shown in figure 1 as it moves, initially unsheared, along the middle of the first tube (remember the shear rate at the tube centre is zero), but then it has to stretch and deform in order to get into the smaller tube. Once it is well inside the smaller tube the stretching ceases. Then as the element emerging from the tube, it experiences compression along the flow axis as it tries to return to its original shape. If the same deformable drop is suspended in a liquid in simple shear flow, it is not deformed as much, see figure 2, and rotates in the flow at a rotation rate (in radians per second) equal to half the shear rate. For these reasons shear flows are called *weak* flows, while extensional flows are called *strong* flows. It is also obvious that extensional flow is irrotational, since our test element did not undergo any rotation in deforming.

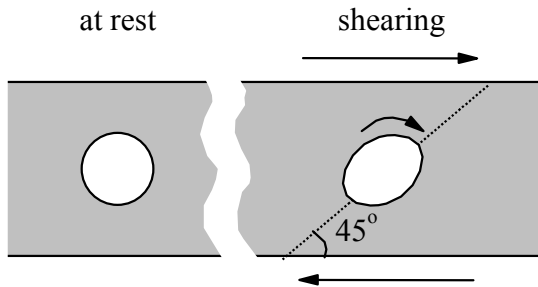


Figure 2: The motion of a droplet in shear flow.

If our test element is a small fibre initially aligned at an angle to the flow lines as it approaches the entrance to the smaller tube, the stretching flow it experiences as it enters the small tube tends to align it along the flow axis, and as it emerges from the smaller tube it would tend to move towards its off-axis angle again, see figure 3.

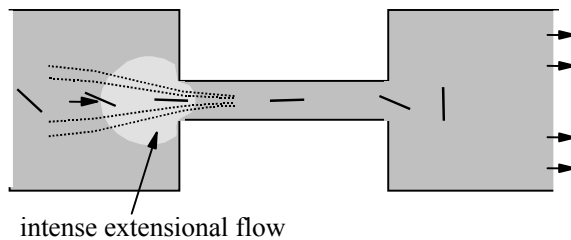


Figure 3 : The motion of a long fibre in and out of a small tube.

17.2 Where do we find extensional flows?

There are many everyday and industrial situations where there is a large element of extensional flow. Some of the following are typical,

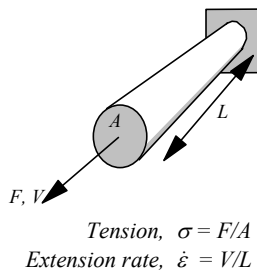
- flow into and out of orifices,
- break-up of liquid jets, droplet break-up, atomisation and spraying,
- expanding bubbles, in foam and doughs,
- unwanted atomisation (misting) in coating and printing operations,
- drinking through a straw (entry flow) and swallowing,
- blow-moulding and other inflation operations for plastic components,
- man-made fibre spinning, and even spinning spiders' webs,
- flow through porous media, and some
- rapid squeezing, forming and stamping operations.

In all these situations we can estimate the extension rate by calculating the appropriate velocity gradient *along* the flow direction. This is done, as usual, by dividing an appropriate *velocity difference* by an pertinent *distance*, as for instance in our example above, by dividing the difference of average velocity between two tubes, see figure 1, by the radius of the smaller tube.

17.3 What's so special about extensional viscosities?

What is the effect of stretching and alignment on the microstructure of real systems, and what resistances to flow (i.e. viscosity) do they show? First consider

one of the simpler forms of stretching flow – uniaxial extensional flow. This is the equivalent of pulling out a filament or thread of liquid, see figure 4, where the velocity gradient is *in* the flow direction, which is quite different from a shear flow where the velocity gradient is *at right angles* to the flow direction. In the same way that we have a stress and a deformation rate in shear flow, so now we have the extensional stress (also called the *tension*), σ_e and the extension (or elongational or stretching) rate, $\dot{\varepsilon}$, with the ratio of the stress and rate giving the uniaxial extensional (or elongational) viscosity, i.e. $\eta_e = \sigma_e / \dot{\varepsilon}$.



$$\text{Tension, } \sigma = F/A$$

$$\text{Extension rate, } \dot{\varepsilon} = V/L$$

Figure 4: Definition diagram for uniaxial extensional flow:
note that the far end of the liquid thread is anchored.

The first major difference between the shear and the extensional viscosity (apart from a mathematical feature which dictates that for *all* liquids at very low shear rate, $\eta_e = 3\eta$) is best illustrated by considering a single fibre suspended in a Newtonian liquid. If the liquid with the suspended fibre is subjected to a **shear** flow, the fibre will align along the flow axis, and then the disturbance it presents to the surrounding liquid is a *minimum*. On the other hand, if the same suspended fibre is subjected to an **extensional** flow, it again aligns, but now the resistance it presents to the flow is *maximised*, since the liquid being stretched tries in turn to stretch the fibre. This is reflected in the viscosity of a suspension made up of such suspended fibres in which the viscosity will *decrease* as a flow aligns the fibre in shear flow, but will *increase* the viscosity as it aligns in extensional flow, see figure 5. The eventual difference between the shear and extensional viscosities at high deformation rates increases with increasing aspect ratio of the fibres [1].

If the fibre concentration is much higher, there are many contacts between individual fibres, and the number of these contacts then dominates the viscosity. In fact the situation is very similar to a polymer solution or melt, in which case the contacts are intermolecular entanglements. In both cases we want to know about the dynamics of these contacts/entanglements as, for instance a function of extension rate.

At rest the transient network formed as the fibres or chains become entangled and disentangled under the action of Brownian motion, and stretching strongly interferes with the dynamics of this transient network. If the inverse of the extension

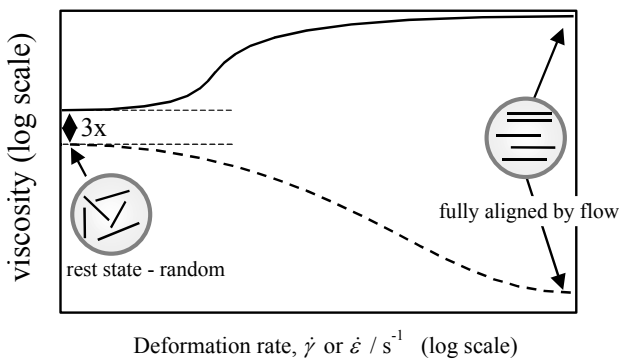


Figure 5: The shear (dotted line) and extensional (solid line) viscosities of a dilute fibre suspension, compared at comparable deformation rates.

rate is greater than the average lifetime of the entanglements forming the network, then momentarily the polymer segment between two entanglements is acting as part of an elastic solid, and the stress increases considerably, until the entanglements would rupture. If, in this situation, the average number of entanglements is constant, then it can be shown that the extensional viscosity *increases* dramatically with extension rate while the shear viscosity remains constant [2]. However, in reality, as the deformation rate increases, the number of entanglements (and possibly their lifetime) begins to decrease with increasing extension rate, then the viscosity—after increasing—drops again, and at the same point the shear viscosity also begins to fall. The overall effect is shown in figure 6. This explains the behaviour of many polymer solutions and melts. This shows another difference between shear and extensional viscosities.

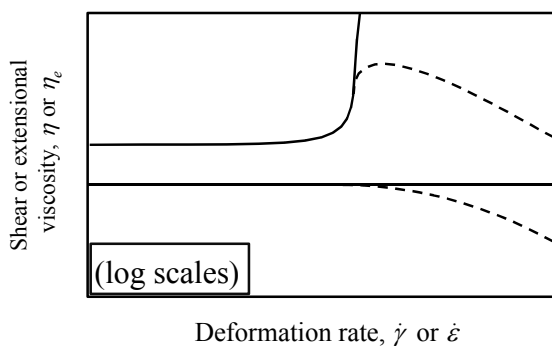


Figure 6: The shear and extensional viscosities of a polymer network, network dynamics effects shown as solid lines, and the effect of loss of junctions shown as dotted lines.

Last we note the most spectacular effect in extensional flow that is seen in very dilute solutions of high-molecular-weight, linear polymers, where the properties are dictated by the isolated individual polymer coils. At low shear and extension rates, the polymer chains are balled up into a loose spherical shape, and the viscosity is low. However, at a critical rate of extensional flow, the polymer suddenly unwinds into a long, stretched string. This is called the *coil-stretch transition*, and results in a spectacular increase in extensional resistance, to give a viscosity that can be up to thousands of times higher than the equivalent viscosity in shear flow, see figures 7 and 8. This is best seen when strings of liquids are pulled

out of the surface of such a solution, and it is virtually impossible to break them, due to their very high viscosity. One practical application of this effect is the suppression of atomisation in such liquids, see figure 8 for a real example of this phenomenon for the ICI aviation-fuel antimisting agent FM9.

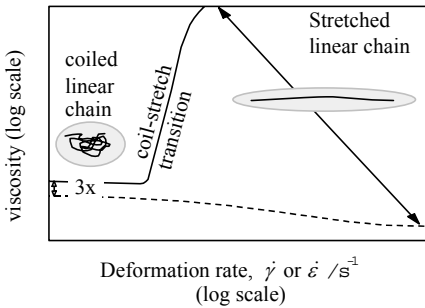


Figure 7: The shear (dotted line) and extensional (solid line) viscosities of a dilute solution of linear polymer, showing the coil-stretch transition from coiled to unwound configuration.

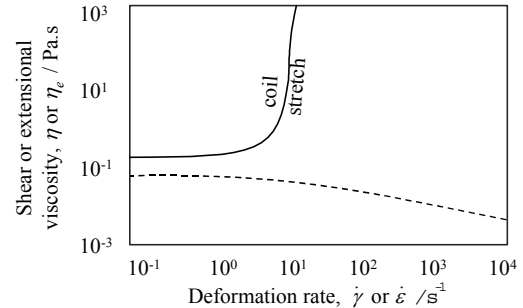


Figure 8: The shear (dotted line) and extensional (solid line) viscosities of an aviation fuel with an anti-misting agent added.

Recap.

The mechanisms that result in the extensional viscosity being much bigger than the shear viscosity are

- aligning particles with the flow results in **maximum** resistance
- strong interaction of extensional flows and network dynamics
- coil-stretch transition giving very long, aligned particles

A good example of what happens when two of these effects are present is shown in figure 9, where the *network dynamics* dictate the first increase and decrease in extensional viscosity, and *coil-stretch* accounts for the second increase, see [3].

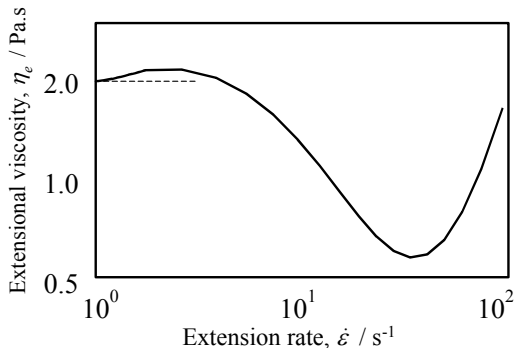


Figure 9: Extensional viscosity versus extension rate for a solution of polybutadiene in decalin, showing the extension/tension thickening, extension/tension thinning and coil stretch regions respectively.

17.4 The Trouton ratio

The difference between the two kinds of viscosities being considered is best illustrated by introducing the so-called Trouton ratio, defined as the ratio of the viscosities as measured at any particular shear rate and *root-three* ($\sqrt{3}$) times the equivalent extension rate. In all cases this ratio starts at 3 for small deformation

rates, and then at some critical point it can begin to rise. This is illustrated in figure 10. The rise can be quite spectacular in the case of the coil-stretch transition for dilute solutions of high-molecular-weight linear polymers.

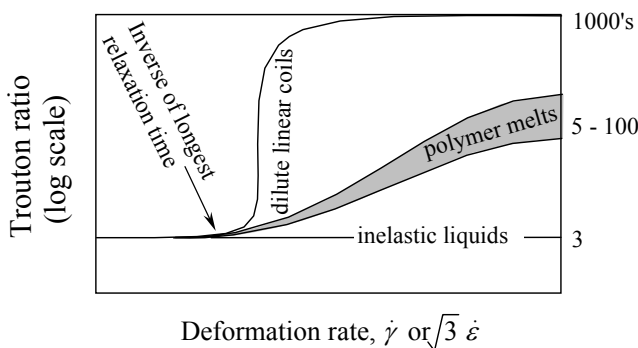


Figure 10: The Trouton ratio (extensional viscosity divided by shear viscosity) for various kinds of liquid.

For some polymer melts the rise can also be marked. In all cases the Trouton ratio levels off at very high deformation rate. The eventual level of the Trouton ratio for the coil-stretch type polymers can be thousands, while for polymer melts it can vary from say 5 to 100, with typical values being around 15. High values of Trouton ratio are coincident with high degrees of elasticity, as seen in *branched* polymer melts and *linear* stretched coils. Colloidal systems where there are no alignable entities in the microstructure will always have a Trouton ratio of around 3, i.e., they show little elastic behaviour. Heavily-branched polymeric thickeners such as Carbopol do not show a high Trouton ratio, and thicken very well without being perceived as 'stringy'.

The fact that the Trouton ratio eventually approaches a constant value means that the shear and extensional viscosities flow curves are 'parallel' in that range, and if the behaviour is power-law, then the power-law index is the same in both cases. (Notice this from the polymer melt examples shown later in the figures 13 - 20.)

17.5 Some examples of extensional viscosity curves

Figures 11 - 13 (see [4] and [5]) show examples of the different kinds of uniaxial extensional viscosities as a function of extension rate, in some cases compared to the equivalent shear viscosities.

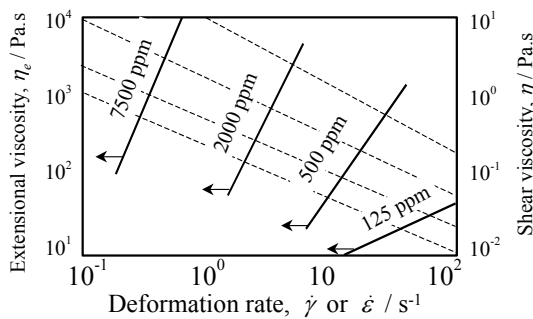


Figure 11: The shear (dotted lines) and extensional viscosities (solid lines) versus deformation rate for aqueous polyacrylamide solutions. Note the (thousand-fold) different viscosity scales, [4].

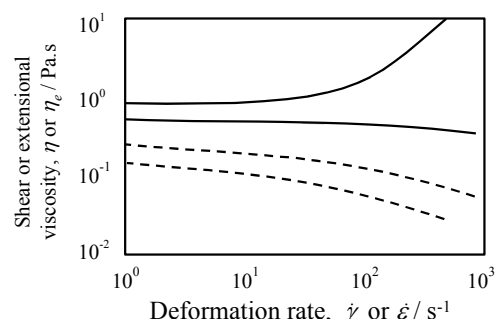


Figure 12: The shear (dotted lines) and extensional (solid lines) flow curves for aqueous solutions of polyacrylamide (tension thickening) and callogen (tension thinning) Rheometrics promotional literature.

The obvious difference between the two kinds of viscosity is most marked in those cases where the extensional viscosity *increases* with increasing extension rate, which even if the viscosity eventually begins to decrease at much higher extension rates, still results in the extensional viscosity being very much larger than the shear viscosity.

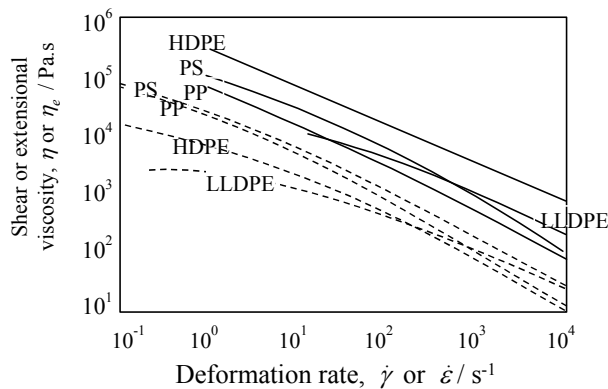


Figure 13: The shear (dotted lines) and extensional (solid lines) flow curves for typical polymer melts at 190 °C.

The degree of branching of the polymer melt is crucial in this situation, as well as molecular weight and temperature. In the case of polymer melts, the presence and kind of fillers (spherical or alignable, i.e. sheets or fibres) is a strong factor in dictating the form of the extensional flow curve. All these general effects are illustrated in figures 14 - 20, shown either in general terms or with specific examples.

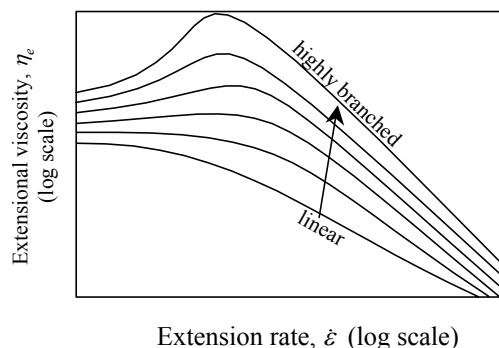


Figure 14: The effect of branching on the extensional viscosity of polymer melts.

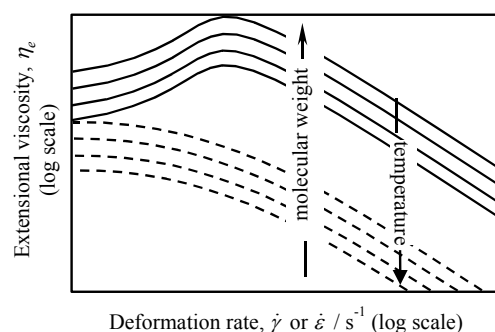


Figure 15: The effect of temperature and molecular weight on the shear (dotted lines) and extensional (solid lines) viscosity of a polymer melt.

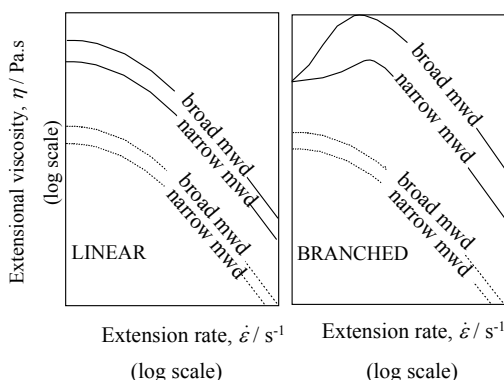


Figure 16: The effect of branching and molecular weight distribution on extensional viscosity of polymer melts.

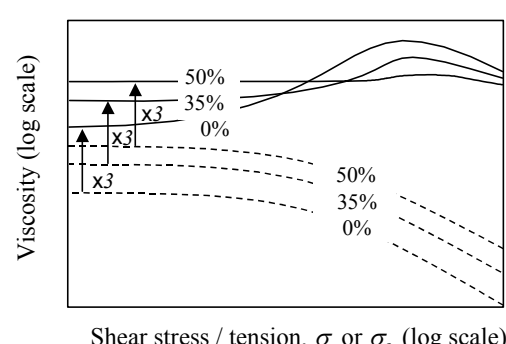


Figure 17: The shear and extensional viscosities of an LDPE melt with various loadings of glass beads.

The overall situation is summarised in figure 21, which shows that behaviour ranges from simple suspensions and emulsions, where the extensional viscosity is only a small multiple of the shear viscosity, to the coil-stretch situation of a possible thousand-fold difference. The behaviour at the highest (relative) extension rates is shown in figure 22, where a concentrated rod-like polymer—say xanthan gum—is stretched very quickly, see [6]. Both shear and extensional viscosities flatten out as the polymer chains are completely untangled and aligned, and show an approximately forty-fold difference.

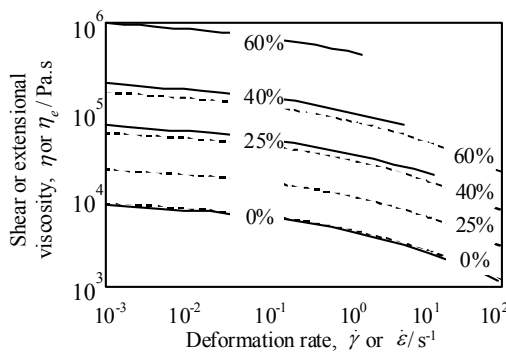


Figure 18: The effect of mica filler level on the shear (dotted lines) and one-third of the extensional (solid lines) viscosity of a polymer melt.

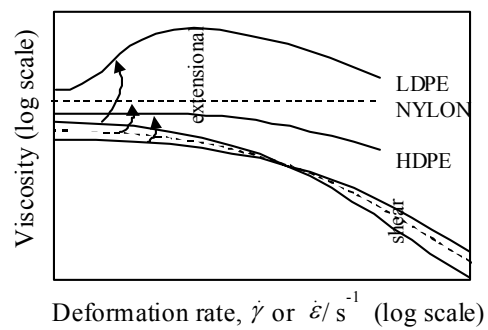


Figure 19: The shear and extensional viscosities of three polymer melts.

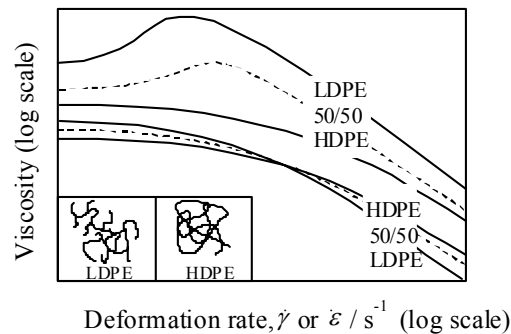


Figure 20: The shear and extensional viscosities of two polymer melts and their 50/50 blend. Note that low density polyethylene is highly branched.

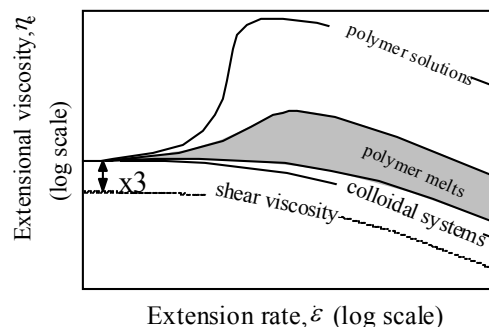


Figure 21: The extensional flow curves of various kinds of liquid.

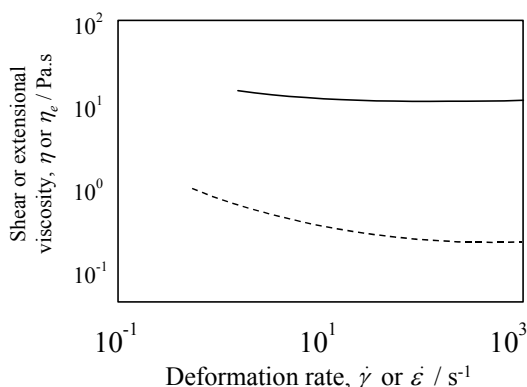


Figure 22: The shear (dotted line) and extensional (solid line) viscosities of 0.04% xanthan gum in a water/syrup mixture.

17.6 The effect of time or extension on extensional viscosity

The typical response of materials with interesting extensional flow curves (i.e. polymer melts) is shown in figure 23 for linear polymer melts and in figure 24 for branched polymer melts. Both take quite a time to come to steady state, showing first the typical viscoelastic response seen in shear flow. The most important point about this data is that it represents not only long times to steady state, but also large extensions. In a fibre-pulling experiment, this can mean an extension of the fibre to over 1000 times its original length! This makes obtaining steady-state values very difficult for very viscoelastic systems.

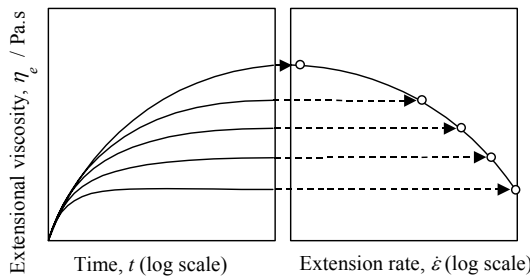


Figure 23 : The extensional viscosity build-up for relatively inelastic polymer melts, as a function of time for different extension rates, projected onto the extensional flow curve.

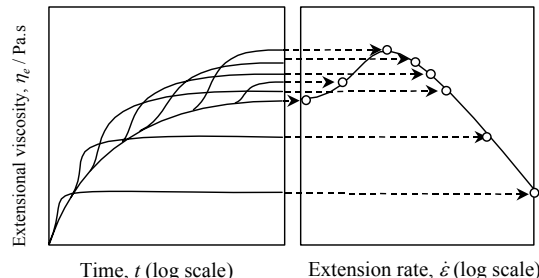


Figure 24: Extensional viscosity build-up for very elastic polymer melts, as a function of time for different extension rates, projected onto the extensional flow curve.

17.7 Other kinds of extensional flows

Apart from the uniaxial extensional flow considered above, there are two other kinds of flows where the material is stretched, see figure 25.

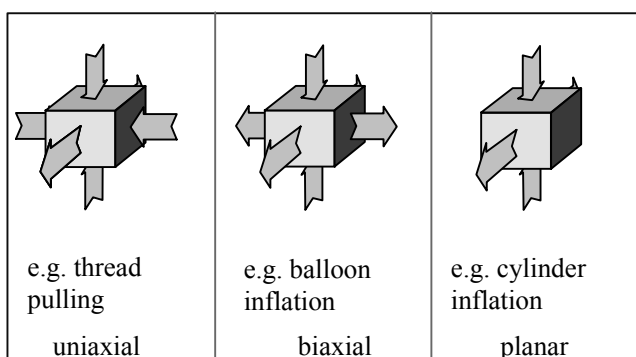


Figure 25: The three different kinds of extensional flow with an example of each.

First we have

biaxial extensional flow, where a sheet of liquid is pulled out in two directions: this is the kind of deformation experienced by a portion of a balloon or a bubble being inflated. Here we have stretching in two directions, and compression in one direction as the thickness of the element decreases.

Then we have

planar extensional flow, as seen for instance when a long cylinder is inflated, and the stretching only takes place in one direction, but the thickness of the sample decreases, i.e. it is effectively compressed, with the third dimension unaffected.

These two kinds of extensional flows are less demanding on microstructures such as individual polymer chains, since uniaxial extension demands that a three-dimensionally random chain be pulled towards a straight extended chain.

All these extensional flows have different values of viscosity associated with them, so that in the simplest case for Newtonian liquids - or for *all* liquids at low enough shear/extension rates - which are as follows

Extensional flow	Extensional Viscosity	
Uniaxial	3η	<i>compared with</i>
Biaxial	4η	<i>shear viscosity = η</i>
Planar	6η	

17.8 Viscometers to measure extensional viscosity

How do we measure extensional viscosity? Apart from a limited number of applications where it is possible to form filaments and sheets and pull them in one or two directions, the answer is that it is much more difficult to perform extensional viscosity measurements than their shear viscosity equivalents. For polymer melts, it is possible to chill the clamps used to hold the melt, and so secure the sample, see figure 26. Sometimes, it is even possible to use a 'super-glue' to attach the sample to the moving clamps!

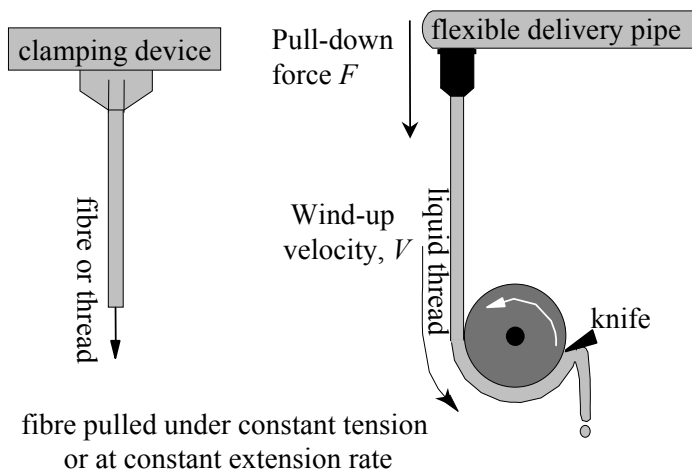


Figure 26: Two thread-pulling methods of measuring extensional viscosity.

Another problem is that even for the simplest stretching flow – uniaxial extension – when we have succeeded in clamping the sample, the nature of extensional flow is such that we need to increase the length of the sample exponentially in order to ensure a constant extension rate. Second, when we are doing this, the cross-section of the sample is continually decreasing, and then if we have decided to initiate the flow by applying a set force, the stress – force divided by cross-sectional area – is constantly increasing as the cross-section decreases. A number of ingenious ways have been found to get around this problem, and it is

possible to apply a constant stress and to measure the deformation, or else to apply a constant extension rate and measure the resulting stress.

However, when we have mobile solutions, the methods described above are impossible, and we have to try to create an extensional flow within a flowing system. This has been done in a number of ways, as shown in figure 26. The method used depends on the liquid of interest being 'spinnable' or not 'spinnable'. If the solution is spinnable, then it is possible to wind up the liquid thread on a rotating drum. In all these cases the average extension rate is measured using a camera system to record the profile of the stretched liquid.

Where a liquid is not spinnable, it is possible to use the opposing jets system. Here two identical jets are immersed in a liquid, quite near to, but opposing each other, an equal amount of liquid being withdrawn through each. The flow in the liquid between the jets contains a high degree of extensional flow, and by noting the jet orifice size and the flow rate as well as the reaction on one of the jets, then a measure of the extensional viscosity can be obtained, see figure 27.

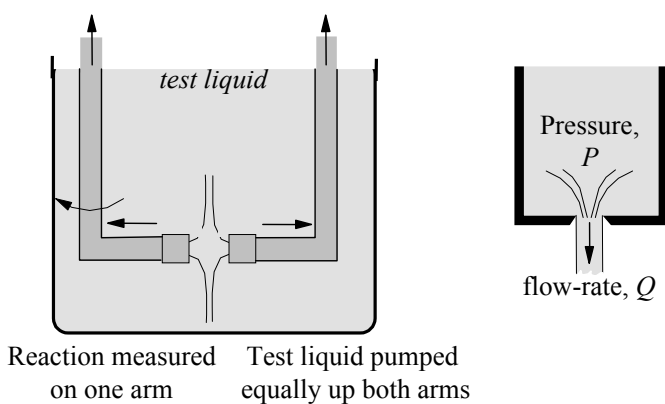


Figure 27 :Two flow geometries for measuring extensional viscosity; the opposed orifice device and the sharp-edged orifice.

In all these measurements there is one great recurring problem—one is never sure if steady state has been achieved. In simple rotational shear instruments, the attainment of steady state is just a matter of waiting. However in extensional instruments the amount of deformation is usually small compared with that necessary to reach equilibrium, which for some polymeric systems—as we have seen—can sometimes only be reached at over 1000 times extension of the undeformed sample at its rest state.

There is one simple experiment that can be performed to obtain a fair estimate of the extensional viscosity in practical situations, this is by measuring the entrance pressure into a capillary of radius a , see figure 27. Then a reasonable expression for the extensional stress is the entrance pressure drop P_e and an equally simple expression for the extension rate is $Q/\pi a^3$. The next level of sophistication is to carry out a power-law analysis, this was done by Cogswell [7] who suggested that

$$\sigma_e = \frac{3}{8}(n+1)P_e \quad \text{and} \quad \dot{\epsilon} = \frac{\sigma_w \dot{\gamma}_w}{2\sigma_e}$$

where σ_w is the wall shear stress inside the small pipe, $Pa/2L$, and $\dot{\gamma}_w$ is the wall shear rate inside the small pipe, $\frac{4Q}{\pi a^3} \left(\frac{3n+1}{4n} \right)$.

17.9 Commercially available extensional viscometers

As we see, these procedures are quite difficult, and thus it is not surprising that few commercial instruments are available to measure extensional viscosity. The present choice is quite small, being limited to Rheometric Scientific's RME extensional viscometer for polymer melts. Anyone interested in measuring extensional viscosity of other systems will have to resort to home-made instruments.

17.10 Some interesting applications

There is a natural tendency for liquid threads to break up due to surface tension forces. This break-up is governed by the extensional viscosity of the liquid thread under the prevailing stretching conditions. If the extensional viscosity is then high, it will oppose any local thinning tendency as a thread is stretched, see figure 28. This resistance is especially enhanced if the stretching takes place in the region where the viscosity is not only high, but is also increasing with extension rate, since the more a thread thins, the greater is the extension rate, and then the greater is the resistance. This is true in at least two situations, first for dilute solutions of high-molecular-weight linear polymers. In this case atomisation of watery liquids is inhibited, see figures 7 and 8, since ligaments of liquid being ripped apart as they fly through the air in the atomisation process undergo strong extensional flow, and the resisting force will be high. In this case the situation is as illustrated in figure 28 where the break-up normally produces small drops called satellites. These are inhibited and a clean break is seen, with the suppression of satellite drops, see also figure 8. If the extensional viscosity is very high, atomisation is completely suppressed.

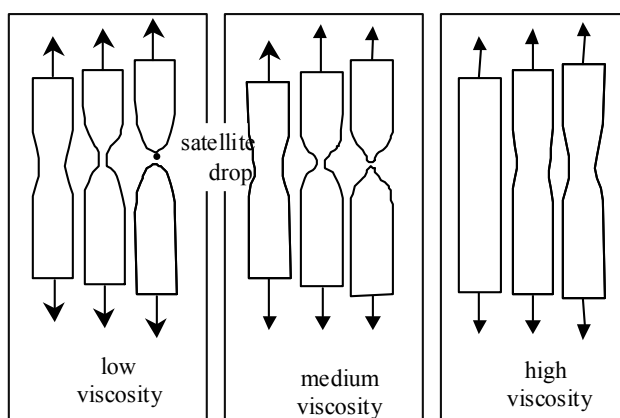


Figure 28 : The break-up of liquid filaments when pulled out.

Then, secondly, in the production of man-made fibres, polymer melts are extruded through many-holed spinnerets, and the hardening threads are quickly wound up unto drums, i.e. they are stretched. If the extensional viscosity of the still-molten stretched portion of the threads is an increasing function of extension rate, the tendency for the thread to neck and break is inhibited, see the right-hand side of

figure 28. In this way the maximum spinning rate is increased for high extensional viscosity.

For mobile liquids with high extensional viscosities, it is possible to perform the inverted siphon experiment, where the spinnable liquid is sucked out of a surface and the tube drawn up to a suitable height, see figure 29. This is the ultimate demonstration of tension along the streamlines and non-breaking of liquid threads!

Last we note the effect of large Trouton ratios on flow through contractions, see figure 30. For this kind of flow, the flow pattern is not predetermined by the geometry, as for instance in simple pipe flow, and in contractions the liquid can choose its own type of flow, so as to minimise the overall energy dissipated in the system. In order to do this, the change in velocity from the large tube into the small tube is more spread out for the high Trouton ratio liquid, so that the average extension rate is lower, thus lowering the overall energy dissipation.

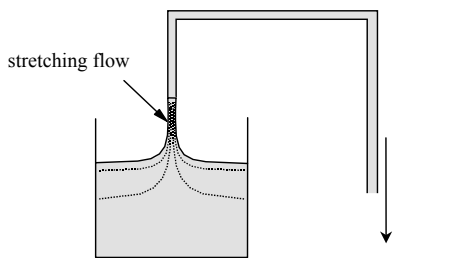


Figure 29: Cross-section of the inverted (tube-less) siphon.

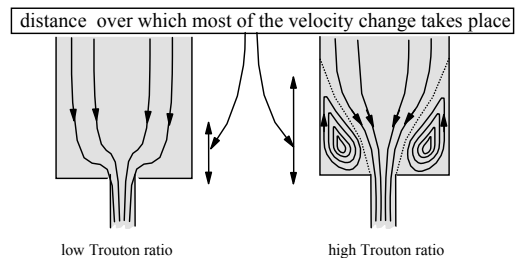


Figure 30 : The flow patterns in converging flow for polymer melts with low and high Trouton ratios respectively, e.g. LDPE and HDPE.

References

- [1] Brenner, H., Int. J. Multiphase Flow, 1, 195 – 341 (1974).
- [2] Lodge, A.S., 'Elastic Liquids', Academic Press, London, 1964.
- [3] Ferguson, J; Kembowski, Z., Applied Fluid Rheology, Elsevier Applied Science, London, 1991.
- [4] Barnes, H.A; Hutton, J.F; Walters, K., '*An Introduction to Rheology*', Elsevier, Amsterdam 1989.
- [5] Barnes, H.A, Polym. Mat. Sci. Enging, 61, 30-37 (1989).
- [6] Zirnsak, M.A; Boger, D.V; Tirtaatmadja, V., J. Rheol. 43(3), 627-650 (1999).
- [7] Cogswell, F.N, Polym. Eng. Sci., 12, 64 (1972).

CHAPTER 18: RHEOLOGY OF SURFACTANT SYSTEMS

'If it's thick, it's strong', a consumer interviewed by the author

18.1 Introduction

The rheology of surfactant (otherwise called detergent) systems is important for such products as

- washing-up liquids,
- shower gels,
- hair shampoos
- liquid fabric surfactants,
- liquid abrasive cleaners and
- rinse conditioners,

as well as playing a role in other household commodities such as toothpastes, or even thickened bleaches. The rheology of such products is important in terms of consumer preference for '*thick and creamy*' liquids, as well as technical aspects that have to be built in, such as slowing down drainage on vertical surfaces by increasing the viscosity, or high viscosity for ease of handling of such products as hair shampoo.

18.2 Surfactant phases

Although surfactant molecules are quite small, they can aggregate together to give large structures of up to $1\mu\text{m}$ in size. (None of these systems are essentially permanent, since the individual surfactant molecules on their outside are constantly interchanging with those in solution.) These remarkable structures give rheological effects that mirror those seen in polymer solutions, or in particulate suspensions with apparent yield stresses. They result from the surfactant molecules' schizophrenic nature in that their head-groups love water (hydrophilic), while their organic tails hate water but love oil (hydrophobic or oliophilic). When a surfactant is dispersed in water, up to a certain low concentration, the molecules disperse monomerically. However, above this level, we see the beginning of the formation of associations of molecules, which are called micelles: this particular concentration is called the critical micelle concentration, or the c.m.c.

The particular shape of the micellar structure that forms above the c.m.c is a function of the shape of the surfactant molecules involved; the electrolytic nature of the water phase and the temperature. Because the tails hate water, the molecules aggregate in such a way as to shield the tails from water by clumping together. There are various shapes that result from this clumping, where the head-groups also line up.

The structures formed include

- spherical micelles
- rod-like micelles
- lamellar phase sheets
- lamellar phase droplets

These structures (which are sometimes called vesicles) are shown schematically in figures 1 - 4 , see also §16.5.

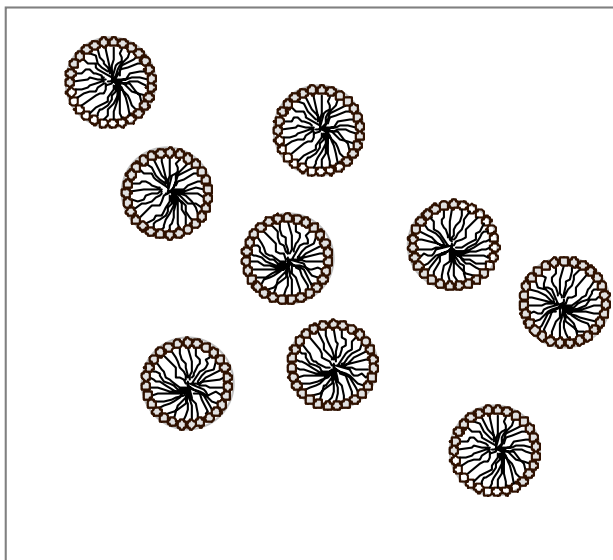


Figure A:diagrammatical representation of spherical micelles;
some shown in cross-section .

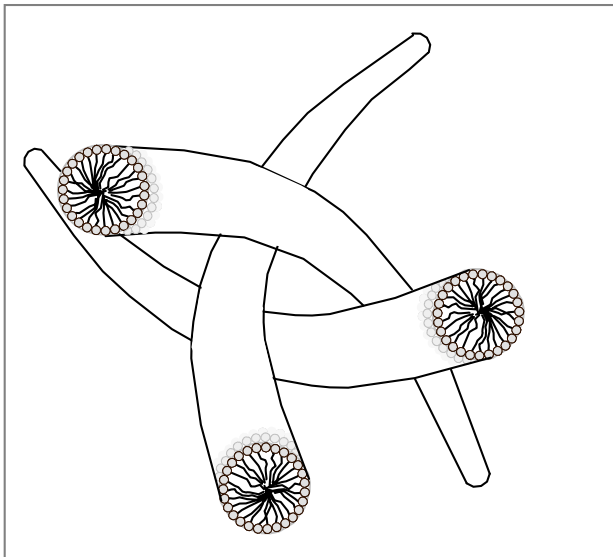


Figure 2: A diagrammatical representation of some rod-like micelles.

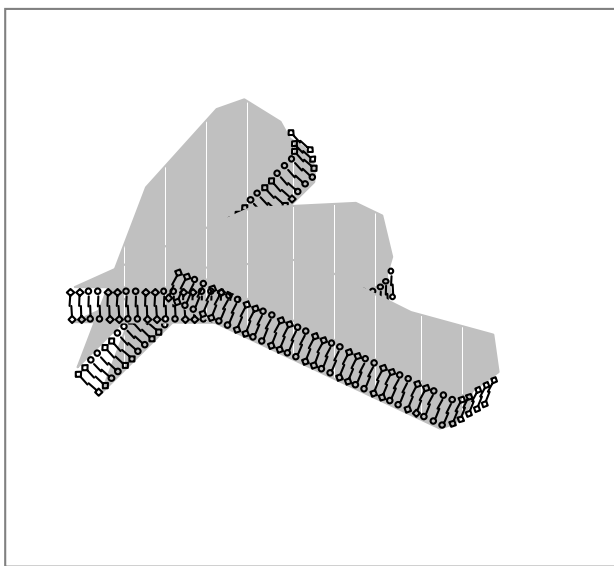


Figure 3: A diagrammatical representation lamellar phase sheets.

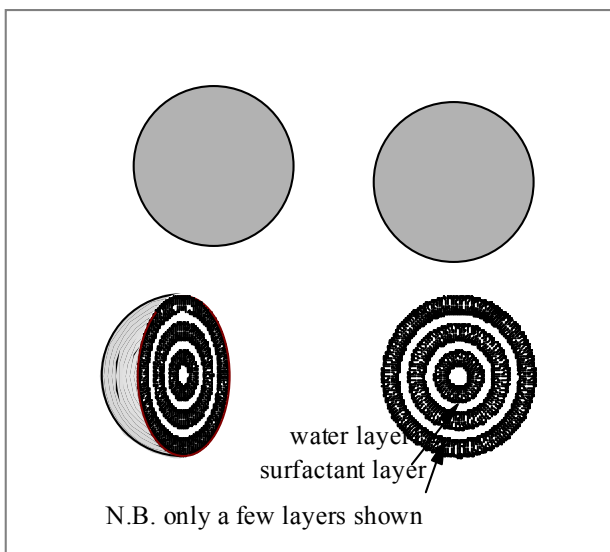


Figure A: diagrammatical representation lamellar-phase droplets with a cross-sectional views of two droplets .

18.3 Rheology of surfactant systems

Clearly the interesting surfactant structures just mentioned will all have important rheological effects. First, the formation of spherical micelles results only in Newtonian behaviour over the normal range of shear rates ($<10^4 \text{ s}^{-1}$), given that the spheres are only a few times greater in diameter than the length of the surfactant molecule, which is around 50 nm. However due to the high phase volumes involved, the viscosity can be many times greater than water. These structures are often present in washing-up liquids, which have viscosities around a few hundred millipascal seconds.

The next degree of complexity comes when—for certain mixtures of surfactant molecules—the structures are present as long rod- or worm-like structures: they are also called living molecules, see chapter 16. These worm-like structures behave as polymers, so they greatly increase the viscosity of the micellar solution via entanglements. They also impart significant viscoelastic properties. However, a special feature is the high degree of shear thinning due to entanglements being lost as the micelles align in the flow. Typically, these systems have a surfactant concentration of less than 10%. Products such as some washing-up liquids, and most shampoos, shower gels, hair shampoos and thickened bleaches rely on this kind of organisation of molecules. The length of these ‘worms’ can be up to $1 \mu\text{m}$, but because the diameters is only a few times the length of the constituent molecules, their length to diameter can be very large, but they are always transparent (a simple check).

The next molecular organisation is more complex. This involves many layers of alternating molecules, intercalated with layers of water—i.e. lamellar phase. It is possible for rafts of these layers to float around in water, but for most real products, they present themselves as fully enclosed multi-layered onion-like droplets. The number of layers can run into hundreds, and these so-called lamellar drops (or vesicles) can be up to several microns in diameter.

The distinctive feature of these structures is the very large amount of water that they trap between the surfactant layers. For a surfactant concentration of around five percent, the total phase volume of the drops can be greater than 70%,

thus giving space-filling, close-packed spheres. These systems are thus very shear thinning and appear to have yield stresses, and hence are good for suspending particles as in liquid abrasive cleaners. These structures also account for the high viscosity of low-concentration rinse conditioners.

18.4 Necessary rheological properties

What are the rheological properties of surfactant-base liquids necessary to fulfil our expectations of them? The following examples might be cited:

(a) lowering viscosity for a high concentration of surfactant:

- washing up liquids
- concentrated rinse conditioners
- liquid fabric-washing liquids
- spray cleaners

(b) keeping viscosity high enough for ease of handling:

- shower gels
- hair shampoos
- liquid soaps

(c) increasing viscosity to slow down run-off from vertical surfaces:

- thickened bleaches

(d) suspension of particles without visible sedimentation:

- liquid abrasive cleaners
- liquid fabric-washing liquids.

These desired properties are best brought about by the manipulation of the micelle structures formed by the proper choice of mixtures of surfactants as well as the correct processing procedures needed to assemble the more complex structures. Other chemical species present in real surfactant formulations (perfumes, hydrotropes etc.) can also play a major role in manipulating micellar form if present at significant levels.

Exercise: Produce a prescription for the rheology of a liquid abrasive cleaner that has to suspend solid particles, but has to readily drain down a vertical surface.



CHAPTER 19: RHEOLOGY OF FOOD PRODUCTS

'Science is nothing but perception', Plato

19.1 Introduction

Apart from the smell, taste and colour of food, their flow properties are high on the list of consumer-perceived attributes. Also, eating and drinking food products are probably the most common applied rheological experiences that the average person encounters. Who has not appreciated the thickness of cream; the creaminess of soup and the texture of creamed potato? The perception of these verbally-expressed properties arises from the interaction between the rheology of the food product and movement in the mouth, tongue and throat. This is a very complex operation, but it is something that is done without real thought but nevertheless from it arises a perception of the food expressed in a wide variety of words. The problem facing the food scientist interested in rheology is first obtaining a proper rheological description of the food being considered and second to describe the flow field in the eating, drinking and swallowing operations.

The processing side of food rheology is how to transform the basic ingredients, viz.

- | | |
|--|--|
| <ul style="list-style-type: none">• Sugars• Polysaccharides• Lipids• Proteins• Colours | <ul style="list-style-type: none">• Flavours• Vitamins• Preservatives• Minerals• Water |
|--|--|

into a palatable form with the correct microstructure that delivers an acceptable rheology.

19.2 Liquid-like food rheology

Liquid-like food is usually made up of a complex mixture of dissolved natural polymers and dispersed insoluble biological material, usually in an aqueous phase with various electrolytes. The rheology varies over the range

• thin liquids	-	e.g.	drinks, consommés, oils
• viscous liquids	-		creamed soup, mayonnaise
• very viscous liquids	-		ketchup, yoghurt
• elastic liquids	-		dough, some soups
• pastes	-		meat paste, processed cheese
• soft solids	-		patés, spreads.

For many of these products, we all know that they can be too thick, or too thin and thus, either way in the situation being considered, unacceptable.

Obviously the rheology of these materials is very diverse, and even at a superficial level, the level of viscosity as well as the degree of non-Newtonianness varies over a wide range, see figure 1.

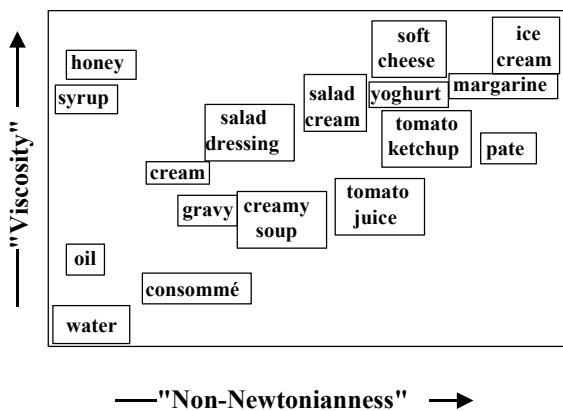


Figure 1: A 'map' of food qualitative rheology.

19.3 In-vivo flow fields

The flow field experienced by a liquid as it is ingested is complex. For the few seconds that the liquid is in the mouth, it obviously experienced shear flows, but also as the tongue is pressed against the pallet, or when the liquid flows around the mouth and moved through small orifices it also encounters extensional flow. For 'simple' non-Newtonian liquids, the average shear rate in the mouth has been estimated as 50 s^{-1} ; the typical extension rates are similar.

The interaction between these flow fields and the perceived experience of eating and drinking is complicated, but it is possible to relate verbal descriptors such as '*creamy*' or '*thick*' to measured rheological properties.

A high degree of viscoelasticity—experienced as stringiness—is obviously unacceptable to consumers, but some viscoelasticity is inevitable, given the kinds of high molecular-weight polymers such as proteins that are dissolved in the aqueous phase.

19.4 Rheology and food processing

Whilst the rheology of finished food products is crucial for a successful brand, there are as many rheology problems encountered in manufacturing. These include mixing, pumping, as well as flow in heat exchangers and even atomisation of powder precursors in spray dryers.

The kind of mixing that can cause a problem is due to severe shear thinning that resembles a yield stress. It is then possible to use the 'cavern' theory approach described in chapter 10. Then we can be assured that the well-mixed zone fills the whole mixer.

Shear thickening in food systems is found for concentrated starch dispersions. Often in the early parts of the production of a food product, this particular situation is encountered, and problems can arise. By following the shear thickening 'map' shown in chapter 15, these difficult areas can be avoided.

Exercise: Using whatever rheometers you have at your disposal, measure the rheological properties of tinned custard.



CHAPTER 20: YOUR RHEOLOGY LIBRARY

'The man who does not read good books has no advantage over the man who can't read them', Mark Twain

20.1 Introduction

There are a number of journals that are primarily concerned with rheology, which you should seriously consider subscribing to:

- Applied Rheology
- Rheologica Acta
- Journal of Rheology
- Journal of Non- Newtonian Fluid Mechanics
- Rheology Abstracts

Your librarian or else your usual journal supplier will be able to arrange this for you.

20.2 Rheology Books in print

To help you move on from being a mere beginner in rheology, you should start your own Rheology library. To assist you, here a list of all the *currently available* books that you can buy on the subject rheology – more than 160 – from which you can begin to build up your collection. Unless otherwise stated, the approximate UK price in pounds sterling of hardback versions for the books is given: sometimes cheaper paperback versions are available.

The list is drawn up according to particular areas of interest – *General Rheology, Theoretical Rheology, Polymeric Systems, Blood, Food, Other Specific Systems, Drag Reduction, Other Meetings, Geological Subjects* – and titles appear within each section in alphabetical order. The abbreviations used for publishers names are well known in the book trade, and the information supplied should be sufficient for any reputable book supplier to obtain copies of the books listed.

20.3 General rheology

Advances in the flow and rheology of non-Newtonian Fluids, Eds. D.A. Siginer, D. De Kee & R.P. Chhabra, Elsevier, 1999, \$380

Applied fluid flow, Cheremisinoff N.P, Marcel Dekker, 1979, \$125

Applied fluid Rheology, Ferguson J, Kembowski Z, Chapman & Hall, 1991, £65

Bubbles, drops and particles in non-Newtonian fluids, Chhabra R.P, CRC Press,

- 1992, £179
Crack and contact problems for viscoelastic bodies, **Graham G.A**, Springer Vienna,
1995, £47
Creep and relaxation of nonlinear viscoelastic materials, **Findley W.N.**,
Dover Pubns., 1989, \$12.95
Developments in non-Newtonian flows (meeting), **Siginer D.A**, ASME, 1994, \$74
Developments & applications of non-Newtonian flows – 1995 (meeting), **Siginer D.A**,
ASME, 1995, £72
Encyclopedia of fluid mechanics: Rheology and non-Newtonian flows, Vol. 7:
Cheremisinoff N, Gulf Publishing, 1988, £157
Engineering Rheology, **Tanner R. I**, Oxford UP, 1985, £65
English-Chinese dictionary of Rheology, **Science Press Staff**, Fr. & Eur., 1990, \$49.95
Free liquid jets and films: hydrodynamics and Rheology: interaction of mechanics and mathematics,
Yarin A, John Wiley & Sons, A\$246
Fundamentals of heat transfer in non-Newtonian fluids, **Chen J**,
Amer. Soc. Mech. Eng., 1991, \$30
Interfacial transport processes and Rheology, **Edwards D**, Butterworth, 1991, £65
(An) Introduction to Rheology, **Barnes H.A, Hutton J.F, Walters K**, Elsevier, 1989, Df 230
(An) Introduction to Rheology, **Laba D**, Micelle Press, Weymouth, 1997, £11.50
Mechanics of viscoelastic fluids, **Drozdov A**, John Wiley Ltd, 1998, £60
Non-Newtonian Flow in the Process Industries, **Chhabra, R.P, Richardson J**, Butterworth-
Heinemann, 1999, £ 35.
Non-Newtonian fluid mechanics, **Bohme G**, North-Holland, 1987, \$256
Non-Newtonian Fluids: Fluid Mechanics Mixing & Heat Transfer, **Wilkinson W. L**,
Elsevier Science, 1999 (ISBN: 0080418635), ?
Optical rheometry of complex fluids, **Fuller G.G**, OUP, 1995, \$60
Physics of flow (A level), **Open University staff**, Heinemann Educational, UK, 1997, £8.50
Large deformation of materials with complex rheological properties at normal and high pressures,
Levitas V.I, Nova Science, 1996, \$97
Progress & trends in Rheology (meeting), **Giesekus H**, Springer Verlag, 1988, \$217
Rheological Measurement, **Collyer A.A & Clegg D.W**, Elsevier Applied Science, 1988, £490
Rheological modelling: thermodynamical and statistical approaches (meeting),
Casas-Vasquez J, Springer-Verlag, 1991, £30
Rheological phenomena in focus, **Boger D.V & Walters K**, Elsevier, 1993, \$149.50
Rheological techniques, **Whorlow R.W**, Ellis Horwood, 1992, £83.95
Rheology : An Historical Perspective, **Tanner R I, Walters K**, Elsevier Science, 1998, \$201.00
Rheology, principles, measurements and applications, **Macosko C.W**,
VCH, 1994, £66
Rheology and elastohydrodynamic lubrication, **Jacobson B.O**, Elsevier, 1991, \$175.75
Rheology & non-Newtonian flow, **Harris J**, Bks Demand (reprint soon), \$107.20
Rheology for Chemists – An Introduction, **Goodwin J.W & Hughes, R.W**, Royal Society of
Chemistry, Cambridge, 2000, £27.50.
Rheology Fundamentals, **Malkin A. Ya**, (Institute of Physics), ChemTec Publishing, 1995, \$135
Rheology of disperse systems (meeting), **Mill C**, Franklin, 1959, \$108
Techniques in rheological measurement, **Collyer A.A**, Chapman & Hall, 1993, £75
The structure and rheology of complex fluids, **Larson R.G**, Oxford, 1999, \$79.95

Synthesis & degradation-Rheology & extrusion, **Cantow H**, J Springer Verlag, 1982, \$62
Transport phenomena, **Bird R. B**, Wiley 1960, \$57.50
Transport properties of fluids: thermal conductivity, viscosity and diffusion coefficient,
 Kestin J, Taylor & Francis, 1988, £96
Understanding Rheology, **Morrison F.A**, OUP, 2001, £50.
(The) vitreous state: thermodynamics, structure, Rheology, crystallisation, **Gutzow I**,
 Springer-Verlag, 1995, £86
Viscoelastic machine elements: elastomers and lubricants in machine systems,
 Moore F, Butterworth Heineman, 1993, £75
Viscoelasticity of Engineering Materials, **Hadda Y**, Chapman & Hall, London, 1995, £75

20.4 Theoretical Rheology

Advances in constitutive laws for engineering materials (meeting), **Fan J**, Elsevier,
 1990, \$345
Advances in finite deformation problems in materials processing and structures,
 Chandra M, Amer. Soc. Mech. Eng, 1992, \$74
Applications of supercomputers in engineering: fluid flow and stress analysis applications: Vol 2,
 Bebbia C.A, Comp. Mechanics, 1989, £69
Approach to Rheology through multivariable thermodynamics, **Hull H.H**, Hull, 1981, \$16
Computer programs for rheologists, **Gordon G.V**, Hanser Garner, 1994, £60
Constitutive equations for anisotropic & isotropic materials, **Smith G. F.**, Elsevier 1994 \$203.25
Constitutive laws & microstructure, **Axelrad D**, Springer Verlag, 1988, \$56.95
Constitutive laws for engineering materials, **Qesai C.S**, ASME, 1991, \$200
Constitutive laws of deformation, **Chandra J**, Soc. Indus. & Applied Mathematics,
 1987, \$40.75
Constitutive equations for engineering materials (meeting) Vol.1, **Chen W.F**,
 Elsevier, 1994, \$359.50
Constitutive laws of plastic deformation and fracture (meeting), **Krausz A.S**,
 Kluwer, 1990, £87.95
Elements of stability in viscoelastic fluid, **Dunwoody J**, Longman, 1990, £22
(The) finite element method: Solid and fluid mechanics: nonlinear problems: Vol. 2,
 Zienkiewicz O.C & Taylor R.L, McGraw-Hill, 1991, £29.95
Fluid dynamics of viscoelastic liquids: Applied mathematical sciences: Vol 84,
 Joseph D.D, Springer-Verlag, 1990, £69
Functional & numerical methods in viscoplasticity, **Ionescu I.R**, OUP, 1993, \$85
Numerical simulation of non-Newtonian flow, **Crochet M.J, Davies R & Walters K**, Elsevier, 1984,
 \$168.75
Mechanics of non-Newtonian fluids, **Schowalter W.R**, Franklin (Pergamon Press Reprint),
 1978, \$146
Mechanics of viscoelastic fluids, **Zahorski S**, Kluwer, 1982, £106.50
Numerical simulations of heat transfer and fluid flow on a personal computer, **Kotake S**,
 Elsevier Science, 1995, \$85.75
Numerical analysis of viscoelastic problems: recherches en mathematiques appliques,
 Le Tallec P, Springer-Verlag, 1990, \$25

- Numerical methods for non-Newtonian fluid dynamics*, **Vradis G.C**, ASME, 1994, \$35
(The) *phenomenological theory of nonlinear viscoelastic behavior: An introduction*,
 Tschoegl N.W, Springer-Verlag, 1989, £79.50
Thermodynamics & constitutive equations, **Grioli G**, Springer Verlag, 1985, \$30
Thermodynamics of irreversible processes: applications to diffusion and Rheology,
 Kuiken G.D.C, John Wiley Ltd, 1994, £35
Thermodynamics & Rheology, **Verhas J.O**, Kluwer, 1996, £74
The thermodynamics of Rheology (or inside the thermodynamic black box), **Hull H.H**, Hull, 1995, £20

20.5 Polymeric systems

- Advances in polymer science*, **Nijenhuis K**, Springer Verlag, 1997, £130
Amorphous polymers and non-Newtonian fluids: Volumes in Mathematics and its application,
 Dafermos C, Springer-Verlag, 1987, \$29
Analytical polymer Rheology: Structure-Processing-Property Relationships,
 Rohn C, Hanser Garner Pubns., 1995, \$125
Chemorheology of thermosetting polymers, **May C.A**, Am. Chemical, 1983, \$49.95
Constitutive equations for polymer melts and solutions, **Larson R**,
 Butterworth Heinemann, 1988, £45
Dynamics of Polymeric Liquids, **Bird R.B, Armstrong R. C & Hassager O**, Volume 1, Fluid
 Mechanics, 2nd ed., Wiley, 1987, £115
Dynamics of Polymeric Liquids, **Bird R.B, Hassager O, Armstrong R. C & Curtiss F.C**, Volume 2,
 Kinetic Theory, 2nd ed., Wiley, 1987, £115
Flow and Rheology in polymer composite processing, **Advani S**, Elsevier, 1994, \$203.25
(The) *flow of high polymers: continuum & molecular Rheology*, **Middleman S**, Bks Demand
 (reprint soon), \$72.70
(An) *introduction to polymer Rheology and processing*, **Cheremisinoff N**,
 CRC Press , 1992, £95
Mechanical properties of polymers & composites, **Neilsen L.E**, 2nd ed., Marcel Dekker, 1994, \$165
Melt Rheology and its role in plastics processing: theory and application, **Dealy J & Wissbrun K.F**,
 V Nostrand Reinhold, 1990, £61.50
Nonlinear viscoelastic effects in flows of polymer melts & concentrated polymer solutions,
 Leonov A.I, Elsevier, 1993, £72
Nonlinear phenomena in flows of viscoelastic polymer fluids, **Leonov A.I & Prokunin A.N**,
 Chapman & Hall, 1994, £95
Polymer alloys and blends: thermodynamics and Rheology, **Utracki L**, Hanser, 1990, £60
Polymer melt Rheology: a guide for industrial practice, **Cogswell F.N**,
 Technomic Pub Co, 1996, \$110
Polymer mixing and extrusion technology, **Cheriminoff P.N**, Marcel Dekker, 1987, \$170
Polymer Rheology: theory & practice, **Yanovsky Y**, Chapman & Hall, 1993, £75
Polymer Rheology, **Nielsen L.E**, Marcel Dekker, 1977, \$125
Polymer Rheology, **Lenk R. S**, Chapman & Hall, 1978, £95
Polymer Rheology and processing, **Collyer A.A**, Chapman & Hall, 1990, £75
Polymers as Rheology modifiers, **Schultz D & Glass J.E**, Amer. Chem. Society, 1991, \$84.95
Principles of polymer engineering Rheology, **White J.L**, John Wiley, 1990, £75
Principles of Rheology for polymer engineers, **White J. L**, JohnWiley, 1990, \$75.95

Rheological fundamentals of polymer processing (meeting), Covas J.A, Kluwer, 1995, £394
Rheology and processing of liquid crystal polymers, 2, Acierno D & Collyer A. A, Chapman & Hall, 1996, £69
Rheology of filled polymer systems, Shenoy, A.V, Kluwer, 1999, £90
Rheology of polymeric systems: principles & applications, Carreau P.J, De Kee D. C. R, & Chhabra R.P, Hanser-Gardner, 1997, \$197.5
Rheology for polymer melt processing, Piau J.M, Elsevier Science, 1996, \$243
Rheology of polymer melts (IUPAC meeting), Kahovec J, Huethig & Wepf, 1992, £28.50
Rheology processing and properties of polymeric materials (meeting), Acierno D, Huethig & Wepf, 1993, £56
Rheology of polymers, Vinogradov G.V, Springer-Verlag, 1981, A\$99.20
Rheometers for molten plastics: a practical guide to testing & property measurement, Dealy J.M, Chapman & Hall, 1981, \$82.95
(The) Theory of Polymer Dynamics, Doi M, Clarendon Press, 1989 (reprint), £25
Thermoplastic melt Rheology and processing, Shenoy A.V & Saini D.R, Marcel Dekker, 1996, \$175
Viscoelastic properties of polymers (3rd Ed), Ferry J.D, John Wiley Inc, 1980, £120

20.6 Blood

Biorheology: proceedings of the second international congress, Copley A, Butterworth-Heinemann, 1975, \$47
Blood cells, Rheology and aging, Platt D, Springer-Verlag, 1987, \$89.70
Blood Rheology, Lowe G.D, Bailliere Tindall, 1987, £27.50
Blood viscosity in heart disease & cancer, Dintenfass L, Franklin (Pergamon Press Reprint), 1981, \$88
Blood viscosity: Hyperviscosity and hyperviscosaemia, Dintenfass L, Kluwer, 1985, £148.75
Clinical blood Rheology, Lowe G.D, CRC Pr, 1988, \$137
Flow properties of blood & other biological systems (meeting), Copley A, Franklin (Pergamon Press Reprint), \$205
Hemorheology (meeting), Copley A, Franklin (Pergamon Press Reprint), 1968, \$378
Hemorheology & thrombosis (meeting), Copley A, Franklin (Pergamon Press Reprint), 1976, \$198
(On the) Rheology of blood & synovial fluids, Chmiel H, Bks Demand, (reprint soon), \$50.80
Rheology, hemolysis, gas & surface interactions, Ghista D.N, S Karger, 1980, \$78.50
Rheology of the circulation, Whitmore R. L, Franklin (Pergamon Press Reprint) 1968, \$99
White blood cells: morphology and Rheology as related to function, Bagge U, Kluwer, 1982, £2.95
White cell Rheology & inflammation, Messmer K, S Karger, 1985, \$57

20.7 Food

Dairy Rheology: a concise guide, Prentice J.H, VCH, 1992, £66
Dough Rheology and baked product texture, Faridi H.A, Aspen, 1989, £75

- Feeding and texture of food (meeting)*, **Vincent J.F.V**, Cambridge UP, 1991, £60
Food texture : measurement and perception, Rosenthal A.J, Aspen Publ., 1999, \$142
Food texture: Instrumental and sensory measurement (meeting), **Moskowitz H.R**,
Marcel Dekker, 1987, \$138
Food texture and viscosity, **Bourne M.C**, 1994, Academic Press, \$85
Measurements in the Rheology of foodstuffs, **Prentice J. H**, Chapman & Hall, 1984, £59
Rheological methods in food process engineering, **Steffe J. F**, Freeman Press, 1992, \$65
Rheology of Fluids and Semisolid Foods : Principles and Applications, **Rao M.A**, Aspen Pub., 1999,
\$125.00
Rheology of foods, **Borwankar R**, Elsevier Adv. Technol., 1993, £75
Rheology of industrial polysaccharides: theory and applications, **Lapasin R & Prich S**,
Chapman & Hall, 1995, £110
Rheology of Foods, **Borwankar R & Shoemaker C.F**, Elsevier Science, 1992, \$135.00
Rheology of food, pharmaceutical and biological materials with general Rheology (meeting), **Carter R.E**,
Chapman & Hall, 1990, £59
Rheology of wheat products, **Faridi H**, Amer. Assn. Cereal, 1986, \$41
Texture measurements of food, **Kramer A & Szczesniak A.S**, Kluwer, 1973, £49.95
Viscoelastic properties of foods, **Rao M.A & Steffe J.F**, Chapman & Hall, 1992, £85

20.8 Other specific systems

- Asphalt Rheology: relationship to mixture*, **Briscoe O**, ASTM, 1987, \$34
Clay-water interface & its rheological implications, **Guven N**, Clay Minerals, 1992, \$15
Coatings Fundamentals: suspension rheology, **Higgins B**, Tappi Press, 1997, \$30
Drilling mud & cement slurry Rheology manual, **French Oil & Gas Ind. Assoc. Publications Staff**, St Mut, 1982, \$250
Electro-rheological flows 1993, **Siginer D.A**, ASME, 1993, \$37.50
Electrorheological fluids: proceedings of the 2nd international conference on ER fluids, **Carlson J.D**,
Technomic, 1990, \$145
Engine oils - Rheology & tribology: 1995 international congress & exposition meeting, **various**, Soc.
Auto. Engineers, 1995, \$49.00
Free liquid jets and films: hydrodynamics and rheology, **Yarin A**, Addison-Wesley Longman Higher
Education, 1993, £83
Free surface flows with viscosity, **Tyvand P. A**, WIT Press/Computational Mechan., 1997, £84
Glass: science and technology: viscosity and relaxation, **Uhlmann D.R**,
Academic Press, 1986, £144
High pressure Rheology of lubricants using the rotating optical micro-viscometer,
Wong P.L, ASME, 1996, ?
Paste flow and extrusion, **Benbow J & Bridgwater J**, Clarendon Press, 1993, £47
Paint flow and pigment: a rheological approach to coating and ink technology, **Patton T**,
John Wiley Inc, 1979, £180
Rheological and thermophysical properties of greases, **Vinogradov G.V & Froishteter G.B**,
Gordon & Breach, 1989, £92
Rheological properties of cosmetics and toiletries, **Laba D**, Marcel Dekker, 1993, £165
Rheological properties of lubricants, **Briant Jean**, Gulf Publishing, 1989, £61
Rheology of emulsions (meeting), **Sherman P**, Franklin, Pergamon Press Reprint, 1963

Rheology & tribology of engine oils, various, Soc. Auto. Engineers, 1992, \$29
Rheology of fresh cement (meeting), **Banfill P.F.G**, E & FN Spon (C&H), 1991, £59
Rheology of liquid crystals, **Khabibullaev P.K**, Allerton Press, 1994, \$95
Rheology of lubricants, **Davenport T**, Elsevier Applied Science, 1973, \$39.75
Viscosity solutions and applications, **Bardi M**, Springer Verlag, 1997, £28

20.9 Drag reduction

Drag reduction by additives: review and bibliography, **White A & Hemmings J.A.G**,
Brit. Hydromechanics Research Assn., 1976, £17
Drag reduction in fluid flows, **Sellin H.J & Moses R**, Horwood Ellis, 1989, £39.95
Drag reduction in turbulent flows by additives, **Gyr A & Bewersdorff H-W**, Kluwer, 1995, £79
Emerging techniques in drag reduction, **Kwing-So C**, Prasad K.K & Truong T.V,
Mech. Engineering Publications, 1996, £98
Fluid mechanics and its applications: Proceedings of the 4th european drag reduction meeting,
Coustoils E, Kluwer, 1990, £70.95
*Recent developments in turbulence management: Proceedings of the 5th drag reduction in
engineering flows meeting*, **Choi K.S**, Kluwer, 1991, \$139.50
Structure of turbulence and drag reduction: IUTAM Symposium, **Gyr A**,
Springer Verlag, 1990, £78

20.10 Geological subjects

Deformation mechanisms, Rheology and tectonics, **Knipe R.J.**,
Geol. Soc. Pub. House, 1990, £85
Earth Rheology, isostasy & eustasy: proceedings of earth Rheology (meeting),
Morner N-A, Bks Demand (reprint soon), \$177
Experimental rheology of clayey soils, **Meschyan S.R**, A A Balkema, 1995, £66
Glacial isostasy, sea-level and mantle Rheology, **Sabadini R**, Kluwer, 1991, £142.25
Geomaterials: Constitutive Equations & Modelling, **Darve F**, Elsevier, 1990, \$117
International conference in Rheology and soil mechanics, **Keedwell M.J.**,
E. & F.N Spon (C&H), 1988, £75
Mudflow rheology and dynamics, **Coussot, P**, A A Balkema, 1997, £60
Proceedings of the international symposium on Rheology & soil mechanics (meeting), **Symposium Staff**, Springer Verlag, 1966, \$113.95
Rheological fundamentals of soil mechanics, **Vyalov S.S**, Elsevier Science, A\$224.50
Rheological parameters of soils and design of foundations, **Ter-Martirosyan Z**,
A.A. Balkema, 1993, £50
Rheology and soil mechanics, **Keedwell M.J**, E. & F.N Spon (C&H), 1984, £79
Rheology of the Earth, **Ranalli G**, Chapman & Hall, 1995, £29.95
Rock and soil Rheology, **Cristescu N**, Springer-Verlag, 1988, \$327
Rheology of solids & of the Earth, **Karato S**, OUP, 1989 \$110
Rock Rheology: mechanics of elastic and inelastic solids, vol. 7,
Cristescu N, Kluwer, 1988, £106.75

20.11 Proceedings of meetings (not mentioned elsewhere)

3rd European Rheology conference (Edin.), Oliver D.R, Chapman & Hall, 1990, £79

Progress and Trends in Rheology V : Proceedings of the Fifth European

Rheology Conference, Eds. Emri I & R. Cvelbar R, Dr Verlag Steinkipff Dietrich, 1998, \$113.00

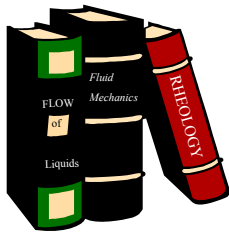
IUTAM symposium on numerical simulation of non-isothermal viscoelastic liquids,

Dijksman J.F, Kluwer, 1995, £61.50

Theoretical and applied Rheology (meeting), Moldenaers P & Keunings R, Elsevier, 1992, \$394.50

Viscoelastic materials: basic science and clinical applications: proceedings of the second international symposium of the Northern Eye Institute, Rosen E.S, Pergamon Press, 1989, £110

Exercise : Log on to the Internet, go to the Amazon Books Website - <http://www.amazon.com/> or amazon.co.uk - or any similar large book-seller site, and search for any new rheology titles.



CHAPTER 21: RHEOLOGY AND COMPUTING

'The world has arrived at an age of cheap complex devices of great reliability, and something is bound to come of it', Vannevar Bush (1945)

21.1 Introduction

The great possibilities opening up following the latest developments in computing mean that many things that were previously not feasible in rheological calculations are now possible. This is especially true with respect to calculating the steady and unsteady flow of rheologically complex fluids in complex geometries, which go far beyond the examples of liquids and geometries given in chapter 10. The particular technique we are referring to is Computational Fluid Dynamics, or simply CFD. The most familiar form of CFD is modern weather forecasting, where the local dynamics and thermodynamics of the atmosphere are calculated using a mathematical description of the flow and physical properties of air, together with the latest knowledge of wind speed, pressure and temperature at certain points, i.e. weather stations and balloons. The output is in terms of the spatial distribution of air velocity, temperature and pressure, and thus the distribution of rain, fog, frost and snow. Some of the largest computers in the world are used for this purpose.

21.2 A brief description of how CFD works

The conservation of mass, momentum and energy govern all fluid flows. These basic principles are expressed in the so-called Navier-Stokes equations. CFD involves the use of a numerical code on a suitable computer to solve these relationships as a series of partial differential equations.

The flow domain of interest has to be subdivided into a number of volumes, or cells, to form the *computational grid*. The conditions at all the boundaries of the grid must then be specified—*the boundary conditions*, e.g. in-flow, outflow, no-slip, velocity or pressure. The next step is to specify the properties of the liquid flowing through the domain—this is called the *constitutive equation*, which might be as simple as a power-law description of viscosity/shear-rate or might be as complicated as any of the most advanced models that account for viscoelasticity and time effects such as thixotropy, see below. The completion of these three steps makes it possible to solve the flow of the liquid throughout the domain.

After the solution stage, the results may be visualised as colour contours or vector plots of, for example, velocity, pressure, temperature, stress components, etc. It is also possible to track virtual ‘particles’ flowing through the flow domain to produce streamlines. It is then possible to create ‘videos’ of results of moving virtual particles.

21.3 The rheological descriptions of a non-Newtonian liquid and CFD codes

Usually mathematical models (or constitutive equations) that are of the following kind can describe the rheological properties of a liquid:

- inelastic - Newtonian, power-law, Cross, Herschel-Bulkley, Bingham
- elastic - differential or integral viscoelastic models, e.g. Oldroyd B.

Popular CFD codes presently available include:

- **CFX** from AEA Technology
- **FLUENT**
FIDAP from Fluent Ltd
POLYFLOW
- **Star CD** from Computational Dynamics
- **PHOENICS** from CHAM

All the codes listed provide a wide range of inelastic models, which adequately cover such liquids as dispersions and emulsions, but the kinds of liquids found in the polymer, personal-product, detergent, pharmaceutical and general chemicals industries might need viscoelastic models, and these presently are only provided by the POLYFLOW code.

21.4 When should CFD be used?

There is no better way to investigate the flow of complex fluids than to perform careful experiments on well-characterised fluids in suitably instrumented experimental geometries. CFD is *not* a cheap way of avoiding such proper, well-planned experiments, since the necessary software, hardware and dedicated trained personnel necessary for its use can be quite expensive. However, it is a very useful adjunct to experimentation, and should be seen as another useful tool for those interested in rheology.

Very often, pre-experiments using CFD will save a lot of time in planning other work, and once one is certain—via practical validation—that a computer code is giving a sufficiently good picture of reality, then systematic changes in both geometry and liquid can be performed with some confidence. This optimisation exercise is then very effective and can be economical in terms of resources that would otherwise have to be used to build and test new geometries, as well as in mixing and characterising new liquids.

21.5 Some typical results of CFD calculations

Figure 1 shows typical example of a flow geometry that has been '*meshed*', and figure 2 shows a typical output of such an exercise.

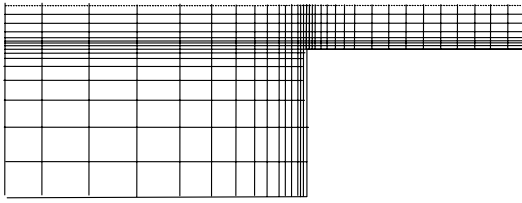


Figure 1 A typical CFD mesh, showing refinement where needed.

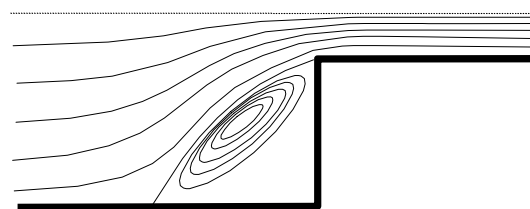
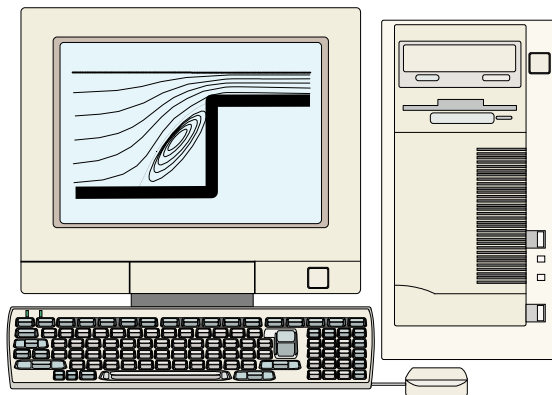


Figure 2: A schematic CFD output, showing flow-lines. Pressure, stress or velocity contours could also be shown.

21.6 A word of caution

CFD calculations are only as good as the mathematical representation of the liquid and the particular calculation procedure being used. The calculation operations used nowadays are however very robust, and given that the mesh used is fine enough in the right places (so it can be established that the results are independent of grid size), then we can be confident that the calculations will converge to a reasonable result. However the greatest problem remaining is the correct choice of a constitutive equation to adequately describe the liquid in a mathematical form. The hierarchy of rheological behaviour we are trying to capture begins at the general viscosity level, and moves up to the precise form of shear thinning behaviour, through possible elastic effects, and then to extensional flow anomalies. Most difficult of all is the inclusion of thixotropic effects at all these levels of sophistication.

Exercise: Look up the CFD website at <http://www.cfd-online.com/Resources/> for a comprehensive list of codes available around the world.



APPENDIX: ON-LINE (PROCESS) VISCOMETRY

'The mere act of observing something changes the nature of the thing observed', Hiesenberg

A.1 Introduction

The advantages—for both batch and continuous process operations—of being able to measure the viscosity of liquid products (or product precursors such as slurries) on-line, *during* their manufacture are obvious:

- time and effort are saved in obtaining the current or batch-end viscosity, which is otherwise obtained by taking a sample to an off-line viscometer, which has to be carefully loaded and subsequently cleaned.
- a control function can be introduced—if means are available to alter the viscosity by process or chemical variables; and
- a continuous monitor of viscosity build-up—and hence structure—is available for batch-mixing operations.

While the term '*process viscometer*' is generic, the terms *in-line* and *on-line* need to be defined: here '*in-line*' is used to describe the situation where *all the liquid* whose viscosity is being measured passes through or around the process viscometer, while '*on-line*' means that *only part of the liquid* is taken and passed through the viscometer—for instance in a bypass loop. We shall usually use the term *on-line* for convenience as it is commonly used for this class of instrument, but it should be noted that the correct place for a viscometer must be carefully chosen, bearing in mind the effect of flow-rate and temperature, so that sometimes it is best to have the viscometer in-line and sometimes on-line.

Here we review briefly the principles on which good practice is based in the area of process viscometry. We will not go over the same ground as Dealy [1] or Cheng et al [2], the former giving some principles, but few viscometer types, while the latter gives lots of viscometers with little '*consumer-preference rating*', and no principles given. Here we shall give an outline of the principles; an overview of the kinds of instruments commercially available and then give some of our own experience with one particular viscometer, the *Brookfield TT100*.

A.2 Desirable features of a good on-line viscometer

A good on-line viscometer should conform to **the three R's** of all process instrumentation:

- **Representative** samples of the liquid must continually pass through the **responsive** viscometer at a reasonable speed, but preferably without noticeably affecting the viscometer reading in doing so;

- **Relatability** must exist between the readings obtained on-line and those obtained from the definitive off-line instrument for **all** liquids of interest;
- **Reliability** and **robustness** of operation is needed for the rigors of a typical factory environment.

In order to have a **representative** sample, liquid must either be taken from a fast-flowing part of the process stream or the instrument be placed directly in the stream. The electro-mechanical response of any viscometer is usually quite fast, but the overall response to a change of viscosity of the liquid stream depends on the rate at which the liquid is substituted by fresh material in the measuring volume of the viscometer. Of course this takes us into a compromise situation because a good flow-through might mean that the flow rate affects the viscosity reading, and then any fluctuations in flow rate are incorrectly interpreted as changes in viscosity, see figure 1. For instance, if we want to place a measuring element directly in the flow stream (say a vibrating element) in order to get an almost instant indication of viscosity change, then it is unlikely to be the kind of measurement that is insensitive to flow rate and it is also unlikely that the viscosity reading easily relates to a conventional off-line measurement.

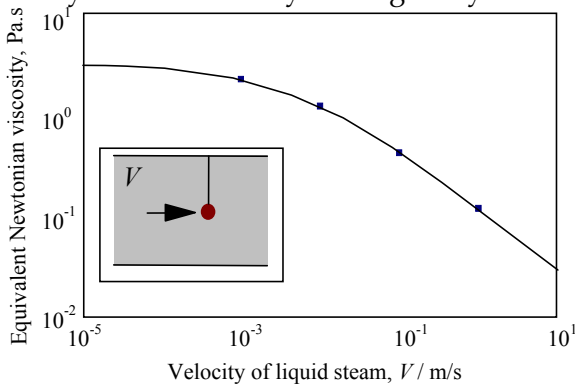


Figure 1: The equivalent Newtonian viscosity indicated by the Nametre vibrating-sphere in-line viscometer as a function of stream velocity.

On the other hand, to make a proper viscosity/shear-rate measurement on-line requires that the liquid be introduced into, and then removed from, a carefully controlled measuring volume which is part of a well-designed viscometer. As we have said, this can take time to carry out, and usually leads to a delay in responding to current viscosity changes in the flow line. What kind of viscometer one chooses depends on one's need for instant information or otherwise. However, data handling systems such as *Connoisseur* (Predictive Control Ltd., Northwich, UK) exist that can make up for slow instrument response because the *form* of the response curve is known and reproducible. This means for instance that if we know the response after say 30 seconds, we can predict where the viscosity will end up. Figure 2 shows a typical response of this kind.

Relatable readings demand that we know quite a lot about the fluid and the flow or else we do the same measurement on-line as off-line to be able to relate the readings, see below.

Reliable and robust machines are designed to withstand the kind of mechanical and chemical environments found in factory situations. They must be mounted in a relatively vibration-free position, and should not be attacked chemically by the liquids flowing through them.

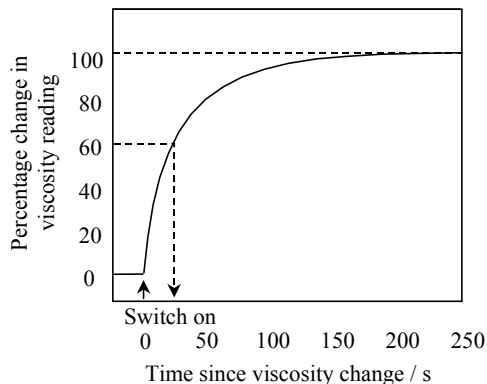


Figure 2: The (normalised) response of a Brookfield TT100 to doubling the viscosity, showing 60% of the change in ~ 30 s.

All these factors mean that the study of on-line viscometry is a subject apart, with its own rules and regulations. This is especially true since most liquids of interest are temperature sensitive and non-Newtonian (and possibly viscoelastic) in nature.

A.3 Types of measurement made by current instruments

On-line viscometers use basically the same kinds of measurements made on off-line instruments, i.e.,

- the drag on rotating geometries or stationary objects in the flow
e.g. *Contraves'* Convimat 101/105, APPA System's Iso-torq, Brookfield TT100;
- the speed of falling/pulled objects
e.g. *Cambridge* piston viscosity sensor;
- the pressure-drop or flow-rate down conduits or through orifices
e.g. *Porpoise's* P5, home-made devices;
- the energy absorbed by vibrating elements, spheres, rods and blades
e.g. *Nametre's* Viscoliner, *AccuTrax's* Electronic vibrating blade, Yamaichi's oscillating cylinder series, plus many others.

Because most liquids of industrial importance are non-Newtonian, we know that the measured viscosity can vary because of the

- type of flow (shear or extension viscosity);
- the rate of oscillation (frequency-dependent viscosity or elasticity) and/or
- the speed of flow (deformation-rate-dependant viscosity).

The result is that the one number usually produced as the output of a process viscometer, purporting to be the measured 'on-line' viscosity, can vary enormously for a non-Newtonian liquid depending on the type of measurement.

Also the measurement will be affected to some extent or other by the need to replenish continuously the fluid in the vicinity of the measuring element with fresh fluid. If this is done continually—as it is in most cases—then there is a strong possibility that the flow could affect the viscosity reading by, for instance, increasing the overall shear rate or even for vibrating

elements give an oscillatory-plus-steady flow which is very difficult to interpret. This can be controlled, accounted for or replaced by a sampling method that ensures no-flow when measurements are made.

One particular problem in the use of vibrational instruments is that if the liquid being measured is viscoelastic to any degree, then care should be taken in analysing the results, because any correlation sought with a conventional viscometer might not be found. The signal, if not split into in-phase and out-of-phase, will include (often non-linear) viscous and elastic components. Because the frequency of these devices is often very high, i.e. ultrasonic, the degree of elasticity can be very high, and hence its contribution to the overall signal is large. In this case it is difficult to relate to an off-line viscosity measurement on a conventional viscometer.

One point that should always be borne in mind is the effect of temperature on viscosity, because the temperature of the liquid being measured on-line is often above that used off-line. Therefore some compensation should be inserted. This is often built into the viscometer but can also be accommodated in any computerised data logging system being used, so that an equivalent standard-temperature viscosity can be displayed. For some measurements however, it might be necessary to pass the material through a heat exchanger to bring the material to the desired temperature for measurement.

A.4 The effect of non-Newtonian viscosity

Many on-line instruments are calibrated with Newtonian liquids, so that the results are presented as **equivalent Newtonian viscosity**—this can be far from the truth! Very few viscometers give the actual unambiguous (non-Newtonian) viscosity as a function of the variable, be it shear rate, frequency, etc. As Dealy has rightly said "*Most commercial process rheometers are designed for use with Newtonian fluids, and when non-Newtonian materials are involved, special problems arise.*" [1].

In cases where we only want a signal that is proportional to some measure of 'thickness', then almost any viscosity reading will suffice. However if anyone has gone to the lengths of putting in an on-line viscometer, this usually means that we have for a long period been accumulating information from off-line measurements—and this is usually the case as few companies install on-line viscometers before off-line—then they will want correspondence between the on-line and off-line reading. This can of course, for the right kind of flow-curve, be accomplished by a simpler method on-line than off-line, when a one-to-one correlation can be established, but this is by no means always the case.

If the particular product is not very non-Newtonian, a single-point measurement might be sufficient. Even then however we must be sure that the flow type is the same. For instance if our experience off-line is built up from steady-state, simple-shear flow curves, then a too-fast measurement might mean the measurement is not made under steady-state conditions. Equally if the on-line flow has an appreciable extensional component, then problems can arise for some liquids, especially polymer solutions. Also if a vibrational mode is used, then it is probable that some non-linear oscillatory function is being measured. All these facts could mean that we end up with no simple one-to-one correlation between on-line and off-line. Hence the safest way is to duplicate on-line what is done off-line. This is possible nowadays for most situations.

Last, we should mention one recurring problem with any kind of viscometry—wall slip. To be more correct, we should speak about the depletion of the dispersed phase of suspensions and emulsions that takes place at a smooth wall. This leads to a lubricating layer at the wall that can greatly interfere with the measurement. This can be overcome by roughening or profiling the surface of the measuring element [3].

A.5 Hygiene and cleaning

Cleaning is an important issue for process viscometers. Anyone with experience of real factory operations knows that process instrumentation is expected to work immediately and it is **never** expected to need adjustment or cleaning, but is used day-in, day-out for months or even years. The best designs of viscometer anticipate this and ensure that little build-up of debris occurs, and if it does, it is easily removed. This will be achieved by either washing the system through with a suitable solvent or by having a built-in cleaning-in-place capability (CIP). The design of the viscometer housing is crucial in this context. Brookfield have introduced a special housing for their TT100 viscometer which was supplied by APV of New York.

A.6 General comments on actual representative instruments

All on-line viscometers have some element of novelty in terms of the way they measure viscosity or how they ensure that liquid is replenished in the measuring region. However, at the same time, because they are in the flow-line, there is some degree of compromise. For instance, for the *Brabender Convimeter*, the novelty lies in the ‘nutation’ of the rotating member which precesses inside the measuring cell without rotating. However, although this novelty ensures that fresh liquid is drawn automatically into the measuring cell and measured liquid is expelled, the actual flow inside the measuring cell is very complicated, and does not necessarily reach steady state. The *Contraves Convimat*’s novelty lies in the magnetic drive through the wall, ensuring complete isolation from the outside. However, the jewelled mounting which holds the driven cylinder often wears out, and lacks robustness. Also, the flow geometry is not well defined, so no true shear rate can be assigned for non-Newtonian liquids, and the flow past the measuring element is too fast.

The *Namtre Viscoliner* (vibrating sphere) is a simple device, easily placed in the flow line, and easy to clean. However, the measurement one obtains is dependent on the flow rate past the vibrating sphere, and the number obtained is at best an oscillatory parameter, possibly the loss modulus, G'' , which for the materials usually being measured, cannot necessarily be correlated with off-line measurements (the same is true for the *Bendix* vibrating reed instrument and the many others of this kind). However, it is rarely the case that the output signal is resolved into its elastic and viscous components.

The *Cambridge* piston viscosity sensor (Cambridge Applied Systems, Cambridge, MA, USA) is ingenious in that the piston is lifted to the top of a slot let into the side wall of a pipe, and allowed to drop, and the cycle then being repeated. The speed of fall is then related to the viscosity. The novelty here is that the action of the cylinder moving up and down which pumps fresh liquid in and out of the tube containing the piston. However, the one number so obtained can only yield the equivalent Newtonian viscosity.

Whether or not one can live with the compromise associated with any instrument depends on the nature of the liquids being measured. Thixotropic, shear-thinning liquids are very difficult to measure even in the best off-line viscometer under ideal laboratory circumstances. To measure such liquids on-line is *extremely* difficult. While most instruments are calibrated to give an *equivalent Newtonian viscosity*, this is not always very useful for difficult materials. If on the other hand the liquids of interest are easy to measure, being virtually time independent and only slightly non-Newtonian, than almost any method will suffice, since a reliable correlation can be established between on-and off-line measurements.

A.7 Detailed analysis of a particular instrument

The *Brookfield TT100* is a typical on-line instrument that fulfils the criteria set out above, in that it follows the **3Rs**, i.e., representative sampling, relatability, reliability and robustness of operation. It is manufactured by the Brookfield Engineering Company of the USA, who are the longest-standing manufacturers of commercial rotational viscometers in the world. It is a concentric-cylinder instrument that can operate in- or on-line, and has an open-ended variant that can be mounted into the wall of a vessel - the *TT200*.

The *TT100* is mounted in a chamber through which the liquid of interest flows—the general arrangement is shown in schematic cross-section in figure 3. The speed of the motor driving the outer cylinder can be varied or fixed and the torque produced on the inner cylinder causes a small twist of the sealed torque-tube supporting it. This small twist is transmitted through the wall without friction and is measured on a rotation transducer mounted outside the chamber.

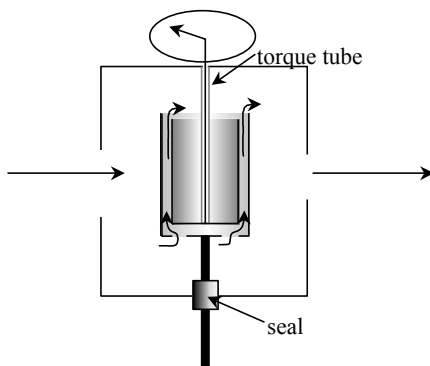


Figure 3: A schematic cross-section of the Brookfield TT100 in-line viscometer.

Some of the flow finds its way down through the gap between the cylinders either by natural means because the flow resistance is asymmetric or as directed using a flow-deflector that drives most the flow downwards, so enhancing enhances the flow between the cylinders. The limits of the viscosity that can be measured by this instrument are set by the onset of instabilities when the viscosity is too low and the torque-tube being twisted too far when the viscosity is too high. The shear rate can be set to any value between about 1 and 1000 s^{-1} , being a combination of the effect of the motor speed and the gap between the cylinders. The latter value is quite small for most pourable liquids and therefore the shear rate is virtually constant throughout the gap. The response time depends on the complete replacement of all the liquid in the measuring volume.

The *TT100* has a very effective CIP set-up. Inlet ports for hot water are positioned to wash the cylinders and keep the all-important gap clean. A special APV hygienic housing is now available that ensures easy cleaning by washing through with cleaning fluids.

A.8 Conclusions

On-line viscometers should be carefully chosen—the amount of care depending on the complexity of the liquid. The viscosity of Newtonian liquids can be measured by any kind of viscometer. If the non-Newtonian liquid of interest is simple, then we will be able to correlate any in- or on- line viscosity with its carefully measured off-line equivalent. If however there is no simple correlation, we need to do our best to measure on-line in the same way as we are measuring off-line. For instance a number of suitable concentric-cylinder type instruments are

now available. Even then, care has to be taken to ensure there is no interference from the flow; either by choice of viscometer or care in regulating the flow through. In the latter situation, single speed or multiple speed models are available. Computer control of course allows us any degree of complexity in measuring.

In terms of response time, we have a compromise situation: fast response times usually come from devices such as vibrating elements (e.g. the Nametre) placed directly in the flow line, however these might be difficult to relate to off-line measurement, and are certainly very sensitive to the local flow rate. On the other hand, the best devices that virtually duplicate off-line measurements are usually much slower in response because of the relatively long time taken to replace the liquid being measured (e.g. the Brookfield TT100). Thus the actual choice of device must be made very carefully.

References

- [1] Dealy, J.M, *Rheol Acta*, 29, 519 (1990).
- [2] Cheng D C-H; Hunt, J A and Madhvi, P, Status Report on Process Viscometers: Current Applications and Future Needs, Warren Spring Laboratory, Rep. No. W85034, 1985, ISBN 0 85624 363 9. (Now available from AEA Technology, Harwell, UK).
- [3] Barnes, H.A, *JNNFM*, 56, 221 - 251 (1995).

INDEX

- abrasive cleaners, 2
absorbed polyelectrolytes, 127
alginate, 55
ammonium salts, effect on viscosity of water, 120
Andrade law, 21, 22
antimisting additive, ICI, 155
apple sauce, 73
Applied Rheology, 175
Arrhenius law, 21
aspect ratio of fibres, 126
associative polymer, 94, 147, 148
atomisation, shear rate in, 7
axial slot, pressure in, 116
axis labels, 17
balloon inflation, 159
battery pastes, 136
beads, particle size distribution, 123
bearings, shear rate in, 7
Bentonite suspension, 72, 97, 102
Bingham equation, fluid or plastic, 59, 61, 64, 69, 75, 76
bleaches, 2
block copolymers, 127
blood and blood flow, 7, 60, 179
body wash, 56
Bonjela, 101
Bouncing Putty, 94
Brabender Convimeter, 191
branching, effect of, 157
break-up of liquid filaments, 162
Brownian motion, 21
brushing, shear rate during, 7
Buckingham-Reiner equation, 64
Burgers model, 83, 85, 86, 87, 91
butter, 74
capillary number, 38
Carbopol, 57, 71, 73, 81, 101, 145, 156
carrageenan, 57
Carreau model, 75
Casson fluid, 64, 75
cavern flow in mixers, 69, 172
cement pastes, 3
centipoise definition, 19
centi-Stokes, definition, 20
ceramic pastes, 136
CFD, 183
 mesh, 185
chewing, shear rate in, 7
CIP (cleaning-in-place), 192
circular hole, pressure at bottom of, 116
clays, 134
coarse sand, particle size distribution, 123
coating and coatings, 7, 134, 148
coil-stretch transition, 154, 155
computational fluid dynamics, see CFD
cone penetrometry, 136
confectionery, 7
consommé, 172
constitutive equation, 183
contraction flow, 117
Contraves Convimat, 191
Couette, 19
cream, 172
creep tests, 84, 86, 88, 89, 100
Cross model, 56, 58
cubic phase detergent, 95
curing, 102
dashpots, 83
delayed elasticity, 85
depletion forces, 128
dextran, effect on viscosity of water, 120
die swell, see extrudate swell
dip coating, shear rate in, 7
disc rotating in power-law liquid, 68
disc-shaped particles, 122
double-layer thickness, 127
dough, 102
drag reduction, 180
drainage down a wall, 7, 31, 65
drilling fluids/muds, 73, 148
Einstein, Albert, 120
elastic moduli, 81
 response, 85
Ellis equation, 78, 79
elongational flow, see extensional flow
engines, shear rate in, 7
entry length in tube flow, 35
epoxy resin, curing of, 103
extensional flow, 5, 150, 152, 159, 160
 biaxial, 159, 160
 planar, 159, 160
 viscosity, 142
extrudate swell, 109, 115
fabric conditioner, 56
 washing liquid, 55, 58
face cream, 2
facial wash, 58
figure legends, 17
fine sand, particle size distribution, 123
flocculated ink, 72
 systems, 43
flocculation, 128
flow along a slot, 31
 at the entrance of tubes, 35
 between squeezed circular discs, 32
curves, 55
in a slit, 66
in a mixer, 69
in a straight circular pipe, 63
in a straight tube, 27, 28, 39

- in inclined trough, 115
- out of a tank, 66
- through a converging nozzle, 67
- through an annulus, 32
- through packed bed, 29
- flows, strong, see extensional flow
 - weak, 151
- food processing, 172, 179
 - rheology, 171
- fractals, 130
- gelling systems, 102
- geological subjects, 181
- geometry, cone-and-plate, 111
 - parallel-plate, 111
 - re-entrant cone, 111
- glassy region, 92
- glucose, 120
- gravy, 172
- greases, 107
- guar gum, 57
 - /borate dispersion, 102
- hair conditioner, 56
 - gel, 101
 - shampoo, 2
 - spray, 2
- Hamaker constant, 127
- HDPE melt, 113, 115, 157, 158, 163
- HDPE/LDPE melt, 158
- Herschel-Bulkley model, 75
- high-speed coating, shear rate in, 7
- holes, pressure in, 115
- honey, 172
- Hooke's law, 82
- hoop stress, 110
- hydrophobic interactions, 165
- hydroxyethyl cellulose, 113
- ice cream, 172
- indenter into a viscous liquid, 34
- inertial effects, 89
 - in cone-and-plate, 116
- inflation of cylinders, 159
- ink, 3
- inverted (see tube-less) siphon, 163
- iron oxide suspension, 71
- ISO 9002, 21
- isoelectric point, 137
- isolated falling sphere, 30
- jet emerging from tubes, 36
- Journal of Non-Newtonian Fluid Mechanics, 175
 - of Rheology, 175
- Kelvin-Voigt element, 83, 86, 87, 92, 104
- Kozeny-Carman equation, 29
- Kreiger-Dougherty equation, 123
- lamellar phase drops, 166-168
 - sheets, 166, 167
- Laponite suspension, 97, 101
- latex suspension, 97, 98, 134
- leathery region, 92
- levelling due to surface tension, 7, 39
- liquid abrasive cleaner, 55
 - laundry additives, 148
- liquid-like behaviour, 90
- living polymers, 107, 146
- locust bean gum, 57
- logarithmic plotting, 11
- log-normal size distribution, 123
- loop tests, 132
- loss modulus, 88
- lotions, 7
- lubricating grease, 97
- lubrication, 7
- maltose, 120
- margarine, 74, 172
- Mark-Houwink equation, 145
- maximum packing fraction, 123, 126
- Maxwell model, 83, 89, 90, 91, 103, 104
- mayonnaise, 2, 72, 73
- mechanical vibrational spectroscopy, 88
- medicines, 7
- mica filler in polymer melt, 158
- micelles, spherical, 166
- micro-gels, 145
- mixing, 7, 134
- modified cellulose, 57
- molecular weight, effect of, 157
- molten chocolate, 71
- mustard, 55, 73
- Navier-Stokes equations, 183
- network dynamics, 155
- Newton, Isaac, 19
- Newtonian behaviour, limit of, 23
 - liquid, 19, 58
 - viscosity, equivalent, 190
- non-linear response, 100
- normal force, 53
 - pump, 109
- normal-stress coefficients, 111
 - difference, 81
 - difference, second, 110
 - difference, first, 109, 112
- nuclear-reactor vessels, 84
- nylon melt, 158
- oil, 172
- oliophilic interactions, 165
- organic glasses, 94
- orthodontic silicone gels, 103
- oscillatory flow and testing, 84, 92, 100
- Ostwald-de Waele, see power law
- paint, 2, 7, 97
- paper manufacture, 7
- parallel-plate plastometer

- (or squeeze-film), 33
 particle deformability, 126
 interactions, 122, 126
 particles, binary mixtures, 124
 particle-size distribution, 123
 pastes, flow of, 136
 paté, 172
 Péclet number, 125, 126
 penetrometers, 51
 penicillin suspension, 71
 personal-care products, 148
 pipe flow, 7, 64
 plastometer, parallel-plate, 67
 plateau modulus, 99
 region, 93
 Poiseuille, 19
 polyacrylamide, 55, 113 – 115, 156
 polyacrylate, 113
 polybutene, 114
 polydimethylsiloxane melt, 96
 polyethylene melt, 95
 low density (LDPE), melt,
 115, 157, 158, 163
 linear LDPE, 157
 polyisobutylene in cetane, 114
 in decalin, 56
 tetradecane, 115
 polymethylmethacrylate (PMMA) melt,
 96, 115
 polymer lattices, suspension of, 124
 polymer melts, 15, 56
 polypropylene (PP) melt, 77, 96, 99, 114,
 115, 157
 polysaccharide, 57
 polystyrene (PS) melt, 96, 113, 114, 157
 polystyrene in toluene, 56, 57, 114, 144
 polyvinyl acetate, 113
 power-law liquid, 56, 57, 58, 59, 61, 63,
 66, 67
 primary minimum, 127
 printing ink, 2, 7, 55
 psycho-physical cognition, 23
 pumping, 134
 radial distribution function, 99
 flow between parallel discs, 66
 rebuilding after shear, 102
 relaxation test, 84, 103
 resins, 134
 Rheologica Acta, 175
 Rheology Abstracts, 175
 rheometer, air turbine, 47, 48
 Carrimed Mk1, 48
 controlled-stress, 47, 53, 74
 Deer, 48
 rheometers, 52
 rod pushed into liquid in cup, 32
 climbing, 108
 rodlike (prolate) particles, 122
 micelles, 107, 146, 166
 rods or fibres, long, 142, 152
 rotating disc in a sea of liquid, 34
 rubbery region, 92
 rubbing, shear rate in, 7
 salad dressing, 7, 172
 saliva, 72
 satellite drops in atomisation, 162
 sauce, 2
 secondary minimum, 127, 128
 sedimentation of small particles, 7, 138
 sepiolite suspension, 103
 shampoo, 56, 60, 146
 sharp-edged orifice, 161
 shear flow, 5
 rate, definition and range of, 6
 stress, 6
 thickening, 133, 172
 thinning, 56
 shower gel, 56, 146
 SI units, 7
 silica gel, 103
 silicone oil, fluid, 57, 89
 Sisko model, 56–58, 60, 61, 64
 skin cream, 7
 slip layer, 65
 slots, pressure in, 115
 sodium salts, effect on viscosity of water,
 120
 soft cheese, 172
 solid-like behaviour, 90
 soup, creamy, 172
 spaghetti sauce, 73
 spectroscopy, mechanical, 100
 sphere in a non-Newtonian liquid, 65
 rolling down inclined tube, 31
 spheres, cloud of, falling/rising, 30, 138
 spray drying, shear rate in, 7
 spraying, shear rate in, 7
 spreadable materials, 74
 springs, 83
 starch, 134
 start-up experiments, 84, 104
 steric repulsion, 127
 stirring, 7
 Stokes flow, law, 30, 65, 88
 with inertia, 36
 stress relaxation test, 84, 103
 stretched exponential model, 132
 stretching flow, see extensional flow
 strong flow, see extensional flow
 structure-breakers for water, 120
 SUA1 polymer solution, 148, 149
 sucrose, effect on viscosity of water, 120
 surface tension, 68
 undulations, 68

- surfactant phases, 165
- solutions, 94
- suspended particles, 46
 - stability, 138
- suspension viscosity control, 137
- swallowing, 7
- Swarfega™, 2
- syrup, 172
- tank drainage, 29
- Tanner equation, 115
- Taylor vortices, 36, 37, 45
- terminal region, 92
- terminally anchored polymer, 127
- ternary mixture of particles, 124
- texture testers, 51
- thixotropic paints, 2
- thixotropy, 56, 82, 130, 131
- thread pulling, 159, 160
- toilet bleaches, 7
- tomato juice, paste, purée, ketchup, 2, 72, 73, 101, 172
- toothpaste, 2, 72, 73, 97
- transient network, 153
- transition region, 92
- transition-to-flow region, 92
- transverse slot, pressure in, 116
- Trouton ratio, 155, 156
- tube emptying under pressure, 29
 - filling under suction, 29
 - flow, 64
- tubeless siphon, 10, 163
- turbulent flow, 35
- uniaxial extension, definition diagram, 10
- van-der-Waals forces, 127, 128
- vane geometry, 43, 74
 - and-basket geometry, 44, 75
- velocity profile in circular pipes, 27
- vesicles, 168
- viscoelasticity, 81
- viscometer, Brookfield, 34, 68
 - calibration, 42
 - Cambridge piston, 191
 - chemical attack, 44
 - concentric-cylinder, 38
 - cone-and-plate, 45, 46
 - controlled-stress, 48
 - effect of gap, 46
 - elongational, 52
 - evaporation in, 43
 - extensional, opposed-orifice/jet, 161
 - flow-cup, 46
 - high-speed testing, 45
 - in-line, Brookfield TT100, 187, 189, 191, 192
 - inertia in a concentric-cylinder, 45
 - in-line, Nametre vibrating-sphere, 188
 - low-viscosity liquids, 45
 - mechanical damage, 45
 - narrow-gap concentric-cylinder, 26
 - on-line, 187
 - parallel-plate, 41, 50
 - pipe/tube, 50
 - process, 187
 - rolling-ball, 31
 - rotational, 25
 - Searle controlled-stress, 47
 - sedimentation/separation, 44
 - small-angle cone/plate, 26
 - standard laboratory, 52
 - U-tube (Ostwald), 19, 46
 - wide-gap concentric-cylinder, 41, 49, 69
- viscometry, on-line (process), 187
- viscosity, α -alumina, 79
 - air, 20
 - asphaltic concrete, 77
 - bitumen, 20, 77
 - butter, 77
 - cement, 77
 - cheddar cheese, 77
 - continuous phase, 20
 - corn syrup, 20
 - definition, 19
 - Earth's mantle, 77
 - effect of pressure, 22
 - effect of temperature, 21
 - everyday perception, 22
 - flocculated suspension as, 129, 131
 - gelatine gel, 77
 - glass, 77
 - glycerol, 20, 23
 - hydrogen, 20
 - ice cream, 77
 - ice, 77, 79
 - infinite-shear, 20
 - international standard, 20
 - intrinsic, 20
 - kinematic, 20
 - lithium fluoride, 79
 - lubricating oil, 20
 - Madeira cake, 77
 - magnesium oxide, 78
 - marble, 77
 - mineral oils, 23
 - mortar, 77
 - Newtonian liquids, 20

olivine, 78
petrol, 20
plastic, 7
Plasticine, 79
relative, 20
resins, 77
silicone oils, 23
sodium chloride, 79
solid soap, 77
solvent, 20
specific, 20
spinel, 79
steel, 77, 99
tin, 77
titanium, 79
uniaxial extensional (or
elongational), 153, 159,
160
water, 20, 172
zero-shear, 20
zinc carbide, 79
viscous region, 92
wall effects or slip, 42, 133
washing-up liquid, 2
water/ethyl-alcohol mixtures, 121
Weissenberg effect, 108, 109
 Rheogoniometer, 47
worm-like micelles, see rod-like micelles
xanthan gum solution, 55, 60, 95, 158
yield stress, 67, 69, 71
 flow equations with, 75
yoghurt, 60, 172

ANSWERS TO SOME EXERCISES

Chap 2, Exercise 4: Answer, $1.0515 \times 10^{-4} \text{ m}^3/\text{s}$.

Chap 6, Exercise: Answer, approximately 10^{-3} litre (or 1 ml) per day.

Chapter 9, Exercise:

Shampoo	-	Cross model
Polymer	-	Sisko model
Yoghurt	-	Sisko model
Blood	-	Cross or Sisko model
Xanthan gum	-	Cross model

Hint: look for turning points in the flow curves.

Chapter 15, Exercise: The viscosity increases smoothly as electrolyte is dissolved until the solubility limit is reached (for that particular temperature). Crystals are then formed, and the solution becomes a suspension. The continuous phase viscosity is given by the electrolyte level at saturation, and the suspended crystals contribute via their phase volume and shape. Temperature changes can change crystal shape (morphology).

Chapter 18 Exercise: The velocity of a cloud of $50 \mu\text{m}$ diameter particles (phase volume 0.3 and density difference with respect to the continuous phase 1000 kg/m^3) is given by

$$V = \frac{2\Delta\rho g a^2}{9\eta} (1 - \varphi)^{4.75}$$

If we can live with 1 mm per year as an acceptable sedimentation rate, then using the equation it is possible to show that the zero shear rate viscosity η_0 needs to be greater than around 10^5 Pa.s . This can be checked on a controlled-stress rheometer.

For a 1 mm thick layer of the liquid to drain down a wall at a superficial velocity greater than 1 mm/s , if we assume the density of the liquid is 1500 kg/m^3 , then the wall shear stress is given by 15 Pa. The order of magnitude of the shear rate is then given by the velocity divided by the thickness, i.e. $\sim 1 \text{ s}^{-1}$, thus the viscosity around unit shear rate has to be less than 15 Pa.s. This can be checked using a laboratory viscometer.

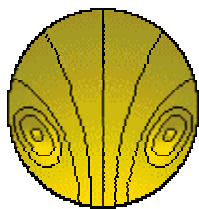
ABOUT THE AUTHOR



Howard Barnes studied Physics as an undergraduate at the University of Wales Aberystwyth, and then did a PhD there with Prof. Ken Walters FRS in the Applied Mathematics department. Since then, he has spent nearly 30 years at Unilever Research Port Sunlight where he is now Science Area Leader in Rheology and Fluid Mechanics. His particular interest is the relationship between the formulation, processing, microstructure and rheology of liquid products. Among his awards for his efforts in this area are a D.Sc. and a visiting professorship from the University of Wales; prizes from the Royal Society of Chemistry and the Institution of Chemical Engineers, and an OBE from Queen Elizabeth II for 'services to science and technology'. He is a fellow of the Royal Academy of Engineering; a past president of the British Society of Rheology, and an associate member of The University of Wales Institute of Non-Newtonian Fluid Mechanics. He is the author of some 60 publications in the area, and together with Professor Ken Walters and Mr John Hutton, he is a co-author of 'An Introduction to Rheology'.

Website: www.rheology.co.uk

ABOUT THE INSTITUTE OF NON-NEWTONIAN FLUID MECHANICS



The University of Wales Institute of Non-Newtonian Fluid Mechanics (UWINNFM) came into being in 1991, bringing together expertise from three constituent colleges of the University of Wales. Its Director is Professor Ken Walters FRS and there are eight other permanent members of staff, in addition to several Associate members, one of whom is Professor H.A. Barnes.

Much of the research carried out within the Institute is driven by the needs of Industry, although significant funding has also been raised from UK Government funding agencies and the EC.

The UWINNFM runs a popular series of annual workshops.

Website: www.aber.ac.uk/~nniwww/

ISBN 0-9538032-0-1